Synthesis and Biological Evaluation of Chalcogen Containing Redox Modulators, and an Analytical Investigation of Potential Mechanisms Responsible for Some Biological Effects of Chalcogen Containing Organic Compounds

Dissertation
zur Erlangung des Grades
des Doktors der Naturwissenschaften
der Naturwissenschaftlich-Technischen Fakultät
der Universität des Saarlandes

Von

Dipl.-Pharm. Ammar Kharma
Saarbrücken
2021

Tag des Kolloquiums:	28. Juni 2021
Dekan:	Prof. Dr. Jörn Eric Walter
Berichterstatter:	Prof. Dr. Claus Jacob Prof. Dr. Andreas Speicher
Akad. Mitglied:	Dr. Michael Ring
Vorsitz:	Prof. Dr. Marc Schneider

Die vorliegende Arbeit wurde von September 2016 bis Dezember 2019 unter Anleitung von Herrn Prof. Dr. Claus Jacob in der Fachrichtung Pharmazie (Bioorganische Chemie) der Naturwissenschaftlich-Technischen Fakultät der Universität des Saarlandes angerfertigt.

Dedicated to my
beloved Family

Table of Contents

Acknowledgements

I would like to express my deepest gratitude to Prof. Dr. Claus Jacob for providing me such a priceless opportunity to work and perform this thesis under his supervision. I am thankful for the support and guidance he offered all the way, and the doors he opened for me, helping me going forward, learning and achieving more and widening the spectrum of my experience.

I would also like to thank Prof. Dr. Andreas Speicher for being my scientific mentor. The valuable advices and insights he offered regarding my progress and his kind friendly approach have been an important support during this journey.

I would like to especially thank Prof. Dr. Eufrânio N. da Silva Júnior for the an unforgettable experience he allowed me to have during my stay at his research group in the Federal University of Minas Gerais, Belo Horizonte, Brazil. The scientific knowledge and techniques he offered me to learn and use and the unlimited support he showed in such an energetic, positive and colourful environment in Brazil has been a huge contribution to my work.

I would also like to thank Dr. Guilherme Jardim. His scientific insights, experience and the help he provided were a vital contribution during my stay in Brazil. I alse extend many thanks to my colleagues and friends in Belo Horizonte. Especially Ícaro A. O. Bozzi , Renata Gomes Almeida, Gleiston Gonçalves, Renato Lúcio, and Luisa Guerra for the great time during the long hours of work and for letting me be a part of the beautiful social and cultural life in Brazil.

I would like thank Dr. Enrique Domínguez Àlvarez, Dr. Miroslav Chovanec, Dr. Karol Ondrias, Marián Grman, and Anton Misak. My work with them, during my stay in the Slovak Academy of Sciences, Bratislava, Slovakia was an important part of my journey.

I would also Like to thank Dr. Jawad Nasim, and Yannick Ney. Both provided me with support, guidance, help and advice during the whole time I spent with them. Their contribution was important and critical for my thesis.

Finally, I would like to extend my endless thanks and gratitude to my family and especially my mother, for her continuous support, encouragement and love during the hardest times.

Abbreviations

BMPO	5-*tert*-Butoxycarbonyl-5-methyl-1-pyrroline-*N*-oxide
·cPTIO	2-(4-carboxyphenyl)-4,4,5,5-tetramethylimidazoline-1-oxyl-3-oxide
CV	Cyclic voltammetry
Cys	Cysteine
DADS	Diallyl disulfide
DATS	Diallyl trisulfide
DNA	Deoxyribonucleic acid
DPP	Different pulse polarography
EC	Electrochemistry
EPR	Electron paramagnetic resonance
ESI-MS	Electrospray ionization mass spectrometry
GPx	Glutathione peroxidase enzymes
GSH	Glutathione
Met	Methionine
NADPH	Nicotinamide adenine dinucleotide phosphate
NQs	Naphthoquinones
OS	Oxidative stress
pDNA	Plasmid DNA
RNS	Reactive nitrogen species
ROS	Reactive oxygen species
RSS	Reactive sulfur species
RSeSS	Reactive selenium and sulfur species
S	Sulfur
SAR	Structure-activity relationship

Se	Selenium
SeCys	Selenocysteine
SeMet	Selenomethionine
TR	Trypanothione reductase

Summary

Redox active modulators have gained the attention of various sectors of the research field. The continuous progress in fields such as synthetic chemistry, medicinal chemistry, and biochemistry have made the redox modulators a topic of interest for the medical and pharmaceutical domains due to the increasing number of advantages obtained from including redox modulators in diets and medications.

In this study, many naphthoquinones-based chalcogen containing compounds were prepared, and their biological activities were evaluated against several cancer cell lines and the parasite *Trypanosoma cruzi*. In general, the compounds demonstrated good biological activities towards the selected targets. The electrochemical synthetic technique was employed as a means to conduct fast and simple reactions performed in mild conditions.

Also, as a part of this study, the sulfur and selenium analogues of phthalic acid anhydride were employed in an analytical study aiming to clarify the mechanisms responsible for the documented biological activities these compounds possess.

Additionally, the redox potentials of a set of compounds synthesized in the study were observed by employing cyclic voltammetry (CV) as a technique. The results showed the changes in the redox potentials that accompanied the structures' chemical transformations after each synthetic step. The results obtained were used to correlate the biological activity and the redox potentials of these compounds.

Zusammenfassung

Redoxaktive Modulatoren haben die Aufmerksamkeit in verschiedenen Bereichen der Forschung gewonnen.

Die kontinuierlichen Fortschritte in Bereichen wie der synthetischen Chemie, der medizinischen Chemie und der Biochemie haben die Redoxmodulatoren zu einem Thema für den medizinischen und pharmazeutischen Bereich gemacht. Aufgrund der zunehmenden Anzahl von Vorteilen können diese Verbindungen relevant für Diäten und Medikamente sein. In dieser Studie wurden eine Reihe von Naphtoquinon-basierten Chalkogen-haltigen Verbindungen hergestellt und ihre biologische Aktivität wurde durch Tests gegen mehrere Krebszelllinien und gegen den Parasiten Trypanosoma cruzi bewertet.

Im Allgemeinen zeigten die synthetisierten Verbindungen eine gute biologische Aktivität gegenüber den ausgewählten Targets.

Die elektrochemische Synthesetechnik wurde eingesetzt, um schnelle und einfache Reaktionen unter milden Bedingungen durchführen zu können.

Im Rahmen dieser Studie wurden auch die Schwefel- und Selenanaloga von Phthalsäureanhydrid in einer analytischen Studie eingesetzt, mit dem Ziel die Mechanismen zu entschlüsseln, die die dokumentierten biologischen Aktivitäten dieser Verbindungen erklären.

Darüber hinaus wurden die Redoxpotentiale einer Reihe von Verbindungen, die während dieser Studie synthetisiert wurden, unter Verwendung der Methode der zyklischen Voltammetrie (CV) verfolgt.

Die Ergebnisse zeigten die Änderungen der Redoxpotentiale, die mit der chemischen Veränderung der Strukturen nach jedem Syntheseschritt einhergingen. Sie wurden genutzt, um die biologische Aktivität und die Redoxpotentiale dieser Verbindungen zu korrelieren.

Publications Included in this thesis

The following publications have been selected for this cumulative thesis:

1. Electrochemical Selenation/Cyclization of Quinones: A Rapid, Green and Efficient Access to Functionalized Trypanocidal and Antitumor Compounds

   Ammar Kharma, Claus Jacob*, Ícaro A. O. Bozzi, Guilherme A. M. Jardim, Antonio L. Braga, Kelly Salomão, Claudia C. Gatto, Maria Francilene S. Silva, Claudia Pessoa, Maximilian Stangier, Lutz Ackermann*, and Eufrânio N. da Silva Júnior*

   European. Journal of Organic Chemistry. 4474-4486. (2020)

2. Release of reactive selenium species from phthalic selenoanhydride in the presence of hydrogen sulfide and glutathione with implications for cancer research

   Ammar Kharma, Anton Misak, Marian Grman, Vlasta Brezova, Lucia Kurakova, Peter Baráth, Claus Jacob, Miroslav Chovanec, Karol Ondrias and Enrique Domĭnguez-Álvarez*

   New Journal of Chemistry, 43, 11771-11783 (2019)

3. Synthesis of quinone imine and sulphur containing-compounds with antitumor and trypanocidal activities: redox and biological implications

   Renata G. Almeida, Wagner O. Valença, Luísa G. Rosa, Carlos A. de Simone, Solange L. de Castro, Juliana M. C. Barbosa, Daniel P. Pinheiro, Carlos R. K. Paier, Guilherme G. C. de Carvalho, Claudia Pessoa, Marilia O. F. Goulart, **Ammar Kharma** and Eufrânio N. da Silva Júnior*

   RSC Medicinal Chemistry, 11, 1145-1160, (2020)

1. Introduction

1.1. Nature is the source and not only an inspiration

The concept of relying on what nature offers from plants, mushrooms, or even animal related products to treat diseases, relieve or stop the pain, and bring the human body to its normal functioning state is not a new idea [1-4]. People have been getting the benefits they seek by simply eating or processing such materials and preparing them as tees, water ,and alcoholic extracts or oils. These practices go back probably to even prior to the point when people began documenting this information as part of the medical literature or as recipes in the records of folk medicine [5].

Such documentation is one of the starting points for researches and studies interested in uncovering the elements and compounds responsible for the therapeutic effects. Researchers' combined efforts in fields such as biochemistry, analytical chemistry, and medicine have led to the characterization of many compounds disguised as gifts from nature [6,7].

1.2. New paths and challenges

These discoveries encouraged a shift in how to deal with the resources and provided an impetus to the extraction and purification efforts, making these compounds available in dosage forms compatible with the efficacy and toxicity studies. In 1805, Friedrich Wilhelm Sertürner (1783-1841) extracted morphine from opium, which was introduced to the market in 1826.

The advancements in areas such as instrumental analysis and intracellular diagnostic techniques, coupled with the curiosity and the desire to explore more profound mysteries of where and how allowed a closer and more detailed look at the mechanisms by which these

compounds of interest operate and what cells and organs they target once they are in the human body[8-10].

Information of this sort spurred new interests for medicinal chemistry and synthetic chemistry, which formed a kind of inspiration that stood behind synthesizing large numbers of novel chemical compounds to integrate the chemical core of interest into more complex structures[11-13]. Besides, improving the chemical priorities such as solubility and stability is a target of high importance to obtain active products suitable for pharmaceutical uses [14-17].

1.3. Redox based approach to dealing with diseases

The naturally available active compounds and the subsequent synthesized ones were and still are, classified according to their chemical structures or the chemical function dominating the structure. However, as a result of the accumulating new findings and insights, another classification has placed them under categories based on the biological activities and roles they demonstrate once introduced to the cellular environment, such as antibiotics and vitamins.

The group of redox active compounds is one of these groups with a renewed interest. The development in pathological diagnostic techniques went beyond observing symptoms and obvious causes and reached the pathological and the cellular functions. One of these investigations' results is the ability to place a frame around the interlaced and interconnected machinery maintaining the redox balance within the cellular environment and identifying the disturbances occurring due to oxidative stress (OS)[18-21]. Subsequently, this led to linking several diseases to imbalanced elevated concentrations of reactive oxygen species (ROS) and reactive nitrogen species (RNS) such as cancer, Alzheimer, and inflammation [22-24].

The redox active compounds, as a term, includes under its umbrella several subgroups such as polyphenols, flavonoids, and xanthenes [25-27]. Among these groups, quinones, secondary

metabolites abundant in the plant kingdom, steal their spotlight [28-30]. Quinones demonstrate biological activities covering a wide range of diseases and disorders [31-34].

1.4. Exploiting the capabilities of naphthoquinones

When moving closer to the quinones groups, the chemists took advantage of the chemical flexibility naphthoquinones (NQs) possess. These compounds can take the roles of dienophiles, electrophiles, pronucleophiles and undergo C-C bond formation reactions [35-39]. Such chemical properties granted the chemists a big space of freedom resulting in various synthesized compounds, including complexes, integrating side chains, and forming heterocyclic compounds, as a few examples [40-43].

In addition to the various synthetic chemistry avenues NQs can roam in, their main structure gives them the ability to interfere with many biological processes and reaction cascades within the living cell. The two carbonyl groups allow these compounds to undergo a redox cycle and accept one electron transforming into semiquinone radicals, such as the case with NADPH-cytochrome P450 reductase enzyme [44]. Additionally, NQs can accept two electrons when enzymes such as NADPH quinone reductase facilitate the reactions [45]. As semiquinone radicals continue their way in the reaction cycle, superoxide is generated [46,47]. Superoxide's presence results in the formation of hydroxyl radicals and hydrogen peroxide, among other ROS [48,49]. Subsequently, ROS activates and modifies various cellular signalling pathways, driving the cell into apoptosis [50-52].

On the other hand, NQs demonstrate high electrophilic properties, allowing them to form covalent bonds with many cellular components, mainly the ones having thiol groups within their structures [53,54]. Such reactions pave the way for other pathways and cascades influencing the cellular signalling process, resulting in apoptosis [55,56].

1.5. The spot chalcogens occupy in the redox realm

Chalcogens are a group of elements that receive an increasing interest in synthetic chemistry, biochemistry, and nutrition. Sulfur (S) and selenium (Se) receive the main focus due to the other group's high toxicity members. [57,58]. These two elements are critical focal points in many vital functions and many intracellular interactions and processes. Their presence in nature and nutrition mirrors their presence in the human body and the daily need the body requires for each of them. The amount of daily requirement of sulfur is estimated to be 14 mg/kg of body weight as the amino acid methionine, and it forms 0.2-0.3% of the mass of the human body [59]. While the human body requires a daily intake of 55 µg of selenium on average, forming 19 x10-9 % of the human body mass [60].

Each of these two elements' importance is manifested in the vital roles they play in the human body. Sulfur is included in key components such as the amino acids cysteine (Cys) and methionine (Met), enzymes depend on sulfur as a cofactor such as hydrogen sulfite reductase, and also glutathione (GSH), the crucial member of the natural mechanism that maintains the redox balance in the living cell [61-63]. While glutathione peroxidase enzymes (GPx), selenoneine, selenocysteine (SeCys), and selenomethionine (SeMet) are examples of the cellular components and sources of nutrition, selenium is included in [64-67].

Both elements can shift between various oxidation states, making them chemically and therefore biologically highly active. They easily join the redox cycles, which facilitate many processes and functions within the cellular environment

1.6. Recruiting chalcogens in pursuit of their redox activity

As a result of such observations, chemists found in chalcogens an investment opportunity, looking at them now with a different perspective, and not only as another element in the

periodic table. Consequently, groups of organic compounds that employed chalcogens were synthesized, aiming for a more potent and wider range of biological activities.

The on-going pursuit already paid off, and many groups of chalcogen containing organic compounds were synthesized. Their biological activities and mechanisms of action were subsequently investigated to know their limitations and promises. Compounds containing thiocyanates, sulfides, and disulfides functional groups and their selenium analogues are the most common examples [68-72].

Furthermore, ebselen and compounds belonging to the sulfonamides group are examples of chalcogen containing structures with stability, safety, bioavailability, and selectivity qualifying them for pharmaceutical use [73-76].

NQs were no exception to this approach, especially since they derive part of their biological activity as redox active compounds. As a result, various selenides, sulfides, disulfides containing NQs were synthesized [77-79].

The idea of synthesizing such compounds aims to benefit from having two components acting as a redox active modulator when present in the living cell. However, each of them interacts with different aspects and processes within the redox cycles in the cell.

Both chalcogens and NQs share the ability to generate ROS and RNS, thereby unleashing the cellular mechanisms associated with elevated concentrations of such species in unhealthy cells. Moreover, NQs interfere with the biological processes facilitated by enzymes such as quinone oxidoreductase-1 and cytochrome b5 reductase, while the chalcogens interfere with the processes that include enzymes such as glutathione peroxidases[80,81] [82].

NQs have taken their share of investigations to clarify the biochemistry behind their effectiveness in the living cell. This was assisted by the clarity of their chemical properties

explaining the readiness to take the roles they play in the cellular environment, and the findings obtained when employing the intracellular diagnostic techniques.

Several parts of the picture framing the chalcogens are still blurry. The reason is mainly the intermediates' high reactivity once they start interacting with the cellular components, which leads to dealing with short living reactive sulfur species (RSS), and reactive selenium species (RSeS) [83-85]. This characteristic opened the door for logical induction and hypotheses about their identity, depending on the aftermath of their activities [84].

1.7. Cyclic voltammetry as an investigation tool

Chemical synthesis is only one of the lanes the researchers have to take in their way to produce an effective chemical compound. In addition to the biological evaluation, several analysis techniques play an essential role in providing many insights and indications of where the researchers have arrived in the drug development process. Electrochemistry (EC) is one item in the toolbox that is used in the field of scientific research during this process.

The accurate and reproducible results of electrochemical methods such as CV and different pulse polarography (DPP) contributed to the widespread use of these methods in many aspects of the scientific research field. Additionally, the fact that the technique itself is relatively fast and cheap made it quickly reliable to obtain valuable information that helped the researchers better understand the compounds studied' chemical and biochemical mechanisms.

The fact that the redox modulators' biochemical behaviour comes initially from these compounds' chemical redox properties has suggested subjecting members of this group of compounds to electrochemical studies. Within this context, investigating the electrochemical properties of NQs helped to understand the chemical transformations that occur on members

of this group of compounds within the living cell that finally unfold as biological activities [86-88].

Also, the information obtained from employing CV when studying natural sulfur compounds such as diallyl disulfide (DADS) and diallyl trisulfide (DATS) clarified that these compounds undergo reduction reactions within the living cell before they interfere with the cellular redox cycle [89].

Understanding the mechanisms responsible for the biological activities of studied compounds and how these compounds interact with the cellular components highlights the importance of the results obtained from similar studies. Such advantages are part of the structure-activity relationship concept, making the EC studies a useful member in the list of techniques used in studies related to this concept. The nature of the information this technique provides makes it possible to predict the biological activity of a novel synthesized compound that shares a structure already went through similar studies.

1.8. Electrochemical synthesis

Synthetic chemists, similar to researchers of any other field, are fast to exploit and employ any new methodologies and techniques that contribute to easing and speeding up the chemical reactions and even unlocking doors for chemical reactions that are not possible with the techniques currently in hand. Photochemistry and electrochemical synthesis are two examples of such techniques. The electrochemical synthesis dates back to 1796, while the first employment for photochemistry was recorded in 1834.

Organic electrochemical synthesis represents an alternative technique that holds characteristics considered advantageous when compared to conventional chemical synthesis.

An essential advantage this technique has is avoiding including conventional oxidants and reductants in the reactions. [90]. In this case, the flow of electrons is the tool that facilitates

the reactions [91]. Additionally, the reactions are often carried out in mild conditions than to those applied during conventional chemical reactions [92]. It is also easy to tag this technique as "green" since it is environmentally friendly due to electricity utilization as a source of energy and the lesser amounts of waste produced by the reactions [93].

On the other hand, some of the disadvantages the researchers go through are the narrow range they move in regarding the solvents and the electrolytes. Also, experimenting on the reaction chamber type and finding the potential that delivers the desired product in satisfying yield are crucial and can be time consuming steps during optimizing the synthesis protocol [94,95].

In a part of this study, this technique was employed to synthesize naphthoquinone based selenium containing compounds. Their biological activity was evaluated against *Trypanosoma cruzi* and various cancer cell lines.

2. Aims of the thesis

The current study's first aim is to employ the electrochemical synthesis technique to incorporate naphthoquinones in selenium based redox modulators. The second aim is to evaluate the biological activity of the resulted compounds against *Trypanosoma cruzi*, and also against several cancer cell lines.

The third aim is to investigate some possible mechanisms responsible for releasing reactive sulfur and selenium species in the biological environment from organic chalcogen compounds and the interaction between these species with cellular components.

The fourth aim of this study is to explore a possible link between the biological efficiency demonstrated by sulfur based redox active compounds and their redox behaviour by employing cyclic voltammetry to observe the changes in the redox behaviour between the starting point and the result of the chemical synthesis.

.

3. Results

3.1. Publication 1

Electrochemical Selenation/Cyclization of Quinones: A Rapid, Green and Efficient Access to Functionalized Trypanocidal and Antitumor Compounds

Ammar Kharma, Claus Jacob*, Ícaro A. O. Bozzi, Guilherme A. M. Jardim, Antonio L. Braga, Kelly Salomão, Claudia C. Gatto, Maria Francilene S. Silva, Claudia Pessoa, Maximilian Stangier, Lutz Ackermann*, and Eufrânio N. da Silva Júnior*

European. Journal of Organic Chemistry. 4474-4486. (2020)

https://doi.org/10.1002/ejoc.202000216

EurJOC
European Journal of Organic Chemistry

Full Paper
doi.org/10.1002/ejoc.202000216

Antitumor Compounds

Electrochemical Selenation/Cyclization of Quinones: A Rapid, Green and Efficient Access to Functionalized Trypanocidal and Antitumor Compounds

Ammar Kharma,[a,b] Claus Jacob,*[b] Ícaro A. O. Bozzi,[a] Guilherme A. M. Jardim,[c] Antonio L. Braga,[c] Kelly Salomão,[d] Claudia C. Gatto,[e] Maria Francilene S. Silva,[f] Claudia Pessoa,[f] Maximilian Stangier,[g] Lutz Ackermann,*[g] and Eufrânio N. da Silva Júnior*[a]

Abstract: Electrochemical selenation in undivided electrochemical cells allows the preparation of selenium-containing naphthoquinones. The rapid, green and efficient protocol avoids chemical oxidants and enables the synthesis of target molecules in a fast and reliable way. This strategy provides and efficient and general method for the synthesis of quinoidal compounds with activity against five cancer cell lines and *Trypanosoma cruzi*, the parasite that causes Chagas disease.

Introduction

A range of naphthoquinoidal compounds obtained from natural sources or via organic synthesis have been associated with impressive biological activities, including antioxidant, chemopreventive, cytotoxic and antimicrobial actions.[1] In this sense, the development of efficient and reliable methods for the functionalization of naphthoquinones is a field of intense pharmaceutical interest and synthetic efforts.[2] Here, the advent of organocatalysis has enabled the straightforward synthesis of complex quinones in their enantiomeric pure form, often employing inexpensive and readily accessible organocatalysts.[3] C–H bond activation reactions were also employed for the synthesis of quinonoid compounds with relevant functionalization pattern prepared in a few synthetic steps, with the use of catalysts based on transition metals.[4] At the same time, electrochemistry has been rediscovered as a powerful and sustainable synthetic tool in organic chemistry.[5] Electrosynthesis enables efficient and selective reactions for the functionalization of diverse organic molecules, as it is based on tightly controlled oxidation and reduction processes. Although electrosynthesis is therefore applicable to a wide variety of organic compounds, its benefits in the field of quinones and chalcogens is still vastly unexplored and warrants a more detailed investigation.[6] Indeed, quinones and chalcogens are both redox active, i.e. in principle amenable to electrosynthetic methods. Furthermore, molecules based on either quinones or chalcogens – or both – are of particular interest in biological chemistry.

A couple of years ago, the Jacob group has described the ability of selenium-containing quinones to act as "intelligent" redox sensor/effector agents.[7] Since then, a wide variety of quinonoid hybrid compounds with two redox centres, i.e. a quinone moiety and a selenium or tellurium atom, have been described in the literature.[7,8] These hybrid chalcogen-containing quinones are often active against cancer cell lines and a range of pathogenic microorganisms (Scheme 1A).[9–12] Following the strategy of insertion of the selenium atom to the quinoidal system, the groups of Braga and da Silva Júnior[12–15] have described the synthesis of selenium-containing quinone derivatives, once more with potent antitumor and trypanocidal activities.

Notably, the relevant seleno-functionalization traditionally involves oxidation with different oxidant sources, as for instance, I_2/DMSO in the presence of diselenide.[13–15] In principle,

[a] Institute of Exact Sciences, Department of Chemistry, Federal University of Minas Gerais, UFMG, 31270-901, Belo Horizonte, MG, Brazil
E-mail: eufranio@ufmg.br
https://www.eufraniolab.com/
[b] Division of Bioorganic Chemistry, School of Pharmacy, University of Saarland, 66123 Saarbruecken, Germany
E-mail: c.jacob@mx.uni-saarland.de
https://www.uni-saarland.de/lehrstuhl/jacob/
[c] Department of Chemistry, Federal University of Santa Catarina, Florianópolis, SC, 88040-900, Brazil
[d] Oswaldo Cruz Institute, FIOCRUZ, Rio de Janeiro, RJ, 21045-900, Brazil
[e] Institute of Chemistry, University of Brasilia, Brasilia, 70904-970, DF, Brazil
[f] Department of Physiology and Pharmacology, Federal University of Ceará, Fortaleza, CE, 60430-270, Brazil
[g] Institut für Organische und Biomolekulare Chemie, Georg-August-Universität, Göttingen, Tammannstraße 2, 37077 Göttingen, Germany
E-mail: lutz.ackermann@chemie.uni-goettingen.de
http://www.ackermann.chemie.uni-goettingen.de/
Supporting information and ORCID(s) from the author(s) for this article are available on the WWW under https://doi.org/10.1002/ejoc.202000216.

Full Paper
doi.org/10.1002/ejoc.202000216

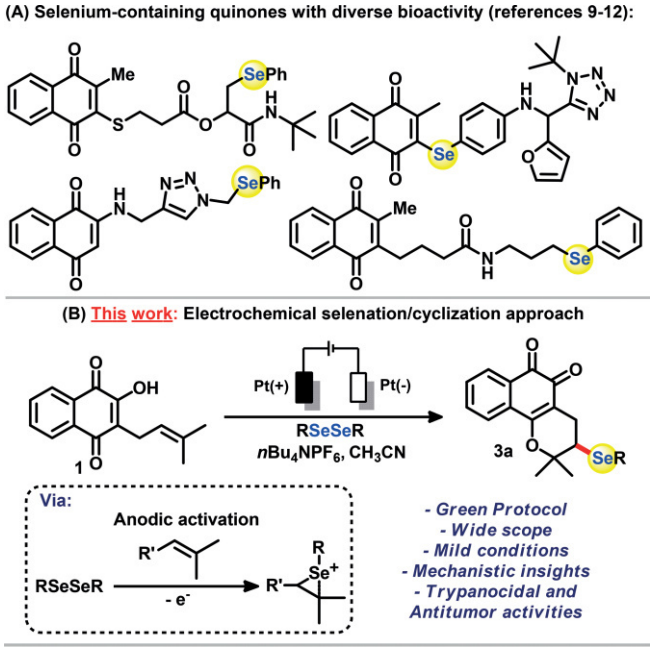

Scheme 1. Overview.

a chemistry employing electrochemical rather than iodine-based oxidation of selenium should be feasible and we are now able to report for the first time an efficient electrochemical selenation/cyclization of naphthoquinones (Scheme 1B).

Results and Discussion

In general, the results obtained in our study confirm the potential of electrochemistry in the synthesis of selenium-containing quinone hybrid molecules which in turn show promising biological activity. The reactivity of lapachol (**1**) towards electrophilic organoselenated species has been described previously by our research group, with an I_2/DMSO oxidative system operating under microwave conditions.[13,14] This kind of oxidative cyclization is also possible in an undivided electrochemical cell. In our first attempt, electrochemical oxidative cyclization of **1** has been performed in an undivided cell reactor with potassium iodide as electrolyte and acetonitrile as solvent (Table 1, entry 1). The presence of iodide was considered as beneficial as the reaction may proceed via the formation of iodine (I_2), as discussed above. Static 10 × 10 × 0.2 mm platinum anodes and cathodes were employed, fully immersed into the solution, with a current up to 5 mA. Under these conditions, a complex mixture of products was observed after 30 min, possibly due to the interference of the electrolyte with electrochemical and subsequent chemical processes. The presence of iodide was therefore seen as counter-productive and the electrolyte was changed to nBu$_4$NBr (1.0 equiv.). Disappointingly, this setup, operating at a current of 5 mA for 1 h yielded only traces of product **3a**. Increasing the current to 10 mA, increased the yield of **3a** to 13 % during the same reaction time (entries 2 and 3). As electrochemical synthesis of **3a** was therefore possible in principle, still with a low yield, we investigated a series of ammonium quaternary salts as alternative electrolytes for the process in order to optimize the conditions and yields. Reaction with 1.0 equiv. of nBu$_4$NClO$_4$ afforded product **3a** in 65 % yield after 1 h, and under the same conditions, nBu$_4$NBF$_4$ as electrolyte resulted in 52 % yield (entries 4 and 5). Astonishingly, exchanging the electrolyte to nBu$_4$NPF$_6$, and employing a current of 10 mA and a reaction time of 1 h afforded **3a** in a stunning 93 % yield (entry 6).

Table 1. Optimization of reaction conditions.[a]

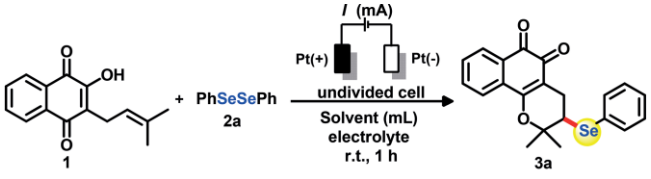

Entry	Solvent (mL)	Electrolyte (equiv)	Current	Time/h	Yield%
1	MeCN (10)	KI (0.5)	5 mA	0.5	mixture
2	MeCN (10)	nBu$_4$NBr (1.0)	5 mA	0.5	NR
3	MeCN (10)	nBu$_4$NBr (1.0)	10 mA	1.0	13
4	MeCN (10)	nBu$_4$NClO$_4$ (1.0)	10 mA	1.0	65
5	MeCN (10)	nBu$_4$NBF$_4$ (1.0)	10 mA	1.0	52
6	MeCN (10)	nBu$_4$NPF$_6$ (1.0)	10 mA	1.0	93
7	MeCN (10)	nBu$_4$NPF$_6$ (0.5)	10 mA	1.0	73
8	MeCN (5)	nBu$_4$NPF$_6$ (1.0)	10 mA	1.0	68
9	MeOH (10)	nBu$_4$NPF$_6$ (1.0)	10 mA	1.0	23
10	H_2O (10)	nBu$_4$NPF$_6$ (1.0)	10 mA	1.0	NR
11	EtOH (10)	nBu$_4$NPF$_6$ (1.0)	10 mA	1.0	11
12	DMC (10)	nBu$_4$NPF$_6$ (1.0)	10 mA	1.0	NR
13	MeCN (10)	nBu$_4$NPF$_6$ (1.0)	10 mA (C+|C-)	1.0	61
14	MeCN (10)	nBu$_4$NPF$_6$ (1.0)	10 mA (Pt+|C-)	1.0	42
15	MeCN (10)	nBu$_4$NPF$_6$ (1.0)	10 mA (C+|Pt-)	1.0	72
16	MeCN (10)	nBu$_4$NPF$_6$ (1.0)	10 mA	1.0	32[b]
17	MeCN (10)	nBu$_4$NPF$_6$ (1.0)	–	24	NR

[a] General reaction conditions: Pt plate electrode (10 mm × 10 mm × 0.05 mm), (**1**) (0.2 mmol), (**2a**) (0.2 mmol); solvent (10 mL), electrolyte (1.0 equiv.), current (10 mA). [b] 0.5 equiv. of **2a** was used. NR = for all cases starting material **1a** was recovered. Yields of isolated products.

Attempts to decrease the amount of electrolyte and solvent (entries 6 and 7) resulted in decreasing yields, which led us to investigate other suitable solvents (entries 9–12). The reaction in methanol or ethanol also resulted in lower yields, and no reaction was observed in water or dimethyl carbonate (DMC), possibly due to the low solubility of the reactants in both of these solvents. As for the electrode material, graphite rods were investigated as a more economical alternative to platinum, and yielded an acceptable yield of 61 % of **3a** under otherwise identical conditions, i.e. in MeCN and at a current of 10 mA (entry 13). In contrast, possible combinations of Pt and graphite as anodes and cathodes (entries 14 and 15), decreased the yield in all cases. Finally, decreasing the amount of diselenide **2a** to 0.5 equiv. resulted in 32 % yield (entry 16). To rule out any chemical processes catalyzed by platinum, the reaction was performed inside the electrochemical cell, albeit without electricity. As expected, no product was observed after 24 h, ruling out any chemical reactions taking place without current applied, and confirming that electricity serves as the terminal oxidant in this transformation (entry 17).

Full Paper
doi.org/10.1002/ejoc.202000216

After optimizing the protocol for electrochemical oxidative selenation/cyclization for the model quinone, lapachol (**1**), different diselenides **2** and different quinones were considered to establish the scope and general applicability of this reaction.

Diselenides with a varied substitution patterns are generally tolerated, as shown by the formation **3a**–**3i** in good to excellent yields, with exception of compound **3h** obtained in a moderate yield of 63 % (Scheme 2). Diselenides containing electron withdrawing groups provided the respective products **3b** and **3c** in 88 % and 83 % yield. Nonetheless, the conditions also tolerate diselenides containing electron donating groups (compounds **3b** and **3c**), or heterocyclic and substitution groups in *meta* position, as demonstrated by the preparation of the quinoidal derivatives **3h** and **3i**. In some cases, suitable crystals were obtained, for instance for compounds **3c**, **3e** and **3g**, and by X-ray crystallographic analysis unambiguously confirmed the formation of the six-membered ring containing an oxygen atom (see ORTEP-3 projection in Figure 1).

Besides being flexible with regard to the diselenide, the electrochemical method of oxidative selenation can also accommodate other naphthoquinones as a nucleophilic partner, as shown in the Scheme 3 and Scheme 4. Initially, we prepared C-allyl lawsone (**4**) via a methodology described in the literature.[16] This quinoidal derivative provides access to an unprecedented range of selenium-containing quinones **5**. In a preliminary study reported by our group,[13] product **5a** was prepared previously via a catalytic chalcogenylation reaction with I_2/DMSO as oxidant in the presence of diphenyl diselenide, still we encountered difficulties in expanding the scope of the reaction, noting that different diselenides, in some cases, did not result in the formation of the respective product in good or moderate yields. In contrast, the electrochemical approach appears to provide access to a wide range of new quinones **5a**–**5i**, regardless of the electronic variety of the substituents. Compounds **5b**–**5e**, for instance, were obtained in moderate yields, and the diselenide containing the heterocyclic also afforded **5h** in 84 % yield.

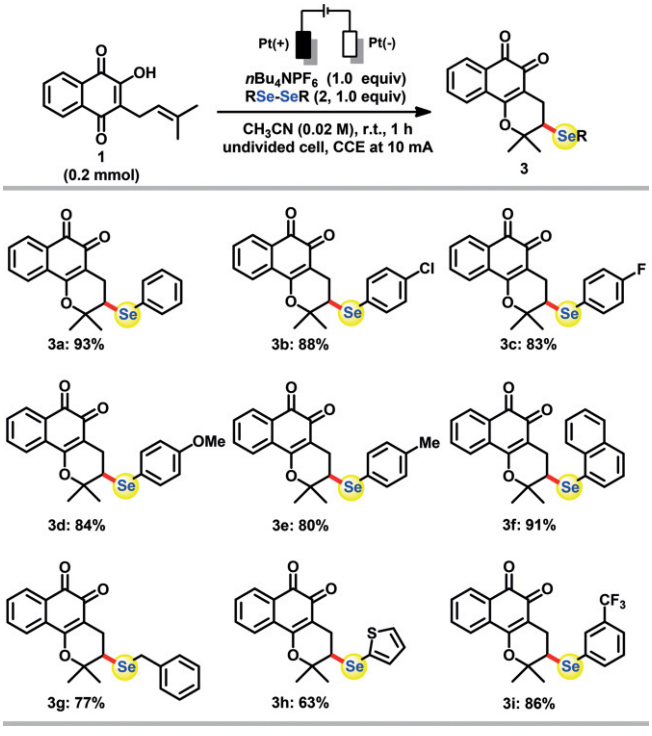

Scheme 2. Scope of the reaction with lapachol as quinone component.

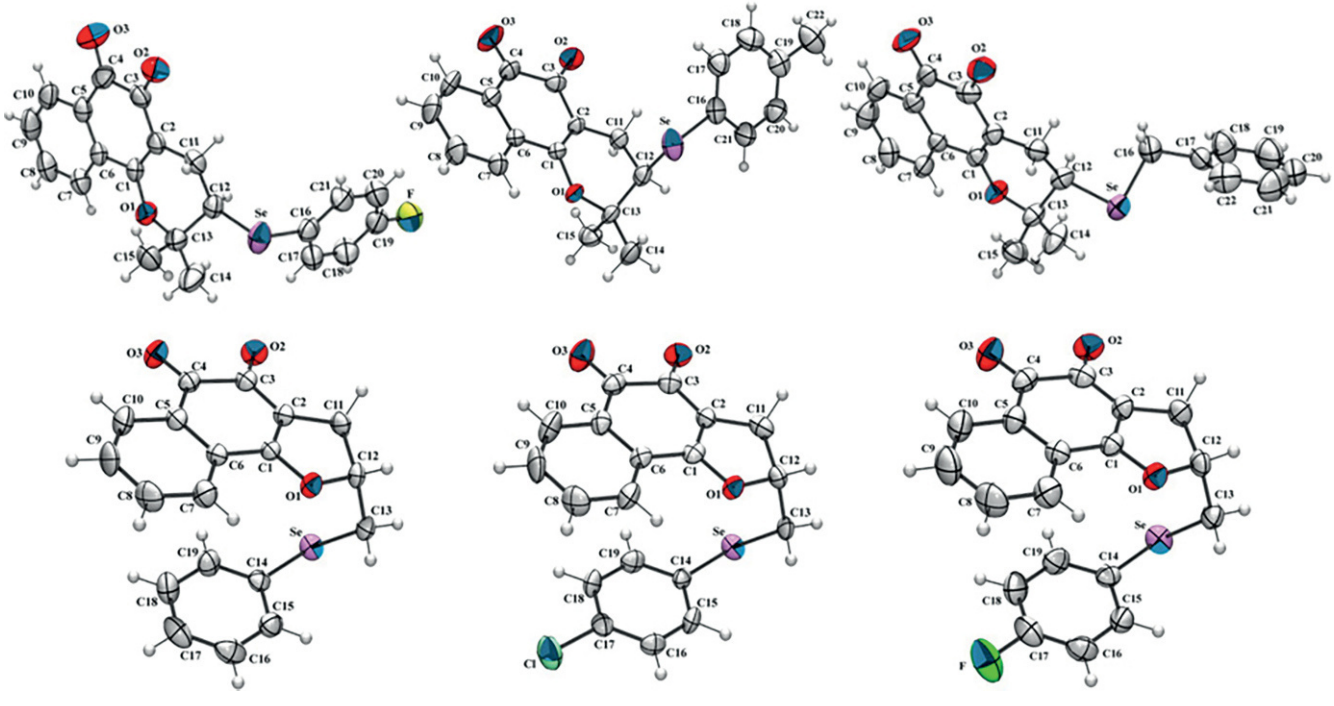

Figure 1. ORTEP-3 projections of **3c**, **3e**, **3g** and **5a**, **5b** and **5c** indicating the atom numbering and displacement ellipsoids at the 50 % probability level.

Full Paper
doi.org/10.1002/ejoc.202000216

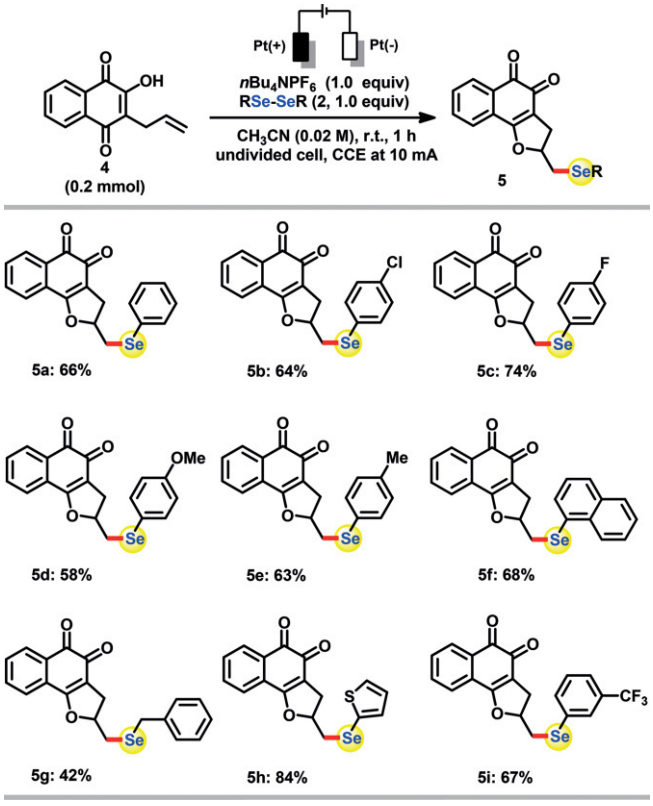

Scheme 3. Scope of the reaction with C-allyl lawsone as quinone component.

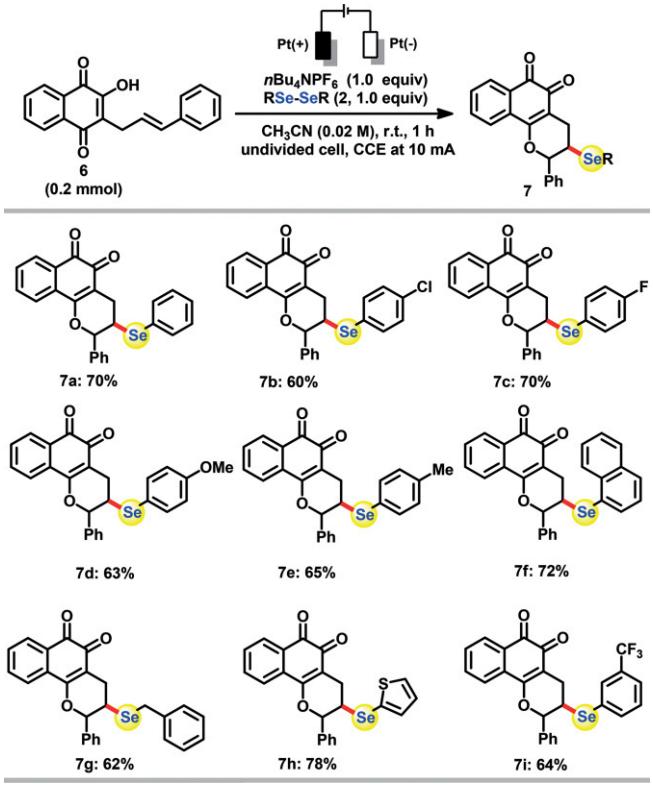

Scheme 4. Scope of the reaction with a quinoidal compound derivative of lawsone as quinone component.

Notably, formation of both, six- and five-membered rings are possible, as the reaction of C-allyl lawsone (**4**) with diselenides indicates. In order to certify the formation of the products, we have obtained suitable crystals for crystallographic studies. The structures of the compounds **5a**, **5b** and **5c** were determined by X-ray crystallography analysis and the ORTEP-3 projections are shown in Figure 1.

The side chain of the quinone, in the case of **4**, may also impact on the reaction, similar to the substituents on the diphenyl diselenide. Besides C-allyl-lawsone (**4**), we have therefore investigated lawsone derivative **6** (Scheme 4). The formation of compounds of the general structure **7** was successful, with moderate to good yields ranging from 60 % to 78 % and as expected for *anti*-addition reactions the products present *trans* stereochemistry and were formed as a racemic mixture. The formation of these compounds from **6** may, in theory, follow two different pathways generating dihydro-furan or -pyran rings. Unfortunately, after several attempts at recrystallization, we have not successfully obtained suitable crystals for X-ray crystallography analysis and compounds of type **7** were characterized by detailed 1D and 2D NMR experiment methods.

We have also investigated derivatizations of **3a** to demonstrate the utility of the selenated naphthoquinones prepared here (Figure 2). Reaction of **3a** with hydroxylamine hydrochloride, *o*-phenylenediamine and phenylhydrazine hydrochloride afforded products **8**, **9** and **10** in yields of 60 %, 72 % and 70 %, respectively. Heterocyclic compounds prepared from lapachones have various applications, for instance, as fluorescent sensors for live-cell imaging of lipid droplets and for imaging NQO1 activity in tumour tissues.[17]

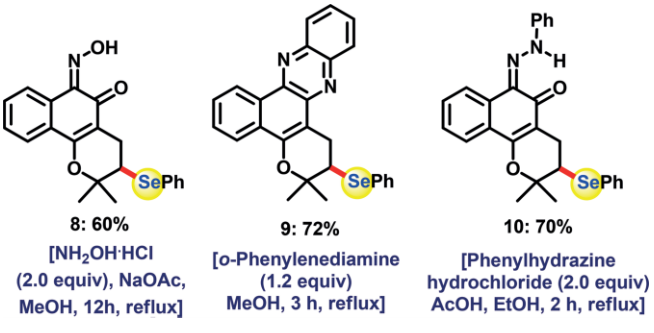

Figure 2. Derivatizations of **3a**.

After successfully performing the first electrochemical selenation/cylcizations of quinones and optimizing the conditions to yield highly competitive yields, we have also turned our attention to the mechanism underlying this – sequence of – reaction(s). Based on literature reports,[18] we expected a mechanism for the electrochemical selenation proceeding via a highly electrophilic, positively charged intermediate (Scheme 1B). To investigate the mechanism of the reaction in greater detail, cyclo voltammetric measurements were conducted.

Diselenide **2a** was found to be irreversibly oxidized at a peak potential of E_p = 1.44 V vs. SCE (Figure 3). Due to its high reactivity, the $[(PhSe)2]^+$ radical cation generated undergoes a fast chemical follow-on reaction, probably forming a dicationic tetramer.[18f,18g,18i] The resulting species shows a cathodic re-

sponse at E_p = 0.02 V vs. SCE, which can be rationalized by reduction of a $[(PhSe)_3]^+$ cation formed according to previous literature reports.[18e]

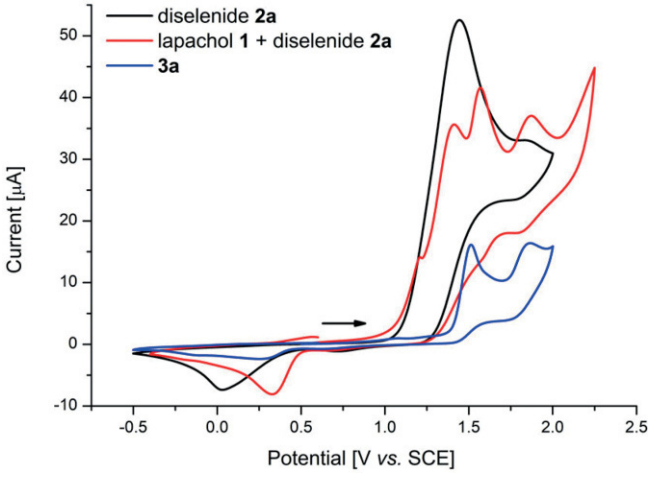

Figure 3. Cyclic voltammograms in MeCN at 100 mV/s. nBu$_4$NPF$_6$ (0.1 M in MeCN), concentration of lapachol (**1**) and diselenide **2a** 5.0 mM. Diselenide **2a** (black); lapachol (**1**) + diselenide **2a** (red); **3a** (blue).

Upon addition of lapachol a new anodic response at E_p = 1.55 V vs. SCE was observed, which can be assigned to the oxidation of product **3a**, as evidenced by an independent analysis of product **3a**. Furthermore, a reductive peak was observed at E_p = 0.33 V vs. SCE, which in comparison to diselenide **2a** takes place at higher potentials and disappears at lower scan rates. Both results, the additional anodic event, together with the diminishing cathodic event at higher scan rates, are suggestive of a rapid carbophilic reaction of the selenium dication with lapachol forming a cationic intermediate, which is rapidly undergoing nucleophilic cyclisation furnishing product **3a** and diselenide **2a** (Scheme 5). Next to the irreversible oxidation peaks at E_p = 1.55 V and E_p = 1.85 V vs. SCE product **3a** shows a reversible reduction at $E_{1/2}$ = –0.75 V vs. SCE confirming that

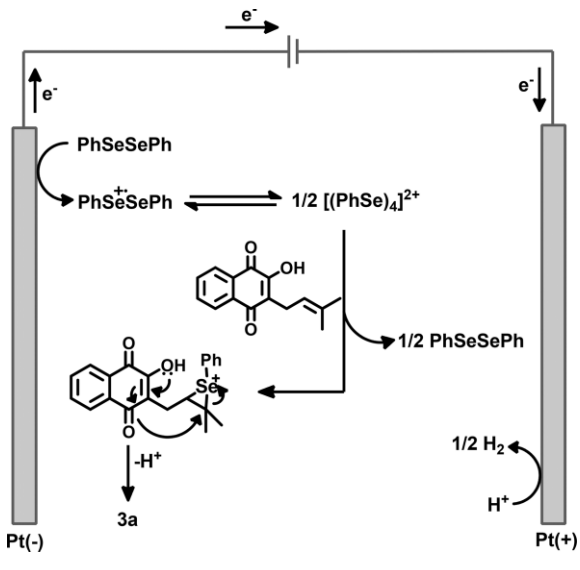

Scheme 5. Proposed mechanism underlying the electrochemical selenation/cyclization reaction(s).

the quinone is obtained in its oxidized form after electrolysis. See Figures S2–S6 in the ESI file for more details.

Once synthesized, the various selenated quinones were also evaluated for possible biological activity. Based on the trypanocidal and antitumor potential of selenium-containing multifunctional redox agents,[9–12,14] the compounds were targeted initially against selected cancer cell lines such as PC3 (prostate carcinoma), SNB-19 (astrocytoma), HCT-116 (human colon carcinoma), MCF-7 (breast carcinoma), B16F10 (murine melanoma), and also against the flagellated protozoan *Trypanosoma cruzi* (*T. cruzi*), which is responsible for Chagas disease.[19] In general terms, quinones are capable of generating reactive oxygen species (ROS) that are intrinsically related to the antitumor and trypanocidal potential of this class of substances.[1e] These deleterious species are able to react directly with DNA, lipids, and proteins leading to cellular damage.[19] In the case of *T. cruzi*, the absence of classical antioxidant machinery, such as the glutathione/glutathione reductase system and catalase, reinforces the parasite rudimentary defenses against ROS.[20]

Chagas disease causes significant mortality and morbidity, especially in low-income populations in endemic countries of Latin America.[21] Since the 1960s, clinical chemotherapy for Chagas' disease is based on two nitro derivatives, benznidazole and nifurtimox, which have important side effects and controversial anti-*T. cruzi* activity in chronic patients.[22] The lack of options for the most serious phase of this disease, gives evidence to the continuous demand for new trypanocidal drugs.[23]

Here, we have identified twelve compounds with activity against the parasite evaluated against bloodstream trypomastigotes of *T. cruzi* (Y strain) at 4 °C with 5 % of blood. Compounds **3c**, **3f**, **3g**, **3h**, **5a**, **5b**, **5e**, **5g**–**5i**, **7a** and **7i** were active against the parasite with IC_{50} values in the range of 97.4 to 38.3 μM (Table 2). Compound **3c** with IC_{50} = 38.3 μM was particularly active, when compared to the standard drug benznidazole (IC_{50} = 103.6 μM), **3c** is 2.6-fold more active. Compound **3i** previously published by our research group also presents activity against *T. cruzi*, and electrochemistry as a synthetic method enabled the preparation of **3i** in higher yield compared to the method previously described.[15]

Table 2. Activity of synthetic derivatives against bloodstream trypomastigotes of *T. cruzi* (Y strain) at 4 °C with 5 % of blood.

Compd	IC_{50}/24 h[a] (μM)	Compd	IC_{50}/24 h[a] (μM)	Compd	IC_{50}/24 h[a] (μM)
3a	102.9 ± 0.0[b]	**5a**	81.6 ± 7.7	**7a**	71.4 ± 22.5
3b	360.5 ± 34.6[b]	**5b**	58.3 ± 2.7	**7b**	337.0 ± 4.2
3c	38.3 ± 2.4	**5c**	241.4 ± 10.9	**7c**	275.0 ± 36.4
3d	207.6 ± 33.52[b]	**5d**	182.5 ± 27.5	**7d**	102.0 ± 2.6
3e	1677.8 ± 113.3[b]	**5e**	82.6 ± 9.0	**7e**	120.5 ± 2.1
3f	57.0 ± 9.6	**5f**	208.4 ± 6.3	**7f**	>500
3g	97.4 ± 17.8	**5g**	85.7 ± 14.7	**7g**	131.5 ± 3.6
3h	63.6 ± 5.1	**5h**	89.4 ± 13.0	**7h**	242.6 ± 46.0
3i	54.9 ± 3.19[b]	**5i**	75.5 ± 9.7	**7i**	95.9 ± 11.6
Bz	103.6 ± 0.6[c]	**Bz**	103.6 ± 0.6[c]	**Bz**	103.6 ± 0.6[c]

[a] Mean ± SD of at least three independent experiments. [b] Ref.[15]. [c] Ref.[24]. Bz = Benznidazole.

Table 3. Cytotoxic activity expressed as IC_{50} μM (95 % CI) of the compounds **3a**–**3i** and **5a**–**5i** in cancer and normal cell lines after 72 h exposure, obtained by nonlinear regression for all cell lines from three independent experiments. nd, not determined. DOXO = doxorubicin, drug used in clinical against cancer.

Compd	IC_{50} μM (95 % CI)					
	PC3	SNB-19	HCT-116	MCF-7	B16F10	L929
3a[a]	0.55	nd	2.41	nd	nd	2.49
	0.30–0.90		2.13–2.76			1.91–2.89
3b[a]	3.28	nd	7.68	nd	nd	5.81
	2.68–4.02		6.43–9.26			5.51–6.39
3c	1.51	1.90	0.95	2.42	0.98	1.55
	1.35- 1.71	1.81–1.99	0.77–1.17	2.30–2.54	0.74–1.30	0.61–3.93
3d[a]	3.06	nd	4.68	nd	nd	1.89
	2.45–3.83		4.08–5.40			1.47–2.38
3e[a]	5.17	nd	19.27	nd	nd	10.47
	4.32–5.76		16.87–20.93			10.13–13.34
3f	10.89	11.72	7.80	9.04	6.49	4.06
	8.17–14.51	9.34–14.71	6.64–9.16	7.41–13.66	5.10–8.26	2.80–5.89
3g	4.51	6.50	5.00	9.76	4.97	3.94
	3.18–6.41	5.92–7.15	4.13–6.07	8.61–11.06	4.40–5.62	2.79–5.56
3h	3.89	5.70	3.85	6.25	3.93	2.97
	3.22–4.73	5.49–5.93	3.25–4.56	5.67–6.88	3.58–4.31	2.27–3.88
3i[a]	1.69	nd	3.78	nd	nd	3.69
	1.26–2.29		3.11–4.57			3.20–4.19
5a	2.51	3.45	2.49	3.81	2.12	1.92
	2.24–3.35	2.86–4.16	2.41–2.97	3.55–4.08	1.99–2.25	0.83–4.46
5b	4.28	3.58	2.78	5.40	2.72	3.03
	3.66–5.00	3.06–4.18	2.28–3.39	4.74–6.14	2.49–2.97	2.76–3.33
5c	9.18	14.62	7.34	12.69	3.72	7.62
	5.90–10.93	12.71–16.80	6.21–8.68	11.37–14.17	3.27–4.24	5.39–10.79
5d	4.30	4.94	4.07	6.56	4.31	3.65
	3.50–5.25	4.36–5.61	3.72–4.46	6.27–6.87	3.71–5.01	2.81–4.74
5e	4.43	6.98	4.09	7.50	2.32	3.85
	3.78–5.23	6.72–7.26	3.61–4.63	7.10–7.93	2.05–2.62	3.07–4.83
5f	3.95	3.11	2.02	5.10	2.12	3.41
	3.96–4.92	2.74–3.53	1.50–2.72	4.28–6.08	1.88–2.40	2.75–4.23
5g	4.19	7.99	5.38	8.96	3.41	3.46
	3.31–5.29	7.38–8.65	4.55–6.36	7.77–10.34	3.07–3.78	2.57–4.67
5h	2.23	3.05	2.36	4.15	2.12	2.36
	1.89–2.50	2.59–3.59	2.09–2.68	3.78–4.56	1.90–2.36	2.05–2.72
5i	3.22	5.85	3.28	4.36	2.62	3.31
	2.47–4.18	5.62–6.09	2.80–3.83	3.60–5.28	2.19–3.13	2.59–4.24
DOXO	0.76	2.07	0.19	0.14	1.34	1.71
	0.59–0.93	1.78–2.40	0.14–0.24	0.12–0.19	1.14–1.59	1.59–1.86

[a] Data obtained from ref.[14].

In previously published studies, we have also demonstrated and discussed the details related to the antitumour activity of selenium-containing quinones.[12,14] In this earlier report, compounds **3a**, **3b**, **3d**, **3e** and **3i** were evaluated against ten cancer cell lines, HL-60 and MOLT-4 (leukaemia), HCT-116 (human colon carcinoma), HCT-8 (colon), PC3 (prostate), PC3M (human metastatic prostate), OVCAR$\bar{3}$ and OVCAR-8 (ovarian), SF295 (central nervous system) and MDA-MB-435 (breast) and normal cell lines, exemplified by peripheral blood mononuclear cells (PBMC), V79 and L929[14] demonstrating the antitumor potential and selectivity of this class of compounds.

In the present study, we selected the quinones related to families **3** (dihydro-pyran ring) and **5** (dihydro-furan ring), here described for the first time, to evaluate any potential activity of these compounds against selected six tumor cell lines, PC3, SNB-19, HCT-116, MCF-7 and B16F10 and one non-tumor cells, L929 (murine fibroblast). The IC_{50} values obtained are summarized in Table 3.

Briefly, compound **3c** (IC_{50} = 0.95 to 2.42 μM) presented the highest cytotoxic potential against all cell lines investigated. This compound exhibited a lower IC_{50} value against the HCT-116 human colon carcinoma cancer cell line than compound **3a**, previously described in the literature (IC_{50} = 2.41 μM).[14] These IC_{50} values in the low micromolar range are promising and demand further investigations. For the PC3 prostate cancer cell line, the compounds with the highest cytotoxic activity were again **3c** and, this time, **5h** with IC_{50} values of 1.51 and 2.23 μM, respectively. These compounds also exhibited higher cytotoxicity against the astrocytoma cells SNB-19, with IC_{50} values of 1.90 and 3.05 μM, respectively.

Compound **3c** presented an IC_{50} value of 2.42 μM in the MCF-7 cell line, where **5a** showed the second highest activity (IC_{50} = 3.81 μM). For colon carcinoma (HCT-116) the IC_{50} was 0.95 μM for **3c**, followed by 2.02 μM for **5f**. The highest cytotoxic for the melanoma lineage (B16F10) were 0.92 μM for **3c** and 2.12 μM for **5f** and **5h**.

For all compounds the selectivity index (SI) was calculated as an indicator of the selectivity of a compound for a neoplastic and a normal lineage, as selectivity is essential before any future clinical evaluation may be carried out (Table S1). The antitumor

potential of new compounds can be considered important when the SI has a value equal to or greater than 2.0, that is, the compound exhibits an activity against in the neoplastic cell line which is double or higher when compared to its activity against normal cells.[22] In some cases, the compounds under investigation exhibited a high selectivity index with values around 1.6. In this context, the substances described here for the first time can be considered as an important starting point for the design of new molecules with powerful antitumor activity and low cytotoxicity against normal cells and consequently a high selectivity index.

Conclusions

In conclusion, we have reported an efficient electrochemical method for the synthesis of a wide range of selenium-containing multifunctional redox quinoidal compounds via an anodic oxidative selenation/cyclization reaction. This reaction is simple and versatile, it results in considerable yields and is insensitive to the character of the diselenide and quinone selected. Some of the quinone-hybrid molecules produced with this electrochemical method also exhibit considerable biological activity, such as compound **3c**, which is active against *T. cruzi* with an IC_{50} of 38.3 μM and against HCT-116 and B16F10 cancer cells with IC_{50} values of 0.95 and 0.98 μM, respectively. Our study provides a simple, fast, green and efficient synthetic access to selenium functionalized quinones. Due to the biological potential of the compounds described and ease of handling and carrying out reactions involving electrochemistry, our methodology enables the synthesis of a wide variety of chalcogen-modified quinones. Their synthesis and biological activities are promising and can be investigated further in a series of follow-on studies.

Experimental Section

General Remarks: Starting materials obtained from commercial suppliers were used as received unless otherwise stated. Flash column chromatography (FCC) was performed using silica gel (Aldrich 40–63 μm, 230–400 mesh). Thin layer chromatography (TLC) was performed using aluminum-backed 60 F254 silica plates. Visualization was achieved by UV fluorescence. Proton nuclear magnetic resonance (NMR) spectra were recorded using a Bruker DRX 400 or a Bruker AVANCE 400 spectrometer. ^{13}C NMR spectra were recorded at 100 MHz as stated. Chemical shifts (δ) are given in parts per million (ppm). Peaks are described as singlets (s), doublets (d), doublet of doublets (dd), triplets (t), doublet of triplets (dt), quartets (q), doublet of quartets (qt) and multiplets (m). The ^{1}H and ^{13}C NMR spectra were referenced to the appropriate residual solvent peak or TMS peak. Coupling constants (*J*) were quoted to the nearest 0.5 Hz. Mass spectra were recorded using a Bruker Daltonics micrOTOF-Q II ($APPI^+$ and ESI^+ mode). Infrared spectra were recorded on a Perkin Elmer Spectrum One FTIR spectrometer as thin films or solids compressed on a diamond plate. IR bands are described by the wavenumber ($\tilde{\nu}$, cm^{-1}). Melting points were determined using the Stuart SMP30 melting point apparatus and are uncorrected. The anode and cathode are platinum plate electrodes (10 × 10 × 0.2 mm). Electrocatalysis was conducted using an AXIOMET AX-3003P potentiostat in constant current mode. CV studies were performed using a Metrohm Autolab PGSTAT204 workstation and Nova 2.1 software.

Synthesis of substrates: Diselenides were synthesized via the Grignard reaction followed by transmetalation with Se powder (200 mesh).[25] Lapachol (1) (2-hydroxy-3-(3′-methyl-2′-butenyl)-1,4-naphthoquinone) was extracted from the heartwood of *Tabebuia sp.* (Tecoma) and purified by a series of recrystallizations in an appropriate solvent. From lawsone, C-allyl-lawsone (4) and compound **6** were synthesized following procedure described by Fieser.[26]

General Electrosynthesis Procedure: A 25 mL electrosynthesis reactor was charged with the corresponding quinone (0.2 mmol), nBu_4NPF_6 (77.4 mg, 0.2 mmol) the corresponding diselenide (0.2 mmol) and acetonitrile (10 mL). The reactor was equipped with two platinum electrodes (10 × 10 × 0.2 mm) immersed in the solution, that was submitted to constant stirring. The constant current was set to 10 mA. The reaction was electrolyzed for 1 hour, and analysis by TLC showed complete consumption of the starting material. The resulting mixture was transferred to a 100 mL round-bottomed flask and after solvent removal by reduced pressure, the crude product was purified by FCC, under the conditions noted.

Characterization Data of Products 3a–i.

2,2-Dimethyl-3-(phenylselanyl)-3,4-dihydro-2*H*-benzo[*h*]chromene-5,6-dione (3a): The general electrosynthesis procedure was followed by using quinone **1** (48.4 mg, 0.2 mmol) and diselenide **2a** (62.4 mg, 0.2 mmol) as starting materials. Purification by column chromatography on silica gel (*n*-hexane/EtOAc, 4:1) yielded **3a** (73.8 mg, 93 %) as an orange solid. ^{1}H NMR (400 MHz, $CDCl_3$) δ: 8.05 (d, *J* = 6.7 Hz, 1H), 7.78 (d, *J* = 7.5 Hz, 1H), 7.71–7.57 (m, 3H), 7.51 (t, *J* = 7.5 Hz, 1H), 7.35–7.24 (m, 3H), 3.41 (dd, *J* = 9.7, 5.6 Hz, 1H), 3.10 (dd, *J* = 17.9, 5.6 Hz, 1H), 2.74 (dd, *J* = 17.9, 9.7 Hz, 1H), 1.68 (s, 3H), 1.54 (s, 3H); ^{13}C NMR (100 MHz, $CDCl_3$) δ: 179.5, 178.0, 161.5, 135.2, 134.9, 132.1, 130.9, 130.1, 129.4, 128.7, 128.5, 128.3, 124.1, 112.5, 83.0, 45.7, 27.8, 25.4, 23.3; ^{77}Se NMR (76 MHz, $CDCl_3$) δ: 379.7; IR (solid): $\tilde{\nu}$ = 2977, 1610, 1377, 743 cm^{-1}; m.p. (°C) = 124.3–125.2; HRMS ($APPI^+$): Calcd. for $C_{21}H_{19}O_3Se$ $[M + H]^+$ 399.0495, found 399.0500.

3-((4-Chlorophenyl)selanyl)-2,2-dimethyl-3,4-dihydro-2*H*-benzo[*h*]chromene-5,6-dione (3b): The general electrosynthesis procedure was followed by using quinone **1** (48.4 mg, 0.2 mmol) and diselenide **2b** (76.2 mg, 0.2 mmol) as starting materials. Purification by column chromatography on silica gel (*n*-hexane/EtOAc, 4:1) yielded **3b** (75.9 mg, 88 %) as a deep orange solid. ^{1}H NMR (400 MHz, $CDCl_3$) δ: 8.06 (d, *J* = 7.5 Hz, 1H), 7.78 (d, *J* = 7.7 Hz, 1H), 7.66 (t, *J* = 8.2 Hz, 1H), 7.54 (d, *J* = 8.3 Hz, 2H), 7.25 (d, *J* = 8.4 Hz, 2H), 3.40 (dd, *J* = 9.5, 5.6 Hz, 1H), 3.09 (dd, *J* = 17.9, 5.6 Hz, 1H), 2.73 (dd, *J* = 17.9, 9.5 Hz, 1H), 1.67 (s, 3H), 1.54 (s, 3H); ^{13}C NMR (100 MHz, $CDCl_3$) δ: 179.4, 178.0, 161.4, 136.5, 134.9, 132.0, 131.0, 130.1, 129.6, 128.8, 126.6, 124.1, 112.3, 82.8, 46.1, 27.8, 25.3, 23.4; ^{77}Se NMR (76 MHz, $CDCl_3$) δ: 375.2; IR (solid): $\tilde{\nu}$ = 2980, 1610, 1302, 821 cm^{-1}; m.p. (°C) = 194.4–194.9; **HRMS** ($APPI^+$): Calcd. for $C_{21}H_{18}ClO_3Se$ $[M + H]^+$ 433.0104, found 433.0103.

3-((4-Fluorophenyl)selanyl)-2,2-dimethyl-3,4-dihydro-2*H*-benzo[*h*]chromene-5,6-dione (3c): The general electrosynthesis procedure was followed by using quinone **1** (48.4 mg, 0.2 mmol) and diselenide **2c** (69.6 mg, 0.2 mmol) as starting materials. Purification by column chromatography on silica gel (*n*-hexane/EtOAc, 4:1) yielded **3c** (68.9 mg, 83 %) as an orange solid. ^{1}H NMR (400 MHz, $CDCl_3$) δ: 8.06 (d, *J* = 7.6 Hz, 1H), 7.78 (d, *J* = 7.2 Hz, 1H), 7.71–7.55 (m, 3H), 7.53 (t, *J* = 7.5 Hz, 1H), 6.99 (t, *J* = 8.7 Hz, 2H), 3.35 (dd, *J* = 9.5, 5.6 Hz, 1H), 3.07 (dd, *J* = 17.9, 5.6 Hz, 1H), 2.72 (dd, *J* = 17.9, 9.6 Hz, 1H), 1.68 (s, 3H), 1.54 (s, 3H); ^{13}C NMR (100 MHz, $CDCl_3$) δ:

179.4, 178.0, 163.1 (d, J = 249.1 Hz), 161.5, 137.7 (d, J = 8.1 Hz), 134.9, 132.0, 131.0, 130.1, 128.7, 124.1, 122.9 (d, J = 3.6 Hz), 116.6 (d, J = 21.9 Hz), 112.3, 82.8, 46.1, 27.8, 25.2, 23.3; ^{77}Se NMR (76 MHz, $CDCl_3$) δ: 371.7; IR (solid): $\tilde{\nu}$ = 2977, 1607, 1217, 778 cm^{-1}; m.p. (°C) = 132.3–132.4; HRMS (APPI$^+$): Calcd. for $C_{21}H_{18}FO_3Se$ [M + H]$^+$ 417.0400, found 417.0405. *The structure of the product was also confirmed by X-ray diffraction* (CCDC number = 1966510).

3-((4-Methoxyphenyl)selanyl)-2,2-dimethyl-3,4-dihydro-2*H*-benzo[*h*]chromene-5,6-dione (3d): The general electrosynthesis procedure was followed by using quinone **1** (48.4 mg, 0.2 mmol) and diselenide **2d** (74.4 mg, 0.2 mmol) as starting materials. Purification by column chromatography on silica gel (*n*-hexane/EtOAc, 4:1) yielded **3d** (71.7 mg, 84 %) as an orange solid. ^{1}H NMR (400 MHz, $CDCl_3$) δ: 8.05 (d, J = 8.3 Hz, 1H), 7.78 (d, J = 7.5 Hz, 1H), 7.65 (t, J = 7.6 Hz, 1H), 7.55–7.52 (m, 3H), 6.80 (d, J = 8.7 Hz, 2H), 3.79 (s, 3H), 3.29 (dd, J = 9.4, 5.6 Hz, 1H), 3.05 (dd, J = 18.0, 5.6 Hz, 1H), 2.70 (dd, J = 17.9, 9.5 Hz, 1H), 1.68 (s, 3H), 1.54 (s, 3H); ^{13}C NMR (100 MHz, $CDCl_3$) δ: 179.5, 178.0, 161.5, 160.1, 137.7, 134.8, 132.2, 130.9, 130.1, 128.7, 124.1, 118.2, 115.0, 112.5, 82.9, 55.3, 45.7, 27.8, 25.1, 23.4; ^{77}Se NMR (76 MHz, $CDCl_3$) δ: 364.1; IR (solid): $\tilde{\nu}$ = 2977, 1610, 1249, 764 cm^{-1}; m.p. (°C) = 142.4–142.9; HRMS (APPI$^+$): Calcd. for $C_{22}H_{21}O_4Se$ [M + H]$^+$ 429.0600, found 429.0602.

2,2-Dimethyl-3-(*p*-tolylselanyl)-3,4-dihydro-2*H*-benzo[*h*]chromene-5,6-dione (3e): The general electrosynthesis procedure was followed by using quinone **1** (48.4 mg, 0.2 mmol) and diselenide **2e** (68.0 mg, 0.2 mmol) as starting materials. Purification by column chromatography on silica gel (*n*-hexane/EtOAc, 4:1) yielded **3e** (65.8 mg, 80 %) as an orange solid. ^{1}H NMR (400 MHz, $CDCl_3$) δ: 8.05 (d, J = 8.4 Hz, 1H), 7.78 (d, J = 7.6 Hz, 1H), 7.65 (t, J = 7.6 Hz, 1H), 7.54–7.49 (m, 3H), 7.08 (d, J = 7.9 Hz, 2H), 3.35 (dd, J = 9.5, 5.6 Hz, 1H), 3.08 (dd, J = 18.0, 5.6 Hz, 1H), 2.72 (dd, J = 18.0, 9.6 Hz, 1H), 2.32 (s, 3H), 1.68 (s, 3H), 1.54 (s, 3H); ^{13}C NMR (100 MHz, $CDCl_3$) δ = –179.5, 178.0, 161.5, 138.6, 135.6, 134.8, 132.1, 130.9, 130.2, 130.1, 128.7, 124.6, 124.1, 112.5, 83.0, 45.6, 27.8, 25.2, 23.4, 21.2; ^{77}Se NMR (76 MHz, $CDCl_3$) δ: 370.3; IR (solid): $\tilde{\nu}$ = 2980, 1607, 1306, 810 cm^{-1}; m.p. (°C) = 190.8–191.3; HRMS (APPI$^+$): Calcd. for $C_{22}H_{21}O_3Se$ [M + H]$^+$ 413.0650, found 413.0658. *The structure of the product was also confirmed by X-ray diffraction* (CCDC number = 1966511).

2,2-Dimethyl-3-(naphthalen-1-ylselanyl)-3,4-dihydro-2*H*-benzo[*h*]chromene-5,6-dione (3f): The general electrosynthesis procedure was followed by using quinone **1** (48.4 mg, 0.2 mmol) and diselenide **2f** (82.4 mg, 0.2 mmol) as starting materials. Purification by column chromatography on silica gel (*n*-hexane/EtOAc, 4:1) yielded **3f** (81.4 mg, 91 %) as an orange solid. ^{1}H NMR (400 MHz, $CDCl_3$) δ: 8.46 (d, J = 8.4 Hz, 1H), 8.03 (d, J = 8.6 Hz, 1H), 7.93 (d, J = 7.1 Hz, 1H), 7.84 (t, J = 8.4 Hz, 2H), 7.74 (d, J = 7.2 Hz, 1H), 7.64–7.47 (m, 4H), 7.38 (t, J = 7.6 Hz, 1H), 3.42 (dd, J = 9.2, 5.6 Hz, 1H), 3.05 (dd, J = 18.0, 5.6 Hz, 1H), 2.77 (dd, J = 18.0, 9.3 Hz, 1H), 1.65 (s, 3H), 1.63 (s, 3H); ^{13}C NMR (100 MHz, $CDCl_3$) δ: 179.4, 178.0, 161.4, 135.9, 134.8, 134.2, 132.1, 130.9, 130.1, 130.0, 128.9, 128.7, 127.9, 127.2, 126.4, 125.9, 124.1, 112.4, 82.9, 45.3, 27.7, 25.2, 23.5; ^{77}Se NMR (76 MHz, $CDCl_3$) δ: 304.4; IR (solid): $\tilde{\nu}$ = 2981, 1607, 1568, 1384, 775 cm^{-1}; m.p. (°C) = 143.4–144.0; HRMS (APPI$^+$): Calcd. for $C_{25}H_{21}O_3Se$ [M + H]$^+$ 449.0650, found 449.0650.

3-(Benzylselanyl)-2,2-dimethyl-3,4-dihydro-2*H*-benzo[*h*]chromene-5,6-dione (3g): The general electrosynthesis procedure was followed by using quinone **1** (48.4 mg, 0.2 mmol) and diselenide **2g** (68.0 mg, 0.2 mmol) as starting materials. Purification by column chromatography on silica gel (*n*-hexane/EtOAc, 4:1) yielded **3g** (63.3 mg, 77 %) as deep orange crystals. ^{1}H NMR (400 MHz, $CDCl_3$) δ: 8.06 (d, J = 8.5 Hz, 1H), 7.77 (d, J = 7.7 Hz, 1H), 7.65 (t, J = 8.3 Hz, 1H), 7.52 (t, J = 8.1 Hz, 1H), 7.38–7.18 (m, 5H), 3.95 (s, 2H), 3.06 (dd, J = 17.5, 5.5 Hz, 1H), 2.92 (dd, J = 10.3, 5.5 Hz, 1H), 2.69 (dd, J = 17.5, 10.4 Hz, 1H), 1.60 (s, 3H), 1.43 (s, 3H); ^{13}C NMR (100 MHz, $CDCl_3$) δ: 179.5, 178.0, 161.5, 138.2, 134.8, 132.1, 130.9, 130.1, 129.0, 128.7, 128.7, 127.2, 124.1, 112.7, 83.2, 40.2, 28.6, 27.7, 25.5, 22.9; ^{77}Se NMR (76 MHz, $CDCl_3$) δ: 336.4; IR (solid): $\tilde{\nu}$ = 2980, 1603, 1571, 1387, 697 cm^{-1}; m.p. (°C) = 134.0–135.1; HRMS (APPI$^+$): Calcd. for $C_{22}H_{21}O_3Se$ [M + H]$^+$ 413.0650, found 413.0650. *The structure of the product was also confirmed by X-ray diffraction* (CCDC number = 1966512).

2,2-Dimethyl-3-(thiophen-2-ylselanyl)-3,4-dihydro-2*H*-benzo[*h*]chromene-5,6-dione (3h): The general electrosynthesis procedure was followed by using quinone **1** (48.4 mg, 0.2 mmol) and diselenide **2h** (64.8 mg, 0.2 mmol) as starting materials. Purification by column chromatography on silica gel (*n*-hexane/EtOAc, 4:1) yielded **3h** (50.8 mg, 63 %) as an orange solid. ^{1}H NMR (400 MHz, $CDCl_3$) δ: 8.06 (d, J = 8.2 Hz, 1H), 7.79 (d, J = 7.6 Hz, 1H), 7.66 (t, J = 7.6 Hz, 1H), 7.52 (t, J = 7.5 Hz, 1H), 7.41 (d, J = 5.3 Hz, 1H), 7.25 (d, J = 4.2 Hz, 1H), 6.98 (dd, J = 5.3, 3.6 Hz, 1H), 3.35 (dd, J = 9.0, 5.6 Hz, 1H), 3.06 (dd, J = 18.0, 5.6 Hz, 1H), 2.73 (dd, J = 18.0, 9.0 Hz, 1H), 1.70 (s, 3H), 1.56 (s, 3H); ^{13}C NMR (100 MHz, $CDCl_3$) δ: 179.4, 178.0, 161.4, 137.7, 134.9, 132.3, 132.1, 130.9, 130.1, 128.7, 128.4, 124.2, 121.6, 112.2, 82.4, 47.5, 27.6, 24.7, 23.5; ^{77}Se NMR (76 MHz, $CDCl_3$) δ: 271.3; IR (solid): $\tilde{\nu}$ = 2977, 1614, 1373, 729 cm^{-1}; m.p. (°C) = 144.5–145.7; HRMS (APPI$^+$): Calcd. for $C_{19}H_{17}O_3SSe$ [M + H]$^+$ 405.0058, found 405.0066.

2,2-Dimethyl-3-((3-(trifluoromethyl)phenyl)selanyl)-3,4-dihydro-2*H* benzo[*h*]chromene-5,6-dione (3i): The general electrosynthesis procedure was followed by using quinone **1** (48.4 mg, 0.2 mmol) and diselenide **2i** (89.6 mg, 0.2 mmol) as starting materials. Purification by column chromatography on silica gel (*n*-hexane/EtOAc, 4:1) yielded **3i** (80.0 mg, 86 %) as an orange oil. ^{1}H NMR (400 MHz, $CDCl_3$) δ: 8.06 (d, J = 7.6 Hz, 1H), 7.85 (s, 1H), 7.79 (d, J = 7.7 Hz, 2H), 7.66 (t, J = 8.0 Hz, 1H), 7.54 (q, J = 8.1, 7.4 Hz, 2H), 7.42 (t, J = 7.7 Hz, 1H), 3.49 (dd, J = 9.3, 5.6 Hz, 1H), 3.13 (dd, J = 18.0, 5.6 Hz, 1H), 2.77 (dd, J = 18.0, 9.4 Hz, 1H), 1.68 (s, 3H), 1.57 (s, 3H); ^{13}C NMR (100 MHz, $CDCl_3$) δ: 179.3, 178.0, 161.5, 138.1, 134.9, 131.9, 131.2 (q, J = 3.8 Hz), 131.0, 130.1, 129.7, 129.6, 128.8, 125.1 (q, J = 3.8 Hz), 124.2, 82.6, 46.1, 27.7, 25.4, 23.5; ^{77}Se NMR (76 MHz, $CDCl_3$) δ: 386.6; IR (solid): $\tilde{\nu}$ = 2991, 1610, 1323, 1122, 697 cm^{-1}; HRMS (APPI$^+$): Calcd. for $C_{22}H_{18}F_3O_3Se$ [M + H]$^+$ 467.0368, found 467.0378.

Characterization Data of Products 5a–i.

2-((Phenylselanyl)methyl)-2,3-dihydronaphtho[1,2-*b*]furan-4,5-dione (5a): The general electrosynthesis procedure was followed by using quinone **4** (48.4 mg, 0.2 mmol) and diselenide **2a** (62.4 mg, 0.2 mmol) as starting materials. Purification by column chromatography on silica gel (*n*-hexane/EtOAc, 3:1) yielded **5a** (48.7 mg, 66 %) as red crystals. ^{1}H NMR (400 MHz, $CDCl_3$) δ: 8.05 (d, J = 8.6 Hz, 1H), 7.66–7.53 (m, 4H), 7.43 (d, J = 7.0 Hz, 1H), 7.27–7.24 (m, 3H), 5.41–5.14 (m, 1H), 3.40–3.19 (m, 3H), 2.97 (dd, J = 15.6, 6.9 Hz, 1H); ^{13}C NMR (100 MHz, $CDCl_3$) δ: 181.0, 175.4, 169.4, 134.5, 133.6, 132.0, 130.6, 129.4, 129.3, 128.6, 127.8, 127.3, 124.6, 115.1, 86.7, 32.4, 32.2; ^{77}Se NMR (76 MHz, $CDCl_3$) δ: 262.8; IR (solid): $\tilde{\nu}$ = 2984, 1614, 1323, 1129, 698 cm^{-1}; m.p. (°C) = 117.6–118.4; HRMS (APPI$^+$): Calcd. for $C_{19}H_{15}O_3Se$ [M + H]$^+$ 371.0181, found 371.0187. *The structure of the product was also confirmed by X-ray diffraction* (CCDC number = 1966513).

2-(((4-Chlorophenyl)selanyl)methyl)-2,3-dihydronaphtho[1,2-*b*]furan-4,5-dione (5b): The general electrosynthesis procedure was followed by using quinone **4** (48.4 mg, 0.2 mmol) and diselenide **2b** (76.2 mg, 0.2 mmol) as starting materials. Purification

by column chromatography on silica gel (*n*-hexane/EtOAc, 3:1) yielded **5b** (51.6 mg, 64 %) as red crystals. ^{1}H NMR (400 MHz, $CDCl_3$) δ: 8.05 (d, *J* = 8.6 Hz, 1H), 7.63–7.55 (m, 2H), 7.48 (d, *J* = 8.4 Hz, 2H), 7.34 (d, *J* = 7.1 Hz, 1H), 7.19 (d, *J* = 8.4 Hz, 2H), 5.34–5.27 (m, 1H), 3.36–3.24 (m, 3H), 2.98 (dd, *J* = 15.6, 6.8 Hz, 1H); ^{13}C NMR (100 MHz, $CDCl_3$) δ: 181.0, 175.3, 169.3, 134.9, 134.5, 134.1, 132.0, 130.6, 129.5, 129.4, 127.2, 126.9, 124.5, 115.0, 86.5, 32.8, 32.2; ^{77}Se NMR (76 MHz, $CDCl_3$) δ: 260.1; IR (solid): $\tilde{\nu}$ = 2920, 1614, 1408, 1246, 807 cm^{-1}; m.p. (°C) = 136.3–137.4; HRMS (APPI$^+$): Calcd. for $C_{19}H_{14}ClO_3Se$ [M + H]$^+$ 404.9791, found 404.9782. *The structure of the product was also confirmed by X-ray diffraction* (CCDC number = 1966514).

2-(((4-Fluorophenyl)selanyl)methyl)-2,3-dihydronaphtho[1,2-*b*]-furan-4,5-dione (5c): The general electrosynthesis procedure was followed by using quinone **4** (48.4 mg, 0.2 mmol) and diselenide **2c** (69.6 mg, 0.2 mmol) as starting materials. Purification by column chromatography on silica gel (*n*-hexane/EtOAc, 3:1) yielded **5c** (57.3 mg, 74 %) as red crystals. ^{1}H NMR (400 MHz, $CDCl_3$) δ: 8.07 (d, *J* = 7.1 Hz, 1H), 7.64–7.54 (m, 4H), 7.42 (d, *J* = 7.0 Hz, 1H), 6.95 (t, *J* = 8.7 Hz, 2H), 5.31–5.24 (m, 1H), 3.37–3.17 (m, 3H), 2.98 (dd, *J* = 15.6, 6.9 Hz, 1H); ^{13}C NMR (100 MHz, $CDCl_3$) δ: 181.0, 175.3, 169.4, 162.7(d, *J* = 249.7 Hz), 136.2 (d, *J* = 8.0 Hz), 134.4, 132.0, 130.6, 129.5, 127.3, 124.5, 123.1 (d, *J* = 3.6 Hz), 116.5 (d, *J* = 21.6 Hz), 115.0, 86.6, 33.2, 32.2; IR (solid): $\tilde{\nu}$ = 3058, 1699, 1610, 1228, 892 cm^{-1}; m.p. (°C) = 183.4–184.1; HRMS (APPI$^+$): Calcd. for $C_{19}H_{14}FO_3Se$ [M + H]$^+$ 389.0087, found 389.0084. *The structure of the product was also confirmed by X-ray diffraction* (CCDC number = 1966515).

2-(((4-Methoxyphenyl)selanyl)methyl)-2,3-dihydronaphtho-[1,2-*b*]furan-4,5-dione (5d): The general electrosynthesis procedure was followed by using quinone **4** (48.4 mg, 0.2 mmol) and diselenide **2d** (74.4 mg, 0.2 mmol) as starting materials. Purification by column chromatography on silica gel (*n*-hexane/EtOAc, 3:1) yielded **5d** (46.3 mg, 58 %) as red crystals. ^{1}H NMR (400 MHz, $CDCl_3$) δ: 8.06 (d, *J* = 8.6 Hz, 1H), 7.63–7.55 (m, 2H), 7.52 (d, *J* = 8.8 Hz, 2H), 7.46 (d, *J* = 7.1 Hz, 1H), 6.79 (d, *J* = 8.8 Hz, 2H), 5.31–5.17 (m, 1H), 3.78 (s, 3H), 3.34–3.21 (m, 2H), 3.13 (dd, *J* = 13.0, 7.0 Hz, 1H), 2.98 (dd, *J* = 15.6, 6.9 Hz, 1H); ^{13}C NMR (100 MHz, $CDCl_3$) δ: 181.1, 175.4, 169.5, 159.8, 136.3, 134.4, 131.9, 130.7, 129.4, 127.4, 124.6, 118.4, 115.1, 115.0, 86.8, 55.3, 33.1, 32.1; ^{77}Se NMR (76 MHz, $CDCl_3$) δ: 251.5; IR (solid): $\tilde{\nu}$ = 2923, 1656, 1614, 1249, 771 cm^{-1}; m.p. (°C) = 140.3–141.0; HRMS (APPI$^+$): Calcd. for $C_{20}H_{17}O_4Se$ [M + H]$^+$ 401.0287, found 401.0284.

2-((*p*-Tolylselanyl)methyl)-2,3-dihydronaphtho[1,2-*b*]furan-4,5-dione (5e): The general electrosynthesis procedure was followed by using quinone **4** (48.4 mg, 0.2 mmol) and diselenide **2e** (68.0 mg, 0.2 mmol) as starting materials. Purification by column chromatography on silica gel (*n*-hexane/EtOAc, 3:1) yielded **5e** (48.3 mg, 63 %) as red crystals. ^{1}H NMR (400 MHz, $CDCl_3$) δ: 8.06 (d, *J* = 7.2 Hz, 1H), 7.58 (p, *J* = 7.5 Hz, 2H), 7.47–7.44 (m, 3H), 7.06 (d, *J* = 7.9 Hz, 2H), 5.25 (dt, *J* = 12.3, 6.1 Hz, 1H), 3.39–3.22 (m, 2H), 3.18 (dd, *J* = 13.0, 7.0 Hz, 1H), 2.98 (dd, *J* = 15.6, 6.9 Hz, 1H), 2.31 (s, 3H); ^{13}C NMR (100 MHz, $CDCl_3$) δ: 181.1, 175.4, 169.5, 138.0, 134.4, 134.1, 131.9, 130.7, 130.1, 129.4, 127.4, 124.7, 124.6, 115.1, 86.8, 32.6, 32.2, 21.1; ^{77}Se NMR (76 MHz, $CDCl_3$) δ: 255.2; IR (solid): $\tilde{\nu}$ = 2923, 1656, 1617, 1249, 771 cm^{-1}; m.p. (°C) = 89.3–90.2; HRMS (APPI$^+$): Calcd. for $C_{20}H_{17}O_3Se$ [M + H]$^+$ 385.0338, found 385.0337.

2-((Naphthalen-1-ylselanyl)methyl)-2,3-dihydronaphtho[1,2-*b*]-furan-4,5-dione (5f): The general electrosynthesis procedure was followed by using quinone **4** (48.4 mg, 0.2 mmol) and diselenide **2f** (82.4 mg, 0.2 mmol) as starting materials. Purification by column chromatography on silica gel (*n*-hexane/EtOAc, 3:1) yielded **5f** (57.0 mg, 68 %) as red crystals. ^{1}H NMR (400 MHz, $CDCl_3$) δ: 8.42 (d, *J* = 8.3 Hz, 1H), 7.97 (dd, *J* = 5.7, 3.2 Hz, 1H), 7.90 (d, *J* = 7.1 Hz, 1H), 7.77 (d, *J* = 8.1 Hz, 2H), 7.60–7.42 (m, 4H), 7.41–7.30 (t, *J* = 7.6 Hz, 1H), 7.16 (dd, *J* = 5.7, 3.1 Hz, 1H), 5.32–5.13 (m, 1H), 3.44–3.18 (m, 3H), 3.06 (dd, *J* = 15.6, 6.9 Hz, 1H); ^{13}C NMR (100 MHz, $CDCl_3$) δ: 181.0, 175.3, 169.4, 134.5, 134.3, 134.3, 134.0, 131.8, 130.5, 129.4, 129.3, 128.7, 127.9, 127.7, 127.1, 127.1, 126.4, 125.7, 124.4, 115.0, 86.7, 32.8, 32.1; ^{77}Se NMR (76 MHz, $CDCl_3$) δ: 192.7; IR (solid): $\tilde{\nu}$ = 3054, 1653, 1614, 1405, 771 cm^{-1}; m.p. (°C) = 75.6–76.3; HRMS (APPI$^+$): Calcd. for $C_{23}H_{17}O_3Se$ [M + H]$^+$ 421.0337, found 421.0340.

2-((Benzylselanyl)methyl)-2,3-dihydronaphtho[1,2-*b*]furan-4,5-dione (5g): The general electrosynthesis procedure was followed by using quinone **4** (48.4 mg, 0.2 mmol) and diselenide **2g** (68.0 mg, 0.2 mmol) as starting materials. Purification by column chromatography on silica gel (*n*-hexane/EtOAc, 3:1) yielded **5g** (32.2 mg, 42 %) as a red solid. ^{1}H NMR (400 MHz, $CDCl_3$) δ: 8.07 (d, *J* = 7.5 Hz, 1H), 7.67–7.56 (m, 3H), 7.41–7.16 (m, 5H), 5.19 (dq, *J* = 12.6, 6.8 Hz, 1H), 3.89 (s, 2H), 3.23 (dd, *J* = 15.6, 9.9 Hz, 1H), 2.89 (qd, *J* = 15.2, 14.1, 6.3 Hz, 3H); ^{13}C NMR (100 MHz, $CDCl_3$) δ: 181.0, 175.3, 169.3, 138.5, 134.6, 132.0, 130.7, 129.5, 128.9, 128.7, 127.4, 127.2, 124.5, 115.2, 87.2, 32.4, 28.2, 28.1; ^{77}Se NMR (76 MHz, $CDCl_3$) δ: 223.5; IR (solid): $\tilde{\nu}$ = 2923, 1656, 1614, 1408, 697 cm^{-1}; m.p. (°C) = 127.9–128.4; HRMS (APPI$^+$): Calcd. for $C_{20}H_{17}O_3Se$ [M + H]$^+$ 385.0337, found 385.0339.

2-((Thiophen-2-ylselanyl)methyl)-2,3-dihydronaphtho[1,2-*b*]-furan-4,5-dione (5h): The general electrosynthesis procedure was followed by using quinone **4** (48.4 mg, 0.2 mmol) and diselenide **2h** (64.8 mg, 0.2 mmol) as starting materials. Purification by column chromatography on silica gel (*n*-hexane/EtOAc, 3:1) yielded **5h** (63.0 mg, 84 %) as an orange solid. ^{1}H NMR (400 MHz, $CDCl_3$) δ: 8.07 (d, *J* = 8.3 Hz, 1H), 7.71–7.53 (m, 3H), 7.41 (dd, *J* = 4.3, 1.1 Hz, 1H), 7.26 (dd, *J* = 3.5, 1.1 Hz, 1H), 6.98 (dd, *J* = 5.3, 3.5 Hz, 1H), 5.44–5.13 (m, 1H), 3.40–3.22 (m, 2H), 3.09 (dd, *J* = 12.9, 7.0 Hz, 1H), 2.96 (dd, *J* = 15.7, 7.0 Hz, 1H); ^{13}C NMR (100 MHz, $CDCl_3$) δ: 181.0, 175.4, 169.5, 136.6, 134.5, 132.0, 131.6, 130.7, 129.5, 128.3, 127.4, 124.6, 122.0, 115.0, 86.4, 35.3, 32.1; ^{77}Se NMR (76 MHz, $CDCl_3$) δ: 177.0; IR (solid): $\tilde{\nu}$ = 3079, 1649, 1575, 1238, 718 cm^{-1}; m.p. (°C) = 143.6–144.7; HRMS (APPI$^+$): Calcd. for $C_{17}H_{13}O_3SSe$ [M + H]$^+$ 376.9745, found 376.9750.

2-(((3-(Trifluoromethyl)phenyl)selanyl)methyl)-2,3-dihydro-naphtho[1,2-*b*]furan-4,5-dione (5i): The general electrosynthesis procedure was followed by using quinone **4** (48.4 mg, 0.2 mmol) and diselenide **2i** (89.6 mg, 0.2 mmol) as starting materials. Purification by column chromatography on silica gel (*n*-hexane/EtOAc, 3:1) yielded **5i** (66.4 mg, 67 %) as an orange solid. ^{1}H NMR (400 MHz, $CDCl_3$) δ: 8.11–8.01 (m, 1H), 7.82 (s, 1H), 7.73 (d, *J* = 7.7 Hz, 1H), 7.57 (td, *J* = 6.7, 5.6, 3.9 Hz, 2H), 7.49 (d, *J* = 7.8 Hz, 1H), 7.42–7.29 (m, 2H), 5.48–5.30 (m, 1H), 3.39 (d, *J* = 5.8 Hz, 2H), 3.31 (dd, *J* = 15.6, 10.0 Hz, 1H), 3.00 (dd, *J* = 15.6, 6.9 Hz, 1H); ^{13}C NMR (100 MHz, $CDCl_3$) δ: 180.9, 175.3, 169.3, 136.4, 134.5, 132.0, 131.7, 131.4, 130.6, 130.1, 129.6 (q, *J* = 4.0 Hz), 129.5, 127.1, 124.9, 124.4 (q, *J* = 3.6 Hz), 122.2, 115.0, 86.3, 32.7, 32.3; ^{77}Se NMR (76 MHz, $CDCl_3$) δ: 269.8; IR (solid): $\tilde{\nu}$ = 2931, 1656, 1621, 1331, 697 cm^{-1}; m.p. (°C) = 94.5–95.3; HRMS (APPI$^+$): Calcd. for $C_{20}H_{14}F_3O_3Se$ [M + H]$^+$ 439.0055, found 439.0051.

Characterization Data of Products 7a–i.

2-Phenyl-3-(phenylselanyl)-3,4-dihydro-2*H*-benzo[*h*]chromene-5,6-dione (7a): The general electrosynthesis procedure was followed by using quinone **6** (58.0 mg, 0.2 mmol) and diselenide **2a** (62.4 mg, 0.2 mmol) as starting materials. Purification by column chromatography on silica gel (*n*-hexane/EtOAc, 3:1) yielded **7a** (62.3 mg, 70 %) as an orange solid. ^{1}H NMR (400 MHz, $CDCl_3$) δ: 8.09 (d, *J* = 7.5 Hz, 1H), 7.77 (d, *J* = 7.2 Hz, 1H), 7.62 (t, *J* = 7.6 Hz, 1H), 7.53 (t, *J* = 7.5 Hz, 1H), 7.42–7.34 (m, 5H), 7.34–7.25 (m, 4H),

7.20 (t, J = 7.3 Hz, 2H), 5.35 (d, J = 7.7 Hz, 1H), 3.73 (td, J = 8.2, 5.3 Hz, 1H), 3.00 (dd, J = 17.8, 5.3 Hz, 1H), 2.73 (dd, J = 17.7, 8.5 Hz, 1H); ^{13}C NMR (100 MHz, $CDCl_3$) δ: 179.3, 178.1, 162.2, 137.6, 135.8, 135.0, 131.6, 131.1, 130.1, 129.2, 129.1, 128.9, 128.7, 128.5, 127.0, 126.8, 124.3, 113.1, 83.7, 39.6, 24.8; ; ^{77}Se NMR (76 MHz, $CDCl_3$) δ: 384.2; IR (solid): $\tilde{\nu}$ = 2923, 1600, 1621, 1391, 930 cm^{-1}; m.p. (°C) = 130.5–132.9; HRMS (APPI$^+$): Calcd. for $C_{25}H_{18}O_3SeNa$ [M + Na]$^+$ 469.0315, found 469.0318.

3-((4-Chlorophenyl)selanyl)-2-phenyl-3,4-dihydro-2*H*-benzo[*h*]chromene-5,6-dione (7b): The general electrosynthesis procedure was followed by using quinone **6** (58.0 mg, 0.2 mmol) and diselenide **2b** (76.2 mg, 0.2 mmol) as starting materials. Purification by column chromatography on silica gel (*n*-hexane/EtOAc, 3:1) yielded **7b** (57.5 mg, 60 %) as an orange solid. ^{1}H NMR (400 MHz, $CDCl_3$) δ: 8.09 (d, J = 7.6 Hz, 1H), 7.75 (d, J = 7.6 Hz, 1H), 7.62 (t, J = 7.6 Hz, 1H), 7.53 (t, J = 7.2 Hz, 1H), 7.38–7.34 (m, 3H), 7.29–7.25 (m, 4H), 7.14 (d, J = 8.4 Hz, 2H), 5.32 (d, J = 8.0 Hz, 1H), 3.69 (td, J = 8.6, 5.3 Hz, 1H), 3.04 (dd, J = 17.7, 5.3 Hz, 1H), 2.71 (dd, J = 17.7, 8.9 Hz, 1H); ^{13}C NMR (100 MHz, $CDCl_3$) δ: 179.2, 178.1, 162.3, 137.3, 137.1, 135.0, 135.0, 131.5, 131.1, 130.0, 129.3, 129.2, 129.0, 128.7, 126.9, 125.3, 124.3, 113.0, 83.9, 40.2, 25.1; ^{77}Se NMR (76 MHz, $CDCl_3$) δ: 377.5; IR (solid): $\tilde{\nu}$ = 2923, 1614, 1398, 1256, 775 cm^{-1}; m.p. (°C) = 152.1–154.2; HRMS (APPI$^+$): Calcd. for $C_{25}H_{18}ClO_3Se$ [M + H]$^+$ 481.0104, found 481.0099.

3-((4-Fluorophenyl)selanyl)-2-phenyl-3,4-dihydro-2*H*-benzo[*h*]chromene-5,6-dione (7c): The general electrosynthesis procedure was followed by using quinone **6** (58.0 mg, 0.2 mmol) and diselenide **2c** (69.6 mg, 0.2 mmol) as starting materials. Purification by column chromatography on silica gel (*n*-hexane/EtOAc, 3:1) yielded **7c** (64.8 mg, 70 %) as an orange solid. ^{1}H NMR (400 MHz, $CDCl_3$) δ: 8.08 (dd, J = 7.6, 1.2 Hz, 1H), 7.75 (d, J = 7.8 Hz, 1H), 7.61 (td, J = 7.6, 1.4 Hz, 1H), 7.52 (td, J = 7.5, 1.2 Hz, 1H), 7.40–7.28 (m, 7H), 6.87 (t, J = 8.7 Hz, 2H), 5.30 (d, J = 7.5 Hz, 1H), 3.65 (td, J = 8.9, 5.3 Hz, 1H), 3.03 (dd, J = 17.7, 5.3 Hz, 1H), 2.69 (dd, J = 17.7, 9.0 Hz, 1H); ^{13}C NMR (100 MHz, $CDCl_3$) δ: 179.2, 178.1, 163.1 (d, J = 249.3 Hz), 162.3, 138.1 (d, J = 8.2 Hz), 137.4, 135.0, 131.6, 131.1, 130.0, 129.2, 128.9, 128.7, 127.0, 124.3, 121.7 (d, J = 3.6 Hz), 116.3 (d, J = 21.6 Hz), 113.0, 83.9, 40.2, 25.1; ^{77}Se NMR (76 MHz, $CDCl_3$) δ: 373.2; IR (solid): $\tilde{\nu}$ = 2916, 1600, 1394, 1221, 831 cm^{-1}; m.p. (°C) = 153.2–154.1; HRMS (APPI$^+$): Calcd. for $C_{25}H_{18}FO_3Se$ [M + H]$^+$ 465.0400, found 465.0399.

3-((4-Methoxyphenyl)selanyl)-2-phenyl-3,4-dihydro-2*H*-benzo[*h*]chromene-5,6-dione (7d): The general electrosynthesis procedure was followed by using quinone **6** (58.0 mg, 0.2 mmol) and diselenide **2d** (74.4 mg, 0.2 mmol) as starting materials. Purification by column chromatography on silica gel (*n*-hexane/EtOAc, 3:1) yielded **7d** (59.9 mg, 63 %) as an orange solid. ^{1}H NMR (400 MHz, $CDCl_3$) δ: 8.12 (d, J = 8.8 Hz, 1H), 8.07 (d, J = 8.9 Hz, 1H), 7.75–7.68 (m, 2H), 7.42 (d, J = 8.7 Hz, 2H), 7.38–7.32 (m, 3H), 7.31–7.27 (m, 2H), 6.77 (d, J = 8.7 Hz, 2H), 5.32 (d, J = 6.8 Hz, 1H), 3.77 (s, 3H), 3.75–3.61 (m, 1H), 2.92 (dd, J = 18.9, 5.5 Hz, 1H), 2.81 (dd, J = 18.9, 7.2 Hz, 1H); ^{13}C NMR (100 MHz, $CDCl_3$) δ: 183.7, 179.0, 160.3, 154.5, 138.3, 137.9, 134.0, 133.2, 132.0, 131.0, 128.8, 128.7, 126.5, 126.4, 126.1, 120.4, 117.0, 114.9, 82.4, 55.3, 55.2, 38.7, 24.5; ^{77}Se NMR (76 MHz, $CDCl_3$) δ: 374.8; IR (solid): $\tilde{\nu}$ = 2926, 1603, 1295, 1210, 777 cm^{-1}; m.p. (°C) = 73.2–74.0; HRMS (APPI$^+$): Calcd. for $C_{26}H_{21}O_4Se$ [M + H]$^+$ 477.0600, found 477.0595.

2-Phenyl-3-(*p*-tolylselanyl)-3,4-dihydro-2*H*-benzo[*h*]chromene-5,6-dione (7e): The general electrosynthesis procedure was followed by using quinone **6** (58.0 mg, 0.2 mmol) and diselenide **2e** (68.0 mg, 0.2 mmol) as starting materials. Purification by column chromatography on silica gel (*n*-hexane/EtOAc, 3:1) yielded **7e** (59.7 mg, 65 %) as an orange solid. ^{1}H NMR (400 MHz, $CDCl_3$) δ: 8.07 (d, J = 7.1 Hz, 1H), 7.76 (d, J = 7.7 Hz, 1H), 7.61 (t, J = 8.1 Hz, 1H), 7.52 (t, J = 7.2 Hz, 1H), 7.40–7.34 (m, 3H), 7.34–7.26 (m, 4H), 7.01 (d, J = 7.9 Hz, 2H), 5.34 (d, J = 7.6 Hz, 1H), 3.72–3.61 (m, 1H), 2.94 (dd, J = 17.8, 5.3 Hz, 1H), 2.71 (dd, J = 17.8, 8.3 Hz, 1H), 2.30 (s, 3H); ^{13}C NMR (100 MHz, $CDCl_3$) δ: 179.3, 178.1, 162.1, 138.8, 137.8, 136.3, 135.0, 131.7, 131.0, 130.1, 130.0, 129.0, 128.9, 128.7, 126.7, 124.3, 123.1, 113.1, 83.6, 39.2, 24.6, 21.2; IR (solid): $\tilde{\nu}$ = 2920, 1607, 1384, 1249, 771 cm^{-1}; m.p. (°C) = 137.2–140.3; HRMS (APPI$^+$): Calcd. for $C_{26}H_{21}O_3Se$ [M + H]$^+$ 461.0650, found 461.0659.

3-(Naphthalen-1-ylselanyl)-2-phenyl-3,4-dihydro-2*H*-benzo[*h*]chromene-5,6-dione (7f): The general electrosynthesis procedure was followed by using quinone **6** (58.0 mg, 0.2 mmol) and diselenide **2f** (82.4 mg, 0.2 mmol) as starting materials. Purification by column chromatography on silica gel (*n*-hexane/EtOAc, 3:1) yielded **7f** (71.3 mg, 72 %) as an orange solid. ^{1}H NMR (400 MHz, $CDCl_3$) δ: 8.32 (d, J = 9.0 Hz, 1H), 8.06 (dd, J = 7.6, 1.2 Hz, 1H), 7.78 (d, J = 7.6 Hz, 2H), 7.61–7.56 (m, 2H), 7.54–7.42 (m, 4H), 7.30–7.23 (m, 5H), 7.20–7.17 (m, 2H), 5.40 (d, J = 7.4 Hz, 1H), 3.77 (td, J = 7.9, 5.4 Hz, 1H), 2.95 (dd, J = 17.8, 5.4 Hz, 1H), 2.78 (dd, J = 17.8, 8.1 Hz, 1H); ^{13}C NMR (100 MHz, $CDCl_3$) δ: 179.2, 178.1, 162.2, 137.5, 136.2, 134.9, 134.0, 131.6, 131.0, 130.0, 130.0, 128.9, 128.9, 128.7, 128.7, 128.6, 128.0, 127.1, 126.9, 126.6, 126.3, 125.7, 124.3, 113.0, 83.8, 39.4, 24.7; ^{77}Se NMR (76 MHz, $CDCl_3$) δ: 309.7; IR (solid): $\tilde{\nu}$ = 2920, 1600, 1391, 1122, 619 cm^{-1}; m.p. (°C) = 142.3–144.1; HRMS (APPI$^+$): Calcd. for $C_{29}H_{21}O_3Se$ [M + H]$^+$ 497.0650, found 497.0650.

3-(Benzylselanyl)-2-phenyl-3,4-dihydro-2*H*-benzo[*h*]chromene-5,6-dione (7g): The general electrosynthesis procedure was followed by using quinone **6** (58.0 mg, 0.2 mmol) and diselenide **2g** (68.0 mg, 0.2 mmol) as starting materials. Purification by column chromatography on silica gel (*n*-hexane/EtOAc, 3:1) yielded **7g** (56.9 mg, 62 %) as an orange solid. ^{1}H NMR (400 MHz, $CDCl_3$) δ: 8.11 (d, J = 8.7 Hz, 1H), 7.79 (d, J = 7.6 Hz, 1H), 7.64 (t, J = 7.6 Hz, 1H), 7.55 (t, J = 7.6 Hz, 1H), 7.53–7.45 (m, 3H), 7.45–7.41 (m, 2H), 7.31–7.16 (m, 5H), 7.14 (d, J = 7.0 Hz, 2H), 5.25 (d, J = 9.1 Hz, 1H), 3.33–3.19 (m, 3H), 3.08 (dd, J = 17.6, 5.4 Hz, 1H), 2.64 (dd, J = 17.5, 10.2 Hz, 1H); ^{13}C NMR (100 MHz, $CDCl_3$) δ: 179.3, 178.1, 162.6, 137.9, 137.8, 135.0, 131.7, 131.1, 130.0, 129.2, 129.0, 128.7, 128.6, 127.4, 127.1, 124.3, 113.4, 85.0, 35.5, 28.0, 26.0; ^{77}Se NMR (76 MHz, $CDCl_3$) δ: 326.4; IR (solid): $\tilde{\nu}$ = 2948, 1632, 1295, 1201, 831 cm^{-1}; m.p. (°C) = 93.2–94.0; HRMS (APPI$^+$): Calcd. for $C_{26}H_{21}O_3Se$ [M + H]$^+$ 461.0650, found 461.0650.

2-Phenyl-3-(thiophen-2-ylselanyl)-3,4-dihydro-2*H*-benzo[*h*]chromene-5,6-dione (7h): The general electrosynthesis procedure was followed by using quinone **6** (58.0 mg, 0.2 mmol) and diselenide **2h** (64.8 mg, 0.2 mmol) as starting materials. Purification by column chromatography on silica gel (*n*-hexane/EtOAc, 3:1) yielded **7h** (70.4 mg, 78 %) as an orange solid. ^{1}H NMR (400 MHz, $CDCl_3$) δ: 8.09 (d, J = 8.6 Hz, 1H), 7.77 (d, J = 7.7 Hz, 1H), 7.62 (t, J = 7.7 Hz, 1H), 7.53 (t, J = 7.5 Hz, 1H), 7.46–7.40 (m, 4H), 7.38–7.32 (m, 2H), 7.10 (d, J = 4.5 Hz, 1H), 6.97 (dd, J = 5.3, 3.5 Hz, 1H), 5.33 (d, J = 7.9 Hz, 1H), 3.61 (td, J = 8.2, 5.3 Hz, 1H), 2.96 (dd, J = 17.8, 5.3 Hz, 1H), 2.72 (dd, J = 17.8, 8.5 Hz, 1H); ^{13}C NMR (100 MHz, $CDCl_3$) δ: 179.3, 178.1, 162.1, 138.4, 137.6, 135.0, 132.6, 131.6, 131.1, 130.0, 129.2, 129.0, 128.8, 128.4, 126.9, 124.3, 119.8, 113.0, 83.0, 40.6, 24.2; IR (solid): $\tilde{\nu}$ = 2920, 1607, 1384, 1253, 697 cm^{-1}; m.p. (°C) = 188.2–190.1; HRMS (APPI$^+$): Calcd. for $C_{23}H_{17}O_3SSe$ [M + H]$^+$ 453.0058, found 453.0056.

2-Phenyl-3-((3-(trifluoromethyl)phenyl)selanyl)-3,4-dihydro-2*H*-benzo[*h*]chromene-5,6-dione (7i): The general electrosynthesis procedure was followed by using quinone **6** (58.0 mg, 0.2 mmol) and diselenide **2i** (89.6 mg, 0.2 mmol) as starting materials. Purification by column chromatography on silica gel (*n*-hexane/EtOAc, 3:1)

yielded **7i** (65.7 mg, 64 %) as an orange solid. ^{1}H NMR (400 MHz, $CDCl_3$) δ: 8.10 (dd, J = 7.6, 1.2 Hz, 1H), 7.74 (d, J = 8.5 Hz, 1H), 7.61 (td, J = 7.6, 1.4 Hz, 1H), 7.55–7.45 (m, 4H), 7.34–7.23 (m, 6H), 5.31 (d, J = 8.5 Hz, 1H), 3.75 (td, J = 9.5, 5.4 Hz, 1H), 3.17 (dd, J = 17.7, 5.3 Hz, 1H), 2.73 (dd, J = 17.7, 9.6 Hz, 1H); ^{13}C NMR (100 MHz, $CDCl_3$) δ: 179.2, 178.1, 162.4, 138.5, 136.9, 135.0, 131.6 (q, J = 4.2 Hz), 131.5, 131.3 (q, J = 33.6 Hz) 131.2, 130.0, 129.4 (q, J = 3.5 Hz), 129.0, 128.6 (q, J = 3.1 Hz), 127.0, 125.0 (q, J = 4.0 Hz), 124.8, 124.3, 122.1, 112.9, 84.3, 40.8, 25.5; ^{77}Se NMR (76 MHz, $CDCl_3$) δ: 384.4; IR (solid): $\tilde{\nu}$ = 2920, 1596, 1391, 1125, 612 cm^{-1}; m.p. (°C) = 134.9–136.1; HRMS (APPI$^+$): Calcd. for $C_{26}H_{18}F_3O_3Se$ [M + H]$^+$ 515.0368, found 515.0366.

General procedure for the synthesis of compound 8: A 5 mL resealable reaction tube was charged with **3a** (79.4 mg, 0.2 mmol), sodium acetate (32.8 mg, 0.4 mmol) and $NH_2OH{\cdot}HCl$ (25.9 mg, 0.4 mmol). Methanol (2 mL) was added, and the mixture was refluxed for 12 hours, until TLC analysis revealed total consumption of **3a**. The mixture was extracted with EtOAc (3 × 5 mL) and the crude product was purified by FCC, under the conditions noted.

6-(Hydroxyimino)-2,2-dimethyl-3-(phenylselanyl)-2,3,4,6-tetrahydro-5*H*-benzo[*h*]chromen-5-one (8): Purification by column chromatography on silica gel (*n*-hexane 7:1 EtOAc) yielded **8** (49.4 mg, 60 %) as an yellow solid. ^{1}H NMR (400 MHz, $CDCl_3$) δ: 8.28 (d, J = 9.0 Hz, 1H), 7.90 (d, J = 9.0 Hz, 1H), 7.64 (d, J = 7.9 Hz, 2H), 7.58–7.45 (m, 2H), 7.37–7.26 (m, 3H), 3.46 (dd, J = 9.9, 5.6 Hz, 1H), 3.15 (dd, J = 17.7, 5.6 Hz, 1H), 2.78 (dd, J = 17.7, 9.9 Hz, 1H), 1.72 (s, 3H), 1.56 (s, 3H); ^{13}C NMR (100 MHz, $CDCl_3$) δ: 180.5, 163.4, 135.2, 130.9, 130.3, 129.4, 129.1, 128.4, 128.4, 125.2, 123.5, 122.6, 109.8, 83.1, 45.5, 27.9, 24.7, 23.2; ^{77}Se NMR (76 MHz, $CDCl_3$) δ: 379.9; IR (solid): $\tilde{\nu}$ = 2973, 1529, 1108, 895 cm^{-1}; m.p. (°C) 166.1–168.0; HRMS (APPI$^+$): Calcd. for $C_{21}H_{20}NO_3Se$ [M + H]$^+$ 414.0603, found 414.0602.

General procedure for the synthesis of compound 9: A 5 mL resealable reaction tube was charged with **3a** (79.4 mg, 0.2 mmol), 1,2-phenylenediamine (25.9 mg, 0.24 mmol) and methanol (6 mL). Then, the mixture was refluxed for 3 hours, until TLC analysis revealed total consumption of **3a**. The mixture was extracted with EtOAc (3 × 5 mL) and the crude product was purified by recrystallization.

3,3-Dimethyl-2-(phenylselanyl)-2,3-dihydro-1*H*-benzo[*a*]pyrano[2,3-*c*]phenazine (9): Purification by recrystallization (CH_2Cl_2/hexane) yielded 9 (67.5 mg, 72 %) as a yellow solid. ^{1}H NMR (400 MHz, $CDCl_3$) δ: 9.43–9.28 (m, 1H), 8.43–8.24 (m, 2H), 8.22 (d, J = 9.5 Hz, 1H), 7.85–7.74 (m, 4H), 7.74–7.66 (m, 2H), 7.35–7.25 (m, 3H), 3.98 (dd, J = 17.8, 5.6 Hz, 1H), 3.74 (dd, J = 9.9, 5.6 Hz, 1H), 3.52 (dd, J = 17.8, 10.0 Hz, 1H), 1.76 (s, 3H), 1.61 (s, 3H); ^{13}C NMR (100 MHz, $CDCl_3$) δ: 151.0, 143.9, 142.5, 140.3, 140.1, 134.6, 130.7, 129.9, 129.6, 129.6, 129.5, 129.2, 128.8, 128.3, 127.9, 127.8, 125.1, 122.2, 109.7, 80.0, 47.8, 28.1, 27.8; ^{77}Se NMR (76 MHz, $CDCl_3$) δ: 374.1; m.p. (°C) 174.9–176.1; IR (solid): $\tilde{\nu}$ = 2980, 1596, 1408, 1115, 739 cm^{-1}; HRMS (APPI$^+$): Calcd. for $C_{27}H_{23}N_2OSe$ [M + H]$^+$ 471.0976, found 471.0972.

General procedure for the synthesis of compound 10: A 5 mL resealable reaction tube was charged with **3a** (79.4 mg, 0.2 mmol) and phenylhydrazine hydrochloride (57.6 mg, 0.4 mmol). Then, EtOH (2 mL) and AcOH (6 drops) were added, and the mixture was refluxed for 2 hours, until TLC analysis revealed total consumption of **3a**. The mixture was extracted with EtOAc (3 × 5 mL) and the crude product was purified by recrystallization.

2,2-Dimethyl-6-(2-phenylhydrazono)-3-(phenylselanyl)-2,3,4,6-Tetrahydro-5*H*-benzo[*h*]chromen-5-one (10): Purification by recrystallization (CH_2Cl_2/hexane) yielded **10** (68.2 mg, 70 %) as an orange solid; ^{1}H NMR (400 MHz, $CDCl_3$) δ: 8.36 (d, J = 8.0 Hz, 1H), 7.90 (d, J = 7.9 Hz, 1H), 7.70–7.59 (m, 2H), 7.58–7.45 (m, 3H), 7.44–7.31 (m, 3H), 7.32–7.23 (m, 3H), 7.14 (t, J = 7.3 Hz, 1H), 3.49 (dd, J = 10.1, 5.6 Hz, 1H), 3.21 (dd, J = 17.6, 5.6 Hz, 1H), 2.84 (dd, J = 17.6, 10.1 Hz, 1H), 1.69 (s, 3H), 1.50 (s, 3H); ^{13}C NMR (100 MHz, $CDCl_3$) δ: 178.8, 159.2, 142.7, 135.0, 133.0, 129.5, 129.3, 129.0, 128.1, 127.8, 126.0, 124.9, 124.0, 122.7, 121.7, 116.2, 111.1, 81.0, 46.6, 28.1, 25.8, 22.8; ^{77}Se NMR (76 MHz, $CDCl_3$) δ: 378.7; IR (solid): $\tilde{\nu}$ = 2920, 1511, 1260, 1023, 750 cm^{-1}; m.p. (°C) 142.1–144.0; HRMS (APPI$^+$): Calcd. for $C_{27}H_{25}N_2O_2Se$ [M + H]$^+$ 489.1076, found 489.1076.

Biological activity. In vitro activity of compounds against bloodstream trypomastigotes of *T. cruzi*: All experiments dealing with animals were performed in accordance with the Brazilian Law 11.794/2008 and regulations of the National Council of Animal Experimentation Control under the license L038/2018 from the Ethics Committee for Animal Use of the Oswaldo Cruz Institute (CEUA/IOC). The mice were housed at a maximum of 6 individuals per cage, kept in a specific-pathogen-free (SPF) room at 20 to 22 °C under a 12/12 h light/dark cycle, 50 to 60 % humidity and provided sterilized water and chow ad libitum. For all the experiments stock solutions of the compounds were prepared in dimethyl sulfoxide, with the final concentration of the solvent in the experiments never exceeding 0.5 %, concentration known to exert no toxicity to the parasite or host cells.[27] Bloodstream trypomastigotes of Y strain[28] were obtained from infected Swiss Webster mice at the peak of parasitaemia by differential centrifugation process. The parasites (5 × 10^6 cells/mL) plus 5 % of blood were incubated for 24 h at 4 °C and 5 % CO_2 atmosphere in absence or presence of the compounds. Cell counts were performed in a Neubauer chamber, by light microscopy and the activity of the compounds was expressed as the IC_{50}/24 h, corresponding to the concentration that led to 50 % lysis of the parasites. At least three independent experiments were performed, and the mean and standard deviation were calculated. The standard drug Bz were used as control.

Determination of cytotoxicity – MTT assay: Cytotoxicity tests were performed against SNB-19 (Astrocytoma), HCT-116 (Colon Carcinoma – Human), PC3 (Prostate Carcinoma), B16F10 (Murine Melanoma), MCF-7 (Breast Carcinoma) were provided by the National Institute Cancer (USA), and L929 (Murine Fibroblast) from the Rio de Janeiro Cell Bank (BCRJ), and were grown in RPMI 1640 and Dulbecco's Modified Eagle Medium (DMEM (L929) medium supplemented with 10 % fetal bovine serum and 1 % antibiotics (100 U mL^{-1} penicillin and 100 μg mL^{-1} streptomycin) at 37 °C and atmosphere containing 5 % CO_2. The L929 cell line was used to evaluate the selectivity of compounds and doxorubicin was used as positive control. Samples were diluted in pure DMSO (dimethyl sulfoxide) for 2 mg mL^{-1}. Viability and metabolic status of the cell was performed by the MTT (3-(4,5-dimethyl-2-thiazolyl)-2,5-diphenyl-2*H*-tetrazoliumbromide) colorimetric method.[29] Cells were plated at concentrations of 0.7 × 10^5 cells/mL (HCT-116, B16F10 and L929) and 0.1 × 10^6 cells/mL (SNB-19, MCF-7 and PC3). Compounds were tested at maximum concentrations, varying according to molecular weight. Compound-treated plates were incubated for 72 hours in a 5 % CO_2 oven at 37 °C. At the end of treatment, the plates were centrifuged, and the supernatant removed. Then 100 μL of MTT (0.5 μg mL^{-1}) solution was added, and plates were incubated for 3 h. After incubation, the MTT solution was removed and the absorbance was read after dissolution of the precipitate with 100 μL of DMSO in the plate spectrophotometer (Multimode Detector, DTX 880, Beckman Coulter) at 595 nm.

Statistical analysis of data activity: All experiments were performed in duplicate and repeated three times. For all compounds, the selectivity index (SI, Table S1) was calculated corresponds to

the division between the IC_{50} value of each test compound in the L929 non-tumor cell line and the IC_{50} value of each compound in the tumor cell line (SI = IC_{50} L929/IC_{50} neoplastic cells).[30] The results were analyzed according to the mean ± standard deviation of the mean of the percentage of inhibition of cell growth using the GraphPad Prism™ 5.0 program.

CCDC 1966510 (for **3c**), 1966511 (for **3e**), 1966512 (for **3g**), 1966513 (for **5a**), 1966514 (for **5b**), 1966515 (for **5c**) contain the supplementary crystallographic data for this paper. These data can be obtained free of charge from The Cambridge Crystallographic Data Centre.

Conflict of interest

The authors declare no conflict of interest.

Acknowledgments

This research was funded by grants from CNPq (404466/2016-8, PQ 305741/2017-9 and 303791/2016-0), FAPEMIG (PPM-00638-16 and PPM-00635-18), FAPERJ, CAPES and INCT-Catálise. ENSJ would also like to thank Capes-Humboldt research fellowship program for experienced researchers (Proc. No. 88881.145517/2017-01) and Return Fellowship of the Alexander-von-Humboldt foundation. GAMJ thanks CNPq for postdoctoral financial support (Project no. 151150/2018-4). LA acknowledges funding from the DFG (Gottfried-Wilhelm-Leibniz prize). MFSS and CP would like to thank INCT BioNat, National Institute of Science and Technology (grant No. 465637/2014-0), Embrapa (SEG 03.14.01.012.00.00). ENSJ and CJ would also like to thank CAPES and DAAD for research cooperation project under the PROBRAL programme (Proc. No. 99999.008126/2015-01) and for financial support to AK. CJ and AK also thanks University of Saarland (through the Landesforschungsförderungsprogramm (LFPP) of the state of Saarland, Grant No. WT/2-LFFP 16/01).

Keywords: Quinones · Electricity · Chagas disease · Cancer · Electrocatalysis · Selenium · Sustainability

[1] a) R. H. Thomson, *Naturally Occurring Quinones*, Academic Press, London, 2nd edn, **1971**; b) R. H. Thomson, *Naturally Occurring Quinones III Recent Advances*, Chapman and Hall, London, 3rd edn, **1987**; c) M. A. Brimble, L. J. Duncalf, M. R. Nairna, *Nat. Prod. Rep.* **1999**, *16*, 267–281; d) C. D. Donner, *Nat. Prod. Rep.* **2015**, *32*, 578–604; e) E. N. da Silva Júnior, G. A. M. Jardim, C. Jacob, U. Dhawa, L. Ackermann, S. L. de Castro, *Eur. J. Med. Chem.* **2019**, *179*, 863–915; f) V. I. Muronetz, R. A. Asryants, P. I. Semenyuk, N. P. Mishchenko, E. A. Vasilieva, S. A. Fedoreyev, E. V. Schmalhausen, *Curr. Org. Chem.* **2017**, *21*, 2125–2133; g) T. Dunlap, R. E. P. Chandrasena, Z. Wang, V. Sinha, Z. Wang, G. R. J. Thatcher, *Chem. Res. Toxicol.* **2007**, *20*, 1903–1912; h) A. Riffel, L. F. Medina, V. Stefani, R. C. Santos, D. Bizani, A. Brandelli, *Braz. J. Med. Biol. Res.* **2002**, *35*, 811–818.

[2] a) A. Baschieri, R. Amorati, L. Valgimigli, L. Sambri, *J. Org. Chem.* **2019**, *84*, 13655–13664; b) A. Borah, A. Sharma, H. Hazarika, P. Gogoi, *ChemistrySelect* **2017**, *2*, 9999–10003; c) Y. Hong, J. Chen, Z. Zhang, Y. Liu, W. Zhang, *Org. Lett.* **2016**, *18*, 2640–2643; d) S. Kim, R. Matsubara, M. Hayashi, *J. Org. Chem.* **2019**, *84*, 2997–3003; e) J. Su, Y. Zhang, M. Chen, W. Li, X. Qin, Y. Xie, L. Qin, S. Huang, M. Zhang, *Synlett* **2019**, *30*, 630–634; f) Z. Sun, N. Zhu, M. Zhou, X. Huo, H. Wu, Y. Tian, J. Yang, G. Ma, Y.-L. Yang, X. Xu, *Org. Chem. Front.* **2019**, *6*, 3759–3765; g) D. R. Sutherland, M. Veguillas, C. L. Oates, A.-L. Lee, *Org. Lett.* **2018**, *20*, 6863–6867; h) D. Yu, X.-L. Chen, B.-R. Ai, X.-M. Zhang, J.-Y. Wang, *Tetrahedron Lett.* **2018**, *59*, 3620–3623; i) M. S. Yusubov, N. S. Soldatova, P. S. Postnikov, R. R. Valiev, A. Yoshimura, T. Wirth, V. N. Nemykin, V. V. Zhdankin, *Chem. Commun.* **2019**, *55*, 7760–7763; j) Y. Zhang, Q. Ye, L. V. Ponomareva, Y. Cao, Y. Liu, Z. Cui, S. G. Van Lanen, S. R. Voss, Q.-B. She, J. S. Thorson, *Chem. Sci.* **2019**, *10*, 7641–7648.

[3] a) B. Hosamani, M. F. Ribeiro, E. N. da Silva Júnior, I. N. N. Namboothiri, *Org. Biomol. Chem.* **2016**, *14*, 6913–6931; b) J. Aleman, S. Cabrera, E. Maerten, J. Overgaard, K. A. Jorgensen, *Angew. Chem. Int. Ed.* **2007**, *46*, 5520–5523; *Angew. Chem.* **2007**, *119*, 5616; c) J. Aleman, B. Richter, K. A. Jorgensen, *Angew. Chem. Int. Ed.* **2007**, *46*, 5515–5519; *Angew. Chem.* **2007**, *119*, 5611; d) G. Zhang, Y. Wang, W. Zhang, X. Xu, A. Zhong, D. Xu, *Eur. J. Org. Chem.* **2011**, *2011*, 2142–2147; e) S.-W. Duan, Y. Li, Y.-Y. Liu, Y.-Q. Zou, D.-Q. Shi, W.-J. Xiao, *Chem. Commun.* **2012**, *48*, 5160–5162.

[4] a) W. Yang, J. Wang, Z. Wei, Q. Zhang, X. Xu, *J. Org. Chem.* **2016**, *81*, 1675–1680; b) N. Guimond, K. Fagnou, *J. Am. Chem. Soc.* **2009**, *131*, 12050–12051; c) Y. Fujiwara, V. Domingo, I. B. Seiple, R. Gianatassio, M. Del Bel, P. S. Baran, *J. Am. Chem. Soc.* **2011**, *133*, 3292–3295; d) Y. Moon, Y. Jeong, D. Kook, S. Hong, *Org. Biomol. Chem.* **2015**, *13*, 3918–3923; e) C. Zhang, M. Wang, Z. Fan, L.-P. Sun, A. Zhang, *J. Org. Chem.* **2014**, *79*, 7626–7632; f) G. A. M. Jardim, E. N. da Silva Júnior, J. F. Bower, *Chem. Sci.* **2016**, *7*, 3780–3784; g) G. A. M. Jardim, J. F. Bower, E. N. da Silva Júnior, *Org. Lett.* **2016**, *18*, 4454–4457; h) G. A. M. Jardim, W. X. C. Oliveira, R. P. de Freitas, R. F. S. Menna-Barreto, T. L. Silva, M. O. F. Goulart, E. N. da Silva Júnior, *Org. Biomol. Chem.* **2018**, *16*, 1686–1691; i) E. N. da Silva Júnior, G. A. M. Jardim, R. S. Gomes, Y.-F. Liang, L. Ackermann, *Chem. Commun.* **2018**, *54*, 7398–7411; j) T. Zhou, L. Li, B. Li, H. Song, B. Wang, *Org. Lett.* **2015**, *17*, 4204–4207; k) A. Ilangovan, S. Saravanakumar, S. Malayappasamy, *Org. Lett.* **2013**, *15*, 4968–4971; l) E. R. Baral, S. H. Kim, Y. R. Lee, *Asian J. Org. Chem.* **2016**, *5*, 1134–1141.

[5] a) C. Tian, U. Dhawa, A. Scheremetjew, L. Ackermann, *ACS Catal.* **2019**, *9*, 7690–7696; b) J. A. Marko, A. Durgham, S. L. Bretz, W. Liu, *Chem. Commun.* **2019**, *55*, 937–940; c) C. Tian, L. Massignan, T. H. Meyer, L. Ackermann, *Angew. Chem. Int. Ed.* **2018**, *57*, 2383–2387; *Angew. Chem.* **2018**, *130*, 2407; d) N. Sauermann, T. H. Meyer, C. Tian, L. Ackermann, *J. Am. Chem. Soc.* **2017**, *139*, 18452–18455; e) J. Wu, Y. Dou, R. Guillot, C. Kouklovsky, G. Vincent, *J. Am. Chem. Soc.* **2019**, *141*, 2832–2837; f) M. D. Kärkäs, *Chem. Soc. Rev.* **2018**, *47*, 5786–5865; g) J. Chen, S. Lv, S. Tian, *ChemSusChem* **2019**, *12*, 115–132; h) C. Ma, P. Fang, T.-S. Mei, *ACS Catal.* **2018**, *8*, 7179–7189.

[6] a) W.-J. Kong, L. H. Finger, A. M. Messinis, R. Kuniyil, J. C. A. Oliveira, L. Ackermann, *J. Am. Chem. Soc.* **2019**, *141*, 17198–17206; b) S. C. Sau, R. Mei, J. Struwe, L. Ackermann, *ChemSusChem* **2019**, *12*, 3023–3027; c) Y. Qiu, J. Struwe, L. Ackermann, *Synlett* **2019**, *30*, 1164–1173; d) Z. Ruan, Z. Huang, Z. Xu, G. Mo, X. Tian, X.-Y. Yu, L. Ackermann, *Org. Lett.* **2019**, *21*, 1237–1240.

[7] V. Jamier, L. A. Ba, C. Jacob, *Chem. Eur. J.* **2010**, *16*, 10920–10928.

[8] G. A. M. Jardim, Í. A. O. Bozzi, W. X. C. Oliveira, C. Mesquita-Rodrigues, R. F. S. Menna-Barreto, R. A. Kumar, E. Gravel, E. Doris, A. L. Braga, E. N. da Silva Júnior, *New J. Chem.* **2019**, *43*, 13751–13763.

[9] S. Shabaan, L. A. Ba, M. Abbas, T. Burkholz, A. Denkert, A. Gohr, L. A. Wessjohann, F. Sasse, W. Weberd, C. Jacob, *Chem. Commun.* **2009**, 4702–4704.

[10] S. Shaaban, A. Negm, A. M. Ashmawy, D. M. Ahmed, L. A. Wessjohann, *Eur. J. Med. Chem.* **2016**, *122*, 55–71.

[11] S. Mecklenburg, S. Shaaban, L. A. Ba, T. Burkholz, T. Schneider, B. Diesel, A. K. Kiemer, A. Röseler, K. Becker, J. Reichrath, A. Stark, W. Tilgen, M. Abbas, L. A. Wessjohann, F. Sasse, C. Jacob, *Org. Biomol. Chem.* **2009**, *7*, 4753–4762.

[12] E. H. G. da Cruz, M. A. Silvers, G. A. M. Jardim, J. M. Resende, B. C. Cavalcanti, I. S. Bomfim, C. Pessoa, C. A. de Simone, G. V. Botteselle, A. L. Braga, D. K. Nair, I. N. N. Namboothiri, D. A. Boothman, E. N. da Silva Júnior, *Eur. J. Med. Chem.* **2016**, *122*, 1–16.

[13] A. A. Vieira, J. B. Azeredo, M. Godoi, C. Santi, E. N. da Silva Júnior, A. L. Braga, *J. Org. Chem.* **2015**, *80*, 2120–2127.

[14] A. A. Vieira, I. R. Brandão, W. O. Valença, C. A. de Simone, B. C. Cavalcanti, C. Pessoa, T. R. Carneiro, A. L. Braga, E. N. da Silva Júnior, *Eur. J. Med. Chem.* **2015**, *101*, 254–265.

[15] G. A. M. Jardim, W. J. Reis, M. F. Ribeiro, F. M. Ottoni, R. J. Alves, T. L. Silva, M. O. F. Goulart, A. L. Braga, R. F. S. Menna-Barreto, K. Salomão, S. L. de Castro, E. N. da Silva Júnior, *RSC Adv.* **2015**, *5*, 78047–78060.

[16] N. Kongkathip, B. Kongkathip, P. Siripong, C. Sangma, S. Luangkamin, M. Niyomdecha, S. Pattanapa, *Bioorg. Med. Chem.* **2003**, *11*, 3179–3191.
[17] a) F. de Moliner, A. King, G. G. Dias, G. F. de Lima, C. A. de Simone, E. N. da Silva Júnior, M. Vendrell, *Front. Chem.* **2018**, *6*, 339; b) G. G. Dias, A. King, F. de Moliner, M. Vendrell, E. N. da Silva Júnior, *Chem. Soc. Rev.* **2018**, *47*, 12–27.
[18] a) L. Sun, Y. Yuan, M. Yao, H. Wang, D. Wang, M. Gao, Y.-H. Chen, A. Lei, *Org. Lett.* **2019**, *21*, 1297–1300; b) G. I. Giles, K. M. Tasker, R. J. K. Johnson, C. Jacob, C. Peers, K. N. Green, *Chem. Commun.* **2001**, 2490–2491; c) G. I. Giles, N. M. Giles, C. A. Collins, K. Holt, F. H. Fry, P. A. S. Lowden, N. J. Gutowski, C. Jacob, *Chem. Commun.* **2013**, *49*, 2030–2031; d) G. I. Giles, M. J. Nasim, W. Ali, C. Jacob, *Antioxidants* **2017**, *6*, 38; e) M. Wilken, S. Ortgies, A. Breder, I. Siewert, *ACS Catal.* **2018**, *8*, 10901–10912; f) A. Kunai, J. Harada, J. Izumi, H. Tachihara, K. Sasaki, *Electrochim. Acta* **1983**, *28*, 1361–1366; g) J. Ludvík, B. Nygard, *J. Electroanal. Chem.* **1997**, *423*, 1–11; h) O. Niyomura, M. Cox, T. Wirth, *Synlett* **2006**, *2*, 251–254; i) B. Mueller, H. Poleschner, K. Seppelt, *Dalton Trans.* **2008**, 4424–4427; j) C. D. Prasad, M. Sattar, S. Kumar, *Org. Lett.* **2017**, *19*, 774–777; k) S. Kumar, R. Kadu, S. Kumar, *Org. Biomol. Chem.* **2016**, *14*, 9210–9214; l) C. D. Prasad, S. J. Balkrishna, A. Kumar, B. S. Bhakuni, K. Shrimali, S. Biswas, S. Kumar, *J. Org. Chem.* **2013**, *78*, 1434–1443.
[19] B. C. Cavalcanti, F. W. A. Barros, I. O. Cabral, J. R. O. Ferreira, H. I. F. Magalhães, H. V. N. Júnior, E. N. da Silva Júnior, F. C. de Abreu, C. O. Costa, M. O. F. Goulart, M. O. Moraes, C. Pessoa, *Chem. Res. Toxicol.* **2011**, *24*, 1560–1574.
[20] A. C. S. Bombaça, P. G. Viana, A. C. C. Santos, T. L. Silva, A. B. M. Rodrigues, A. C. R. Guimarães, M. O. F. Goulart, E. N. da Silva Júnior, R. F. S. Menna-Barreto, *Free Radical Biol. Med.* **2019**, *130*, 408–418.
[21] WHO. Chagas disease – Epidemiology, **2017**, https://www.who.int/chagas/epidemiology/en/, Accessed November 2019.
[22] C. A. Morillo, J. A. Marin-Neto, A. Avezum, S. Sosa-Estani, A. Rassi Júnior, F. Rosas, E. Villena, R. Quiroz, R. Bonilla, C. Britto, F. Guhl, E. Velazquez, L. Bonilla, B. Meeks, P. Rao-Melacini, J. Pogue, A. Mattos, J. Lazdins, A. Rassi, S. J. Connolly, S. Yusuf, *N. Engl. J. Med.* **2015**, *373*, 1295–1306.
[23] a) R. F. Menna-Barreto, S. L. de Castro, *Curr. Top. Med. Chem.* **2017**, *17*, 1212–1234; b) S. B. Scarim, D. H. Jornada, R. C. Chelucci, L. de Almeida, J. L. dos Santos, M. C. Chung, *Eur. J. Med. Chem.* **2018**, *155*, 824–838.
[24] E. N. da Silva Júnior, R. F. S. Menna-Barreto, M. C. F. R. Pinto, R. S. F. Silva, D. V. Teixeira, M. C. B. V. de Souza, C. A. de Simone, S. L. de Castro, V. F. Ferreira, A. V. Pinto, *Eur. J. Med. Chem.* **2008**, *43*, 1774–1780.
[25] H. J. Reich, J. M. Renga, I. L. Reich, *J. Am. Chem. Soc.* **1975**, *97*, 5434–5447.
[26] a) L. F. Fieser, M. Fieser, *J. Am. Chem. Soc.* **1948**, *70*, 3215–3222; b) L. F. Fieser, *J. Am. Chem. Soc.* **1926**, *48*, 2922–2937.
[27] K. Salomão, E. M. de Souza, S. A. Carvalho, E. F. da Silva, C. A. M. Fraga, H. S. Barbosa, S. L. de Castro, *Antimicrob. Agents Chemother.* **2010**, *54*, 2023–2031.
[28] L. H. P. Silva, V. Nussenszweig, *Folia Clin. Biol.* **1953**, *20*, 191–207.
[29] T. Mossmann, *J. Immunol. Methods* **1983**, *65*, 55–63.
[30] M. F. S. Silva, L. M. A. Silva, A. L. Quintela, A. G. dos Santos, F. A. N. Silva, F. C. E. de Oliveira, E. G. Alves Filho, E. S. de Brito, K. M. Canuto, C. Pessoa, G. J. Zocolo, *J. Chromatogr. B* **2019**, *1120*, 51–61.

Received: February 17, 2020

Antitumor Compounds

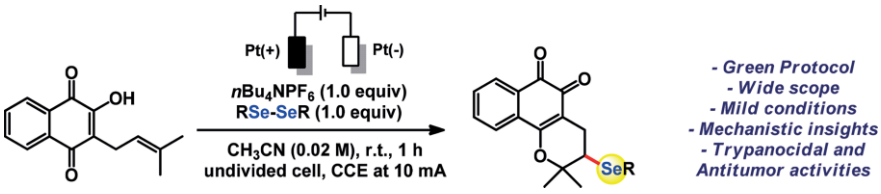

Electrochemical selenation in undivided electrochemical cells allows the preparation of selenium-containing naphthoquinones with potent bioactivity. The rapid, green and efficient protocol avoids chemical oxidants and enables the synthesis of target molecules in a fast and reliable way.

0

doi.org/10.1002/ejoc.202000216

3.2. Publication 2

Release of reactive selenium species from phthalic selenoanhydride in the presence of hydrogen sulfide and glutathione with implications for cancer research

Ammar Kharma, Anton Misak, Marian Grman, Vlasta Brezova, Lucia Kurakova, Peter Baráth, Claus Jacob, Miroslav Chovanec, Karol Ondrias and Enrique Domĭnguez-Álvarez*

New Journal of Chemistry, 43, 11771-11783 (2019)

https://doi.org/10.1039/C9NJ02245G

NJC

PAPER

View Article Online
View Journal | View Issue

Check for updates

Cite this: *New J. Chem.*, 2019, **43**, 11771

Release of reactive selenium species from phthalic selenoanhydride in the presence of hydrogen sulfide and glutathione with implications for cancer research†

Ammar Kharma,[ab] Anton Misak,[a] Marian Grman,[a] Vlasta Brezova,[c] Lucia Kurakova,[d] Peter Baráth,[e] Claus Jacob,[b] Miroslav Chovanec,[f] Karol Ondrias[a] and Enrique Domínguez-Álvarez *[g]

The last decade has witnessed a renewed interest in selenium (Se) as an element able to prevent a range of illnesses in humans, mainly through supplementation. However, such supplementation relies on species such as sodium selenite or selenomethionine, which proved to have limited solubility and bioavailability, thus leading to limited activity. To overcome this limitation, other selenium species need to be explored, such as phthalic selenoanhydride (R-Se), which is soluble in physiological media. R-Se releases various reactive selenium species (RSeS), including hydrogen selenide (H_2Se), that can interact with cellular components, such as glutathione (GSH) and hydrogen sulfide (H_2S). This interplay between R-Se and the cellular components provides a sophisticated biochemical release mechanism that could be behind the noteworthy biological activities observed for this compound. In order to investigate the interactions of phthalic chalcogen anhydrides with H_2S or GSH, we have employed UV-vis spectrophotometry, electron paramagnetic resonance spectroscopy (EPR) and plasmid DNA (pDNA) cleavage assay. We found that apart from R-Se, the other analogues do not have the ability to scavenge the $^{\bullet}$cPTIO radical or to cleave pDNA on their own. In contrast, the scavenging potency for the $^{\bullet}$cPTIO radical and for the $O_2^{\bullet-}$ radical exerted by R-Se and its sulfur analogue (R-S) significantly increased when they were evaluated in the presence of H_2S. However, GSH only changed the radical scavenging activity of R-Se. These new discoveries may explain some of the biological activities associated with this class of compounds and open a new approach to ascertain the possible mechanisms underlying their biological actions.

Received 1st May 2019,
Accepted 1st July 2019

DOI: 10.1039/c9nj02245g

rsc.li/njc

Introduction

Selenium (Se) is an essential element for human health and its deficiency causes severe disorders, such as Keshan or Kashin-Beck diseases, which are endemic in farming self-sufficient regions with low levels of Se in the soil.[1,2] Both Se-containing compounds and the Se atom present in the active sites of 25 mammalian selenoproteins identified so far participate in key cellular and physiological processes, as well as diseases such as cancer, inflammation, immunity, type 2 diabetes or liver diseases.[3–8] However, the molecular mechanism of action is not fully understood yet for some of these selenoproteins.

During recent years, Se-compounds have gained substantial interest as H_2Se donors, as potential anti-cancer agents or as selenocompounds with potential use in selenium supplementation.[8–11] Among other effects of Se-compounds related to cancer, they could induce apoptosis in cancer cells through the production of Reactive Oxygen Species (ROS), thus

[a] *Institute of Clinical and Translational Research, Biomedical Research Center, University Science Park for Medicine, Slovak Academy of Sciences, Dúbravská cesta 9, 845 05 Bratislava, Slovak Republic*
[b] *Division of Bioorganic Chemistry, School of Pharmacy, Saarland University, Campus B2 1, D-66123 Saarbruecken, Germany*
[c] *Faculty of Chemical and Food Technology, Slovak University of Technology, Radlinskeho 9, 812 37 Bratislava, Slovak Republic*
[d] *Department of Pharmacology and Toxicology, Faculty of Pharmacy, Comenius University, Ulica Odbojárov 10, 832 32 Bratislava, Slovak Republic*
[e] *Institute of Chemistry, Slovak Academy of Sciences, Dúbravská cesta 9, 845 38 Bratislava, Slovak Republic*
[f] *Cancer Research Institute, Biomedical Research Center, University Science Park for Medicine, Slovak Academy of Sciences, Dúbravská cesta 9, 845 05 Bratislava, Slovak Republic*
[g] *Instituto de Química Orgánica General, Consejo Superior de Investigaciones Científicas (IQOG, CSIC), Juan de la Cierva 3, 28006 Madrid, Spain. E-mail: e.dominguez.alvarez@csic.es*

† Electronic supplementary information (ESI) available. See DOI: 10.1039/c9nj02245g

inducing oxidative stress (OS).[12,13] Furthermore, certain Se-compounds can damage DNA. Then, they may not protect against cancer and other chronic diseases, and can even cause or enhance some types of cancer. These facts indicate that Se may exert a broad pattern of toxic effects.[14,15] The exact mechanisms underlying the beneficial and toxic effects of Se-compounds are not fully understood yet and they are still under intensive investigation, due to the interest in the potential applications of this dual behaviour: these pro-oxidant/antioxidant Se-compounds could act as novel cellular redox modulators.

In this context, the accessibility and reactivity of the selenols (mainly deprotonated at biological pH values) and selenol-derived compounds, such as Se-methyl selenocysteine and diselenides,[16–19] may be behind the reported chemopreventive activity of different Se-containing compounds, which has been reviewed extensively by numerous authors.[11,20–25] Several mechanisms have been proposed to explain the chemopreventive activity, such as the direct scavenging of free radicals,[26,27] the amelioration of the toxic effects of anticancer drugs,[28] the glutathione peroxidase (GPx)-like activity,[29,30] the protection from toxic elements such as arsenic by protecting PC12 cells from arsenic induced oxidative stress[31] or the protection from radiotherapy,[32] and the modulation of the intracellular redox homeostasis[33] and of the protein kinases.[34]

In the last twenty years, H_2S ($H_2S/HS^-/S^{2-}$) has been emerging as a new gaseous signalling molecule besides nitric oxide ($^{\bullet}NO$) and carbon monoxide (CO). H_2S is produced endogenously in almost all mammalian cells and affects many physiological and pathological processes.[35–37] H_2S has mostly beneficial effects under conditions of oxidative stress by reacting with reactive oxygen and nitrogen species.[38–42] It has both pro- and anti-cancer effects depending on the cell type, concentration and interaction with other cellular molecules.[43–45] Glutathione (GSH) is another intracellular natural antioxidant, which has many biological roles including modulation of cellular redox homeostasis and protection against reactive oxygen and nitrogen species.[46,47] As has been determined in previous work, sodium selenite (Na_2SeO_3) and selenium tetrachloride ($SeCl_4$) have the ability to interact separately with GSH and H_2S. This fact could be behind their biological effects.[48] However, as mentioned above, sodium selenite can have reduced bioavailability and can also exert toxic effects.[14,15] Thus, it is desirable to move towards novel Se-containing compounds that retain this observed ability to interact with relevant sulfur compounds (herein, GSH and H_2S) and, at the same time, show reduced toxicity in comparison with sodium selenite. This would improve the applicability of these new selenium-based redox modulators and simultaneously opens a new approach in Se-supplementation, by finding redox-active derivatives with less toxicity.

In this context, our previous data showed promising chemopreventive, antiproliferative, cytotoxic, free radical scavenging, pro-apoptotic and multidrug-resistance (MDR) reversing activity of phthalic selenoanhydride (R-Se, Fig. 1), the Se-analogue of phthalic-anhydride.[49–52] Probably, these reported biological activities are directly related to the Se atom, as no relevant biological effects were displayed by its oxygen analogue, phthalic anhydride (R-O).[51] A hypothesis which may explain the amazing

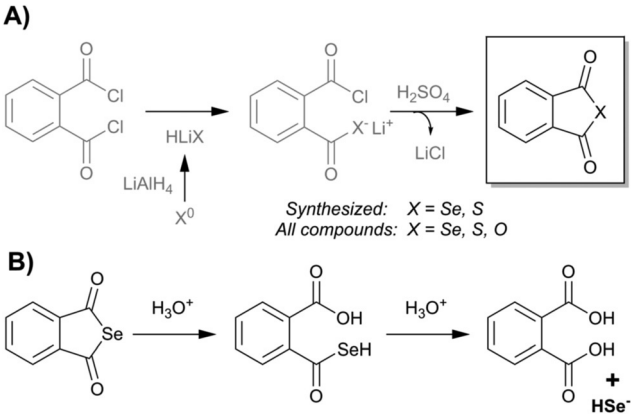

Fig. 1 (A) Chemical structure of the chalcogen derivatives of phthalic anhydride. X = Se → R-Se; S → R-S; O → R-O. Synthetic procedure for R-Se and R-S. (B) Hypothesized reactions that would lead to the release of hydrogen selenide (H_2Se) from R-Se in physiological media.

biological properties of R-Se draws attention to the lability of the CO–Se chemical bond.[49] This lability suggests the interesting possibility that R-Se behaves in the organism as a prodrug: it enables the internalization of the compound in the cells and once inside it can release selenium slowly inside the cell, in the form of H_2Se, of other uncharged Se-species such as nanoparticles of selenium or of charged Se-anions able to interact swiftly with cellular components.[49,51] Due to their particular chemical affinity towards thiol-containing agents, such as hydrogen sulfide (H_2S) or glutathione (GSH), and with the enzymes and proteins which are components of the cell thiolstat, such reactivity may initiate pronounced biological responses. In this way, R-Se could be a very simple, elegant and straightforward method to transport selenium inside cells and, at the same time, it would enable its release in an "activated" form as a reactive selenium species, ready to exert immediately a wide variety of biological effects. Besides, these compounds have been proven in previous studies to exert a selective action to be less toxic in non-tumour cells than in cancer cells.[49,51] Thus, they could be used as safer redox modulators.

Herein, we have studied further the possible mechanism(s) underlying these initial promising biological activities of R-Se, and we will ascertain if these hypothesized interactions with H_2S and GSH take place effectively. The activities of R-O and phthalic thioanhydride (R-S) were examined in parallel for comparison. Since H_2S and GSH interact with several biologically active molecules, modulating their activities,[42,46–48,53] the interactions of H_2S and GSH with these three phthalic anhydride derivatives and their molecular consequences were also analysed, expecting that in these instances R-Se would be the most reactive one thanks to its higher expected reactivity. The reduction of the $^{\bullet}$cPTIO and superoxide ($O_2^{\bullet-}$) radicals, and plasmid DNA (pDNA) cleavage assay were employed to monitor these consequences. We show that only R-Se displays any significant biological activity on its own. This activity was augmented considerably when tested in combination with H_2S or GSH. In contrast, GSH showed no impact on the activities of R-S or of R-O, whilst H_2S was efficient to some extent in this context. Hence, the products of the H_2S or

GSH interaction with R-Se and R-S show free radical scavenging properties and appear to cleave pDNA, potentially explaining some of their biological activities.

Results and discussion

To unveil the possible mechanisms underlying the reported activities of R-Se against cancer, we have designed different experiments with R-Se, R-S and R-O, such as mass spectrometry (ESI-MS), spectrophotometrically-monitored radical scavenging and electron paramagnetic resonance (EPR), in an attempt to ascertain how this promising Se-containing compound can interact with different cellular redox targets.

Chemistry

In the present work, we have evaluated three chalcogen phthalic anhydrides, as shown in Fig. 1: phthalic selenoanhydride (X = Se → R-Se), phthalic thioanhydride (X = S → R-S) and phthalic anhydride (X = O → R-O), as well as phthalic acid (R-OH). R-O and R-OH were commercially available, whereas R-Se and R-S were synthesized following an adaption of the procedure previously described for the synthesis of R-Se (Fig. 1).[49]

In brief, elemental selenium or sulfur is reduced with lithium aluminium hydride, and the *in situ* formed hydrogen chalcogenide attacks the phthaloyl chloride to form a reactive intermediate. Sulphuric acid is added to form the desired final R-Se or R-S. Compounds were isolated in the form of stable solids, whose purity was assessed through NMR and LC-MS.

ESI-MS

R-Se showed a complex pattern of fragmentation (Fig. 2) in the ESI-MS (electrospray ionization mass spectrometry) spectrum taken in a 50% methanol/H_2O solution (Fig. 3). The possible fragments corresponding to the main peaks observed in ESI are suggested in Fig. 2.

The M^+H molecular peak of R-Se is easily recognisable thanks to the characteristic isotopic pattern of the Se-containing fragments, and the remaining peaks of low *m/z* can be assigned to specific fragments (Fig. 2). Briefly, the protonated molecular peak (*m/z* = 212.94487) is attacked by methanol to generate the fragment with *m/z* = 244.97104 (also with the characteristic isotopic pattern of Se). This fragment loses a molecule of hydrogen selenide, leading to *m/z* = 163.03906, which can suffer additional fragmentation (release of CO, *m/z* = 135.04408) or can incorporate a molecule of water to later generate protonated R-O (*m/z* = 181.04956). The majority of these peaks can be seen when R-Se is analysed together with Na_2S (Fig. 4). The remaining peaks, especially those with *m/z* > 245, are the result of complex couplings with other R-Se molecules/fragments, and with water or with the solvent (methanol). The low abundance of the protonated molecular peak in the ESI-MS spectrum may be an indicator of the readiness of the R-Se compound to react with different compounds, and this reactivity can explain the biological activities found so far for this bioactive compound.

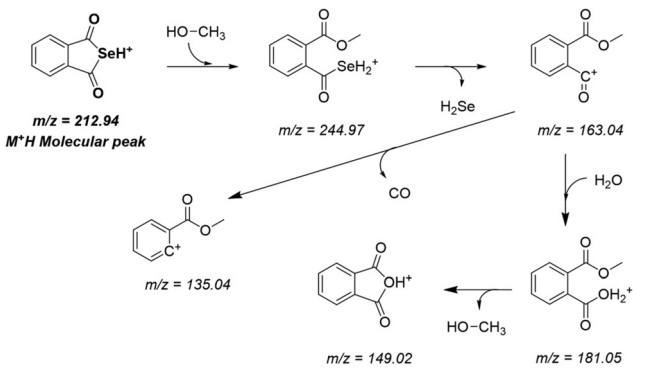

Fig. 2 Hypothesized fragmentation pattern for protonated R-Se in ESI-MS.

When Na_2S is added to the R-Se solution in 50% methanol/H_2O (Fig. 4), the protonated molecular peak of R-Se (*m/z* = 212.94487) disappears, although *m/z* = 244.97110 (the result of methanol addition to this peak and also with the Se isotopic pattern) can be observed, but with a significant lower abundance than in the spectrum of R-Se alone. It is also possible to observe the peaks of lower *m/z* that were hypothesized above in Fig. 2: *m/z* = 135.04414, *m/z* = 149.02, *m/z* = 163.03908 and *m/z* = 181.04958. Besides, new peaks appear. The most relevant of them is *m/z* = 197.02664, which is the equivalent of *m/z* = 244.97110 but replacing the Se atom by sulfur (Fig. 4, inset). This peak can be formed through the coupling of H_2S (generated *in situ* from Na_2S) with *m/z* = 163.03908. Finally, two peaks (*m/z* = 266.95303 and *m/z* = 219.00859) with a difference of 48 Da are found, a difference that can be attributed to a Se–S change, taking into account that the first peak presents the characteristic isotopic pattern of Se. Tentative structures that could explain these two peaks are the polyhydroxy-containing compounds drawn in the Fig. 4 inset. In any case, the absence of the R-Se protonated molecular peak and the two sulfur-containing peaks (*m/z* = 197.02664 and *m/z* = 219.00859) together is indicative of an interaction between R-Se and Na_2S.

According to the data obtained, ESI-MS experiments show how this Se-compound, in the electrospray ionization conditions, suffers specific fragmentation (Fig. 2) and how it forms complex couplings with the solvent and other R-Se molecules/fragments (Fig. 3), indicating that this compound has high reactivity. This fact could be indicative of potential interactions of R-Se with reactive species present in the cell, such as ROS, Reactive Nitrogen Species (RNS) and the sulfur compounds of the redox thiolstat. To prove this hypothetical interaction between R-Se and sulfur species present in cells such as H_2S, we also applied the ESI-MS methodology to a mixture of R-Se and Na_2S (Fig. 4). In this second ESI-MS spectrum, it is observed how the peaks of the initial R-Se are practically irrelevant, whereas its fragment peaks are the main peaks. Additionally, new peaks related to coupling of its fragments with the added sulfur atoms start to be observed, proving also the reaction between the two chalcogen compounds.

Results of the reduction of •cPTIO by phthalic-anhydride derivatives and H_2S

Since H_2S is endogenously produced in living organisms, we studied the interaction of H_2S with R-Se. We observed that H_2S

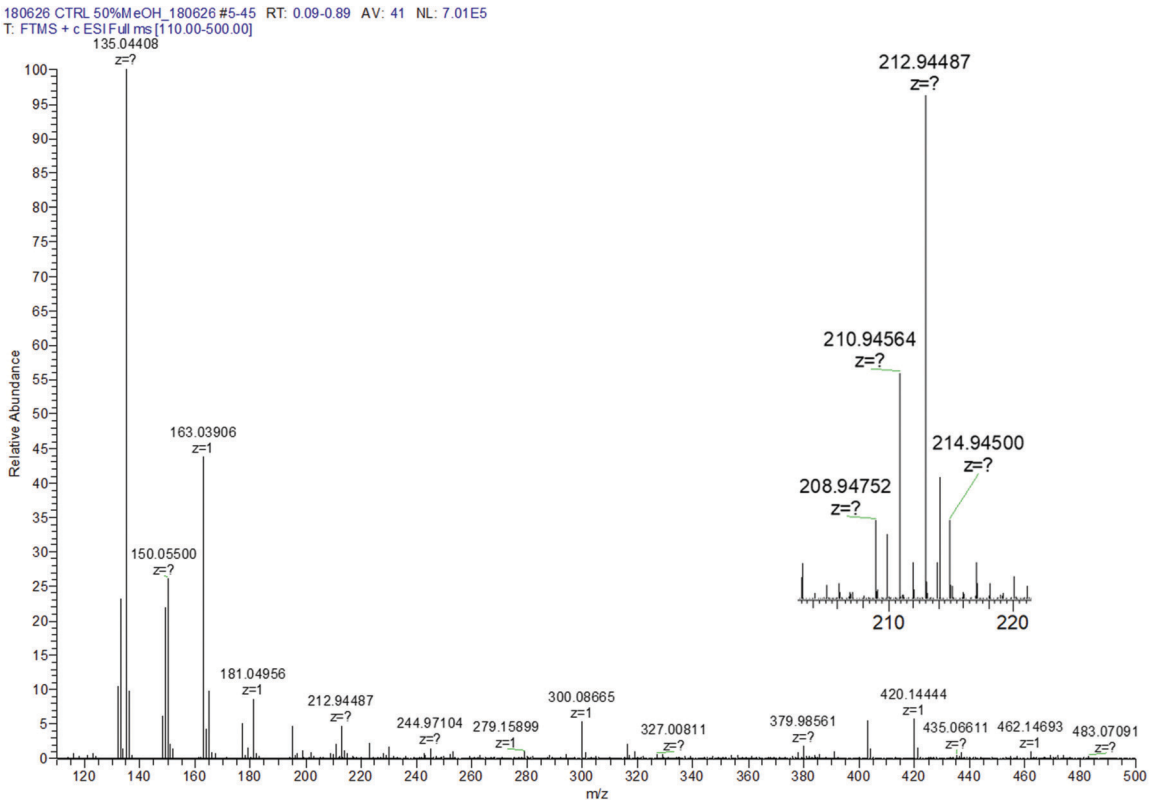

Fig. 3 Control R-Se ESI spectrum in 50% methanol/H_2O. Inset: Zoom of the protonated molecular peak showing the characteristic isotopic pattern of Se.

interacts with R-Se. Since H_2S and Se derivatives were reported to interact with radicals,[54] it was of high interest to reveal whether the products of the H_2S/R-Se reaction interact with radicals and how this interaction is unique in comparison to other phthalic-anhydride derivatives. Therefore, we studied the potency of H_2S, R-Se, R-S, R-O and R-OH and the interaction products of H_2S/R-Se, H_2S/R-S, H_2S/R-O and H_2S/R-OH to reduce the •cPTIO radical.

H_2S potentiates R-Se and R-S (but not R-O or R-OH) in reducing •cPTIO. Since H_2S is endogenously produced in organisms and exogenous H_2S donors are being considered to be used in medicine, we have studied the interaction of H_2S with anhydride derivatives and the ability of the products of this interaction to reduce the •cPTIO radical. H_2S in the presence of R-Se or R-S, but not R-O or R-OH, significantly increased the rate and potency of the compounds to reduce •cPTIO (Fig. 5A, inset, Fig. 5B and 6).

Notably, 6.25, 12.5 and 25 μM of R-Se in the presence of 100 μM H_2S had two time-dependent phases of decreasing the concentration of 100 μM •cPTIO. The first was a fast decrease (in $\leq$2 min) followed by a second gradual decrease (Fig. 6A). On the other hand, 6.25, 12.5 and 25 μM of R-S decreased •cPTIO in the first phase slower than what was observed when R-Se was employed ($\leq$5 min), but later the •cPTIO concentration did not decrease significantly (Fig. 6C). This indicates that the molecular mechanism of •cPTIO reduction by H_2S/R-Se and H_2S/R-S is different. The •cPTIO reduction potency of the H_2S/R-Se mixture was several fold higher than ($\geq$5×) that of H_2S/R-S (Fig. 6E). The reduction of •cPTIO strongly depended on the H_2S/R-Se molar ratio: it was low at 0.5 and 1 H_2S/R-Se molar ratios but increased significantly at 2 and 4 molar ratios (Fig. 6B and F). On the other hand, the reduction of •cPTIO gradually increased with the H_2S/R-Se molar ratio (Fig. 6D and F). The results show that H_2S interacting with R-Se and R-S (but not with R-O or R-OH) forms reactive products which reduce the •cPTIO radical. The order of potency is as follows: H_2S/R-Se > H_2S/R-S ≫ H_2S/R-O ∼ R-OH = 0.

GSH potentiates R-Se and R-S (but not R-O or R-OH) in reducing •cPTIO. GSH is a tripeptide (glutamate–cysteine–glycine) natural antioxidant, whose intracellular concentrations are in the range of 0.5 to 10 mM.[46,47] Therefore, we studied the effect of GSH on the reducing potency of the phthalic-anhydride derivatives. GSH (100 and 500 μM) did not reduce the •cPTIO (100 μM) radical alone (Fig. 7), as observed in our previous study.[42] However, the GSH/R-Se (200/50 and 500/50 μM/μM) and GSH/R-S (200/50 and 500/50 μM/μM) mixtures significantly reduced •cPTIO (Fig. 7). The kinetics of •cPTIO reduction by the mixtures were different for R-Se and R-S. In the case of R-S, it was an exponential decay, but in the case of R-Se an induction period was observed. The addition of R-O to the •cPTIO/GSH mixture did not cause •cPTIO reduction (Fig. 7). The results indicate that the reducing potency of GSH is significantly enhanced upon its interaction with R-Se and R-S. In control experiments, R-O and phthalic acid did not reduce •cPTIO themselves, nor in the presence of 500 μM GSH (Fig. 7). This indicates that the presence

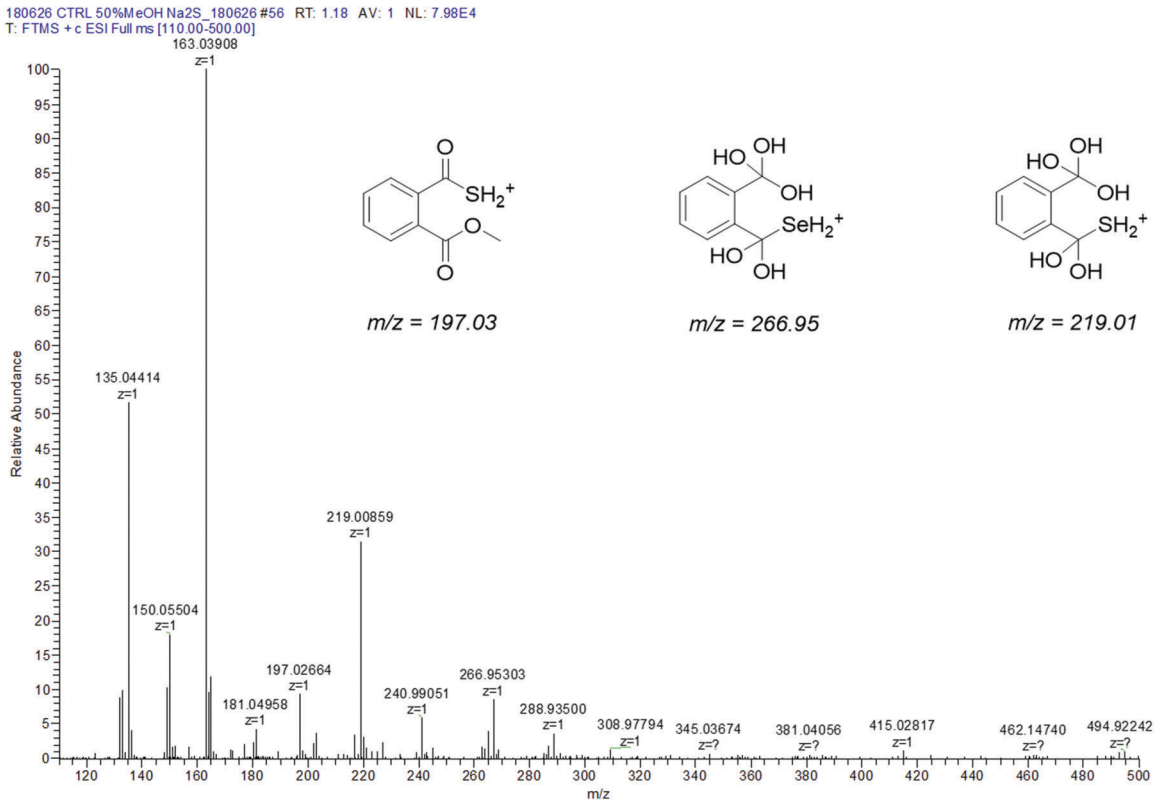

Fig. 4 Experimental ESI-MS spectrum of R-Se + Na_2S in 50% methanol/H_2O. Inset: Structures suggested to explain the differential peaks with respect to the R-Se ESI-MS spectrum.

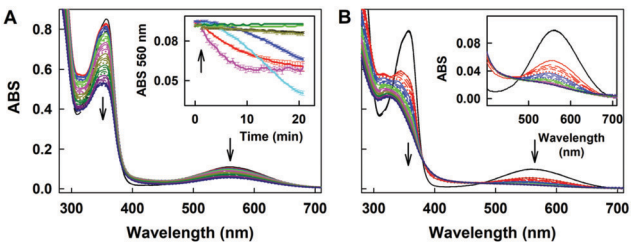

Fig. 5 Reduction of •cPTIO by H_2S, R-Se, R-S, RO and the R-Se/H_2S mixture. (A) Time resolved UV-vis spectra of 100 μM •cPTIO after addition of 100 μM R-S. Spectra were recorded every 30 s for 20 min. The first spectrum was recorded 15 s after R-S addition. Arrows indicate the decrease of ABS at 356 and 560 nm. Inset: Kinetics of changes in absorbance at 560 nm of 100 μM •cPTIO after addition (indicated by an arrow) of: 100 μM H_2S (black); 50 and 100 μM R-Se (red and pink); 50 and 100 μM R-S (blue and cyan); 50 and 100 μM R-O (green and dark green) and a mixture of 100 μM H_2S with 100 μM R-O (dark yellow). Means ± SEM, n = 2–4. (B) Time resolved UV-vis spectra of the interaction of 100 μM •cPTIO with 100 μM H_2S (3 times repeated every 30 s, black) and subsequent addition of 12.5 μM R-Se. Spectra were recorded every 30 s for 20 min, the first spectrum, indicated by the red line, was measured 15 s after addition of R-Se. Inset: Details of the time resolved spectra of the •cPTIO/H_2S (100/100 μM/μM) interaction before (black) and after addition of R-Se (12.5 μM, the first spectrum is indicated by the solid red line, which is followed each 30 s by: long dashed red, medium dashed red, short dashed red, dotted red, solid blue, long dashed blue, medium dashed blue, *etc.*).

of Se and S in phthalic anhydride derivatives after interaction with H_2S and GSH is responsible for the reduction of •cPTIO.

H_2S and GSH interacting with Na_2Se-derivatives reduce •cPTIO. ESI-MS experiments (Fig. 3 and 4) show that H_2S interacts with R-Se (and its derivatives). We observed that the H_2S/R-Se mixture, but not the H_2S/R-O or H_2S/phthalic acid mixtures, reduced •cPTIO (Fig. 6). Based on these data, we suppose that the intermediates and/or products of the H_2S interaction with Se (released from R-Se) and/or with R-Se derivatives are responsible for •cPTIO reduction. To confirm this, we studied the interaction of H_2S and GSH with Se derivatives using Na_2Se. The UV-vis spectra of freshly prepared 100 μM Na_2Se changed gradually for 20 min (Fig. 8A), which could be an indication of a potential slow unspecific interaction with any of the compounds present in the solution, such as diethylenetriaminepentaacetic acid (DTPA), sodium phosphate, the solvent (water) or most probably with oxygen, which acts as an oxidant. The UV-vis spectra of H_2S/Na_2Se (100/100 μM/μM) also changed gradually for 20 min (Fig. 8B). Since the time dependence of the UV-vis spectra of Na_2Se (Fig. 8A) and the Na_2Se/H_2S mixture (Fig. 8B) were different (marked by arrows), we confirm the interaction of H_2S with Na_2Se derivatives.

The time resolved UV-vis spectra of •cPTIO/Na_2Se (100/100 μM/μM) show no •cPTIO reduction by Na_2Se alone, since ABS at 356 nm (marked by an arrow) did not decrease over the time (Fig. 8C and F), nor ABS at 560 nm (Fig. 8C, inset). H_2S (100 μM) or GSH (500 μM) had only minor effects (≤7%) on their own in terms of •cPTIO (100 μM) reduction within 20 min. However, addition of freshly prepared Na_2Se (100 μM) to the H_2S/•cPTIO

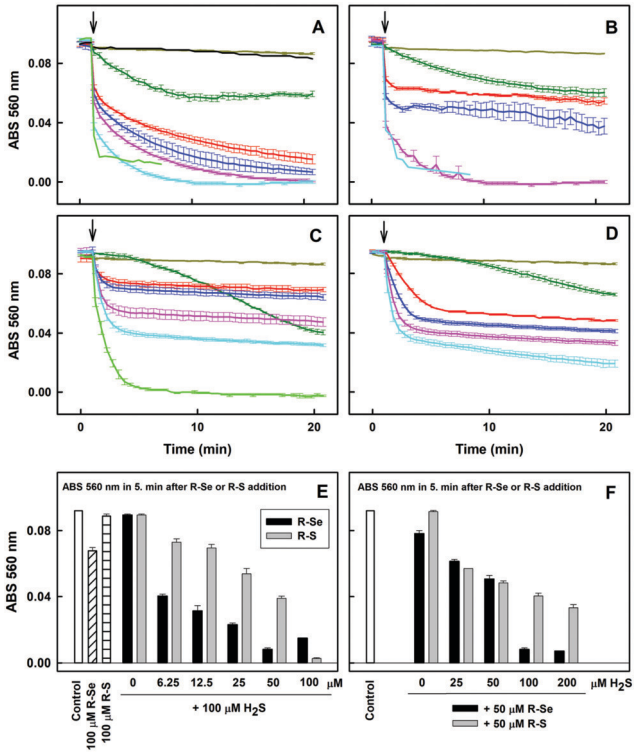

Fig. 6 The effect of R-Se and R-S on the kinetics of •cPTIO reduction in the absence and presence of H_2S. (A) The effect of R-Se and R-OH on the time-dependent reduction of •cPTIO/H_2S. Kinetics of changes in absorbance at 560 nm of 100 μM •cPTIO after addition (indicated by an arrow) of 100 μM R-Se alone (dark green) and compared to the addition of 0 (dark yellow), 6.25 (red), 12.5 (blue), 25 (pink), 50 (cyan) and 100 μM (green) R-Se to •cPTIO/H_2S (100/100 μM/μM). 50 μM R-OH added to •cPTIO/H_2S (black; 100/100 μM/μM). Data were collected from UV-vis spectra every 30 s for 20 min. (B) The effect of H_2S on the kinetics of reduction of •cPTIO in the presence of R-Se. Kinetics of changes in absorbance at 560 nm of 100 μM •cPTIO after addition (indicated by an arrow) of 100 μM H_2S alone (dark yellow) and after addition of 50 μM R-Se to 0 μM (dark green), 25 μM (red), 50 μM (blue), 100 μM (pink) and 200 μM H_2S (cyan). (C) The effect of R-S on the kinetics of •cPTIO reduction in the presence of H_2S. Kinetics of changes in absorbance at 560 nm of 100 μM •cPTIO after addition (indicated by an arrow) of 100 μM R-S alone (dark green) and compared to the addition of 0 (dark yellow), 6.25 (red), 12.5 (blue), 25 (pink), 50 (cyan) and 100 μM (green) R-S to •cPTIO/H_2S (100/100 μM/μM). (D) The effect of H_2S on the kinetics of •cPTIO reduction in the presence of R-S. Kinetics of changes in absorbance at 560 nm of 100 μM •cPTIO after addition (indicated by an arrow) of 100 μM H_2S alone (dark yellow) and after addition of 50 μM R-S to 0 μM (dark green), 25 μM H_2S (red), 50 μM (blue), 100 μM (pink) and 200 μM H_2S (cyan). (E) Comparison of the potency of R-Se and R-S to reduce •cPTIO in the presence of H_2S. Reduction of •cPTIO (100 μM) by R-Se and R-S (100 μM) and reduction of •cPTIO in the presence of H_2S (100 μM) after addition of 0, 6.12, 12.5, 25, 50 and 100 μM R-Se or R-S. The changes in absorbance at 560 nm of 100 μM •cPTIO were taken from (A and C) at the 5th min after the addition of the compound. (F) Comparison of the potency of R-Se and R-S to reduce •cPTIO in the presence of different concentrations of H_2S. Reduction of •cPTIO (100 μM) by R-Se and R-S (50 μM) in the presence of 0, 25, 50, 100 and 200 μM H_2S. The changes in absorbance at 560 nm of 100 μM •cPTIO were taken from (B and D) at the 5th min after the addition of the compound. Mean ± SEM, n = 2–4.

(100/100 μM/μM) or GSH/•cPTIO (500/100 μM/μM) mixture reduced •cPTIO (decreased ABS at 356 and 560 nm) in <1 min

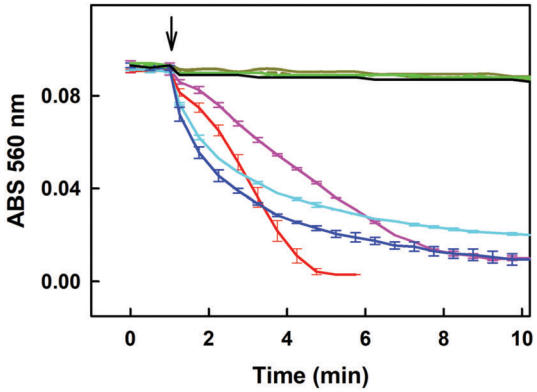

Fig. 7 Effect of GSH on the •cPTIO reduction kinetics in the presence of R-Se, R-S, R-O and R-OH. Kinetics of the changes in absorbance at 560 nm of 100 μM •cPTIO after addition (indicated by an arrow) of 100 (dashed dark-yellow) and 500 μM GSH (solid dark yellow); after addition of 50 μM R-Se to •cPTIO/GSH (100/200 μM/μM; pink), and to •cPTIO/GSH (100/500 μM/μM; red); after addition of 50 μM R-S to •cPTIO/GSH (100/200 μM/μM; cyan), and to •cPTIO/GSH (100/500 μM/μM; blue); after addition of 50 μM R-O to •cPTIO/GSH (100/200 μM/μM; dashed green), and to •cPTIO/GSH (100/500 μM/μM; solid green); and after addition of 50 μM R-OH to •cPTIO/GSH (100/500 μM/μM; black). Mean ± SEM, n = 2–3.

(Fig. 8D–F), indicating formation of reducing species during the interaction of Na_2Se-derivatives with H_2S and GSH which reduce the •cPTIO radical. The results support the suggestion that H_2S and GSH significantly potentiated the reducing properties of Se derivatives which are released from R-Se.

Discussion of the reduction of •cPTIO by phthalic-anhydride derivatives and H_2S

Regarding the reduction of the •cPTIO radical, R-S and R-Se showed a higher capacity to reduce this radical in comparison with H_2S. But H_2S was most effective in the reduction of the •cPTIO free radical compared to phthalic acid and phthalic anhydride. This fact suggests that the mechanism that explains this reduction must be related to a characteristic reaction of R-S and R-Se that is not demonstrated by R-O or by R-OH. A potential candidate for the reaction that led to this observation could be then the release of sulfide or selenide anions, respectively, as the release of O^{2-} is non-existent. All sulfide or selenide anions would probably be partially protonated in buffered solution. H_2S is produced endogenously and exerts relevant biological effects and functions. It can be found in tissue cells in non-negligible physiological concentrations that reach even higher than 1 μM.[55] Besides, its local space–time concentration in microenvironments can be even several times higher. This fact indicates that the H_2S/R-Se interaction may be involved also in the biological activities of R-Se. Thus, we have evaluated how it interacts with these chalcogen phthalic derivatives. The results were in line with the previous observations and supported our hypothesis of the S^{2-} and Se^{2-} release: the addition of H_2S to R-S and R-Se potentiated the above mentioned reduction of the •cPTIO radical. It is noteworthy that the addition of H_2S promoted the reduction exerted by R-Se more than the one induced by R-S. In contrast, the addition of H_2S to R-O and R-OH did not exert any effect. Interestingly, the

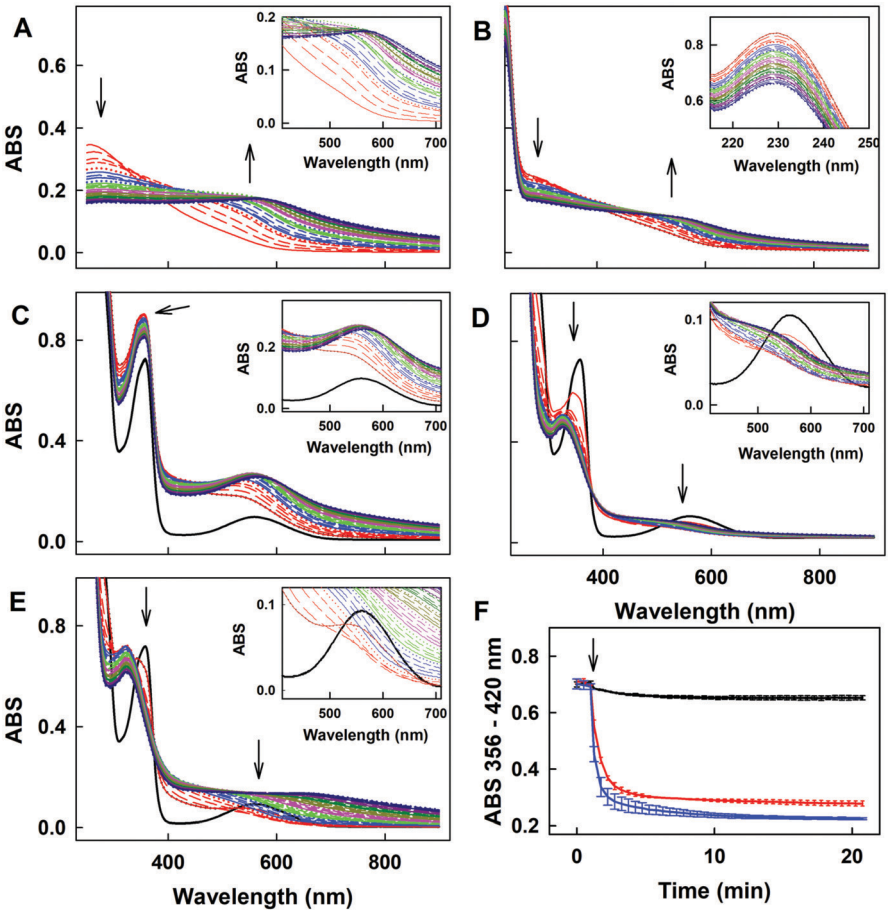

Fig. 8 UV-vis spectra of the interaction of Na_2Se with •cPTIO/H_2S and •cPTIO/GSH. (A) Time resolved UV-vis spectra of 100 μM Na_2Se in 100 mM sodium phosphate, 100 μM DTPA, pH 7.4 buffer at 37 °C. Spectra were collected every 30 s for 20 min, the first spectrum was measured 15 s after addition of Na_2Se. Insets are details. The first spectrum is indicated by the solid red line, which is followed each 30 s by: long dashed red, medium dashed red, short dashed red, dotted red, solid blue, long dashed blue, medium dashed blue, *etc.* (B) Time resolved UV-vis spectra of the interaction of 100 μM Na_2Se with 100 μM H_2S. Spectra were collected every 30 s for 20 min, the first spectrum, indicated by the solid red line, was measured 15 s after addition of Na_2Se to H_2S. Inset: Details of the time resolved spectra of HS^-, peak at 230 nm. (C) Time resolved UV-vis spectra of the interaction of 100 μM •cPTIO with 100 μM Na_2Se (•cPTIO – 3 times repeated every 30 s, black) and subsequent addition of 100 μM Na_2Se. Spectra were collected every 30 s for 20 min, the first spectrum, indicated by the solid red line, was measured 15 s after addition of Na_2Se. The arrow indicates ABS at 356 nm. Inset: Details of the time resolved spectra of the •cPTIO/Na_2Se (100/100 μM/μM) interaction before (black) and after addition of Na_2Se (100 μM). (D) Time resolved UV-vis spectra of the interaction of Na_2Se with •cPTIO/H_2S. Control •cPTIO/H_2S (100/100 μM/μM; 3 times repeated every 30 s, black), and subsequent addition of 100 μM Na_2Se. Spectra were collected every 30 s for 20 min, the first spectrum, indicated by the red line, was measured 15 s after addition of Na_2Se. The arrows indicate the decrease of ABS at 356 and 560 nm. Inset: Details of the time resolved spectra of the •cPTIO/H_2S (100/100 μM/μM) interaction before (black) and after addition of Na_2Se (100 μM). (E) Time resolved UV-vis spectra of the interaction of Na_2Se with •cPTIO/GSH. Control •cPTIO/GSH (100/500 μM/μM; 3 times repeated every 30 s, black), and subsequent addition of 100 μM Na_2Se. Spectra were collected every 30 s for 20 min, the first spectrum, indicated by the solid red line, was measured 15 s after addition of Na_2Se. The arrows indicate the decrease of ABS at 356 and 560 nm. Inset: Details of the time resolved spectra of the •cPTIO/GSH (100/500 μM/μM) interaction before (black) and after addition of Na_2Se (100 μM). (F) Kinetics of the interaction of Na_2Se (100 μM, marked by an arrow) with •cPTIO (100 μM, black), •cPTIO/H_2S (100/100 μM/μM, blue) and •cPTIO/GSH (100/500 μM/μM, red) monitored as changes of ABS at 356 nm with correction to 420 nm; mean ± SEM, n = 2–3.

interaction of H_2S with R-Se is dependent on the molar ratio between the Se analogue and H_2S: when R-Se is predominant or when both are equimolar, a low reduction is observed. However, when the molar ratio H_2S/R-Se is 2 to 4, the detected reduction increased significantly. This fact could suggest that a reaction between H_2S and R-Se takes place and that the concentration of the first potentiates this reaction, although the R-Se is also crucial as its replacement by R-S reduced the observed potentiation effect.

Another sulfur-containing biogenic compound with crucial functions is GSH, which can reach intracellular concentrations in the range 0.5–10 mM. Thus, we have also evaluated its interaction with the phthalic anhydride derivatives, as this interaction may be involved in the R-Se biological effects. And effectively similar results of potentiation of the R-Se and R-S ability to reduce the •cPTIO radical were obtained, being then again more significant for R-Se than for R-S. The phthalic anhydride derivatives could interact also with other components of the cellular thiolstat, or even with other different enzymes. For example, they could be activated through different cellular enzymes, such as disulfide reductases and esterases. However, further research

needs to be conducted in future work to confirm this extent. In this study we have selected GSH and H_2S as representative compounds of the sulfur containing components involved in the redox thiolstat. The enhancement of the R-Se activity with respect to the potentiation observed for R-S by the two thiols evaluated (H_2S and GSH) was observed and therefore we tested how H_2S and GSH reduced the •cPTIO radical in the absence of R-Se, finding that in this case there was no interaction. This confirms the key role of R-Se in this interaction, and the requirement of having both Se and S species to have a more effective interaction.

Cleavage of pDNA

We wanted to ascertain whether the products of the H_2S/R-Se and/or GSH/R-Se interaction can directly attack pDNA without the contribution of other (unknown) biologically important molecules and/or pathways. Briefly, the pDNA cleavage assay can detect any activity that attacks and disrupts the sugar-phosphate backbone of DNA (*e.g.*, reactive oxygen species, free radicals *etc.*).

H_2S and GSH interacting with phthalic-anhydride derivatives cleave pDNA. To compare the pDNA cleavage activity caused or mediated by the phthalic-anhydride derivatives, increasing concentrations of these compounds were incubated with pDNA *in vitro* and the resulting reaction mixtures were subjected to electrophoretic separation to resolve the individual pDNA forms. R-S, R-O or R-OH had only minor effects on pDNA cleavage. In contrast, R-Se cleaved pDNA in a concentration-dependent manner at concentrations $\geq$50 μM (Fig. 9).

Notably, H_2S modulated the pDNA cleavage activity of the anhydride derivatives depending on the H_2S/anhydride derivative molar ratio. In the presence of 50 μM of R-Se, increasing concentrations of H_2S caused bell-shaped effects with a maximum level being reached at 100/50 and 200/50 μM/μM H_2S/R-Se molar ratios. The effect of 50 μM of R-S, R-O and R-OH increased with increasing H_2S concentrations (Fig. 10A). In the presence of 100 μM H_2S, the pDNA cleavage activity of R-Se was several times higher in comparison to R-S, R-O or R-OH. Also GSH modulated the pDNA cleavage activity of the anhydride derivatives. In the presence of 50 μM R-Se, increasing concentrations of GSH mediated bell-shaped effects with a maximum level being seen at a 100/50 μM/μM GSH/R-Se molar ratio. In the presence of 50 μM R-S, R-O or R-OH, increasing concentrations of GSH had no effects on the pDNA cleavage (Fig. 10B).

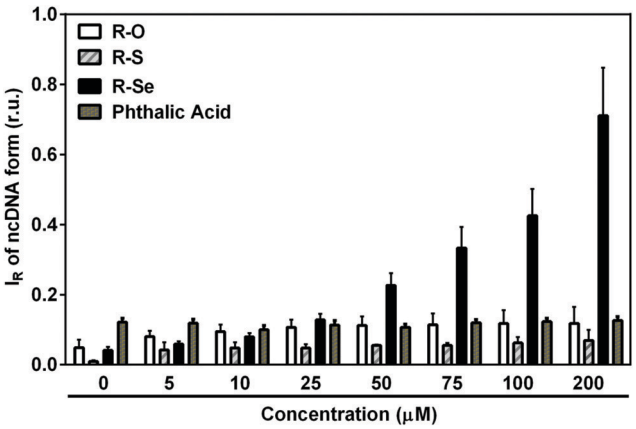

Fig. 9 The effect of anhydride-derivatives on pDNA integrity. Increasing concentrations of R-Se, R-S, R-O or phthalic acid were incubated with pDNA for 30 min at 37 °C and the resulting pDNA forms were resolved using agarose gel electrophoresis. Mean ± SEM, n = 3.

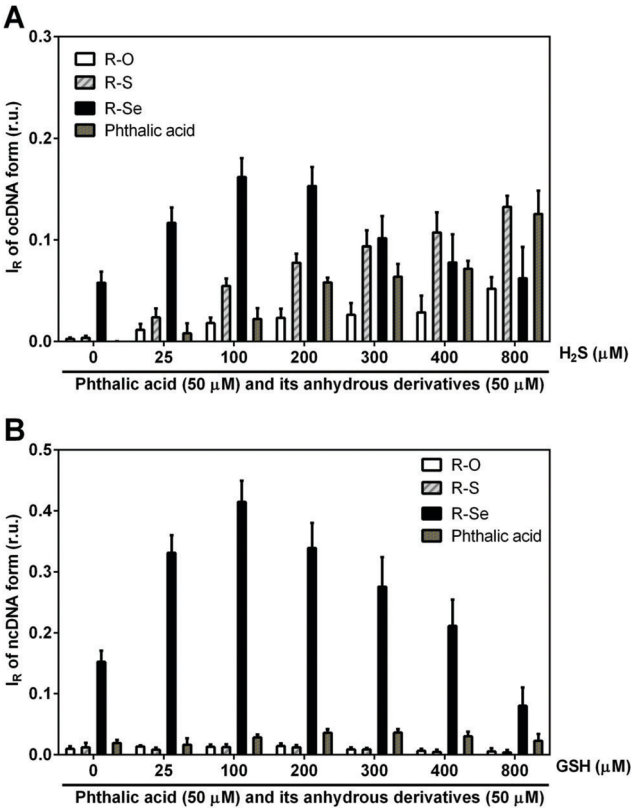

Fig. 10 The effect of increasing concentrations of H_2S (A) and GSH (B) on the pDNA integrity in the presence of the anhydride-derivatives R-Se, R-S, R-O and R-OH at 50 μM concentrations. Mean ± SEM, n = 3–5.

As we detected relatively similar pDNA cleavage efficiencies at 1 : 1 and 1 : 3 molar ratios of R-Se : H_2S, we checked whether there was a difference in kinetics between the two reactions. However, the two reactions displayed the same (linear) time-dependent pDNA cleavage efficiency, suggesting that within a 1 : 1–1 : 3 (R-Se : H_2S) molar ratio window, R-Se is a rate-limiting factor in the reaction (Fig. 11).

Summing up, we have observed that R-S, R-O and R-OH only exerted limited pDNA cleavage activity, whereas this activity increased significantly when R-Se was employed in a concentration-dependent manner. Interestingly, the addition of H_2S and GSH modulated strongly this pDNA cleavage action, and showed a bell-shaped effect, suggesting that the kinetics may be a rate-limiting factor in this action. In this case, the pDNA cleavage exerted by the remaining phthalic derivatives tested in the presence of H_2S increased in a concentration dependent manner with H_2S, which may be caused by the H_2S-related pDNA cleavage effect. Thus, it is noteworthy that the pDNA cleavage in the absence of H_2S and the bell-shaped modulation in the presence of H_2S and

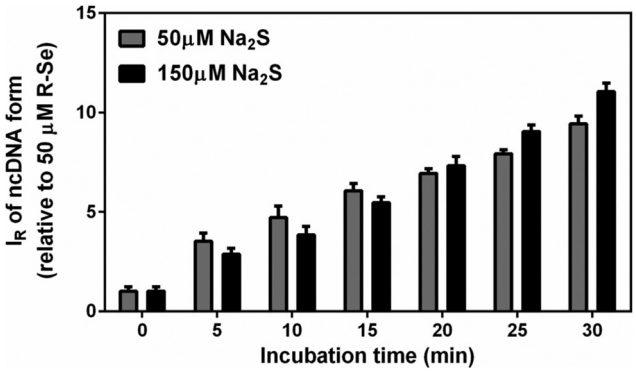

Fig. 11 Comparison of time-dependent pDNA cleavage by H_2S/R-Se at molar ratios 50/50 and 150/50 μM/μM. The H_2S/R-Se mixture was incubated with pDNA for the given time. I_R of ncDNA was normalized relative to 50 μM R-Se. Mean ± SEM, n = 3.

GSH are only observed when R-Se is employed, which underlines the unique redox-modulating properties of R-Se and indicates the possibility of the formation of a S–Se intermediate when H_2S interacts with R-Se.

The ability of R-Se, R-S and R-O without and with H_2S to scavenge the $O_2^{\bullet-}$ radical or its derivatives. Since we observed that the mixture of H_2S and R-Se or R-S significantly potentiated •cPTIO reduction, it was of interest to study if the mixture can scavenge $O_2^{\bullet-}$ radicals. The EPR spin trap method based on the reaction of $O_2^{\bullet-}$ with BMPO to form the •BMPO-OOH adducts (conformer I and II) were employed.[56] The $O_2^{\bullet-}$ radical anion solution (prepared by dissolving KO_2 in DMSO) was diluted in phosphate buffer (pH 7.4; 37 °C) and trapped by BMPO.

Under these conditions, the relative intensity of the •BMPO-OOH adducts decreased slowly over the time and was comparable to the values reported under physiological conditions (Fig. 12A1–A3).[56] The addition of R-Se or R-O (25 μM) had a minor effect on the •BMPO-OOH adducts formation, their concentration or rate of decay (Fig. 12B1–B3, D1–D3, 13A and B). In contrast, R-S (25 μM) significantly decreased the quantity of the •BMPO-adducts (Fig. 12C1–C3, 13A and B) and from the decreased ratio of the •BMPO-OOH/•BMPO-adducts (Fig. 12C and D), a superposition of at least two radicals, •BMPO-OOH and •BMPO-OH, was recognized. H_2S (50 μM) had similar effects to R-S, however its potency to decrease the quantity of the •BMPO-adducts and ratio of •BMPO-OOH/•BMPO-OH was lower in comparison to R-S (Fig. 12E1–E3 and 13).

The presence of H_2S (50 μM) in the R-Se or R-S (25 μM) solution significantly decreased the quantity of the •BMPO-adducts (Fig. 12F1–F3, G1–G3, 13A and B) and significantly decreased the ratio of the •BMPO-OOH/•BMPO-adducts (Fig. 13C and D), where a superposition of at least two radicals, •BMPO-OOH and •BMPO-OH, was recognized. Alternatively, a mixture of H_2S (50 μM) with R-O (25 μM) caused a similar effect to H_2S alone (Fig. 12H1–H3 and 13). Based on the decreasing quantity of the •BMPO-adducts, we suggest that R-S, H_2S/R-Se and H_2S/R-S scavenge the •BMPO-OOH/OH adducts, which may include direct scavenging of $O_2^{\bullet-}$ or its derivatives. The decreasing ratio of the •BMPO-OOH/•BMPO-adducts indicates that the compounds cause the decomposition

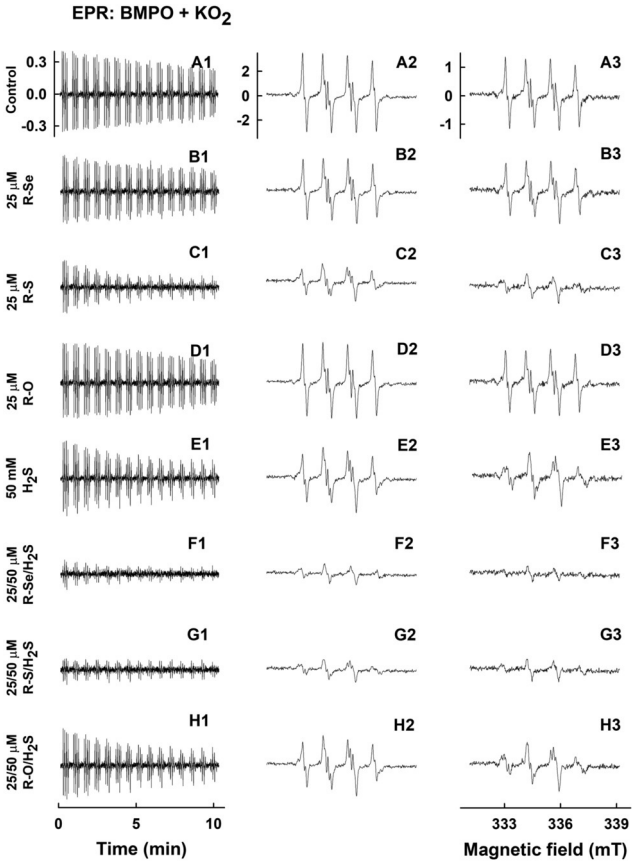

Fig. 12 EPR spectra of •BMPO in the presence of $O_2^{\bullet-}$ and modulated by R-Se, R-S and R-O without and with H_2S. Representative EPR spectra of the •BMPO-adducts were monitored in 10% v/v saturated KO_2/DMSO solution in 50 mM sodium phosphate buffer, 0.1 mM DTPA, pH 7.4, 37 °C in the presence of the studied species investigated and 20 mM BMPO. Sets of individual EPR spectra of the •BMPO-adducts monitored with 15 sequential scans, each 42 s (A1–H1), starting acquisition 2 min after sample preparation in: control 10% v/v KO_2/DMSO in the buffer (A1); KO_2/DMSO in the presence of 25 μM R-Se (B1); 25 μM R-S (C1); 25 μM R-O (D1); 50 μM H_2S (E1); a mixture of 25/50 μM/μM R-Se/H_2S (F1); a mixture of 25/50 μM/μM R-S/H_2S (G1) and a mixture of 25/50 μM/μM R-O/H_2S (H1). The spectra A2–H2 show details of the accumulated first ten A1–H1 spectra. The spectra A3–H3 show details of the accumulated last five A1–H1 spectra. The intensities of the time-dependent EPR spectra (A1–H1) and detailed spectra (A2–H2 and A3–H3) are comparable, as they were measured under identical EPR settings.

of •BMPO-OOH to •BMPO-OH and scavenge both •BMPO-adducts. However, we cannot exclude the possibility of trapping an unknown radical by BMPO which decomposed to •BMPO-OH before measurement of the sample. Our data suggest that R-S, H_2S/R-Se and H_2S/R-S have high potency to scavenge different radicals.

To summarize this section, taking into account the ability of the phthalic derivatives to reduce the •cPTIO radical, we have studied also how these derivatives interact with $O_2^{\bullet-}$, observing how they interfere with the formation of the •BMPO-OOH adduct in the presence of KO_2 and BMPO. In this experiment, R-Se and R-O showed a minor interaction with the $O_2^{\bullet-}$ radical, whereas R-S significantly decreased the formation of the •BMPO-OOH adducts. Interestingly, the addition of H_2S to R-Se and to R-S

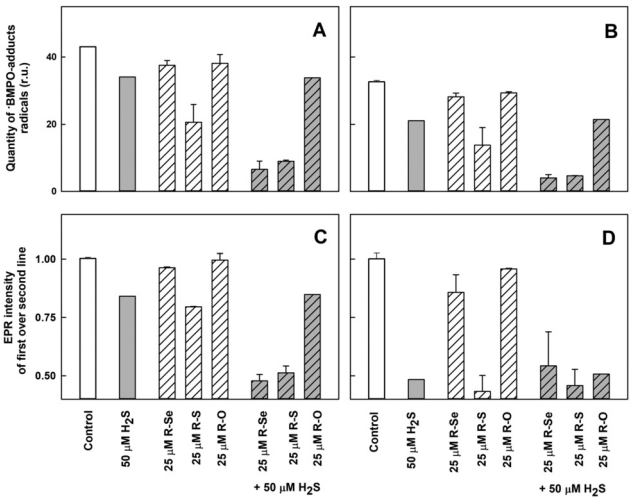

Fig. 13 The effects of the compounds on the •BMPO-adduct radicals. The effects of the compounds (25 μM) and their mixture with H_2S (50 μM) on the quantity of the •BMPO-adduct radicals (double integral of the EPR spectra from Fig. 12) in the presence of 10% v/v saturated KO_2/DMSO solution. Average radical quantity during 2–9 (A, from Fig. 12A2–H2) and 10–13 (B, from Fig. 12A3–H3) min after sample preparation. The effects of the compounds (25 μM) and their mixture with H_2S (50 μM) on the ratio of the EPR intensity of the first over the second line spectra of the •BMPO-adduct radicals (data from Fig. 12). Average ratio during 2–9 (C, from Fig. 12A2–H2) and 10–13 (D, from Fig. 12A3–H3) min after sample preparation. Buffer: 50 mM sodium phosphate, 0.1 mM DTPA, pH 7.4, 37 °C. Mean ± SEM, n = 2.

significantly enhances their capacity to decrease the formation of the •BMPO-OOH adduct, again highlighting the enhanced activity of the products of the interaction between H_2S and R-Se: the presence of both Se and S atoms seems to be crucial for all these activities.

Final discussion

At the sight of the results presented herein, we suggest that the products of the H_2S or GSH interaction with R-Se, having free radical scavenging and pDNA cleavage activities, can also affect intracellular molecules other than DNA. Based on the well-known consequences of oxidative stress, protein oxidation is also highly expected. We are aware of the fact that many more effects should be examined to obtain a more complete picture of the action of the products of the H_2S or GSH interaction with R-Se and our intention is to present these promising initial results.

In summary, the results confirm our initial hypothesis: selenoanhydride (R-Se) can act as a H_2Se donor, serving as a prodrug that enables the internalisation of selenium into cells, and the subsequent release of H_2Se and ionic species of Se inside the cell. Besides, we have proven that H_2S and GSH interact with R-Se, and that the intermediates and/or products of this interaction have significant properties to reduce (scavenge) the •cPTIO and superoxide ($O_2^{\bullet-}$) radicals or their derivatives and to cleave pDNA. The antioxidant (reducing) properties observed of the intermediates and/or products of the H_2S/R-Se and GSH/R-Se interaction to reduce •cPTIO, scavenge $O_2^{\bullet-}$ and decompose •BMPO-OOH to •BMPO-OH, indicate that they may modulate redox properties and free radical signalling. However, qualifying the significance of these observations is a challenge for future research.

Experimental

Chemical synthesis of the anhydride-derivatives

R-Se and R-S (Fig. 1) were synthetized according to a procedure based on the one previously described in the literature,[49] with minor modifications, whereas R-O was commercially available. Briefly, a suspension of grey selenium (for R-Se) or elemental sulfur (for R-S) in water-free tetrahydrofuran is reduced by dropwise addition of lithium aluminium hydride. Once the reaction is completed (visible by the ceasing of the generation of molecular hydrogen), phthaloyl chloride is added to the reaction and left reacting till the end of the reaction (usually 1 h). Then, the solution is filtered to eliminate the metallic salts generated during the process, and over the filtrate, 10 ml of concentrated sulfuric acid is added dropwise. The mixture is left reacting and the solid formed is filtered and washed with chloroform. The product isolated from the organic fraction is recrystallized in hexane.

The structure of the compounds R-Se and R-S was confirmed by ^{1}H-NMR, and their purity by LC-MS. Spectra are provided in the ESI† and they are in accordance with the literature. The purity of both compounds was 100% according to LC-MS (see data in the ESI†), so both derivatives were suitable for biological evaluation as they accomplished the 95% purity considered as the minimum threshold purity value required for biological assays. The chemical reactions of this synthetic procedure are shown in Fig. 1. It is quite interesting to see how the reaction normally used to get oxygen anhydrides (dehydration of phthalic acid) also serves to synthesize the sulfur and selenium anhydride analogues. What is more, it is noteworthy to point out the selectivity of the formation of the respective thio- and selenoanhydride when an oxygen atom is bound to the second carbonyl of the intermediate chalcogen phthalate.

In previous work in a PhD dissertation,[57] to learn more about the reactivity of different phthalic derivatives to form phthalic selenoanhydride (R-Se) following this procedure, a synthetic study was performed. R-Se was synthesized according to the procedure mentioned above, departing from phthaloyl chloride and using lithium aluminium hydride for the reaction. The yield before recrystallization in this case was 94%. When the reaction was carried out using water as a solvent and employing sodium borohydride as a reducing agent, the yield before recrystallization was 47%. The reaction could also use different phthalic derivatives as substrates (always employing lithium aluminium hydride), in this case with different yields. We explored phthalic anhydride and *N*-hydroxyphthalimide, achieving yields of 16% and 62%, respectively. Interestingly (unpublished results), phthalimide did not render R-Se after dehydration with sulfuric acid. It seems that a selenazine is formed instead of the selenoanhydride, obtaining 1*H*-benzo[*d*][1,2]selenazine-1,4(3*H*)-dione. Unfortunately, this

compound could not be obtained with a satisfactory purity and more research needs to be done to isolate and characterize this compound.

For the pDNA cleavage assay, the anhydride-derivatives were dissolved in ultrapure deionized water at a 1 mM final concentration by vortexing and 1 min water bath sonication, subsequently aliquoted and stored at −80 °C before their use. For UV-vis, EPR and ESI studies, the anhydride-derivatives were dissolved in anhydrous DMSO at a 50 mM concentration, aliquoted and stored at −80 °C before being used.

ESI-MS measurement

Saturated R-Se was prepared in 50% methanol/H_2O, vortexed for 2–3 min, sonicated in a water bath for 1–2 min and centrifuged for 2 min. The sample without and with 7 mM Na_2S (∼9 pH) was incubated for 1 min at 37 °C and 55 μl of the supernatant was used to measure ESI-MS spectra (Orbitrap Elite, ThermoScientific).

Chemicals for UV-vis and EPR measurements

The studied compounds R-Se, R-S and R-O in DMSO (50 mM) were used after thawing. The spin trap 5-*tert*-butoxycarbonyl-5-methyl-1-pyrroline-*N*-oxide (BMPO, 100 mM, ENZO Life Sciences AG, Switzerland) was prepared in deionized H_2O, stored at −80 °C and used after thawing. The radical 2-(4-carboxyphenyl)-4,4,5,5-tetramethylimidazoline-1-oxyl-3-oxide (•cPTIO, 10 mM, Cayman 81540 or Sigma C221) in deionized H_2O was stored at −20 °C for several weeks. Na_2S as a source of H_2S (100 mM; SB01, DoJindo, Japan) was prepared in deionized H_2O, stored at −80 °C and used after thawing. Na_2S dissociates in solution and reacts with H^+ to yield H_2S, HS^- and a trace of S^{2-}. We use the term H_2S to encompass the total mixture of H_2S, HS^- and S^{2-}. To Na_2Se powder (Alfa Aesar, 36187, stored under argon) H_2O was added, and in 10 s an aliquot of the stock Na_2Se solution (10 mM) was added to a UV-vis cuvette containing the studied compounds. 100 mM sodium phosphate buffer supplemented with 100 μM DTPA, pH 7.4, 37 °C, was employed for UV-vis experiments. 50 and 25 mM sodium phosphate buffer, supplemented with 100 and 50 μM DTPA (diethylenetriaminepentaacetic acid), pH 7.4, 37 °C was used for electron paramagnetic resonance (EPR) studies.

UV-vis of •cPTIO

To a basic 900–990 μl solution of 100 mM sodium phosphate, 100 μM DTPA buffer (pH 7.4, 37 °C) the required aliquots of 100 μM •cPTIO and Na_2S were added to obtain the desired final concentrations of •cPTIO and Na_2S. Then, the UV-vis spectra (900–190 nm) were recorded, 3 × 30 s. The studied compounds R-Se, R-S and R-O (50 mM in DMSO), firstly dissolved in 50 μl buffer and vortexed for 3 s, were added and the spectra were recorded every 30 s for 20 min using a Shimadzu 1800 (Kyoto, Japan) spectrometer at 37 °C (the blank was H_2O). For our study, the •cPTIO extinction coefficient at 560 nm of 920 M^{-1} cm^{-1} was used. Scavenging of the •cPTIO radical by Na_2S (H_2S) or GSH and its mixture with the studied compounds R-Se, R-S and R-O was determined as a decrease of absorbance at 356 and 560 nm (the absorption maximum of •cPTIO) after subtraction of the baseline absorbance, which was determined at 730 or 420 nm, respectively.[42]

Plasmid DNA cleavage

The pDNA cleavage assay, which detects a disruption of the sugar-phosphate backbone of DNA, was used to study if the products of the H_2S/R-Se and/or GSH/R-Se interaction can directly attack pDNA. In this assay, even a single hit is trapped, as it converts the circular supercoiled DNA molecule into its nicked relaxed circular form. These two forms display distinct mobility in agarose gels, and therefore they can easily be distinguished and quantified.

The pBR322 vector (4.361 kb, New England Biolabs, N3033L) was used in the pDNA cleavage assay. In this assay, all samples contained 200 ng of pDNA in a final volume of 20 μl of buffer composed of 25 mM sodium phosphate and 50 μM DTPA (pH 7.4). Three different assay conditions were used: (i) pDNA *per se* (control), (ii) pDNA + phthalic-anhydride derivatives, and (iii) pDNA + anhydride-derivative + Na_2S or GSH. The resulting mixtures were incubated for 30 min at 37 °C. Afterwards, the reaction mixtures were subjected to 0.6% agarose gel electrophoresis. The samples were electrophoresed in TBE buffer (89 mM Tris, 89 mM boric acid, 2 mM EDTA, pH 8.0) at 5.5 V cm^{-1} for 2 h. The gel was stained with Gel Red™ nucleic acid gel stain. Finally, the gels were photographed using a UV transilluminator. To quantify the pDNA cleavage efficiency, the integrated densities of two identified pBR322 forms (a supercoiled and a nicked circular form) in each lane were quantified using Total Lab TL100 image analysis software (Nonlinear Dynamic Ltd, USA).

EPR of •BMPO-adducts

To study the ability of R-Se, R-S and R-O without and with H_2S to scavenge the $O_2^{\bullet-}$ radical produced in DMSO/KO_2 solution, sample preparation and EPR measurements were conducted in accordance with previously reported protocols.[42] A solution (final concentrations) of BMPO (20 mM) and DTPA (100 μM) in sodium phosphate buffer (50 mM, pH 7.4) was incubated for 1 min at 37 °C. An aliquot of the compounds studied was added, followed by the addition of Na_2S in 3 s and saturated KO_2/DMSO solution (10% v/v DMSO/final buffer) 3 s later. The sample was mixed for 5 s and the first EPR spectrum was recorded 2 min after the addition of KO_2/DMSO solution at 37 °C. Sets of individual EPR spectra of the •BMPO spin-adducts were recorded as 15 sequential scans, each 42 s, with a total time of 11 min. Each experiment was repeated at least twice. EPR spectra of the •BMPO spin-adducts were measured on a Bruker EMX spectrometer, X-band ∼9.4 GHz, 335.15 mT central field, 8 mT scan range, 20 mW microwave power, 0.1 mT modulation amplitude, 42 s sweep time, 20.48 ms time constant, and 20.48 ms conversion time at 37 °C.

The relative quantity of the •BMPO-adduct radicals was calculated as a double integral of the EPR spectra. Since the EPR spectra were mostly low intensity, which did not permit spectral simulation, to quantify the relative ratio of the •BMPO-OOH/•BMPO-adducts, the ratio of the EPR intensity of the first line over the second line was used. The ratio is ∼1 at ∼100% of

•BMPO-OOH (Fig. 12A2) and ~0.5 at ~0% of •BMPO-OOH.[42] A lower ratio (lower than 1) indicates a higher concentration of other •BMPO-adducts, in which mostly •BMPO-OH radicals are present.

Conclusions

Understanding the molecular mechanism of the biological effects of phthalic-anhydride derivatives could lead to development of more efficient drugs for treatment of cancer and ROS related diseases. To achieve this, we found that phthalic-anhydride derivatives R-Se, R-S, R-O and R-OH (≤ 50 μM) on their own have minor potency to reduce/scavenge radicals or cleave pDNA. However, the potency of R-Se and R-S, but not R-O or R-OH, significantly increased after interacting with H_2S and GSH.

Our *in vitro* data revealed unique properties of the H_2S/R-Se, GSH/R-Se and H_2S/R-S mixtures to reduce the •cPTIO and superoxide radicals. The unique potency of the H_2S/R-Se mixture to cleave pDNA has a bell-shaped dependence on the H_2S and GSH concentrations, whereas the potency of H_2S/R-S increased linearly with H_2S, but did not increase with the GSH concentration. The results underline that the interactions of R-Se and R-S with H_2S and GSH enhanced significantly the different activities monitored, thus indicating that the intermediates and/or the products of the interaction of R-Se and R-S with endogenous H_2S and GSH, which appear to include reactive selenium species such as H_2Se, have significant antioxidant properties and that they can damage DNA. These findings may contribute to a more-in-depth understanding of the unique biological effects reported so far for R-Se and R-S. Besides, these findings open a new so far unexplored approach to study the action of Se-containing compounds. These experiments, for example, can be applied to the different selenium species that have been used until now in supplementation, to ascertain which ones have more ability to interact with GSH and H_2S. This is of crucial importance, as it would enable detecting new compounds that could behave as Se-based redox modulators in potential Se supplementation. An example would be the phthalic selenoanhydride (R-Se) reported in this work, which retains the capacity of sodium selenite to react with key components of the redox thiolstat (such as GSH and H_2S) and simultaneously, according to previous work, shows lower toxicity against non-tumour cells.

Author contributions

Conceptualization, E. D.-A., C. J., M. C., and K. O.; methodology, K. O., M. C., and V. B.; validation, K. O., M. C., V. B., A. M., M. G., and E. D.-A.; formal analysis, A. M., and K. O.; investigation, A. M., M. G., A. K., V. B., L. K., P. B., M. C., K. O., and E. D.-A.; resources, A. K., C. J., and E. D.-A.; writing – original draft preparation, K. O., M. C., and E. D.-A.; visualization, K. O., A. M., M. G., and E. D.-A.; supervision, K. O., C. J., M. C., and E. D.-A.; project administration, K. O., C. J., M. C., and E. D.-A.; funding acquisition, K. O.

Conflicts of interest

There are no conflicts to declare.

Acknowledgements

This research was funded by the Slovak Research & Development Agency, grant numbers APVV-15-0371, 15-0565 and 17-0384, and the Scientific Grant Agency of the Slovak Republic, grant numbers VEGA 1/0026/18, 2/0079/19, 2/0014/17 and 2/0053/19. The authors would also like to acknowledge the financial support of the Agencia Estatal Consejo Superior de Investigaciones Científicas (Spain, project 201780I027) and of the University of Saarland (through the Landesforschungsförderungsprogramm (LFPP) of the state of Saarland, Grant No. WT/2-LFFP 16/01). We also acknowledge the INTERREG-VA GR program (BIOVAL, Grant No. 4-09-21) and the NutRedOx (COST Project CA16112), as well as the support of the Erasmus+ program. We also thank Prof. Dr Anna K. H. Hirsch and Dr Eleonora Diamanti from Helmholtz Institute for Pharmaceutical Research in Saarland (HIPS) for helping with MS spectra measurements.

Notes and references

1 S. J. Fairweather-Tait and K. Cashman, in *Nutrition for the Primary Care Provider. World Rev. Nutr. Diet.*, ed. D. M. Bier, J. Mann, D. H. Alpers, H. H. E. Vorster and M. J. Gibney, Karger AG, Basel, Switzerland, 2015, ch. 8, vol. 111, pp. 45–52.
2 S. Li, T. Xiao and B. Zheng, *Sci. Total Environ*, 2012, **421–422**, 31–40.
3 S. Stranges, J. R. Marshall, R. Natarajan, R. P. Donahue, M. Trevisan, G. F. Combs, F. P. Cappuccio, A. Ceriello and M. E. Reid, *Ann. Intern. Med.*, 2007, **147**, 217–223.
4 D. L. Hatfield, M. H. Yoo, B. A. Carlson and V. N. Gladyshev, *Biochim. Biophys. Acta, Gen. Subj.*, 2009, **1790**, 1541–1545.
5 J. C. Avery and P. R. Hoffmann, *Nutrients*, 2018, **10**, 1203.
6 N. Shang, X. Wang, Q. Shu, H. Wang and L. Zhao, *J. Nanosci. Nanotechnol.*, 2019, **19**, 1875–1888.
7 K. M. Peters, B. A. Carlson, V. N. Gladyshev and P. A. Tsuji, *Free Radical Biol. Med.*, 2018, **127**, 14–25.
8 V. Gandin, P. Khalkar, J. Braude and A. P. Fernandes, *Free Radical Biol. Med.*, 2018, **127**, 80–97.
9 M. Bodnar, M. Szczyglowska, P. Konieczka and J. Namiesnik, *Crit. Rev. Food Sci. Nutr.*, 2016, **56**, 36–55.
10 A. Tarze, M. Dauplais, I. Grigoras, M. Lazard, N. T. Ha Duong, F. Barbier, S. Blanquet and P. Plateau, *J. Biol. Chem.*, 2007, **282**, 8759–8767.
11 A. P. Fernandes and V. Gandin, *Biochim. Biophys. Acta, Gen. Subj.*, 2015, **1850**, 1642–1660.
12 J. J. An, K. J. Shi, W. Wei, F. Y. Hua, Y. L. Ci, Q. Jiang, F. Li, P. Wu, K. Y. Hui, Y. Yang and C. M. Xu, *Cell Death Dis.*, 2013, **4**, e973.
13 G. Nilsonne, X. Sun, C. Nyström, A. K. Rundlöf, A. Potamitou Fernandes, M. Björnstedt and K. Dobra, *Free Radical Biol. Med.*, 2006, **41**, 874–885.

14 J. Brozmanová, D. Mániková, V. Vlčková and M. Chovanec, *Arch. Toxicol.*, 2010, **84**, 919–938.
15 E. Jablonska and M. Vinceti, *J. Environ. Sci. Health, Part C: Environ. Carcinog. Ecotoxicol. Rev.*, 2015, **33**, 328–368.
16 H. J. Reich and R. J. Hondal, *ACS Chem. Biol.*, 2016, **11**, 821–841.
17 R. Mousa, R. Notis Dardashti and N. Metanis, *Angew. Chem., Int. Ed.*, 2017, **56**, 15818–15827.
18 C. Jacob, G. I. Giles, N. M. Giles and H. Sies, *Angew. Chem., Int. Ed.*, 2003, **42**, 4742–4758.
19 L. Sancineto, M. Palomba, L. Bagnoli, F. Marini and C. Santi, *Curr. Org. Chem.*, 2016, **20**, 122–135.
20 D. Bartolini, L. Sancineto, A. Fabro de Bem, K. D. Tew, C. Santi, R. Radi, P. Toquato and F. Galli, in *Advances in Cancer Research*, ed. K. D. Tew and F. Galli, Academic Press Inc., Cambridge, USA, 2017, ch. 10, vol. 136, pp. 259–302.
21 C. Santi, C. Tomassini and L. Sancineto, *Chimia*, 2017, **71**, 592–595.
22 M. Álvarez-Pérez, W. Ali, M. A. Marć, J. Handzlik and E. Domínguez-Álvarez, *Molecules*, 2018, **23**, 628.
23 W. Ali, M. Álvarez-Pérez, M. A. Marć, N. Salardón-Jiménez, J. Handzlik and E. Domínguez-Álvarez, *Curr. Pharmacol. Rep.*, 2018, **4**, 468–481.
24 S. Misra, M. Boylan, A. Selvam, J. E. Spallholz and M. Björnstedt, *Nutrients*, 2015, **7**, 3536–3556.
25 C. M. Weekley and H. H. Harris, *Chem. Soc. Rev.*, 2013, **42**, 8870–8894.
26 R. Terazawa, D. R. Garud, N. Hamada, Y. Fujita, T. Itoh, Y. Nozawa, K. Nakane, T. Deguchi, M. Koketsu and M. Ito, *Bioorg. Med. Chem.*, 2010, **18**, 7001–7008.
27 B. Romano, D. Plano, I. Encío, J. A. Palop and C. Sanmartín, *Bioorg. Med. Chem.*, 2015, **23**, 1716–1727.
28 Y. Zakharia, A. Bhattacharya and Y. M. Rustum, *Oncotarget*, 2018, **9**, 10765–10783.
29 C. Santi, C. Tidei, C. C. Scalera, M. Piroddi and F. Galli, *Curr. Chem. Biol.*, 2013, **7**, 25–36.
30 D. Bartolini, M. Piroddi, C. Tidei, S. Giovagnoli, D. Pietrella, Y. Manevich, K. D. Tew, D. Giustarini, R. Rossi, D. M. Townsend, C. Santi and F. Galli, *Free Radical Biol. Med.*, 2015, **78**, 56–65.
31 M. M. Rahman, R. A. Uson-Lopez, M. T. Sikder, G. Tan, T. Hosokawa, T. Saito and M. Kurasaki, *Chemosphere*, 2018, **196**, 453–466.
32 M. Mix, N. Ramnath, J. Gomez, C. De Groot, S. Rajan, S. Dibaj, W. Tan, Y. Rustum, M. B. Jameson and A. K. Singh, *World J. Clin. Oncol.*, 2015, **6**, 156–165.
33 D. Mániková, L. M. Letavayová, D. Vlasáková, P. Košík, E. C. Estevam, M. J. Nasim, M. Gruhlke, A. Slusarenko, T. Burkholz, C. Jacob and M. Chovanec, *Molecules*, 2014, **19**, 12258–12279.
34 C. Sanmartín, D. Plano, M. Font and J. A. Palop, *Curr. Cancer Drug Targets*, 2011, **11**, 496–523.
35 R. Wang, *Physiol. Rev.*, 2012, **92**, 791–896.
36 C. Szabo and A. Papapetropoulos, *Pharmacol. Rev.*, 2017, **69**, 497–564.
37 H. Kimura, *Antioxid. Redox Signaling*, 2015, **22**, 362–376.
38 M. Whiteman, J. S. Armstrong, S. H. Chu, S. Jia-Ling, B. S. Wong, N. S. Cheung, B. Halliwell and P. K. Moore, *J. Neurochem.*, 2004, **90**, 765–768.
39 M. Whiteman, N. S. Cheung, Y. Z. Zhu, S. H. Chu, J. L. Siau, B. S. Wong, J. S. Armstrong and P. K. Moore, *Biochem. Biophys. Res. Commun.*, 2005, **326**, 794–798.
40 A. Staško, V. Brezová, M. Zalibera, S. Biskupič and K. Ondriaš, *Free Radical Res.*, 2009, **43**, 581–593.
41 B. Olas, *Chem.-Biol. Interact.*, 2014, **217**, 46–56.
42 A. Misak, M. Grman, Z. Bacova, I. Rezuchova, S. Hudecova, E. Ondriasova, O. Krizanova, V. Brezova, M. Chovanec and K. Ondrias, *Nitric oxide*, 2018, **76**, 136–151.
43 C. Szabo, C. Coletta, C. Chao, K. Módis, B. Szczesny, A. Papapetropoulos and M. R. Hellmich, *Proc. Natl. Acad. Sci. U. S. A.*, 2013, **110**, 12474–12479.
44 D. Wu, W. Si, M. Wang, S. Lv, A. Ji and Y. Li, *Nitric oxide*, 2015, **50**, 38–45.
45 J. Breza Jr., A. Soltysova, S. Hudecova, A. Penesova, I. Szadvari, P. Babula, B. Chovancova, L. Lencesova, O. Pos, J. Breza, K. Ondrias and O. Krizanova, *BMC Cancer*, 2018, **18**, 591.
46 V. I. Lushchak, *J. Amino Acids*, 2012, 736837.
47 C. Gaucher, A. Boudier, J. Bonetti, I. Clarot, P. Leroy and M. Parent, *Antioxidants*, 2018, **7**, 62.
48 A. Kharma, M. Grman, A. Misak, E. Domínguez-Álvarez, M. J. Nasim, K. Ondrias, M. Chovanec and C. Jacob, *Molecules*, 2019, **24**, 1359.
49 E. Domínguez-Álvarez, D. Plano, M. Font, A. Calvo, C. Prior, C. Jacob, J. A. Palop and C. Sanmartín, *Eur. J. Med. Chem.*, 2014, **73**, 153–166.
50 M. J. Nasim, W. Ali, E. Domínguez-Álvarez, E. N. da Silva Júnior, R. S. Z. Saleem and C. Jacob, in *Organoselenium Compounds in Biology and Medicine: Synthesis, Biological and Therapeutic Treatments*, ed. V. K. Jain and K. I. Priyadarsini, The Royal Society of Chemistry, Croydon, UK, 2018, ch. 10, pp. 277–302.
51 M. Gajdács, G. Spengler, C. Sanmartín., M. A. Marć, J. Handzlik and E. Domínguez-Álvarez, *Bioorg. Med. Chem. Lett.*, 2017, **27**, 797–802.
52 E. Domínguez-Álvarez, M. Gajdács, G. Spengler, J. A. Palop, M. A. Marć, K. Kieć-Kononowicz, L. Amaral, J. Molnár, C. Jacob, J. Handzlik and C. Sanmartín, *Bioorg. Med. Chem. Lett.*, 2016, **26**, 2821–2824.
53 M. M. Cortese-Krott, G. G. C. Kuhnle, A. Dyson, B. O. Fernandez, M. Grman, J. F. DuMond, M. P. Barrow, G. McLeod, H. Nakagawa, K. Ondrias, P. Nagy, S. B. King, J. E. Saavedra, L. K. Keefer, M. Singer, M. Kelm, A. R. Butler and M. Feelisch, *Proc. Natl. Acad. Sci. U. S. A.*, 2015, **112**, E4651–E4660.
54 M. T. Zimmerman, C. A. Bayse, R. R. Ramoutar and J. L. Brumaghim, *J. Inorg. Biochem.*, 2015, **145**, 30–40.
55 Y. H. Liu, M. Lu, L. F. Hu, P. T. H. Wong, G. D. Webb and J. S. Bian, *Antioxid. Redox Signaling*, 2012, **17**, 141–185.
56 H. Zhao, J. Joseph, H. Zhang, H. Karoui and B. Kalyanaraman, *Free Radical Biol. Med.*, 2001, **31**, 599–606.
57 E. Domínguez-Álvarez, PhD Dissertation, University of Navarra, Spain, 2012.

3.3. Publication 3

Synthesis of quinone imine and sulphur containing-compounds with antitumor and trypanocidal activities: redox and biological implications

Renata G. Almeida, Wagner O. Valença, Luísa G. Rosa, Carlos A. de Simone, Solange L. de Castro, Juliana M. C. Barbosa, Daniel P. Pinheiro, Carlos R. K. Paier, Guilherme G. C. de Carvalho, Claudia Pessoa, Marilia O. F. Goulart, **Ammar Kharma** and Eufrânio N. da Silva Júnior*

RSC Medicinal Chemistry, 11, 1145-1160, (2020)

https://doi.org/10.1039/D0MD00072H

RSC Medicinal Chemistry

ROYAL SOCIETY OF CHEMISTRY

RESEARCH ARTICLE

View Article Online
View Journal

Cite this: DOI: 10.1039/d0md00072h

Synthesis of quinone imine and sulphur-containing compounds with antitumor and trypanocidal activities: redox and biological implications†

Renata G. Almeida, ‡[a] Wagner O. Valença, ‡[ab] Luísa G. Rosa, [a] Carlos A. de Simone,[c] Solange L. de Castro, [d] Juliana M. C. Barbosa, [d] Daniel P. Pinheiro, [e] Carlos R. K. Paier, [e] Guilherme G. C. de Carvalho,[e] Claudia Pessoa, [e] Marilia O. F. Goulart, [f] Ammar Kharma [ag] and Eufrânio N. da Silva Júnior *[a]

Received 3rd March 2020,
Accepted 8th June 2020

DOI: 10.1039/d0md00072h

rsc.li/medchem

Ortho-Quinones represent a special class of redox active compounds associated with a spectrum of pronounced biological activities, including selective cytotoxicity and antimicrobial actions. The modification of the quinone ring by simple nitrogen and sulphur substitutions leads to several new classes of compounds with their own, distinct redox behaviour and equally distinct activities against cancer cell lines and *Trypanosoma cruzi*. Some of the compounds investigated show activity against *T. cruzi* at concentrations of 24.3 and 65.6 μM with a selectivity index of around 1. These results demonstrate that simple chemical modifications on the *ortho*-quinone ring system, in particular, by heteroatoms such as nitrogen and sulphur, transform these simple redox molecules into powerful cytotoxic agents with considerable "potential", not only in synthesis and electrochemistry, but also, in a broader sense, in health sciences.

1. Introduction

The rapid expansion and simultaneous ageing of populations around the globe represent a demographical change and a challenge that, among many other issues, such as shortage of nutrition and increase of pollution, is also associated with higher incidence of new cases of cancer and related deaths. The projection for the year 2030 estimates 27 million new cases of cancer with 17 million cancer-related deaths worldwide.[1] At the same time, an increased global population is also more susceptible to the outbreak and spread of infectious diseases, such as Chagas disease. This disease is caused by the protozoan *Trypanosoma cruzi*, which is considered by the World Health Organization (WHO) as one of the twenty neglected tropical diseases, affecting more than 5 million people worldwide. Its current chemotherapy is still restricted to the nitroderivatives benznidazole and nifurtimox, available for half a century, which present limited activity and severe adverse effects.[2–8] These demographical developments and new ways of transmission, combined with the emergence of drug resistance, require new and effective drugs for the treatment of such diseases, *i.e.* agents which may be effective as (cyto)toxins and also selective for their targets.

Within this context, naphthoquinoidal compounds have been studied widely.[9–13] The derivatization of naphthoquinones has been a subject of considerable interest among medicinal chemists and a wide variety of natural and synthetic naphthoquinones have already been reported as potent trypanocidal and anticancer agents.[14–17] Mechanistically, the quinone core may undergo one-electron reduction under aerobic conditions to form a semiquinone radical which will redox cycle to release reactive oxygen species (ROS).[10,18–20] Within the context of cancer, the cytotoxicity of quinones is therefore mainly associated with the catalytic generation of ROS and the alkylation of crucial proteins and nucleic acids, both

[a] Institute of Exact Sciences, Department of Chemistry, Federal University of Minas Gerais, Belo Horizonte, 31270-901, MG, Brazil. E-mail: eufranio@ufmg.br
[b] Center for the Development of Chemical Technologies, State University of Mato Grosso do Sul, Naviraí, 79950-000, MS, Brazil
[c] Department of Physics and Informatics, Institute of Physics, University of São Paulo, São Carlos, 13560-160, SP, Brazil
[d] Oswaldo Cruz Institute, FIOCRUZ, Rio de Janeiro, 21045-900, RJ, Brazil
[e] Department of Physiology and Pharmacology, Federal University of Ceará, Fortaleza, CE, 60430-270, Brazil
[f] Institute of Chemistry and Biotechnology, Federal University of Alagoas, CEP 57072-970, Maceió, AL, Brazil
[g] Division of Bioorganic Chemistry, School of Pharmacy, University of Saarland, D-66123 Saarbruecken, Germany

† Electronic supplementary information (ESI) available. CCDC 1928261, 1928296, 1928326, 1928361, 1928382 and 1928407. For ESI and crystallographic data in CIF or other electronic format see DOI: 10.1039/d0md00072h

‡ These authors contributed equally to this work.

processes, which provoke cell damage.[14–16] Similar considerations also apply to pathogenic microorganisms, some of which are affected considerably by – similar – redox modulating agents thanks to their weak(er) cellular antioxidant defence systems. Indeed, the concept of catalytic "sensor/effector" agents, *i.e.* "smart" redox molecules responding to specific intracellular redox signatures and peculiarities, and thereby combining considerable activity with selectivity, has been evaluated for over a decade now, often with amazing results.[21–23]

For almost twenty years, our groups have been involved in the synthesis and biological evaluation of naphthoquinones.[24–26] Whilst initial studies on such catalytic agents have employed comparably simple redox agents, subsequent ones have developed hybrid molecules with two or more redox sites integrated into one molecule. The hybridization of a triazole nucleus with β-lapachone, for instance, has already resulted in a derivative with high antitumor activity ($IC_{50} < 2$ μM) for different cancer lineages and, more recently, we have also reported the antitumor activity of selenium-containing quinone-based triazoles, which were inspired by earlier quinone–chalcogen structures tested more than a decade ago (Scheme 1A).[21,27–29] Quinone-based *N*-sulfonyl-1,2,3-triazoles were also prepared by our group using click chemistry reactions (Scheme 1B).[30] In this

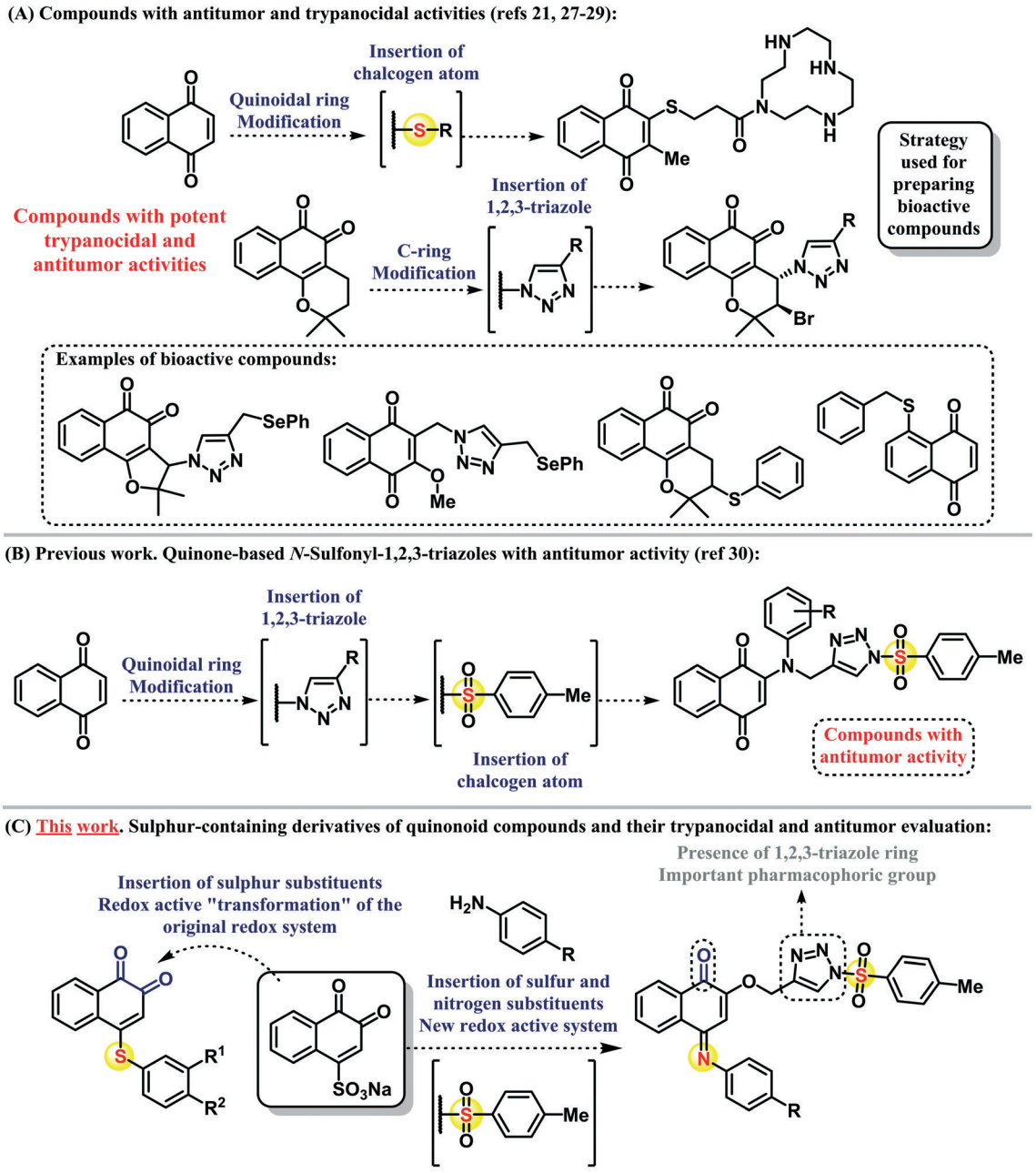

Scheme 1 A schematic overview of the strategies employed in the preparation of bioactive compounds and transformation of *ortho*-quinones into *para*-quinone imines and sulphur containing compounds.

work, we employed as a strategy the insertion of the 1,2,3-triazolic nucleus associated with a chalcogen atom, allowing the formation of a redox active system. The compounds were subsequently evaluated against eight types of cancer cell lines and some derivatives exhibited potent antitumor activity.[30] Interestingly, the application of such "smart" catalytic agents is not limited to cancer research, and a pronounced – and selective – cytotoxicity also affects protozoan pathogens, such as *T. cruzi*, with some molecules exhibiting trypanocidal activity about two or six times higher than that of the standard drug benznidazole.[31–35]

Interestingly, the *ortho*-quinone redox centre found in β-lapachone is prone to chemical modifications which impact considerably the redox behaviour of these agents.[10] Here, we have investigated modifications with nitrogen and sulphur substituents, as both heteroatoms are redox active and, besides electronic effects, promise a major "transformation" of the original redox system into considerably more active species (Scheme 1C). We are now able to report the synthesis, electrochemistry, anticancer and trypanocidal evaluation of quinoidal derivatives containing alkynes and *N*-sulfonyl triazoles and propose a distinct relationship between the chemical structure and redox system, and their electrochemical potentials and biological activities.

2. Results and discussion

2.1. Chemistry

The first class of compounds with a nitrogen substituent at the ring was prepared from commercially available 1,2-naphthoquinone-4-sulfonic acid sodium salt (**1**). Initially, we prepared arylamino naphthoquinones (**2a–h**) by the reaction of **1** and the respective anilines following a procedure published previously in the literature with minor modifications.[36–38] In general, the desired products were obtained in moderate to excellent yields (Scheme 2). It should be noted from the outset that these compounds now possess more complicated redox cores spanning the original *ortho*-quinone and the amine functionality in the *para*-position.

With the quinoidal compounds **2a–h** available, the changed "redox core" was modified further, this time by alkylation of one of the oxygen atoms. Notably, this kind of alkylation not only simply "blocks" one of the oxygen atoms of the *ortho*-quinone, it also transforms the electronic structure of the entire ring system by engaging the nitrogen in the *para*-position in the form of a distinctive *para*-quinone imine redox core (Scheme 3).[39,40] The consequences of this apparently innocent *O*-alkylation for the redox and biological activity will be discussed later. Eight alkyne derivatives **3a–h** were synthesized in moderate to excellent yields ranging from 48% to 99% according to Scheme 3 and in the presence of DMF as a solvent, excess K_2CO_3 as a base, and propargyl bromide.

Alkynes derived from *ortho*-naphthoquinones represent important intermediates for the synthesis of 1,2,3-triazole derivatives, and such molecules can be synthesized easily by means of a 1,3-dipolar cycloaddition reaction between an azide and alkyne using copper(I) as a catalyst, in a process known as a click chemistry reaction (Scheme 4). This type of reaction is considered an important tool to synthesize hybrid molecules with two or more redox centres and pronounced

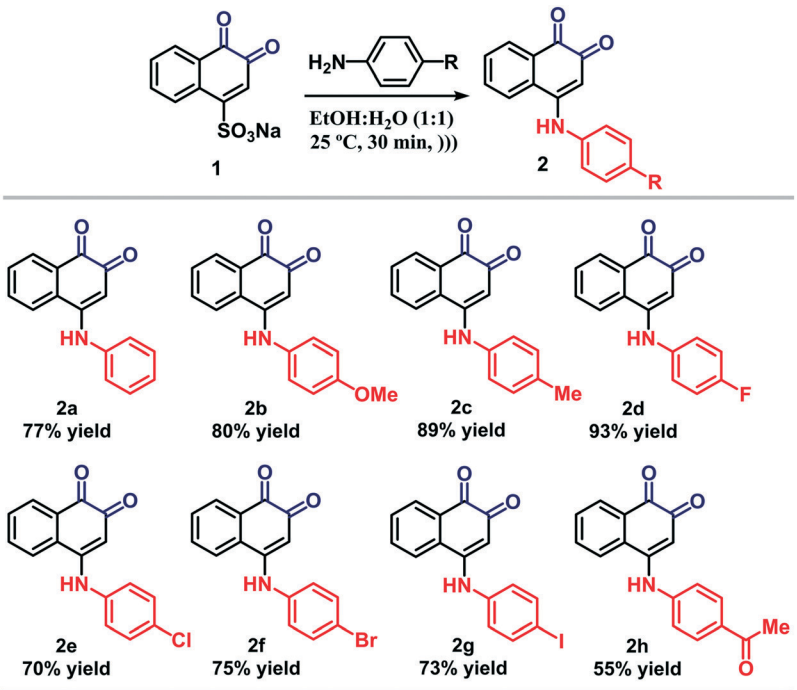

Scheme 2 Synthesis of arylamino *ortho*-naphthoquinones **2a–h**.

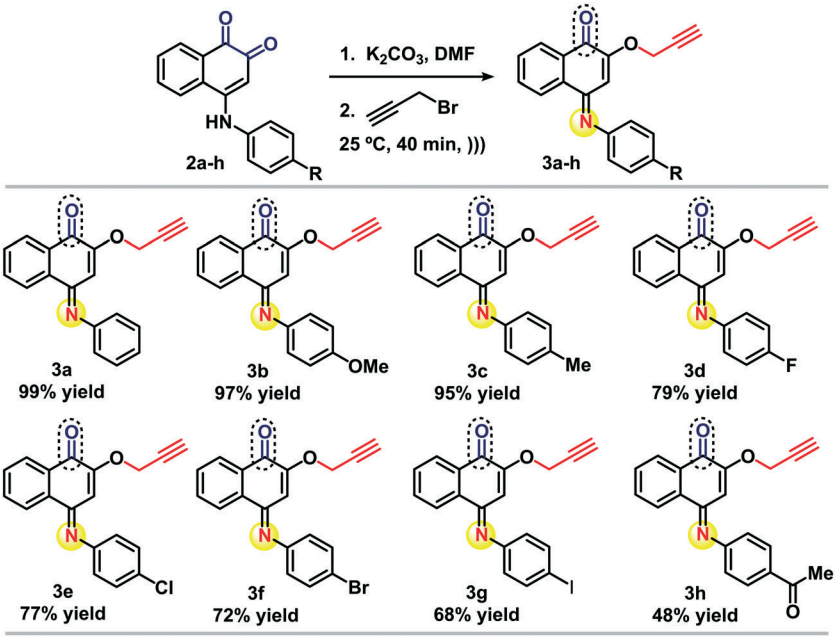

Scheme 3 Synthesis of alkynes derived from arylamino *ortho*-naphthoquinones **3a–h**.

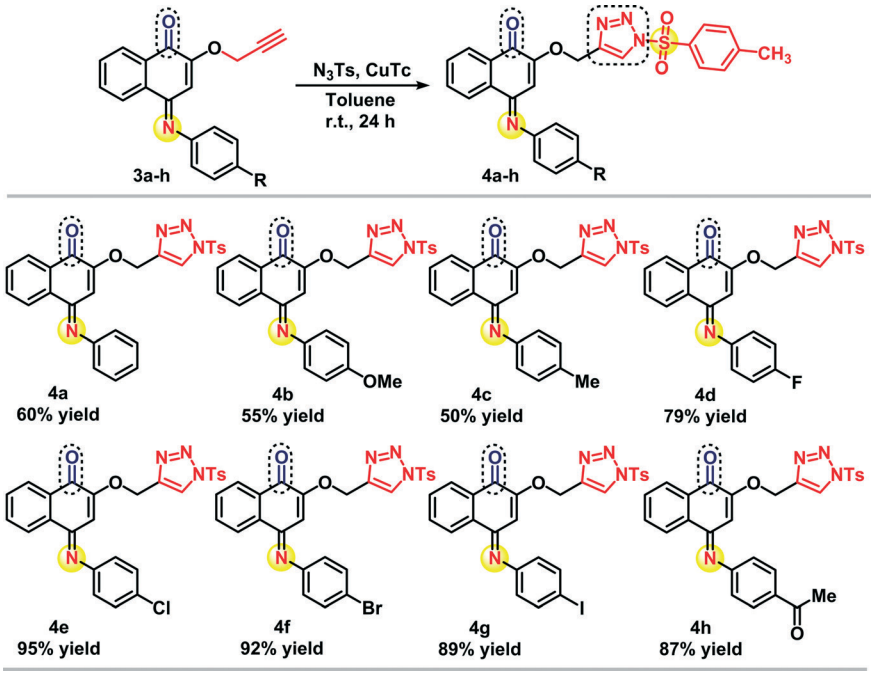

Scheme 4 Synthesis of *N*-sulfonyl-1,2,3-triazoles **4a–h**.

biological activities.[41] In this context, the synthesis of the *N*-sulfonyl-1,2,3-triazoles was accomplished according to the methodology described by Fokin *et al.*, employing copper(I)-thiophene-2-carboxylate (CuTC) as a catalyst, as this catalyst promises high yields and selective formation of the 1,4-regioisomer of the product.[42] The reaction was carried employing the corresponding alkynes (**3a–h**) (Scheme 3) with an excess of tosyl azide in toluene, as a solvent, and at room temperature according to Scheme 4. In general, novel compounds were obtained in moderate to excellent (50–95%) yields.

Nitrogen is not the only nucleophile able to replace the sulfonate group in compound **1**. Sulphur has a similar nucleophilic character and is also redox active. Indeed, recent studies have shown that naphthoquinone compounds substituted with chalcogen atoms often exhibit considerable

biological activity.[17,43] Whilst these studies have focused primarily on *para*-quinones, compound **1** provides the basis for a series of similar *ortho*-quinones. For this synthesis, a methodology adapted from the literature[36,37] yielded compounds **5a–5d** in low to moderate yields (30–40%) (Scheme 5).

The structures of the novel compounds were determined initially by ^{1}H and ^{13}C NMR, and were corroborated further using electrospray ionization mass spectra. In the case of compounds **3a**, **3d**, **3f**, **3g**, **3h** and **5d**, X-ray crystallographic analysis with suitable crystals obtained by the slow evaporation method was performed. Here, the bond lengths and angles are in good agreement with the expected values reported in the literature.[44] The atoms of the naphthoquinonic ring (C1–C10) of all structures are coplanar and the largest deviation from the least-squares plane for each one is: 0.077(3) Å for atom C1 in **3a**; 0.044(3) Å for atom C5 in **3d**; 0.035(2) Å for atom C1 in **3f**; 0.039(2) Å for atom C5 in **3g**; 0.039(2) Å for atom C8 in **3h** and 0.017(4) Å for atom C5 in **5d**. The dihedral angles between the planes of the rings (C1–C10) and (C11–C12) are: 48.5(3)° for **3a**; 57.4(2)° for **3d**; 86.9(3)° for **3g**; 57.1(4)° for **3h**; 61.01° for **3f** and 86.9° for **5d**. ORTEP-3 diagrams of each molecule are shown in Fig. 1.

2.2. Redox transformations

The process of substituting the sulfonate group in compound **1** for the nitrogen or sulphur in **2** and **5**, respectively, and also by *O*-alkylation when moving from **2** to **3** and **4**, changes the "redox core" of these molecules, as an additional redox active element is added to the initial *ortho*-quinone system. Some of the resulting redox systems therefore appear to differ significantly from the original structures, and these differences should also be reflected in the redox behaviour and biological activities associated with them. As such, cyclic voltammetry (CV) was employed to study redox changes, as it represents a readily applicable, fast, informative and also fairly reliable method to obtain initial information about reversible and irreversible reduction and oxidation processes associated with such molecules. CV was performed in mixed medium, *i.e.* phosphate buffer + 30% methanol, on a glassy carbon working electrode, with *E vs.* Ag/AgCl as a reference electrode (SSE), at 200 mV s^{-1}. In the presence of a protic organic solvent (methanol), the reduction occurs in two monoelectronic steps, different from the mechanism in totally aqueous medium, where the reduction occurs through the capture of $2e^- + 2H^+$.

The cyclic voltammograms of selected compounds belonging to class 1 (compounds **1** and **2**), class 3 (compound **3a**) and class 5 (compound **5b**) were obtained and are shown in Fig. S39 (see the ESI† file), together with the values for the relevant reduction signals (E_{pc}) and corresponding oxidation (E_{pa}) ones for various quinones, in Table 1. We have focused here on the prime signals associated with the quinone redox centre, as these waves are important to rationalize the relevant biological activities (see below).

By analysis of the first reduction potential (E_{pc1}), the ease of reduction is the following: **5c** > **5b** > **1** ≈ **5d** > **3e** > **3h** ≈ **3b** > **3a** > **2a**.

As anticipated, the redox behaviour changes significantly, once the original *ortho*-quinone **1** is modified by a nitrogen substituent in the *para*-position to yield compounds of class **2**, due to the electron donating character of the amino group. Interestingly, the subsequent *O*-alkylation converting **2** into **3** also – quite dramatically – changes the entire redox system, since there is a direct modification on the redox system. This significant change from an *ortho*-quinone to a *para*-quinone imine is also observed electrochemically, and is associated with a shift of the first reduction potentials to more negative potentials. Generally, the potentials for the *para*-quinone imine are 150 to 200 mV more negative, when compared to those for the *ortho*-quinones, pointing towards a less electrophilic compound, being reduced at more negative potentials. Modifying the compounds of class **2** (less electrophilic) to yield class **3** brings an anodic shift of the relevant potentials, however less intense, when compared to

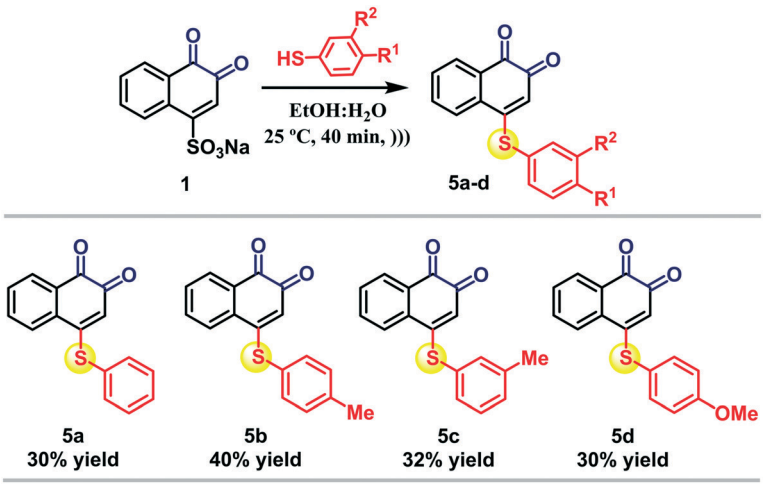

Scheme 5 Synthesis of chalcogenic aryl *ortho*-quinones **5a–d**.

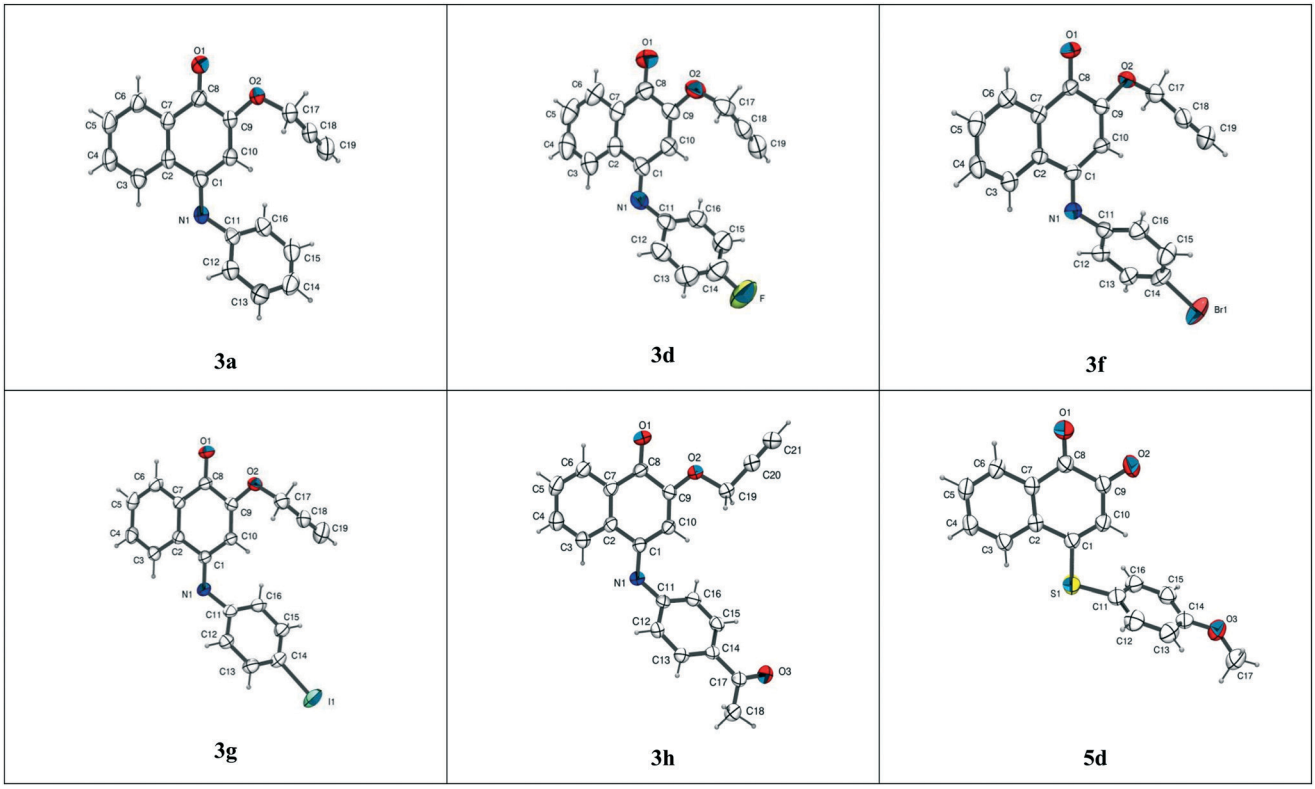

Fig. 1 ORTEP-3 projections of **3a**, **3d**, **3f**, **3g**, **3h** and **5d**, showing the atom-numbering and displacement ellipsoids at the 50% probability level.

the original compound **1**, and introducing another factor involved in the redox cycle with the quinone imines, once they are known to undergo a redox cycle through aminophenols. Another important fact should be considered: arylquinone imines can suffer from hydrolysis, to generate back the original quinone,[45] possibly behaving as a pro-drug.[40]

In contrast, the substitution of the initial "redox core" with a sulfur atom seems to change the original redox properties to a quasi-reversible electron transfer with potentials in the range of −168 mV up to −254 mV (E_{pc1}) and from −500 mV up to −574 mV (E_{pc2}). A significant change from an *ortho*-quinone to a chalcogenic quinone is observed electrochemically, and is associated with a shift of the relevant potentials to more positive potentials. Generally, the potentials for the chalcogenic quinone are 20 to 100 mV more positive, when compared to those for the *ortho*-quinone, pointing towards a more oxidizing species. Hence, its influence on the overall redox behaviour of these compounds is primarily due to electronic effects.

Table 1 Reduction potential values (E_{pc1} and E_{pc2}) and corresponding oxidation potentials (E_{pa1} and E_{pa2}), representing three different classes of compounds and their synthetic precursor (**1**)

	1st wave		2nd wave	
Compounds	E_{pc1}	E_{pa1}	E_{pc2}	E_{pa2}
1	−250 mV	−340 mV	−602 mV	−28 mV
2a	−490 mV	−420 mV	−716 mV	−202 mV
3a	−429 mV	−493 mV	−669 mV	−259 mV
3b	−387 mV	−475 mV	−687 mV	−292 mV
3e	−339 mV	−415 mV	−690 mV	−235 mV
3h	−384 mV	−414 mV	−614 mV	−190 mV
5b	−210 mV	−304 mV	−552 mV	−132 mV
5c	−168 mV	−324 mV	−500 mV	−110 mV
5d	−254 mV	−360 mV	−574 mV	−178 mV

2.3. Antiparasitic activity

Based on the strategy of modifying and hence modulating the initial "redox core" of the *ortho*-quinone, and the insights obtained by electrochemistry, it was then interesting to see if these modifications also translate into specific – changes in – biological activities. Here, two distinct models indicative of the activity of quinones have been selected, *i.e.* cancer cell lines and *T. cruzi* (see section 1 Introduction).

The selection of these models was based on studies previously described in the literature that demonstrate the antitumor and trypanocidal activity of quinoidal compounds containing the 1,2,3-triazole nucleus and the sulphur atom.[27,29,30] As discussed in the Introduction, our research group demonstrated that quinone-based *N*-sulfonyl-1,2,3-triazoles exhibited cytotoxicity against various tumour cell lines. These compounds were not evaluated against *T. cruzi*, the parasite that causes Chagas disease, but it is well documented that active redox systems are potential candidates to present

Table 2 Activity of the naphthoquinones on trypomastigote forms of *T. cruzi*[a]

Compounds	IC_{50}/24 h (μM)	LC_{50}/24 h[b] (μM)	SI
4a	>500	80.8 ± 6.5	>6.19
4b	>500	44.3 ± 6.4	>11.29
4c	>500	88.5 ± 3.5	>5.65
4d	>500	26.9 ± 1.2	>18.59
4e	>500	>100	nd
4f	>500	>100	nd
4g	>500	>100	nd
4h	>500	40.6 ± 2.5	>12.31
5a	**24.3 ± 7.9**	**36.9 ± 2.6**	**1.52**
5b	**88.7 ± 10.1**	**81.4 ± 3.7**	**0.92**
5c	**65.6 ± 10.2**	**67.3 ± 6.9**	**1.03**
5d	112.0 ± 10.6	41.5 ± 0.2	0.37
Bz	103.6 ± 0.6	>4000	>38.6

[a] Mean ± SD of at least three independent experiments, 5% blood at 4 °C. [b] Cytotoxicity assays were performed using primary cultures of peritoneal macrophages obtained from Swiss Webster mice. nd: not determined. Bz: benznidazole. SI = selectivity index, represented by the ratio LC_{50}/IC_{50}.

trypanocidal activity, since in general such activity may be intrinsically related to the generation of ROS.

Whilst none of the *N*-sulfonyl triazoles **4a–4h** appears to be particularly active against *T. cruzi*, with IC_{50} values higher than 500 μM, the sulphur-containing quinones **5a–5d** exhibit rather promising IC_{50} values between 24.3 and 112.0 μM (Table 2). It therefore appears that this particular microorganism is sensitive towards the substituted *ortho*-quinone series, and less so towards the quinone imines. From the perspective of redox chemistry, this may be explained by the fact that the *ortho*-quinones with their more positive electrochemical potentials are also generally more oxidizing and hence toxic, whilst the quinone imines, with their somewhat more negative potentials, are less oxidizing. Nonetheless, practical applications of such compounds may be compromised by a wider toxicity, as the selectivity index (SI) is rather low, with values ranging from 0.37 for compound **5d** to 1.52 for compound **5a**.

It is already established in the literature that naphthoquinones are inactivated in the presence of certain components present in human blood.[46,47] Compounds **5a–5d** were therefore also assayed in the absence of blood at 37 °C (Table 3).[46] These "blood-free" assays resulted in IC_{50} values between 1.3 μM for compound **5a** and 3.9 μM for compound **5d**. The SI was also improved, with values above 10 observed for virtually all compounds of class **5** under investigation. When compared to the standard drug benznidazole, which under these experimental conditions shows an IC_{50} of 9.7 μM, the quinones **5a–5d** were even more active. Nonetheless, the selectivity for the parasite is notoriously low for the quinones when compared to benznidazole (SI > 413.2), regardless of the assay conditions.

The sulphur-containing quinones **5a–5d** also exhibited some activity against macrophages with LC_{50} values between 36.9 and 81.4 μM. The quinones **5a–5d** were, however, more cytotoxic when compared to the standard drug benznidazole, which under these experimental conditions shows LC_{50} > 4000 μM, and it is worth noting here the correlation between the observed activity and the recorded electrochemical potentials for the chosen compounds.

2.4. Cytotoxic activity

In the case of the cancer cell lines, cytotoxicity was evaluated *in vitro* by the 3-(4,5-dimethylthiazol-2-yl)-2,5-diphenyltetrazolium bromide (MTT) colorimetric assay representative of six cancer cell lines, *i.e.* colon cancer cells (HCT-116), lung cancer cells (NCI-H460), prostate cancer cells (PC3), human promyelocytic leukemia cells (HL-60), human immortalized myelogenous leukemia cells (K-562) and multidrug resistant leukemia cells (Lucena 1) (Table 4). The murine, non-tumorigenic fibroblast immortalized cell line (L929) was employed as a control to evaluate the selectivity index of the compounds for tumour cells, once its IC_{50} is compared to the corresponding values of neoplastic cell lines through selectivity index calculation. Doxorubicin was employed as a positive control and benchmark drug. The compounds were classified according to their activity as highly active ($IC_{50} < 2$ μM), moderately active (2 μM < IC_{50} < 10 μM), or inactive ($IC_{50} > 10$ μM).[48]

As expected and reflected in Table 4, the redox active quinones exhibit significant cytotoxicity against a range of cancer cell lines, with IC_{50} values for some compounds in the low micromolar range. For instance, some alkynes of class **3** are moderately active and generally present a non-selective cytotoxicity against the tumour cells evaluated. Compound **3d** is an exception, as it is particularly active and selective against HL-60 cells, with an IC_{50} of 9.20 μM (Table 4) and a

Table 3 Activity of the synthetic derivatives against bloodstream trypomastigotes of *T. cruzi* (Y strain) at 37 °C in the absence of blood[a]

Compounds	IC_{50}/24 h (μM) at 37 °C, absence of blood	LC_{50}/24 h[b] (μM) macrophages	SI at 37 °C, absence of blood
5a	1.3 ± 0.2	36.9 ± 2.6	28.38
5b	3.4 ± 1.0	81.4 ± 3.7	23.94
5c	4.6 ± 1.1	67.3 ± 6.9	14.63
5d	3.9 ± 1.4	41.5 ± 0.2	10.64
Bz	9.7 ± 2.4	>4000	>413.2

[a] Mean ± SD of at least three independent experiments, absence of blood at 37 °C. [b] Cytotoxicity assays were performed using primary cultures of peritoneal macrophages obtained from Swiss Webster mice. nd: not determined. Bz: benznidazole. SI = selectivity index, represented by the ratio LC_{50}/IC_{50}.

Table 4 Cytotoxic activity of the compounds expressed as IC_{50} (μM) in cancer and non-cancer cell lines after 72 h exposure, obtained by nonlinear regression for all cell lines from three independent experiments

	HCT-116	NCI-H460	PC-3	HL-60	K-562	Lucena 1	L929
3a	>20.00	>20.00	14.10 (12.18–16.29)	17.44 (14.79–20.50)	>20.00	>20.00	>20.00
3b	10.71 (9.61–12.35)	**9.45** (7.88–9.45)	**8.82** (8.04–9.67)	**7.18** (5.64–9.11)	>20.00	11.41 (9.36–13.90)	>20.00
3c	>20.00	16.92 (13.94–20.91)	18.45 (16.36–20.77)	11.98 (10.22–14.00)	>20.00	14.07 (12.51–15.80)	>20.00
3d	18.67 (16.51–21.13)	17.03 (15.07–19.32)	>20.00	**9.20** (7.73–10.97)	13.48 (11.69–15.57)	17.00 (13.92–20.74)	>20.00
3e	18.87 (16.29–21.88)	16.16 (13.99–18.65)	14.64 (11.66–18.37)	11.03 (9.39–13.02)	12.80 (10.38–15.78)	16.43 (13.44–20.11)	>20.00
3f	>20.00	>20.00	15.87 (14.25–17.69)	14.20 (11.25–17.94)	>20.00	12.52 (10.31–15.20)	>20.00
3g	16.46 (13.07–20.81)	>20.00	>20.00	11.90 (10.38–13.65)	16.96 (14.33–20.09)	15.13 (12.27–18.66)	>20.00
3h	>20.00	>20.00	12.51 (10.93–14.33)	>20.00	>20.00	16.25 (11.87–22.23)	>20.00
4a	**5.37** (4.75–6.40)	**7.22** (6.40–8.05)	>20.00	**6.71** (4.93–9.08)	12.24 (10.13–14.79)	**3.67** (3.01–4.46)	>20.00
4b	**7.43** (6.48–8.58)	**8.39** (7.24–9.72)	>20.00	**6.96** (5.75–8.46)	>20.00	**4.58** (3.55–5.93)	>20.00
4c	**3.61** (3.01–4.21)	**8.02** (7.62–8.62)	**2.65** (2.25–3.11)	**5.42** (4.42–6.64)	**6.22** (4.97–7.76)	**1.44** (0.98–2.11)	17.73 (13.91–22.61)
4d	**5.75** (4.96–6.69)	**7.36** (6.77–7.96)	**2.03** (1.65–2.49)	**7.52** (6.07–9.33)	**7.70** (6.39–9.27)	**6.58** (5.57–7.78)	>20.00
4e	**9.44** (8.48–10.79)	**12.14** (10.98–13.30)	>20.00	**6.92** (5.57–8.57)	**9.80** (7.64–12.58)	**3.16** (2.47–4.09)	>20.00
4f	**9.25** (8.55–9.99)	**9.41** (8.34–10.47)	**3.41** (2.88–4.05)	**4.22** (3.44–5.16)	**5.40** (4.06–7.15)	**3.32** (2.45–4.51)	>17.75
4g	>16.38	>16.38	>16.38	**6.31** (5.29–7.49)	10.76 (8.08–14.32)	**2.90** (2.44–3.44)	>16.38
4h	**6.27** (5.32–7.41)	15.76 (14.43–17.47)	**3.91** (3.42–4.50)	**5.30** (4.51–6.28)	**5.52** (4.77–6.39)	**6.46** (5.05–8.26)	10.75 (8.77–13.17)
5a	12.77 (10.14–16.15)	>20.00	>20.00	**6.08** (4.88–7.55)	15.71 (13.59–18.16)	15.58 (12.58–19.30)	>20.00
5b	>20.00	>20.00	>20.00	**4.14** (3.21–5.31)	14.91 (11.38–19.54)	12.84 (10.52–15.66)	>20.00
5c	19.62 (16.77–22.83)	>20.00	>20.00	**5.42** (4.21–6.99)	16.24 (12.86–19.87)	12.66 (10.20–15.73)	>20.00
5d	>20.00	>20.00	>20.00	**9.38** (7.49–11.78)	13.33 (9.97–17.84)	>20.00	>20.00
Dox	0.21 (0.16–0.29)	0.15 (0.13–0.18)	0.76 (0.59–0.93)	0.02 (0.01–0.02)	0.49 (0.47–0.51)	0.18 (0.15–0.22)	1.72 (1.58–1.87)

Table 5 Selectivity index for the most active compounds[a]

Compounds	HCT116	NCI-H460	PC3	HL-60	K-562	Lucena I
3a	1.2	1.6	**2.5**	**2.0**	1.0	1.5
3b	**2.9**	**3.3**	**3.6**	**4.4**	1.0	**2.8**
3c	1.6	**2.0**	1.8	**2.8**	1.5	**2.4**
3d	1.8	1.9	1.0	**3.6**	**2.4**	1.9
3e	1.6	1.9	**2.1**	**2.8**	**2.4**	1.9
3f	1.2	1.3	1.7	1.9	1.2	**2.2**
3g	1.5	1.0	1.0	**2.0**	1.4	1.6
3h	1.0	1.0	**24**	1.1	1.0	1.9
4a	**3.8**	**2.9**	1.0	**3.1**	1.7	**5.6**
4b	**2.9**	**2.6**	1.0	**3.3**	1.0	**5.4**
4c	**4.9**	**2.2**	**6.7**	**3.3**	**2.9**	**12.3**
4d	**3.5**	**2.7**	**9.8**	**2.6**	**2.6**	**3.0**
4e	**2.0**	1.6	1.0	**2.8**	**2.0**	**6.1**
4f	1.9	1.9	**5.2**	**4.2**	**3.3**	**5.3**
4g	1.0	1.0	1.0	**2.6**	1.5	**5.6**
4h	1.7	0.7	**2.7**	**2.0**	1.9	1.7
5a	**2.2**	0.7	0.7	**4.6**	1.8	1.8
5b	1.3	0.8	0.8	**6.6**	1.8	**2.1**
5c	1.8	1.0	1.0	**6.6**	**2.2**	**2.8**
5d	1.0	1.0	1.0	**3.6**	**2.5**	1.0

[a] Selectivity index, represented by the ratio of cytotoxicities between normal cells and different lines of cancer cells.

selectivity index (SI) superior to 3.6 (Table 5). Compound **3b** presents a broader cytotoxicity against NCI-H460 (IC_{50} = 9.45 μM), PC-3 (IC_{50} = 8.82 μM) and HL-60 (IC_{50} = 7.18 μM) cells with a SI higher than 1.8. Generally, the members of class **4** exhibit a more selective cytotoxic activity against all the cell lines, with IC_{50} values ranging from 1.44 to > 20 μM. For example, **4d** presents IC_{50} values between 2.03 and 7.70 μM (Table 4), with a SI higher than 2.6 (Table 5), while **4f** presents an IC_{50} from 3.32 to 9.41 μM (Table 4) and a SI higher than 1.9 (Table 5). Interestingly, the only difference between these molecules is the deactivating halogen substituent in the benzene ring, –F in **4d** and –Br in **4f**, suggesting that the more electronegative the halogen substituent, the more cytotoxic the compound. This pattern is followed by **4g**, which possesses an –I substituent and is a less cytotoxic compound against the cell lines tested, except for a particularly high selectivity for Lucena 1, *i.e.* IC_{50} of 2.90 μM and SI higher than 5.6 (Table 4).

Notable differences can be observed in the SI values shown in Table 5. The sulphur containing quinones seem to be fairly selective against certain cancer cell lines, such as HL-60, as observed in the case of compounds **5b** and **5c**. Indeed, compounds of class **5** are particularly attractive as far as observed activity and selectivity are considered, reflecting the potential of the redox core in concert with the sulfur atom added to this analogue. Compounds **5b** and **5c** present IC_{50} values of 4.14 μM and 5.42 μM against HL-60, respectively, with an SI of 6.6.

In general, generation of intracellular ROS is a key mechanism associated with the cytotoxic effects of quinones in tumor cells. Thus, the redox status of treated K-562 cells was monitored using the oxidation-sensitive fluorescent dye CM-H_2DCFDA after 1 and 3 hours of incubation. Fig. 2 shows that all three tested compounds induced a significant increase in intracellular ROS levels, reaching a higher ROS + cell count at 3 hours. Compound **5a** was the most potent in inducing significant changes ($p < 0.05$) in ROS levels, at both 1 and 3 hours. In contrast, compound **4f** generated lower levels of ROS, but still significant ($p < 0.05$) at 3 hours. As expected, menadione and hydrogen peroxide increased ROS generation in treated cells.

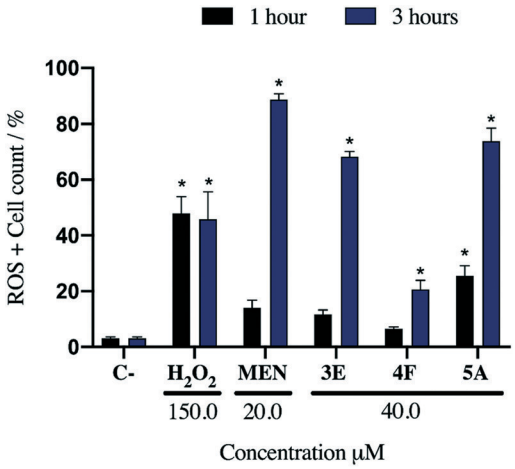

Fig. 2 Effect of compounds **3e**, **4f** and **5a** on ROS production in K-562 cells determined by flow cytometry using CM-H_2DCFDA, after 1 and 3 hours incubation. Menadione (MEN, 20 μM) and hydrogen peroxide (H_2O_2, 150 μM) were used as positive controls. A total of 10 000 events were analyzed per sample. Data are expressed as mean ± SEM from three independent experiments. *, $p < 0.05$ compared to the negative control by ANOVA followed by Tukey's test, performed using GraphPad Prism 8.

3. Conclusions

Considered together, the modification of the *ortho*-quinone lead **1** provides access to a wide range of different classes of

compounds with distinctive "redox cores", electrochemical potentials, biological activities and SI values. Here, the underlying mode(s) of action and also possible selectivity need to be investigated, together with potential applications against different human diseases. Whilst some of the compounds synthesised as part of this study already exhibit a combination of high activity and selectivity, these aspects may need to be further improved. It remains to be shown, for instance, against which cells or organisms these compounds are especially active, and if there is some selectivity associated with this activity, which may be exploited in practice.

Fortunately, the synthetic chemistry associated with these compounds is straightforward and provides wide opportunities for structural modifications, from the initial nucleophilic substitution and alkylation to the side chains and prospects provided by click chemistry reactions. Similarly, electrochemical investigations by cyclic voltammetry are fast and simple, and may provide initial information on the redox behaviour and activities one may expect.

4. Experimental section

4.1. Chemistry

Starting materials available from commercial suppliers were employed as received, unless stated otherwise. All other reagents requiring purification were purified by standard laboratory techniques, according to methods published by Perrin, Armarego and Perrin.[49] Catalytic reactions were performed under nitrogen or argon atmosphere. Glassware, syringes and needles were either flame-dried immediately prior to use or placed in an oven (200 °C), for at least 2 h, and allowed to cool either in a desiccator or under an atmosphere of nitrogen or argon. Liquid reagents, solutions or solvents were added *via* a syringe through rubber septa. Melting points of solid compounds were measured on a Thomas Hoover melting point apparatus and are uncorrected. Column chromatography was performed on silica gel (SiliaFlash G60 Ultrapure 60–200 μm, 60 Å). ^{1}H and ^{13}C NMR spectra were recorded at room temperature on a Bruker AVANCE DRX200 and DRX400, in the solvents indicated. Chemical shifts (δ) are given in parts per million (ppm) and coupling constants (J) are reported in Hertz (Hz). MS analyses were performed on a LC-MS/ESI TOF spectrometer (Model Xevo G2-XS QTof, Waters). The compounds are named in accordance with IUPAC rules as applied by ChemBioDraw Ultra (version 12.0).

General procedure for the synthesis of compounds 2a–h. The synthesis of compounds **2a–h** was performed according to the methodology described in the literature by the Potter and Chen groups with minor modifications.[36,37] To a solution of sodium 3,4-dioxo-3,4-dihydronaphthalene-1-sulfonate (**1**) (2.5 mmol) in EtOH : H_2O 1 : 1 (75 mL), the respective aniline (2.7 mmol) was added. The reaction mixture was stirred at room temperature monitored by TLC until the total consumption of the starting material. After completion of the reaction, the solvent was removed *in vacuo* and the resulting residue was purified by column chromatography over silica gel, using as the eluent a gradient mixture of hexane/ethyl acetate with increasing polarity. In some cases, ultrasound can be used to promote the reaction. The analytical data for compounds **2a–h** are in accordance with those reported in the literature.[36–38]

General procedure for the synthesis of compounds 3a–h. To a stirred solution of a type **2** compound (2.0 equiv.) in DMF (4 mL), K_2CO_3 (250 mg, 0.18 mmol, 1.1 equiv.) was added and the reaction mixture was stirred at room temperature. After 10 min, propargyl bromide (80 mg, 0.7 mmol, 2.1 equiv.) was added dropwise and stirred under ultrasound for 40 min. The solvent was evaporated *in vacuo* and water (5 mL) was added to the crude reaction mixture. The aqueous phase was extracted with ethyl acetate (3 × 10 mL) and the organic phases were combined and dried over anhydrous sodium sulfate and concentrated under reduced pressure. The crude residue was purified by silica gel column chromatography by eluting with an increasing polarity gradient mixture of hexane and ethyl acetate to afford the respective alkynes (**3a–h**).

(*E*)-4-(Phenylimino)-2-(prop-2-yn-1-yloxy)naphthalen-1(4*H*)-one (3a). The product was obtained as an orange solid (99% yield); mp 139–141 °C; ^{1}H NMR (400 MHz, $CDCl_3$): δ 8.52 (1H, d, J = 7.8 Hz), 8.24 (1H, d, J = 7.8 Hz), 7.74 (1H, t, J = 7.7 Hz), 7.67 (1H, t, J = 7.7 Hz), 7.43 (2H, t, J = 7.8 Hz), 7.21 (1H, t, J = 7.4 Hz), 6.96 (2H, d, J = 7.4 Hz), 6.60 (1H, s), 4.61 (2H, d, J = 2.2 Hz), 2.55 (1H, t, J = 2.2 Hz); ^{13}C NMR (100 MHz, $CDCl_3$): δ 180.3, 154.8, 154.3, 150.5, 134.8, 133.5, 131.3, 131.3, 129.2, 126.7, 125.5, 125.0, 120.6, 104.6, 77.5, 76.6, 56.2; IR ν_{max} (cm^{-1}, KBr): 3264, 3067, 2974, 2117, 1670, 1612, 1483, 1383, 1332, 1255, 1189, 1044, 1019, 949, 857, 769, 694, 648; EI/HRMS (m/z) $[M + H]^+$: 288.1023. Cald. for $[C_{19}H_{14}NO_2]^+$: 288.1024.

(*E*)-4-((4-Methoxyphenyl)imino)-2-(prop-2-yn-1-yloxy)-naphthalen-1(4*H*)-one (3b). The product was obtained as a red solid (97% yield); mp 149–150 °C; ^{1}H NMR (400 MHz, $CDCl_3$): δ 8.51 (1H, d, J = 7.8 Hz), 8.22 (1H, d, J = 7.8 Hz), 7.73 (1H, t, J = 7.9 Hz), 7.65 (1H, t, J = 7.9 Hz), 6.98 (4H, s), 6.72 (1H, s), 4.65 (2H, d, J = 2.3 Hz), 3.78 (3H, s), 2.59 (1H, t, J = 2.3 Hz); ^{13}C NMR (100 MHz, $CDCl_3$): δ 180.4, 157.7, 154.3, 154.1, 143.6, 135.1, 133.4, 131.2, 131.0, 126.6, 125.3, 122.7, 114.6, 104.6, 77.5, 76.8, 56.2, 55.7; IR ν_{max} (cm^{-1}, KBr): 3264, 2930, 2843, 2128, 1675, 1597, 1497, 1461, 1354, 1320, 1260, 1243, 1201, 1044, 1022, 847, 777, 682, 653; EI/HRMS (m/z) $[M + H]^+$: 318.1122. Cald. for $[C_{20}H_{16}NO_3]^+$: 318.1125.

(*E*)-2-(Prop-2-yn-1-yloxy)-4-(*p*-tolylimino)naphthalen-1(4*H*)-one (3c). The product was obtained as an orange solid (95% yield); mp 148–150 °C; ^{1}H NMR (400 MHz, $CDCl_3$): δ 8.50 (1H, d, J = 7.6 Hz), 8.21 (1H, d, J = 7.6 Hz), 7.71 (1H, t, J = 7.2 Hz), 7.64 (1H, t, J = 7.2 Hz), 7.22 (2H, d, J = 7.4 Hz), 6.88 (2H, d, J = 7.4 Hz), 6.65 (1H, s), 4.62 (2H, s), 2.59 (1H, s), 2.40 (3H, s); ^{13}C NMR (100 MHz, $CDCl_3$): δ 180.1, 154.3, 153.9, 147.7, 134.8, 134.6, 133.2, 131.1, 130.9, 129.6, 126.4, 125.2, 120.7,

104.4, 76.8, 76.6, 56.0, 21.0; IR ν_{max} (cm^{-1}, KBr): 3269, 2117, 1672, 1614, 1597, 1500, 1335, 1257, 1192, 1044, 1019, 772; EI/HRMS (*m*/*z*) $[M + H]^+$: 302.1170. Cald. for $[C_{20}H_{16}NO_2]^+$: 302.1176.

(*E*)-4-((4-Fluorophenyl)imino)-2-(prop-2-yn-1-yloxy)-naphthalen-1(4*H*)-one (3d). The product was obtained as an orange solid (79% yield); mp 147–149 °C; ^{1}H NMR (400 MHz, $CDCl_3$): δ 8.45 (1H, d, *J* = 7.7 Hz), 8.18 (1H, d, *J* = 7.7 Hz), 7.70 (1H, t, *J* = 7.4 Hz), 7.63 (1H, t, *J* = 7.4 Hz), 7.10 (2H, t, *J* = 8.6 Hz), 6.93–6.90 (2H, m), 6.56 (1H, s), 4.61 (2H, d, *J* = 2.1 Hz), 2.57 (1H, t, *J* = 2.1 Hz); ^{13}C NMR (100 MHz, $CDCl_3$): δ 180.1, 161.6, 159.2, 155.2, 154.3, 146.4, 134.6, 133.5, 131.3, 131.2, 126.6, 125.3, 122.2, 122.1, 116.1, 115.9, 104.1, 76.5, 56.2; IR ν_{max} (cm^{-1}, KBr): 3296, 2990, 2123, 1667, 1624, 1597, 1497, 1339, 1264, 1221, 1204, 1184, 1044, 1019, 862, 772, 697, 648; EI/HRMS (*m*/*z*) $[M + H]^+$: 306.0919. Cald. for $[C_{19}H_{13}FNO_2]^+$: 306.0925.

(*E*)-4-((4-Chlorophenyl)imino)-2-(prop-2-yn-1-yloxy)-naphthalen-1(4*H*)-one (3e). The product was obtained as an orange solid (77% yield); mp 145–147 °C; ^{1}H NMR (400 MHz, $CDCl_3$): δ 8.44 (1H, dd, *J* = 1.5 and 7.8 Hz), 8.19 (1H, dd, *J* = 1.5 and 7.8 Hz), 7.75–7.59 (2H, m), 7.36 (2H, d, *J* = 8.6 Hz), 6.89 (2H, d, *J* = 8.6 Hz), 6.51 (1H, s), 4.62 (2H, d, *J* = 2.4 Hz), 2.58 (1H, t, *J* = 2.4 Hz); ^{13}C NMR (50 MHz, $CDCl_3$): δ 180.0, 155.2, 154.4, 148.8, 134.5, 133.5, 131.4, 131.1, 130.4, 129.3, 126.7, 125.4, 122.0, 104.0, 77.6, 76.5, 56.2; IR ν_{max} (cm^{-1}, KBr): 3275, 1670, 1614, 1483, 1337, 1252, 1192, 1044, 1019, 854, 772, 639; EI/HRMS (*m*/*z*) $[M + H]^+$: 322.0629. Cald. for $[C_{19}H_{13}ClNO_2]^+$: 322.0629.

(*E*)-4-((4-Bromophenyl)imino)-2-(prop-2-yn-1-yloxy)-naphthalen-1(4*H*)-one (3f). The product was obtained as a red solid (72% yield); mp 156–158 °C; ^{1}H NMR (400 MHz, $CDCl_3$): δ 8.48 (1H, d, *J* = 7.8 Hz), 8.23 (1H, d, *J* = 7.8 Hz), 7.75 (1H, t, *J* = 7.4 Hz), 7.68 (1H, t, *J* = 7.4 Hz), 7.54 (2H, d, *J* = 8.4 Hz), 6.85 (2H, d, *J* = 8.4 Hz), 6.54 (1H, s), 4.65 (2H, d, *J* = 2.1 Hz), 2.58 (1H, t, *J* = 2.1 Hz); ^{13}C NMR (50 MHz, $CDCl_3$): δ 180.1, 155.3, 154.6, 149.4, 134.6, 133.6, 132.3, 131.5, 131.3, 126.8, 125.5, 122.4, 118.2, 104.2, 77.6, 76.5, 56.3; IR ν_{max} (cm^{-1}, KBr): 3275, 2117, 1667, 1612, 1478, 1337, 1255, 1192, 1046, 1024, 852, 772, 685, 641; EI/HRMS (*m*/*z*) $[M + H]^+$: 366.0120. Cald. for $[C_{19}H_{13}BrNO_2]^+$: 366.0124.

(*E*)-4-((4-Iodophenyl)imino)-2-(prop-2-yn-1-yloxy)-naphthalen-1(4*H*)-one (3g). The product was obtained as a red solid (68% yield); mp 123–125 °C; ^{1}H NMR (400 MHz, $CDCl_3$): δ 8.46 (1H, d, *J* = 7.8 Hz), 8.21 (1H, d, *J* = 7.8 Hz), 7.73–7.65 (4H, m), 6.72 (2H, d, *J* = 8.2 Hz), 6.52 (1H, s), 4.64 (2H, s), 2.59 (1H,s); ^{13}C NMR (50 MHz, $CDCl_3$): δ 179.8, 154.9, 154.2, 149.7, 137.9, 134.3, 133.3, 131.2, 130.9, 126.5, 125.2, 122.5, 103.8, 88.6, 77.4, 76.2, 56.1; IR ν_{max} (cm^{-1}, KBr): 3280, 1668, 1609, 1473, 1476, 1253, 1187, 1044, 1020, 770; EI/HRMS (*m*/*z*) $[M + H]^+$: 413.9989. Cald. for $[C_{19}H_{13}INO_2]^+$: 413.9985.

(*E*)-4-((4-Acetylphenyl)imino)-2-(prop-2-yn-1-yloxy)-naphthalen-1(4*H*)-one (3h). The product was obtained as a yellow solid (48% yield); mp 172–174 °C; ^{1}H NMR (400 MHz, $CDCl_3$): δ 8.49 (1H, dd, *J* = 1.0 and 7.7 Hz), 8.25 (1H, dd, *J* = 1.0 and 7.7 Hz), 8.05 (2H, d, *J* = 8.6 Hz), 7.77 (1H, t, *J* = 7.5 Hz), 7.70 (1H, t, *J* = 7.5 Hz), 7.01 (2H, d, *J* = 8.6 Hz), 6.44 (1H, s), 4.62 (2H, d, *J* = 2.3 Hz), 2.65 (3H, s), 2.56 (1H, t, *J* = 2.3 Hz); ^{13}C NMR (50 MHz, $CDCl_3$): δ 197.0, 179.8, 155.1, 154.8, 154.5, 134.1, 133.6, 133.5, 131.4, 131.1, 129.7, 126.7, 125.6, 120.1, 104.0, 77.5, 76.1, 56.1, 26.5; IR ν_{max} (cm^{-1}, KBr): 3264, 2925, 2134, 1679, 1614, 1592, 1560, 1359, 1267, 1209, 1019, 726, 685; EI/HRMS (*m*/*z*) $[M + H]^+$: 330.1122. Cald. for $[C_{21}H_{16}NO_3]^+$: 330.1125.

General procedure for preparing the 1,2,3-triazole derivatives. To a stirred solution of copper(I) thiophene-2-carboxylate (CuTC, 8 mg, 0.04 mmol, 0.08 equiv.) in toluene (5 mL), the respective propargylated aminonaphthoquinones (0.5 mmol, 1 equiv.) were added and the reaction mixture was cooled in an ice–water bath. Subsequently, the sulfonyl azide (0.5 mmol, 1 equiv.) was added dropwise. The reaction mixture was then allowed to warm to room temperature and stirred until the reaction was complete (as evidenced by TLC). The reaction mixture was extracted with EtOAc (3 × 30 mL). The combined organic layers were dried over sodium sulfate and filtered through Celite®. The eluent was concentrated under vacuum and the product was purified by silica gel column chromatography using eluents with an increasing polarity gradient mixture of hexane and ethyl acetate to afford compounds **4a–h**.

(*E*)-4-(Phenylimino)-2-((1-tosyl-1*H*-1,2,3-triazol-4-yl)-methoxy)naphthalen-1(4*H*)-one (4a). The product was obtained as a red solid (60% yield); mp 153–155 °C; ^{1}H NMR (400 MHz, $CDCl_3$): δ 8.48 (1H, d, *J* = 7.5 Hz), 8.22 (1H, s), 8.19 (1H, d, *J* = 7.5 Hz), 7.99 (2H, d, *J* = 8.0 Hz), 7.72 (1H, t, *J* = 7.5 Hz), 7.65 (1H, t, *J* = 7.5 Hz), 7.43–7.37 (4H, m), 7.19 (1H, t, *J* = 7.1 Hz), 6.84 (2H, d, *J* = 8.0 Hz), 6.52 (1H, s), 5.02 (2H, s), 2.44 (3H, s); ^{13}C NMR (100 MHz, $CDCl_3$): δ 180.0, 154.6, 154.5, 150.2, 147.7, 141.8, 134.6, 133.4, 132.7, 131.1, 131.0, 130.5, 129.2, 129.2, 126.5, 125.3, 124.9, 123.2, 120.2, 120.1, 103.8, 61.7, 21.8; IR ν_{max} (cm^{-1}, KBr): 3132, 2922, 1668, 1607, 1392, 1254, 1193, 1014, 667, 587; EI/HRMS (*m*/*z*) $[M + H]^+$: 485.1208. Cald. for $[C_{26}H_{21}N_4O_4S]^+$: 485.1278.

(*E*)-4-((4-Methoxyphenyl)imino)-2-((1-tosyl-1*H*-1,2,3-triazol-4-yl)methoxy)naphthalen-1(4*H*)-one (4b). The product was obtained as a red solid (55% yield); mp 123–125 °C; ^{1}H NMR (400 MHz, $CDCl_3$): δ 8.52 (1H, d, *J* = 7.8 Hz), 8.26 (1H, s), 8.22 (1H, d, *J* = 7.8 Hz), 8.02 (2H, d, *J* = 7.5 Hz), 7.74 (1H, t, *J* = 7.3 Hz), 7.66 (1H, t, *J* = 7.3 Hz), 7.41 (2H, d, *J* = 7.5 Hz), 6.98 (2H, d, *J* = 7.2 Hz), 6.86 (2H, d, *J* = 7.2 Hz), 6.67 (1H, s), 5.09 (2H, s), 3.89 (3H, s), 2.47 (3H, s); ^{13}C NMR (100 MHz, $CDCl_3$): δ 180.0, 157.5, 154.4, 154.0, 147.7, 143.3, 142.0, 134.8, 133.3, 132.8, 131.0, 130.9, 130.5, 128.9, 126.5, 125.2, 123.1, 122.2, 114.6, 104.0, 61.7, 55.5; IR ν_{max} (cm^{-1}, KBr): 3139, 2958, 2922, 1659, 1601, 1499, 1391, 1261, 1193, 1020, 670, 583; EI/HRMS (*m*/*z*) $[M + H]^+$: 515.1372. Cald. for $[C_{27}H_{23}N_4O_5S]^+$: 515.1384.

(*E*)-4-(*p*-Tolylimino)-2-((1-tosyl-1*H*-1,2,3-triazol-4-yl)-methoxy)naphthalen-1(4*H*)-one (4c). The product was obtained as a yellow solid (50% yield); mp 157–159 °C; ^{1}H NMR (400 MHz, $CDCl_3$): δ 8.52 (1H, d, *J* = 7.8 Hz), 8.23–8.21 (2H, m), 8.03 (2H, d, *J* = 8.2 Hz), 7.75 (1H, t, *J* = 7.6 Hz), 7.67 (1H, t, *J* = 7.6 Hz), 7.41 (2H, d, *J* = 8.2 Hz), 7.23 (2H, d, *J* = 8.0

Hz), 6.78 (2H, d, J = 8.0 Hz), 6.59 (1H, s), 5.06 (2H, s), 2.47 (3H, s), 2.42 (3H, s); ^{13}C NMR (100 MHz, $CDCl_3$): δ; 180.2, 154.8, 154.6, 147.9, 142.3, 135.0, 135.0, 133.6, 133.1, 131.3, 131.2, 130.8, 130.1, 129.1, 126.7, 125.5, 123.3, 120.6, 104.1, 62.0, 22.1, 21.2; IR ν_{max} (cm^{-1}, KBr): 3132, 2917, 1665, 1597, 1396, 1260, 1197, 1015, 670, 587; EI/HRMS (m/z) [M + H]$^+$: 499.1421. Cald. for [$C_{27}H_{23}N_4O_4S$]$^+$: 499.1435.

(*E*)-4-((4-Fluorophenyl)imino)-2-((1-tosyl-1*H*-1,2,3-triazol-4-yl)methoxy)naphthalen-1(4*H*)-one (4d). The product was obtained as a yellow solid (79% yield); mp 162–164 °C; ^{1}H NMR (400 MHz, $CDCl_3$): δ 8.46 (1H, d, J = 7.6 Hz), 8.23 (1H, s), 8.19 (1H, d, J = 7.6 Hz), 8.00 (2H, d, J = 7.8 Hz), 7.72 (1H, t, J = 7.2 Hz), 7.65 (1H, t, J = 7.2 Hz), 7.39 (2H, d, J = 7.8 Hz), 7.11 (2H, t, J = 8.2 Hz), 6.83–6.81 (2H, m), 6.55 (1H, s), 5.06 (2H, s), 2.45 (3H, s); ^{13}C NMR (100 MHz, $CDCl_3$): δ 179.9, 155.0, 154.6, 147.7, 141.7, 134.5, 133.5, 132.6, 131.2, 131.0, 130.6, 128.9, 126.5, 125.3, 123.3, 121.8, 121.8, 116.2, 116.0, 61.5, 21.8; IR ν_{max} (cm^{-1}, KBr): 3127, 2925, 1670, 1607, 1495, 1388, 1260, 1197, 1015, 854, 670, 587; EI/HRMS (m/z) [M + H]$^+$: 503.1154. Cald. for [$C_{26}H_{20}FN_4O_4S$]$^+$: 503.1184.

(*E*)-4-((4-Chlorophenyl)imino)-2-((1-tosyl-1*H*-1,2,3-triazol-4-yl)methoxy)naphthalen-1(4*H*)-one (4e). The product was obtained as an orange solid (95% yield); mp 155–157 °C; ^{1}H NMR (400 MHz, $CDCl_3$): δ 8.47 (1H, d, J = 7.6 Hz), 8.25 (1H, s), 8.21 (1H, d, J = 7.6 Hz), 8.03 (2H, d, J = 7.5 Hz), 7.75 (1H, t, J = 7.2 Hz), 7.68 (1H, t, J = 7.2 Hz), 7.43–7.39 (4H, m), 6.82 (2H, d, J = 7.2 Hz), 6.53 (1H, s), 5.07 (2H, s), 2.47 (3H, s); ^{13}C NMR (100 MHz, $CDCl_3$): δ 180.1, 155.3, 155.1, 148.9, 147.9, 142.0, 134.7, 133.8, 133.0, 131.6, 131.3, 130.8, 130.6, 129.7, 129.2, 126.9, 125.6, 123.5, 121.9, 61.7, 21.9; IR ν_{max} (cm^{-1}, KBr): 3138, 2919, 1670, 1609, 1391, 1260, 1194, 1088, 1010, 852, 670, 583; EI/HRMS (m/z) [M + H]$^+$: 519.0883. Cald. for [$C_{26}H_{20}ClN_4O_4S$]$^+$: 519.0888.

(*E*)-4-((4-Bromophenyl)imino)-2-((1-tosyl-1*H*-1,2,3-triazol-4-yl)methoxy)naphthalen-1(4*H*)-one (4f). The product was obtained as a yellow solid (92% yield); mp 175–177 °C; ^{1}H NMR (400 MHz, $CDCl_3$): δ 8.47 (1H, d, J = 7.7 Hz), 8.24 (1H, s), 8.21 (1H, d, J = 7.7 Hz), 8.03 (2H, d, J = 8.4 Hz), 7.75 (1H, t, J = 7.4 Hz), 7.68 (1H, t, J = 7.4 Hz), 7.54 (2H, d, J = 8.4 Hz), 7.42 (2H, d, J = 8.2 Hz), 6.76 (2H, d, J = 8.2 Hz), 6.52 (1H, s), 5.07 (2H, s), 2.48 (3H, s); ^{13}C NMR (100 MHz, $CDCl_3$): δ 179.8, 154.9, 154.8, 149.1, 147.7, 141.7, 134.4, 133.5, 132.7, 132.3, 131.3, 131.0, 130.6, 128.9, 126.6, 125.4, 123.2, 122.0, 118.1, 103.4, 61.7, 21.9; IR ν_{max} (cm^{-1}, KBr): 3127, 1670, 1609, 1393, 1260, 1192, 1015, 852, 774, 670, 587, 540; EI/HRMS (m/z) [M + H]$^+$: 563.0364. Cald. for [$C_{26}H_{20}BrN_4O_4S$]$^+$: 563.0383.

(*E*)-4-((4-Iodophenyl)imino)-2-((1-tosyl-1*H*-1,2,3-triazol-4-yl)-methoxy)naphthalen-1(4*H*)-one (4g). The product was obtained as a yellow solid (89% yield); mp 173–175 °C; ^{1}H NMR (400 MHz, $CDCl_3$): δ 8.45 (1H, d, J = 7.8 Hz), 8.21 (1H, s), 8.19 (1H, d, J = 7.8 Hz), 8.01 (2H, d, J = 8.2 Hz), 7.75–7.69 (3H, m), 7.66 (1H, t, J = 7.4 Hz), 7.39 (2H, d, J = 8.2 Hz), 6.62 (2H, d, J = 8.3 Hz), 6.79 (1H, s), 5.05 (2H, s), 2.45 (3H, s); ^{13}C NMR (100 MHz, $CDCl_3$): δ 179.8, 154.9, 149.7, 147.7, 141.7, 138.2, 134.4, 133.5, 132.7, 131.3, 131.0, 130.6, 128.9, 126.6, 125.4, 123.2, 122.3, 103.4, 88.8, 61.7, 21.9; IR ν_{max} (cm^{-1}, KBr): 3138, 2919, 1670, 1609, 1396, 1260, 1194, 1017, 668, 585; EI/HRMS (m/z) [M + H]$^+$: 611.0246. Cald. for [$C_{26}H_{20}IN_4O_4S$]$^+$: 611.0244.

(*E*)-4-((4-Acetylphenyl)imino)-2-((1-tosyl-1*H*-1,2,3-triazol-4-yl)methoxy)naphthalen-1(4*H*)-one (4h). The product was obtained as a yellow solid (87% yield); mp 174–176 °C; ^{1}H NMR (400 MHz, $CDCl_3$): δ 8.46 (1H, d, J = 7.6 Hz), 8.22–8.20 (2H, m), 8.04–7.99 (4H, m), 7.76 (1H, t, J = 7.3 Hz), 7.68 (1H, t, J = 7.3 Hz), 7.40 (2H, d, J = 8.1 Hz), 6.91 (2H, d, J = 8.1 Hz), 6.39 (1H, s), 5.03 (2H, s), 2.65 (3H, s), 2.46 (3H, s); ^{13}C NMR (100 MHz, $CDCl_3$): δ 197.0, 179.7, 155.0, 154.6, 147.7, 141.6, 134.1, 133.7, 133.6, 132.7, 131.5, 131.1, 130.6, 129.8, 128.9, 126.6, 125.5, 123.2, 119.9, 103.6, 61.8, 29.7, 26.5, 21.8; IR ν_{max} (cm^{-1}, KBr): 3133, 2919, 2859, 1670, 1594, 1393, 1269, 1194, 1019, 670, 590; EI/HRMS (m/z) [M + H]$^+$: 527.1378. Cald. for [$C_{28}H_{23}N_4O_5S$]$^+$: 527.1384.

General procedure for the synthesis of compounds 5a–d. The synthesis of compounds **5a–d** was performed according to the methodology described in the literature by the Potter and Chen groups with minor modifications.[36,37] To a 25 mL round bottom flask, 5 mL of ethanol and 5 mL of water, and then sodium 3,4-dioxo-3,4-dihydronaphthalene-1-sulfonate (**1**) (1 mmol) and the corresponding thiophenol (2 mmol) were added. The reaction mixture was stirred at room temperature under ultrasound energy, and monitored by TLC until the total consumption of the starting material. After completion of the reaction, the organic phase was extracted with dichloromethane and dried over sodium sulphate. The solvent was removed under reduced pressure to afford the crude product, which was purified by column chromatography over silica gel, using as the eluent a gradient mixture of hexane/ethyl acetate with increasing polarity. The analytical data for compounds **5a** are in accordance with those reported in the literature.[17b]

4-(*p*-Tolylthio)naphthalene-1,2-dione (5b). The product was obtained as an orange solid (40% yield); mp 205–206 °C; ^{1}H NMR (200 MHz, $CDCl_3$): δ 8.09 (1H, d, J = 7.4 Hz), 7.87 (1H, d, J = 7.6 Hz), 7.65 (t, 1H, J = 7.2 Hz), 7.52 (1H, t, J = 7.4 Hz), 7.37 (2H, d, J = 8.0 Hz), 7.25 (2H, d, J = 8.0 Hz), 5.80 (s, 1H), 2.36 (s, 3H); ^{13}C NMR (50 MHz, $CDCl_3$): 179.5, 176.6, 161.9, 141.7, 135.8, 135.0, 133.4, 131.1, 130,3, 129.4, 125.0, 122.6, 121.1, 21.3; EI/MS (m/z) [M + H]$^+$: 281.0. Cald. for [$C_{17}H_{13}O_2S$]$^+$: 281.0.

4-(*m*-Tolylthio)naphthalene-1,2-dione (5c). The product was obtained as an orange solid (32% yield); mp 210–212 °C; ^{1}H NMR (400 MHz, $CDCl_3$): δ 8.19 (1H, d, J = 7.4 Hz), 7.97 (1H, d, J = 7.6 Hz), 7.74 (1H, t, J = 7.2 Hz), 7.62 (1H, t, J = 7.4 Hz), 7.44–7.35 (m, 4H), 5.92 (s, 1H), 2.43 (s, 3H); ^{13}C NMR (100 MHz, $CDCl_3$): 179.5, 176.6, 161.9, 140.6, 136.5, 135.0, 133.4, 131.1, 130,3, 129.4, 125.0, 122.6, 121.1, 21.3; EI/MS (m/z) [M + H]$^+$: 281.0. Cald. for [$C_{17}H_{13}O_2S$]$^+$: 281.0.

4-((4-Methoxyphenyl)thio)naphthalene-1,2-dione (5d). The product was obtained as a red solid (30% yield); mp 215–216 °C; ^{1}H NMR (400 MHz, $CDCl_3$): δ 8.17 (1H, d, J = 7.6 Hz), 7.95 (1H, d, J = 7.7 Hz), 7.73 (1H, t, J = 7.6 Hz), 7.60 (1H, t, J = 7.5 Hz), 7.48 (2H, d, J = 8.4 Hz), 7.03 (2H, d, J = 8.4 Hz), 5.88 (1H, s), 3.89 (3H,

s); ^{13}C NMR (100 MHz, $CDCl_3$): 179.5, 176.6, 162.0, 137.5, 135.8, 135.0, 133.4, 131.1, 130,3, 129.4, 125.0, 122.6, 121.1, 55.6; EI/MS (*m*/*z*) $[M + H]^+$: 297.0. Cald. for $[C_{17}H_{13}O_3S]^+$: 297.0.

4.2. Biological assays

4.2.1. Animals. All experiments dealing with animals were performed in accordance with the Brazilian Law 11.794/2008 and regulations of the National Council of Animal Experimentation Control under the license L038/2018 from the Ethics Committee for Animal Use of the Oswaldo Cruz Institute (CEUA/IOC).

4.2.2. Cytotoxicity assays. The compounds were tested for cytotoxic activity in cell culture *in vitro* employing several human cancer cell lines obtained from the National Cancer Institute, NCI (Bethesda, MD). Cytotoxicity was investigated against six cancer cell lines, *i.e.* HCT-116 (human colon carcinoma cells), NCI-H460 (human lung cancer cells), PC3 (human prostate cells), HL-60 (human promyelocytic leukemia cells), K-562 (myelogenous leukemia cell line) and Lucena 1 (MDR-cell line). The murine fibroblast immortalized cell line (L929) was used as control lineage. All culture media were supplemented with 10% fetal bovine serum, 2 mM L-glutamine, 100 IU mL^{-1} penicillin, and 100 μg mL^{-1} streptomycin at 37 °C with 5% CO_2. In cytotoxicity experiments, cells were plated in 96-well plates (0.1×10^6 cells per well for leukaemia cells, 0.7×10^5 cells per well for HCT-116, and 0.1×10^6 cells per well for PC3, L929 and NCI-H460). All the compounds tested were dissolved in DMSO. The final concentration of DMSO in the culture medium was kept constant (0.1%, v/v). Doxorubicin (0.001–1.10 μM) served as positive control, and negative control groups received the same amount of vehicle (DMSO). The cell viability was determined by reduction of the yellow dye 3-(4,5-dimethyl-2-thiazol)-2,5-diphenyl-2*H*-tetrazolium bromide (MTT) to a blue formazan product as described by Mosmann.[50a] At completion of the incubation after 72 h, the plates were centrifuged and the medium was replaced by fresh medium (200 μL) containing 0.5 mg mL^{-1} MTT. Three hours later, the MTT formazan product was dissolved in DMSO (150 μL) and the absorbance was measured on a multiplate reader (SpectraCount, Packard, Ontario, Canada). The influence of the compound on cell proliferation and survival was quantified as the percentage of control absorbance of the reduced dye at 550 nm. The results were obtained by nonlinear regression for all the cell lines from three independent experiments. All cell treatments were performed with three replicates. All cells were mycoplasma-free.

4.2.3. Measurement of intracellular reactive oxygen species levels. Intracellular reactive oxygen species (ROS) accumulation was monitored using 5-(6)-chloromethyl-2′,7′-dichlorodihydrofluorescein diacetate (CM-H_2DCFDA), which is converted to the highly fluorescent dichlorofluorescein (DCF) in the presence of intracellular ROS.[50b] K-562 cells (myelogenous leukemia cell line) were pre-loaded with 10 μM CM-H_2DCFDA and incubated for 1 hour, in the dark, at 37 °C/5% CO_2. After that time, the cells were centrifuged, the medium containing CM-H_2DCFDA was removed and the cells were washed with PBS buffer. From this stage, the cells were always protected from light. Fresh medium containing compounds **3e**, **4f** and **5a** was added and the cells were incubated at the times of interest (1 and 3 hours). After the incubation time, the cells were centrifuged, washed and re-suspended in PBS containing propidium iodide (PI) to a final concentration of 1 μg mL^{-1}. Tubes were placed on ice and immediately analyzed by flow cytometry. Living cells, which are PI negative, were selected by gating. In those living cells, the DCF fluorescence was recorded using excitation and emission wavelengths of 490 and 525 nm, respectively. Menadione (MEN, 20 μM) and hydrogen peroxide (H_2O_2, 150 μM) were used as positive controls. A total of 10 000 events were analyzed per sample. Data are expressed as mean ± SEM from three independent experiments.

4.2.4. Trypanocidal assay and selectivity index. Stock solutions of the compounds were prepared in dimethyl sulfoxide (DMSO), with the final concentration of the latter in the experiments never exceeding 0.4%. Preliminary experiments showed that DMSO has no deleterious effect on the parasites when its concentration is up to 4%. *T. cruzi* bloodstream trypomastigotes (Y strain) were obtained at the peak of parasitaemia from infected albino mice, purified by differential centrifugation and resuspended in RPMI to a parasite concentration of 10^7 cells per mL in the presence of 10% mouse blood. This suspension (100 μL) was added in the same volume of each compound previously prepared at twice the desired final concentrations for 24 h at 4 °C. Cell quantification was performed in a Neubauer chamber and the trypanocidal activity was expressed as IC_{50}/24 h, corresponding to the concentration that leads to lysis of 50% of the parasites. In order to determine the SI, cytotoxicity assays were performed with primary cultures of peritoneal macrophages obtained from Albino Swiss mice. For the experiments, 2.5×10^4 cells in 200 μL of RPMI-1640 medium (pH 7.2 plus 10% foetal bovine serum and 2 mM glutamine) were added to each well of a 96-well microtitre plate and incubated for 24 h at 37 °C. The treatment of the cultures was performed in fresh supplemented medium (200 μL per well) for 24 h at 37 °C. After this period, 110 μL of the medium was discarded and 10 μL of PrestoBlue (Invitrogen) was added to complete the final volume of 100 μL. Thus, the plate was incubated for 2 h and the measurement was performed at 560 and 590 nm, as recommended by the manufacturer. The results were expressed as the difference in the percentage of reduction between treated and untreated cells being the LC_{50} value, corresponding to the concentration that leads to damage of 50% of the mammalian cells.

5. X-ray crystallography

X-ray diffraction data collection for the compounds was performed on an Enraf-Nonius Kappa-CCD diffractometer (95

mm CCD camera on a κ-goniostat) and XtaLAB Mini (ROW) two-circle diffractometer employing graphite monochromated MoK_radiation (0.71073 Å), at room temperature. Data collection was carried out using the COLLECT software and CrysAlisPro.[51,52] Integration and scaling of the reflections, and correction for Lorentz and polarization effects were performed with the HKL DENZO-SCALEPACK and the CrysAlisPro system of programs.[53] The structure of the compounds was solved by direct methods with SHELXS-97.[54] The models were refined by full-matrix least squares on F^2 using SHELXL-97.[54] The program ORTEP-3 was used for graphic representation and the program WINGX was used to prepare materials for publication.[55,56] All H atoms were located by geometric considerations placed (C–H = 0.93–0.96 Å; N–H = 0.86 Å) and refined as riding with U_{iso}(H) = 1.5U_{eq}(C-methyl) or 1.2U_{eq}(other). Crystallographic data for the structures were deposited in the Cambridge Crystallographic Data Centre, with CCDC numbers 1928261 (**3a**), 1928296 (**3d**), 1928326 (**3f**), 1928361 (**3g**), 1928382 (**3h**) and 1928407 (**5d**).

6. Electrochemical studies

Cyclic voltammetry was performed on a 100B/W electrochemical workstation (BASI®, West Lafayette, USA) at ambient temperature. Cyclic voltammograms of the compounds (1 mM) were recorded in phosphate buffer (pH 7.4), employing a glassy carbon working electrode cleaned and polished with Al_2O_3 after each scan, an Ag/AgCl reference electrode (SSE) and a platinum wire counter electrode, at a potential range between −1 and +1 V. Quinone derivatives required 30% methanol due to limited solubility in aqueous media. Buffers were purged with nitrogen for 30 min prior to use. The sensitivity of the cell was adjusted to 10 μA V^{-1} and the compounds were scanned at the rate of 200 mV s^{-1}.

Conflicts of interest

Authors declare no conflict of interest.

Acknowledgements

This research was funded by grants from CNPq (404466/2016-8 and PQ 305741/2017-9, PDS 110818/2016-4 and PQ SR 302613/2013-9), Chamada Universal MCTI/CNPq No 01/2016, FAPEMIG (Edital 01/2014 APQ-02478-14 and Programa Pesquisador Mineiro – PPM-00638-16 and PPM-00635-18), FAPERJ (CNE Proc. E-26/203.083/2016), CAPES and INCT-Catalysis. ENSJ would like to thank CAPES and DAAD for the PROBRAL exchange program (99999.008126/2015-01). ENSJ thanks the Capes-Humboldt research fellowship for experienced researchers (Proc. No. 88881.145517/2017-01), Return Fellowship of the Alexander-von-Humboldt foundation and the Royal Society of Chemistry for the research fund grant (R19-9781). CAS would like to thank the Institute of Physics of the University of São Paulo (São Carlos). The authors would like to thank the Multi-User Facility of Drug Research and Development Center of the Federal University of Ceará for technical support. AK also thanks the University of Saarland, CAPES and DAAD for the PROBRAL exchange program that provided financial support for his exchange period at the Federal University of Minas Gerais. The authors are grateful to Prof. Claus Jacob from the University of Saarland for his excellent suggestions during the preparation of this manuscript.

References

1 J. Ferlay, I. Soerjomataram, R. Dikshit, S. Eser, C. Mathers, M. Rebelo, D. M. Parkin, D. Forman and F. Bray, *Int. J. Cancer*, 2015, **136**, E359–E386.
2 WHO, *Weekly epidemiological record.*, 2015, **90**, 33–43.
3 J. C. P. Dias, A. N. Ramos Jr., E. D. Gontijo, A. Luquetti, M. A. Shikanai-Yasuda, J. R. Coura, R. M. Torres, J. R. D. C. Melo, E. A. D. Almeida, W. D. Oliveira Jr., A. C. Silveira, J. M. D. Rezende, F. S. Pinto, A. W. Ferreira, A. Rassi, A. A. F. Filho, A. S. D. Sousa, D. C. Filho, A. M. Jansen, G. M. Q. Andrade, C. F. D. P. D. C. Britto, A. Y. D. N. Pinto, A. Rassi Jr., D. E. Campos, F. Abad-Franch, S. E. Santos, E. Chiari, A. M. Hasslocher-Moreno, E. F. Moreira, D. S. D. O. Marques, E. L. Silva, J. A. Marin-Neto, L. M. D. C. Galvão, S. S. Xavier, S. A. D. S. Valente, N. B. Carvalho, A. V. Cardoso, R. A. E. Silva, V. M. D. Costa, S. M. Vivaldini, S. M. Oliveira, V. D. C. Valente, M. M. Lima and R. V. Alves, *Epidemiol. Serv. Saude*, 2016, **25**, 7–86.
4 G. A. Schmunis and Z. E. Yadon, *Acta Trop.*, 2010, **115**, 14–21.
5 A. Requena-Méndez, S. Bussion, E. Aldasoro, Y. Jackson, A. Angheben, D. Moore, M.-J. Pinazo, J. Gascón, J. Muñoz and E. Sicuri, *Lancet*, 2017, **5**, e439–e447.
6 J. Gascon, C. Bern and M. J. Pinazo, *Acta Trop.*, 2010, **115**, 22–27.
7 S. Antinori, L. Galimberti, R. Bianco, R. Grande, M. Galli and M. Corbellino, *Eur. J. Intern. Med.*, 2017, **43**, 6–15.
8 K. Salomão, R. F. Menna-Barreto and S. L. de Castro, *Curr. Top. Med. Chem.*, 2016, **16**, 2266–2289.
9 R. P. Verma, *Anti-Cancer Agents Med. Chem.*, 2006, **6**, 489–499.
10 (*a*) S. L. de Castro, F. S. Emery and E. N. da Silva Junior, *Eur. J. Med. Chem.*, 2013, **69**, 678–700; (*b*) E. N. da Silva Júnior, G. A. M. Jardim, C. Jacob, U. Dhawa, L. Ackermann and S. L. de Castro, *Eur. J. Med. Chem.*, 2019, **179**, 863–915.
11 E. I. Parkinson and P. J. Hergenrother, *Acc. Chem. Res.*, 2015, **48**, 2715–2723.
12 H. Hussain and I. R. Green, *Expert Opin. Ther. Pat.*, 2017, **27**, 1111–1121.
13 H. Y. Qiu, P. F. Wang, H. Y. Lin, C. Y. Tang, H. L. Zhu and Y. H. Yang, *Chem. Biol. Drug Des.*, 2018, **91**, 681–690.
14 A. V. Pinto and S. L. de Castro, *Molecules*, 2009, **14**, 4570–4590.
15 D. Trachootham, J. Alexandre and P. Huang, *Nat. Rev. Drug Discovery*, 2009, **8**, 579–591.
16 S. Shaaban, R. Diestel, B. Hinkelmann, Y. Muthukumar, R. P. Verma, F. Sasse and C. Jacob, *Eur. J. Med. Chem.*, 2012, **58**, 192–205.

17 (*a*) Y. G. Paiva, T. L. Silva, A. F. A. Xavier, M. F. C. Cardoso, F. C. da Silva, M. F. S. Silva, D. P. Pinheiro, C. Pessoa, V. F. Ferreira and M. O. F. Goulart, *J. Braz. Chem. Soc.*, 2019, **30**, 658–672; (*b*) A. K. Mishra and J. N. Moorthy, *J. Org. Chem.*, 2016, **81**, 6472–6480.

18 C. J. Li, Y. Z. Li, A. V. Pinto and A. B. Pardee, *Proc. Natl. Acad. Sci. U. S. A.*, 1999, **96**, 13369–13374.

19 J. I. Lee, D. Y. Choi, H. S. Chung, H. G. Seo, H. J. Woo, B. T. Choi and Y. H. Choi, *Exp. Oncol.*, 2006, **28**, 30–35.

20 M. R. Gunner, J. Madeo and Z. Zhu, *J. Bioenerg. Biomembr.*, 2008, **40**, 509.

21 M. Doering, L. A. Ba, N. Lilienthal, C. Nicco, C. Scherer, M. Abbas, A. A. Zada, R. Coriat, T. Burkholz, L. Wessjohann, M. Diederich, F. Batteux, M. Herling and C. Jacob, *J. Med. Chem.*, 2010, **53**, 6954–6963.

22 G. I. Giles, K. M. Tasker, R. J. K. Johnson, C. Jacob, C. Peers and K. N. Green, *Chem. Commun.*, 2001, 2490–2491.

23 G. I. Giles, N. M. Giles, C. A. Collins, K. Holt, F. H. Fry, P. A. S. Lowden, N. J. Gutowski and C. Jacob, *Chem. Commun.*, 2003, 2030–2031.

24 E. N. da Silva Júnior, M. C. de Souza, A. V. Pinto, C. Pinto Mdo, M. O. Goulart, F. W. Barros, C. Pessoa, L. V. Costa-Lotufo, R. C. Montenegro, M. O. de Moraes and V. F. Ferreira, *Bioorg. Med. Chem.*, 2007, **15**, 7035–7041.

25 E. N. da Silva Júnior, M. A. B. F. D. Moura, A. V. Pinto, M. D. C. F. R. Pinto, M. C. B. V. D. Souza, A. J. Araújo, C. Pessoa, L. V. Costa-Lotufo, R. C. Montenegro, M. O. D. Moraes, V. F. Ferreira and M. O. F. Goulart, *J. Braz. Chem. Soc.*, 2009, **20**, 635–643.

26 E. N. da Silva Júnior, C. F. de Deus, B. C. Cavalcanti, C. Pessoa, L. V. Costa-Lotufo, R. C. Montenegro, M. O. de Moraes, M. D. C. F. R. Pinto, C. A. de Simone, V. F. Ferreira, M. O. F. Goulart, C. K. Z. Andrade and A. V. Pinto, *J. Med. Chem.*, 2010, **53**, 504–508.

27 (*a*) E. N. da Silva Júnior, B. C. Cavalcanti, T. T. Guimaraes, C. Pinto Mdo, I. O. Cabral, C. Pessoa, L. V. Costa-Lotufo, M. O. de Moraes, C. K. de Andrade, M. R. Dos Santos, C. A. de Simone, M. O. Goulart and A. V. Pinto, *Eur. J. Med. Chem.*, 2011, **46**, 399–410; (*b*) S. Shabaan, L. A. Ba, M. Abbas, T. Burkholz, A. Denkert, A. Gohr, L. A. Wessjohann, F. Sasse, W. Weber and C. Jacob, *Chem. Commun.*, 2009, 4702–4704; (*c*) S. Mecklenburg, S. Shaaban, L. A. Ba, T. Burkholz, T. Schneider, B. Diesel, A. K. Kiemer, A. Roseler, K. Becker, J. Reichrath, A. Stark, W. Tilgen, M. Abbas, L. A. Wessjohann, F. Sasse and C. Jacob, *Org. Biomol. Chem.*, 2009, **7**, 4753–4762.

28 E. H. G. da Cruz, M. A. Silvers, G. A. M. Jardim, J. M. Resende, B. C. Cavalcanti, I. S. Bomfim, C. Pessoa, C. A. de Simone, G. V. Botteselle, A. L. Braga, D. K. Nair, I. N. N. Namboothiri, D. A. Boothman and E. N. da Silva Júnior, *Eur. J. Med. Chem.*, 2016, **122**, 1–16.

29 (*a*) G. A. M. Jardim, E. H. G. da Cruz, W. O. Valença, D. J. B. Lima, B. C. Cavalcanti, C. Pessoa, J. Rafique, A. L. Braga, C. Jacob and E. N. da Silva Júnior, *Molecules*, 2018, **23**, 83; (*b*) G. A. M. Jardim, W. X. C. Oliveira, R. P. de Freitas, R. F. S. Menna-Barreto, T. L. Silva, M. O. F. Goulart and E. N. da Silva Júnior, *Org. Biomol. Chem.*, 2018, **16**, 1686–1691.

30 W. O. Valença, T. V. Baiju, F. G. Brito, M. H. Araujo, C. Pessoa, B. C. Cavalcanti, C. A. de Simone, C. Jacob, I. N. N. Namboothiri and E. N. da Silva Júnior, *ChemistrySelect*, 2017, **2**, 4300–4307.

31 E. N. da Silva Júnior, R. F. Menna-Barreto, M. C. Pinto, R. S. Silva, D. V. Teixeira, M. C. de Souza, C. A. De Simone, S. L. De Castro, V. F. Ferreira and A. V. Pinto, *Eur. J. Med. Chem.*, 2008, **43**, 1774–1780.

32 E. N. da Silva Júnior, G. A. M. Jardim, R. F. S. Menna-Barreto and S. L. D. Castro, *J. Braz. Chem. Soc.*, 2014, **25**, 1780–1798.

33 (*a*) R. L. de Carvalho, G. A. M. Jardim, A. C. C. Santos, M. H. Araujo, W. X. C. Oliveira, A. C. S. Bombaça, R. F. S. Menna-Barreto, E. Gopi, E. Gravel, E. Doris and E. N. da Silva Júnior, *Chem. – Eur. J.*, 2018, **24**, 15227–15235; (*b*) G. G. Dias, T. Rogge, R. Kuniyil, C. Jacob, R. F. S. Menna-Barreto, E. N. da Silva Júnior and L. Ackermann, *Chem. Commun.*, 2018, **54**, 12840–12843.

34 S. B. B. B. Bahia, W. J. Reis, G. A. M. Jardim, F. T. Souto, C. A. de Simone, C. C. Gatto, R. F. S. Menna-Barreto, S. L. de Castro, B. C. Cavalcanti, C. Pessoa, M. H. Araujo and E. N. da Silva Júnior, *MedChemComm*, 2016, **7**, 1555–1563.

35 E. N. da Silva Júnior, T. T. Guimarães, R. F. S. Menna-Barreto, M. C. F. R. Pinto, C. A. de Simone, C. Pessoa, B. C. Cavalcanti, J. R. Sabino, C. K. Z. Andrade, M. O. F. Goulart, S. L. de Castro and A. V. Pinto, *Bioorg. Med. Chem.*, 2010, **18**, 3224–3230.

36 M. J. Hatfield, J. Chen, E. M. Fratt, L. Chi, J. C. Bollinger, R. J. Binder, J. Bowling, J. L. Hyatt, J. Scarborough, C. Jeffries and P. M. Potter, *J. Med. Chem.*, 2017, **60**, 1568–1579.

37 C. H. Tseng, C. M. Cheng, C. C. Tzeng, S. I. Peng, C. L. Yang and Y. L. Chen, *Bioorg. Med. Chem.*, 2013, **21**, 523–531.

38 (*a*) C. H. Tseng, C. K. Lin, Y. L. Chen, C. K. Tseng, J. Y. Lee and J. C. Lee, *Eur. J. Med. Chem.*, 2018, **143**, 970–982; (*b*) T. P. Fragoso, J. W. M. Carneiro and M. D. Vargas, *J. Mol. Model.*, 2010, **16**, 825–830.

39 P. H. Di Chenna, V. Benedetti-Doctorovich, R. F. Baggio, M. T. Garland and G. Burton, *Eur. J. Med. Chem.*, 2001, **44**, 2486–2489.

40 K. E. Reinicke, E. A. Bey, M. S. Bentle, J. J. Pink, S. T. Ingalls, C. L. Hoppel, R. I. Misico, G. M. Arzac, G. Burton, W. G. Bornmann, D. Sutton, J. Gao and D. A. Boothman, *Clin. Cancer Res.*, 2005, **11**, 3055–3064.

41 G. A. M. Jardim, I. A. O. Bozzi, W. X. C. Oliveira, C. Mesquita-Rodrigues, R. F. S. Menna-Barreto, R. A. Kumar, E. Gravel, E. Doris, A. L. Braga and E. N. da Silva Júnior, *New J. Chem.*, 2019, **43**, 13751–13763.

42 J. Raushel and V. V. Fokin, *Org. Lett.*, 2010, **12**, 4952–4955.

43 A. A. Vieira, I. R. Brandao, W. O. Valença, C. A. de Simone, B. C. Cavalcanti, C. Pessoa, T. R. Carneiro, A. L. Braga and E. N. da Silva Júnior, *Eur. J. Med. Chem.*, 2015, **101**, 254–265.

44 F. H. Allen, O. Kennard, D. G. Watson, L. Brammer, A. G. Orpen and R. Taylor, *J. Chem. Soc., Perkin Trans. 2*, 1987, **12**, S1–S19.

45 R. I. Misico and E. S. Forzani, *Electrochem. Commun.*, 2003, **5**, 449–454.

46 K. Salomão, N. A. Santana, M. T. Molina, S. L. de Castro and R. F. S. Menna-Barreto, *BMC Microbiol.*, 2013, **13**, 196.
47 (*a*) J. N. Lopes, F. S. Cruz, R. Docampo, M. E. Vasconcellos, M. C. Sampaio, A. V. Pinto and B. Gilbert, *Ann. Trop. Med. Parasitol.*, 1978, **72**, 523–531; (*b*) G. A. M. Jardim, W. J. Reis, M. F. Ribeiro, F. M. Ottoni, R. J. Alves, T. L. Silva, M. O. F. Goulart, A. L. Braga, R. F. S. Menna-Barreto, K. Salomão, S. L. de Castro and E. N. da Silva Júnior, *RSC Adv.*, 2015, **5**, 78047–78060.
48 E. Perez-Sacau, R. G. Diaz-Penate, A. Estevez-Braun, A. G. Ravelo, J. M. Garcia-Castellano, L. Pardo and M. Campillo, *J. Med. Chem.*, 2007, **50**, 696–706.
49 D. D. Perrin, W. L. F. Armarego and D. R. Perrin, *Purification of Laboratory Chemicals*, 2nd edn, Pergamon, Oxford, 1980.
50 (*a*) T. Mosmann, *J. Immunol. Methods*, 1983, **65**, 55–63; (*b*) C. P. LeBel, H. Ischiropoulos and S. C. Bondy, *Chem. Res. Toxicol.*, 1992, **5**, 227–231.
51 B. V. Nonius, *Enraf-Nonius COLLECT*, Delft, The Netherlands, 1997–2000.
52 O. D. Rigaku, *CrysAlisPro*, 2015.
53 Z. Otwinowski and W. Minor, *Methods Enzymol.*, 1997, **276**, 307–326.
54 C. Schnitter, H. W. Roesky, T. Albers, H. G. Schmidt, C. Röpken, E. Parisini and G. M. Sheldrick, *Chem. – Eur. J.*, 1997, **3**, 1783–1792.
55 L. Farrugia, *J. Appl. Crystallogr.*, 1997, **30**, 565.
56 L. Farrugia, *J. Appl. Crystallogr.*, 1999, **32**, 837–838.

4. Discussion

The impressive broad spectrum of the biological activities the quinones demonstrate, and the accumulating evidence and results regarding the importance and effectiveness of both sulfur and selenium elements played a part in inspiring and encouraging the concept of synthesizing many groups of chalcogen based quinones, with the hope of introducing structures loaded with promising biological activities.

The biological studies that accompanied the chemical synthesis of this category of compounds proved these compounds highly active. Still, the pursuit of structures with good selectivity and high bioavailability among their characteristics remains an ongoing challenge in the fields of synthetic and medicinal chemistry.

As a part of this study, several chalcogen containing redox active compounds, based on natural naphthoquinones, i.e., lapachol, lawsone, and α-naphtoquinone, have been synthesized, which demonstrated a promising activity when tested against *Trypanosoma cruzi* and several cancer cell lines.

When viewing from the perspective of chemistry, as mentioned before, designing and synthesizing new redox active agents is an ongoing effort, aiming to reach the point where bioavailability, activity, and selectivity are satisfying.

In this regard, the compounds synthesized revolved around integrating sulfur and selenium in quinones based structures equipped with two abilities. First, generating ROS due to undergoing a one electron reduction reaction or alkylating agents after a two electron reduction reaction [96,97]. In addition to exploiting the chalcogen elements' redox activity and the reactive selenium species, reactive sulfur species and reactive selenium and sulfur species

(RSeSS), which form once the compounds are within the cellular environment, including and not limited to hydrogen sulfide and hydrogen selenide [98,84,99].

Electrochemical technique facilitated the synthesis of naphthoquinones based selenides. Using various diselenide as a source of a selenium dication which was involved in a fast carbophilic reaction with the naphtoquinone, followed with a cyclization reaction introducing the final products.

Additionally, one of the compounds synthesized was used as a precursor of three derivatizations, showcasing another capability this route offers, i.e., synthesizing new compounds by integrating the electrochemical synthesis as one step among other synthesis steps or techniques.

Due to the adjusted metabolism processes the cancer cells demonstrate, they become an easy target against such compounds [24,100]. The chemical properties the compounds synthesized hold led directly to the biological activity observed when tested against the cancer cell lines assigned for this study.

Similarly, due to the same characteristic of producing ROS, the synthesized compounds demonstrated the ability to affect *Trypanosoma cruzi* [101].

CV is included in many fields of scientific research and even in industry. Although it is not itself the backbone of any of the majors or fields, it is employed by; its data is a reliable reference for redirecting the efforts, whether in research studies or development of projects in the industrial sector. This technique has been commonly employed as an identification tool, a purification method, and a step within manufacturing processes [102-104]. The role this technique plays is crucial during the development of enzyme mimics, for example. One of the prerequisites for such compounds is to have an identical redox potential to that of the

inspiring enzyme. Employing CV in this step of the development process helps determine the researcher's distance to the target compound [105-107].

Within this study, one particular application of CV in synthetic chemistry has been employed in this study. The redox potentials of the sulfur containing quinone based compounds were monitored and recorded. The aim was to rely on this data as a form of structure-activity relationship (SAR) to link and interpret these compounds' biological activity testing results.

Two points might interfere with the extent the CV data can serve as a source of information. First, considering a compound as biologically active or highly active, based on its redox potentials, is not necessarily compatible with the biological testing results. One of the requirements needed to label a compound as biologically active is the selectivity, and the nature of results obtained by CV does not provide such information. While CV draws an image of a compound's redox activity, it cannot predict how the elements, side chains, and moieties added to the core structure affect the final compound's selectivity and cell toxicity.

Another point to consider is that the redox potentials might overlap as the complexity of the compound being synthesized increases. This makes interpreting and explaining the results more difficult, especially with compounds containing multiple redox centres and redox active elements such as the chalcogens.

Still, the data obtained from CV studies remains very valuable as a starting point and an initial filter that narrows down the scope of the studies performed. It helps determine a more precise direction for the next steps when taken, whether it is expanding the chemical synthesis for the structure of interest or using the image both CV data and biological testings' results drew and modifying the chemical synthesis to improve the activity.

A wide range of the natural and synthesized redox active groups and families of compounds had their fair share of studies in both fields, chemistry and biochemistry. It is not entirely the

case for a specific group of redox active agents. i.e., chalcogens, and also chalcogen based organic compounds. The short life span of the species the chalcogens form within the cellular environment, and their high chemical reactivity slowed down navigating this region. These species do not take long between their formation and engaging in chemical or biochemical reactions and subsequently transforming into other species. Besides, their low concentrations within the cellular environment is another reason that held back the progress in the studies dealing with them. It needed to wait till the analytical methods and the instruments able to detect and quantify such concentration were developed.

As a result, many studies that dealt with the identity of these, almost instantaneous, species relied in part on the expectation of their chemical structure, based on the traces they leave behind, i.e., biological effects or final chemical products.

In the second part of this study, sulfur and selenium analogues of phthalic acid anhydride were recruited in an analytical study to shed light on the mechanism responsible for the already known efficiency and put the finger on the possible species leading to it. Additionally, the two analogues were employed in a biological study, seeking more clarification regarding the source of biological effects the selenium analogue had already demonstrated in previous studies.

The ESI-MS (electrospray ionization mass spectrometry) findings indicate the Se- phthalic acid anhydride analogue's preparedness to release hydrogen selenide and couple with other components present in the media with the protonated Se at the center of such couplings. This outcome can be generalized and extended to include other organo-selenium compounds, presenting Se as an essential player in the biological activity of these compounds. Not only because of its own chemical and redox activities. But also due to its involvement in interacting with cellular components forming other intermediates and active species responsible for following cascades of reactions and effects.

In the following step, and to build on what was observed in the previous experiment, the centric role of the Se and S in the compounds employed was highlighted. The free radicals scavenging activity was investigated using BMPO and cPTIO based methods. Additionally, the experiment provides compelling evidence of the interaction between RSS, RSeS, and the cellular components. Here, GSH and hydrogen sulfide are the examples subjected to the experiment to form new species that demonstrate more efficient free radicals scavenging activities.

Finally, this study addressed the idea that RSeS and RSS's impact is directly related to their concentrations in the cellular medium or the target cell component. It has been previously concluded from the findings of this study that both RSeS and RSS exhibit protective antioxidant efficiency, while at the same time, they show damaging effects when the concentrations applied are adjusted.

The results credit a big part of the recorded activity to the formations of Se-S species within the cellular environment, which carry out their own interactions and reactions within the cell leading to the final effects.

These results are not limited to the compounds employed in this study. It is possible to extend and expand the concept to cover many organic chalcogen compounds to explain some of their recorded biological activity. The chalcogen element is responsible for the activity, while the organic part plays the carrier's role and facilitates the delivery of the element to the target point.

.

5. Conclusions

This study covers the synthesis and the biological evaluation of new redox active, chalcogen containing organic compounds based on natural naphthoquinones against *Trypanosoma cruzi*, the parasite that causes Chagas disease, and against several cancer cell lines. The study also, within the synthesis part, involves the electrochemical synthesis technique, a method that holds many advantages and opens the door for new possibilities regarding the structures which can be obtained when utilizing it.

This study also covers an analytical approach conducted in conditions close to the ones within the biological range to shed some light on some of the paths taken by chalcogen based redox active agents within the living organisms to demonstrate their biological impact.

And additionally, this study presents an attempt to link the bioactivity of the redox active compounds to their redox potentials, using cyclic voltammetry as a means to investigate the possible relation between these two aspects and the extent to which these two activities and redox behaviour of these compounds coincide.

Obtaining new redox active compounds, whether containing chalcogen elements or not, is a "still in progress" process in a continuous attempt to reach a compound or a group of compounds that guarantees a good biological activity, as antibacterial, antifungal, antiparasitic or anticancer, as examples from the range covered by the compounds that have been synthesized and biologically investigated so far. These efforts also include overcoming the challenges that improve the stability, bioavailability, and selectivity of these compounds.

Within this context, the work is underway to find new lead structures based on natural naphthoquinones and shift from merely adding functional moieties to the basic structure to design and synthesize more complex structures.

Here, the electrochemical synthesis technique helped introduce new selenium based redox active compounds comprising multiple redox centres, crafted from natural naphthoquinones by selenation and cyclization. An outlook to aim for is to exploit the electrochemical synthesis technique to synthesize the sulfur analogues of the selenium based compounds obtained in this study. Also, expanding the investigation of the biological activity to include bacteria and other parasites helps obtain a better idea of the range covered by these compounds.

In another chapter, this study employed phthalic anhydride and its sulfur and selenium derivatives as an example of chalcogen containing redox active compounds in an analytical study in biological conditions aiming for using the findings of the study not only for its direct output, which is a better understanding, and additional clarification of the biological effects and where they come from. But also to take advantage of these findings when new redox active compounds are being planned.

Finally, this study dealt with the attempt to follow the changes in the redox behaviour that occurred during the steps of the chemical synthesis of quinone based, amine, or sulfur containing new compounds.

For this purpose, cyclic voltammetry was used to record and observe the changes in the redox potentials, investigating the possibility of linking these findings to the compounds' biological activity as an additional attempt to build the chemists' efforts more oriented and fruitful when new synthesis protocols are being developed.

The interest in the topic of redox active modulators is not limited to the field of synthetic chemistry only. It also extends to understanding the paths these compounds take within the living cell and the chemical and biochemical reactions that occur and lead to the manifestation of the effects on the cellular process.

Both concepts, redox modulators and cellular redox chemistry overlap and include many layers worth exploring. The new techniques enriching chemical synthesis, intracellular diagnosis, and instrumental analysis will help to raise the bar each time it is reached.

6. References

1. Angeletti, L. R.; Agrimi, U.; Curia, C.; French, D.; Mariani-Costantini, R. Healing rituals and sacred serpents. *Lancet* **1992**, *340*, 223-225.
2. Jima, T. T.; Megersa, M. Ethnobotanical Study of Medicinal Plants Used to Treat Human Diseases in Berbere District, Bale Zone of Oromia Regional State, South East Ethiopia. *Evidence-Based Complementary and Alternative Medicine* **2018**,.
3. Lee, K.-H.; Morris-Natschke, S. L.; Yang, X.; Huang, R.; Zhou, T.; Wu, S.-F.; Shi, Q.; Itokawa, H. Recent progress of research on medicinal mushrooms, foods, and other herbal products used in traditional Chinese medicine. *Journal of traditional and complementary medicine* **2012**, *2*, 84-95.
4. Park, H.-L.; Lee, H.-S.; Shin, B.-C.; Liu, J.-P.; Shang, Q.; Yamashita, H.; Lim, B. Traditional Medicine in China, Korea, and Japan: A Brief Introduction and Comparison. *Evidence-Based Complementary and Alternative Medicine* **2012**.
5. Yu, F.; Takahashi, T.; Moriya, J.; Kawaura, K.; Yamakawa, J.; Kusaka, K.; Itoh, T.; Morimoto, S.; Yamaguchi, N.; Kanda, T. Traditional Chinese Medicine and Kampo: A Review from the Distant past for the Future. *Journal of International Medical Research* **2006**, *34*, 231-239.
6. Ching, J.; Soh, W.-L.; Tan, C.-H.; Lee, J.-F.; Tan, J.-Y. C.; Yang, J.; Yap, C.-W.; Koh, H.-L. Identification of active compounds from medicinal plant extracts using gas chromatography-mass spectrometry and multivariate data analysis. *Journal of Separation Science* **2012**, *35*, 53-59.
7. Sasidharan, S.; Chen, Y.; Saravanan, D.; Sundram, K. M.; Yoga Latha, L. Extraction, isolation and characterization of bioactive compounds from plants' extracts. *African journal of traditional, complementary, and alternative medicines : AJTCAM* **2011**, *8*, 1-10.
8. Mániková, D.; Letavayová, L. M.; Vlasáková, D.; Košík, P.; Estevam, E. C.; Nasim, M. J.; Gruhlke, M.; Slusarenko, A.; Burkholz, T.; Jacob, C.; Chovanec, M. Intracellular diagnostics: hunting for the mode of action of redox-modulating selenium compounds in selected model systems. *Molecules (Basel, Switzerland)* **2014**, *19*, 12258-12279.
9. Schneider, T.; Muthukumar, Y.; Hinkelmann, B.; Franke, R.; Döring, M.; Jacob, C.; Sasse, F. Deciphering intracellular targets of organochalcogen based redox catalysts. *MedChemComm* **2012**, *3*, 784-787.
10. Talib, W. H.; Alsalahat, I.; Daoud, S.; Abutayeh, R. F.; Mahmod, A. I. Plant-Derived Natural Products in Cancer Research: Extraction, Mechanism of Action, and Drug Formulation. *Molecules (Basel, Switzerland)* **2020**, *25*, 5319.
11. Forgan, R. S.; Sauvage, J.-P.; Stoddart, J. F. Chemical Topology: Complex Molecular Knots, Links, and Entanglements. *Chemical Reviews* **2011**, *111*, 5434-5464.
12. Zhang, Q.; Deng, Y.-X.; Luo, H.-X.; Shi, C.-Y.; Geise, G. M.; Feringa, B. L.; Tian, H.; Qu, D.-H. Assembling a Natural Small Molecule into a Supramolecular Network with High Structural Order and Dynamic Functions. *Journal of the American Chemical Society* **2019**, *141*, 12804-12814.
13. Zhang, Q.; Shi, C. Y.; Qu, D. H.; Long, Y. T.; Feringa, B. L.; Tian, H. Exploring a naturally tailored small molecule for stretchable, self-healing, and adhesive supramolecular polymers. *Sci Adv* **2018**.
14. Anna Rita, B.; Vieri, P.; Laura, R.; Giulia, V.; Marta, C.; Meng, W.; Maria Camilla, B. Nanocarriers: A Successful Tool to Increase Solubility, Stability and Optimise

Bioefficacy of Natural Constituents. *Current Medicinal Chemistry* **2019**, *26*, 4631-4656.
15. Coimbra, M.; Isacchi, B.; Van Bloois, L.; Torano, J. S.; Ket, A.; Wu, X.; Broere, F.; Metselaar, J. M.; Rijcken, C. J.; Storm, G.; Bilia, R.; Schiffelers, R. M. Improving solubility and chemical stability of natural compounds for medicinal use by incorporation into liposomes. *Int J Pharm* **2011**, *416*, 433-442.
16. Gu, T.; Zhong, Y.; Lu, Y.-T.; Sun, Y.; Dong, Z.-X.; Wu, W.-Y.; Shi, Z.-H.; Li, N.-G.; Xue, X.; Fang, F.; Li, H.-M.; Tang, Y.-P. Synthesis and Bioactivity Characterization of Scutellarein Sulfonated Derivative. *Molecules (Basel, Switzerland)* **2017**, *22*, 1028.
17. Yao, H.; Liu, J.; Xu, S.; Zhu, Z.; Xu, J. The structural modification of natural products for novel drug discovery. *Expert Opinion on Drug Discovery* **2017**, *12*, 121-140.
18. Chen, Y.; Cai, J.; Jones, D. P. Mitochondrial thioredoxin in regulation of oxidant-induced cell death. *FEBS Letters* **2006**, *580*, 6596-6602.
19. Dröge, W. Free Radicals in the Physiological Control of Cell Function. *Physiological Reviews* **2002**, *82*, 47-95.
20. Go, Y.-M.; Park, H.; Koval, M.; Orr, M.; Reed, M.; Liang, Y.; Smith, D.; Pohl, J.; Jones, D. P. A key role for mitochondria in endothelial signaling by plasma cysteine/cystine redox potential. *Free Radical Biology and Medicine* **2010**, *48*, 275-283.
21. Liu, Y.; Zhao, H.; Li, H.; Kalyanaraman, B.; Nicolosi, A. C.; Gutterman, D. D. Mitochondrial Sources of H_2O_2 Generation Play a Key Role in Flow-Mediated Dilation in Human Coronary Resistance Arteries. *Circulation Research* **2003**, *93*, 573-580.
22. Gupta, K. Reactive Oxygen species: The main culprit of Alzheimer Disease. *Nthrys E library (http://nthrys.org/main/user-access/applications/e-library?view=files&id=16)* **2013**.
23. Laskin, D. L.; Sunil, V. R.; Fakhrzadeh, L.; Groves, A.; Gow, A. J.; Laskin, J. D. Macrophages, reactive nitrogen species, and lung injury. *Annals of the New York Academy of Sciences* **2010**, *1203*, 60-65.
24. Liou, G.-Y.; Storz, P. Reactive oxygen species in cancer. *Free radical research* **2010**, *44*, 479-496.
25. De Marchi, U.; Biasutto, L.; Garbisa, S.; Toninello, A.; Zoratti, M. Quercetin can act either as an inhibitor or an inducer of the mitochondrial permeability transition pore: A demonstration of the ambivalent redox character of polyphenols. *Biochimica et Biophysica Acta (BBA) - Bioenergetics* **2009**, *1787*, 1425-1432.
26. Munday, R.; Munday, J. S.; Munday, C. M. Comparative effects of mono-, di-, tri-, and tetrasulfides derived from plants of the Allium family: redox cycling in vitro and hemolytic activity and Phase 2 enzyme induction in vivo. *Free Radic Biol Med* **2003**, *34*, 1200-1211.
27. Santos, P. M.; Telo, J. P.; Vieira, A. J. Structure and redox properties of radicals derived from one-electron oxidised methylxanthines. *Redox Rep* **2008**, *13*, 123-133.
28. Bakasso, S.; Lamien-Meda, A.; Lamien, C. E.; Kiendrebeogo, M.; Millogo, J.; Ouedraogo, A. G.; Nacoulma, O. G. Polyphenol contents and antioxidant activities of five Indigofera species (Fabaceae) from Burkina Faso. *Pak J Biol Sci* **2008**, *11*, 1429-1435.
29. Bringmann, G.; Mutanyatta-Comar, J.; Knauer, M.; Abegaz, B. M. Knipholone and related 4-phenylanthraquinones: structurally, pharmacologically, and biosynthetically remarkable natural products. *Nat Prod Rep* **2008**, *25*, 696-718.

30. Salem, M. L. Immunomodulatory and therapeutic properties of the Nigella sativa L. seed. *Int Immunopharmacol* **2005**, *5*, 1749-1770.
31. Fotie, J. Quinones and Malaria. *Anti-Infective Agents in Medicinal Chemistry (Formerly Current Medicinal Chemistry - Anti-Infective Agents)* **2006**, *5*, 357-366.
32. Futuro, D. O.; Ferreira, P. G.; Nicoletti, C. D.; Borba-Santos, L. P.; Silva, F. C. D.; Rozental, S.; Ferreira, V. F. The Antifungal Activity of Naphthoquinones: An Integrative Review. *Anais da Academia Brasileira de Ciências* **2018**, *90*, 1187-1214.
33. Jin, S.; Sato, N. Benzoquinone, the substance essential for antibacterial activity in aqueous extracts from succulent young shoots of the pear Pyrus spp. *Phytochemistry* **2003**, *62*, 101-107.
34. Lu, J. J.; Bao, J. L.; Wu, G. S.; Xu, W. S.; Huang, M. Q.; Chen, X. P.; Wang, Y. T. Quinones derived from plant secondary metabolites as anti-cancer agents. *Anticancer Agents Med Chem* **2013**, *13*, 456-463.
35. Hammam, A. S.; Hassan, M. A.; Fandy, R. F. 2,3-Dicyano-1,4-naphthoquinone as a dienophile in Diels-Alder reactions. *Afinidad* **2003**, *60*, 42-46.
36. He, Z.; Liu, T.; Tao, H.; Wang, C.-J. A Facile Access to Enantioenriched Isoindolines via One-Pot Sequential Cu(I)-Catalyzed Asymmetric 1,3-Dipolar Cycloaddition/Aromatization. *Organic Letters* **2012**, *14*, 6230-6233.
37. Ibis, C.; Tuyun, A. F.; Bahar, H.; Ayla, S. S.; Stasevych, M. V.; Musyanovych, R. Y.; Komarovska-Porokhnyavets, O.; Novikov, V. Nucleophilic substitution reactions of 1,4-naphthoquinone and biologic properties of novel S-, S,S-, N-, and N,S-substituted 1,4-naphthoquinone derivatives. *Medicinal Chemistry Research* **2014**, *23*, 2140-2149.
38. Skrzyńska, A.; Romaniszyn, M.; Pomikło, D.; Albrecht, Ł. The Application of 2-Benzyl-1,4-naphthoquinones as Pronucleophiles in Aminocatalytic Synthesis of Tricyclic Derivatives. *The Journal of Organic Chemistry* **2018**, *83*, 5019-5026.
39. Sun, K.; Zhang, B. Y.; Liu, X. X. Catalysis of ruthenium 1,2-naphthoquinone-1-oxime complexes towards aldol C-C bond formation reactions. *Chinese Journal of Organic Chemistry* **2005**, *25*, 424-426.
40. Garge, P.; Chikate, R.; Padhye, S.; Savariault, J. M.; De Loth, P.; Tuchagues, J. P. Iron(II) complexes of ortho-functionalized naphthoquinones. 2. Crystal and molecular structure of bis(aquo)bis(lawsonato)iron(II) and intermolecular magnetic exchange interactions in bis(3-aminolawsonato)iron(II). *Inorganic Chemistry* **1990**, *29*, 3315-3320.
41. Krohn, K.; Böker, N. Attachment of Ketide Side Chains on Methyl-1,4-naphthoquinones for biomimetic type angucycline syntheses. *Journal für Praktische Chemie/Chemiker-Zeitung* **1997**, *339*, 114-120.
42. Ravichandiran, P.; Vasanthkumar, S. Synthesis of heterocyclic naphthoquinone derivatives as potent organic fluorescent switching molecules. *Journal of Taibah University for Science* **2015**, *9*, 538-547.
43. Wu, C.; Johnson, R. K.; Mattern, M. R.; Wong, J. C.; Kingston, D. G. Synthesis of furanonaphthoquinones with hydroxyamino side chains. *J Nat Prod* **1999**, *62*, 963-968.
44. Wardman, P. Bioreductive Activation of Quinones: Redox Properties and Thiol Reactivity. *Free Radical Research Communications* **1990**, *8*, 219-229.
45. Brunmark, A.; Cadenas, E. Redox and addition chemistry of quinoid compounds and its biological implications. *Free Radical Biology and Medicine* **1989**, *7*, 435-477.
46. Crofts, A. R.; Lhee, S.; Crofts, S. B.; Cheng, J.; Rose, S. Proton pumping in the bc1 complex: A new gating mechanism that prevents short circuits. *Biochimica et Biophysica Acta (BBA) - Bioenergetics* **2006**, *1757*, 1019-1034.

47. Muller, F.; Crofts, A. R.; Kramer, D. M. Multiple Q-Cycle Bypass Reactions at the Qo Site of the Cytochrome bc1 Complex. *Biochemistry* **2002**, *41*, 7866-7874.
48. Collin, F. Chemical Basis of Reactive Oxygen Species Reactivity and Involvement in Neurodegenerative Diseases. *Int J Mol Sci* **2019**, *20*.
49. Phaniendra, A.; Jestadi, D. B.; Periyasamy, L. Free radicals: properties, sources, targets, and their implication in various diseases. *Indian journal of clinical biochemistry : IJCB* **2015**, *30*, 11-26.
50. Circu, M. L.; Aw, T. Y. Reactive oxygen species, cellular redox systems, and apoptosis. *Free radical biology & medicine* **2010**, *48*, 749-762.
51. Redza-Dutordoir, M.; Averill-Bates, D. A. Activation of apoptosis signalling pathways by reactive oxygen species. *Biochim Biophys Acta* **2016**, *12*, 17.
52. Zhang, J.; Wang, X.; Vikash; Ye, Q.; Wu, D.; Liu, Y.; Dong, W. ROS and ROS-mediated cellular signaling. *Oxidative Medicine and Cellular Longevity* **2016**.
53. López López, L. I.; Nery Flores, S. D.; Silva Belmares, S. Y.; Sáenz Galindo, A. NAPHTHOQUINONES: BIOLOGICAL PROPERTIES AND SYNTHESIS OF LAWSONE AND DERIVATIVES - A STRUCTURED REVIEW. *Vitae* **2014**, *21*, 248-258.
54. Wilson, I.; Wardman, P.; Lin, T.-S.; Sartorelli, A. C. Reactivity of thiols towards derivatives of 2- and 6-methyl-1,4-naphthoquinone bioreductive alkylating agents. *Chemico-Biological Interactions* **1987**, *61*, 229-240.
55. Shinkai, Y.; Iwamoto, N.; Miura, T.; Ishii, T.; Cho, A. K.; Kumagai, Y. Redox cycling of 1,2-naphthoquinone by thioredoxin1 through Cys32 and Cys35 causes inhibition of its catalytic activity and activation of ASK1/p38 signaling. *Chem Res Toxicol* **2012**, *25*, 1222-1230.
56. Wang, H.; Luo, Y. H.; Shen, G. N.; Piao, X. J.; Xu, W. T.; Zhang, Y.; Wang, J. R.; Feng, Y. C.; Li, J. Q.; Zhang, T.; Wang, S. N.; Xue, H.; Wang, H. X.; Wang, C. Y.; Jin, C. H. Two novel 1,4-naphthoquinone derivatives induce human gastric cancer cell apoptosis and cell cycle arrest by regulating reactive oxygen species-mediated MAPK/Akt/STAT3 signaling pathways. *Mol Med Rep* **2019**, *20*, 2571-2582.
57. Ansoborlo, E. Poisonous polonium. *Nature Chemistry* **2014**, *6*, 454-454.
58. Taylor, A. Biochemistry of tellurium. *Biological Trace Element Research* **1996**, *55*, 231-239.
59. Nimni, M. E.; Han, B.; Cordoba, F. Are we getting enough sulfur in our diet? *Nutrition & metabolism* **2007**, *4*, 24-24.
60. Thomson, C. D. Assessment of requirements for selenium and adequacy of selenium status: a review. *European Journal of Clinical Nutrition* **2004**, *58*, 391-402.
61. Mendoza-Cózatl, D.; Loza-Tavera, H.; Hernández-Navarro, A.; Moreno-Sánchez, R. Sulfur assimilation and glutathione metabolism under cadmium stress in yeast, protists and plants. *FEMS Microbiology Reviews* **2005**, *29*, 653-671.
62. Oliveira, T. F.; Franklin, E.; Afonso, J. P.; Khan, A. R.; Oldham, N. J.; Pereira, I. a. C.; Archer, M. Structural insights into dissimilatory sulfite reductases: structure of desulforubidin from desulfomicrobium norvegicum. *Frontiers in microbiology* **2011**, *2*, 71-71.
63. Parey, K.; Warkentin, E.; Kroneck, P. M. H.; Ermler, U. Reaction Cycle of the Dissimilatory Sulfite Reductase from Archaeoglobus fulgidus. *Biochemistry* **2010**, *49*, 8912-8921.
64. Baker, R. D.; Baker, S. S.; Larosa, K.; Whitney, C.; Newburger, P. E. Selenium regulation of glutathione peroxidase in human hepatoma cell line Hep3B. *Arch Biochem Biophys* **1993**, *304*, 53-57.

65. Johansson, L.; Gafvelin, G.; Arnér, E. S. J. Selenocysteine in proteins-properties and biotechnological use. *Biochimica et biophysica acta* **2005**, *1726*, 1-13.
66. Schrauzer, G. N. Selenomethionine: A Review of Its Nutritional Significance, Metabolism and Toxicity. *The Journal of Nutrition* **2000**, *130*, 1653-1656.
67. Yamashita, M.; Yamashita, Y.; Suzuki, T.; Kani, Y.; Mizusawa, N.; Imamura, S.; Takemoto, K.; Hara, T.; Hossain, M. A.; Yabu, T.; Touhata, K. Selenoneine, a novel selenium-containing compound, mediates detoxification mechanisms against methylmercury accumulation and toxicity in zebrafish embryo. *Mar Biotechnol* **2013**, *15*, 559-570.
68. Ito, Y.; Touyama, A.; Uku, M.; Egami, H.; Hamashima, Y. Thiocyanation of Aromatic and Heteroaromatic Compounds with 1-Chloro-1,2-benziodoxol-3-1*H*-one and (Trimethylsilyl)isothiocyanate. *Chemical and Pharmaceutical Bulletin* **2019**, *67*, 1015-1018.
69. Kazemi, M.; Sajjadifar, S.; Abdelkarim, A. Biological and Pharmaceutical Organosulfur Molecules. **2018**.
70. Pacuła, A.; Obieziurska-Fabisiak, M.; Ścianowski, J.; Kaczor, K.; Antosiewicz, J. Water-dependent synthesis of biologically active diaryl diselenides. *Arkivoc* **2018**, *2018*, 144-155.
71. Romano, B.; Plano, D.; Encío, I.; Palop, J. A.; Sanmartín, C. In vitro radical scavenging and cytotoxic activities of novel hybrid selenocarbamates. *Bioorg Med Chem* **2015**, *23*, 1716-1727.
72. Santos, E. D. a. D.; Prado, P. C.; Carvalho, W. R. D.; Lima, R. V. D.; Beatriz, A.; Lima, D. P. D.; Hamel, E.; Dyba, M. A.; Albuquerque, S. Synthesis and biological activity of sulfur compounds showing structural analogy with combretastatin A-4. *Química Nova* **2013**, *36*, 279-283.
73. Branowska, D.; Karczmarzyk, Z.; Wolińska, E.; Wysocki, W.; Morawiak, M.; Urbańczyk-Lipkowska, Z.; Bielawska, A.; Bielawski, K. 1,2,4-Triazine Sulfonamides: Synthesis by Sulfenamide Intermediates, In Vitro Anticancer Screening, Structural Characterization, and Molecular Docking Study. *Molecules (Basel, Switzerland)* **2020**, *25*.
74. Jacob, C.; Maret, W.; Vallee, B. L. Ebselen, a selenium-containing redox drug, releases zinc from metallothionein. *Biochem Biophys Res Commun* **1998**, *248*, 569-573.
75. P Thomas, S.; Jayatilaka, D.; Row, T. S...O Chalcogen Bonding in Sulfa Drugs: Insights from Multipole Charge Density and X-ray Wavefunction of Acetazolamide. *Physical chemistry chemical physics : PCCP* **2015**, *17*.
76. Zhang, D.-W.; Yan, H.-L.; Xu, X.-S.; Xu, L.; Yin, Z.-H.; Chang, S.; Luo, H. The selenium-containing drug ebselen potently disrupts LEDGF/p75-HIV-1 integrase interaction by targeting LEDGF/p75. *Journal of enzyme inhibition and medicinal chemistry* **2020**, *35*, 906-912.
77. Panetta, C. A.; Fan, P. W.-J.; Fattah, R.; Greever, J. C.; He, Z.; Hussey, C. L.; Sha, D.; Wescott, L. D. 1,4-Naphthoquinone Disulfides and Methyl Sulfides: Self-Assembled Monolayers on Gold Substrates. *The Journal of Organic Chemistry* **1999**, *64*, 2919-2923.
78. Sakakibara, M.; Watanabe, Y.; Toru, T.; Ueno, Y. New selenenylation method. Synthesis of setenonaphthoquinones and selenoquinolinequinones mediated by phenyl selenide ion. *Journal of the Chemical Society, Perkin Transactions 1* **1991**, 10.1039/p19910001231, 1231-1234.

79. Wellington, K. W.; Kolesnikova, N. I.; Hlatshwayo, V.; Saha, S. T.; Kaur, M.; Motadi, L. R. Anticancer activity, apoptosis and a structure-activity analysis of a series of 1,4-naphthoquinone-2,3-bis-sulfides. *Invest New Drugs* **2020**, *38*, 274-286.
80. Klotz, L.-O.; Hou, X.; Jacob, C. 1,4-naphthoquinones: from oxidative damage to cellular and inter-cellular signaling. *Molecules (Basel, Switzerland)* **2014**, *19*, 14902-14918.
81. Szilagyi, J. T.; Fussell, K. C.; Wang, Y.; Jan, Y. H.; Mishin, V.; Richardson, J. R.; Heck, D. E.; Yang, S.; Aleksunes, L. M.; Laskin, D. L.; Laskin, J. D. Quinone and nitrofurantoin redox cycling by recombinant cytochrome b5 reductase. *Toxicol Appl Pharmacol* **2018**, *359*, 102-107.
82. Bortoli, M.; Torsello, M.; Bickelhaupt, F. M.; Orian, L. Role of the Chalcogen (S, Se, Te) in the Oxidation Mechanism of the Glutathione Peroxidase Active Site. *ChemPhysChem* **2017**, *18*, 2990-2998.
83. Giles, G. I.; Nasim, M. J.; Ali, W.; Jacob, C. The Reactive Sulfur Species Concept: 15 Years On. *Antioxidants (Basel, Switzerland)* **2017**, *6*, 38.
84. Kharma, A.; Grman, M.; Misak, A.; Domínguez-Álvarez, E.; Nasim, M. J.; Ondrias, K.; Chovanec, M.; Jacob, C. Inorganic Polysulfides and Related Reactive Sulfur–Selenium Species from the Perspective of Chemistry. *Molecules (Basel, Switzerland)* **2019**, *24*, 1359.
85. Kolluru, G. K.; Shen, X.; Kevil, C. G. Reactive Sulfur Species. *Arteriosclerosis, Thrombosis, and Vascular Biology* **2020**, *40*, 874-884.
86. Ashnagar, A.; Bruce, J. M.; Dutton, P. L.; Prince, R. C. One- and two-electron reduction of hydroxy-1,4-naphthoquinones and hydroxy-9,10-anthraquinones. The role of internal hydrogen bonding and its bearing on the redox chemistry of the anthracycline antitumour quinones. *Biochim Biophys Acta* **1984**, *801*, 351-359.
87. Koyama, J.; Morita, I.; Kobayashi, N.; Osakai, T.; Hotta, H.; Takayasu, J.; Nishino, H.; Tokuda, H. Correlation of redox potentials and inhibitory effects on Epstein-Barr virus activation of 2-azaanthraquinones. *Cancer Lett* **2004**, *212*, 1-6.
88. Kumbhar, A.; Padhye, S.; Ross, D. Cytotoxic properties of iron-hydroxynaphthoquinone complexes in rat hepatocytes. *Biometals* **1996**, *9*, 235-240.
89. Anwar, A.; Burkholz, T.; Scherer, C.; Abbas, M.; Lehr, C.-M.; Diederich, M.; Jacob, C. Naturally occurring reactive sulfur species, their activity against Caco-2 cells, and possible modes of biochemical action. *Journal of Sulfur Chemistry* **2008**, *29*, 251-268.
90. Yuan, Y.; Lei, A. Is electrosynthesis always green and advantageous compared to traditional methods? *Nature Communications* **2020**, *11*, 802.
91. Möhle, S.; Zirbes, M.; Rodrigo, E.; Gieshoff, T.; Wiebe, A.; Waldvogel, S. R. Modern Electrochemical Aspects for the Synthesis of Value-Added Organic Products. *Angewandte Chemie International Edition* **2018**, *57*, 6018-6041.
92. Kärkäs, M. D. Electrochemical strategies for C–H functionalization and C–N bond formation. *Chemical Society Reviews* **2018**, *47*, 5786-5865.
93. Leech, M. C.; Garcia, A. D.; Petti, A.; Dobbs, A. P.; Lam, K. Organic electrosynthesis: from academia to industry. *Reaction Chemistry & Engineering* **2020**, *5*, 977-990.
94. Perry, S. C.; Ponce De León, C.; Walsh, F. C. Review—The Design, Performance and Continuing Development of Electrochemical Reactors for Clean Electrosynthesis. *Journal of The Electrochemical Society* **2020**, *167*, 155525.
95. Schotten, C.; Nicholls, T. P.; Bourne, R. A.; Kapur, N.; Nguyen, B. N.; Willans, C. E. Making electrochemistry easily accessible to the synthetic chemist. *Green Chemistry* **2020**, *22*, 3358-3375.

96. Anand, A.; Chen, K.; Yang, L.; Sastry, A. V.; Olson, C. A.; Poudel, S.; Seif, Y.; Hefner, Y.; Phaneuf, P. V.; Xu, S.; Szubin, R.; Feist, A. M.; Palsson, B. O. Adaptive evolution reveals a tradeoff between growth rate and oxidative stress during naphthoquinone-based aerobic respiration. *Proceedings of the National Academy of Sciences* **2019**, *116*, 25287-25292.
97. Giulivi, C.; Cadenas, E. One- and two-electron reduction of 2-methyl-1,4-naphthoquinone bioreductive alkylating agents: kinetic studies, free-radical production, thiol oxidation and DNA-strand-break formation. *Biochemical Journal* **1994**, *301*, 21-30.
98. Cupp-Sutton, K. A.; Ashby, M. T. Biological Chemistry of Hydrogen Selenide. *Antioxidants (Basel, Switzerland)* **2016**, *5*, 42.
99. Olson, K. R. Hydrogen sulfide, reactive sulfur species and coping with reactive oxygen species. *Free Radic Biol Med* **2019**, *140*, 74-83.
100. Zhou, D.; Shao, L.; Spitz, D. R. Reactive oxygen species in normal and tumor stem cells. *Advances in cancer research* **2014**, *122*, 1-67.
101. Lazarin-Bidóia, D.; Desoti, V. C.; Martins, S. C.; Ribeiro, F. M.; Ud Din, Z.; Rodrigues-Filho, E.; Ueda-Nakamura, T.; Nakamura, C. V.; De Oliveira Silva, S. Dibenzylideneacetones Are Potent Trypanocidal Compounds That Affect the *Trypanosoma cruzi* Redox System. *Antimicrobial Agents and Chemotherapy* **2016**, *60*, 890-903.
102. Alatraktchi, F. a. A.; Breum Andersen, S.; Krogh Johansen, H.; Molin, S.; Svendsen, W. E. Fast Selective Detection of Pyocyanin Using Cyclic Voltammetry. *Sensors* **2016**, *16*, 408.
103. Chooto, P. Cyclic Voltammetry and Its Applications. 2019.
104. Kilmartin, P. A.; Zou, H.; Waterhouse, A. L. A Cyclic Voltammetry Method Suitable for Characterizing Antioxidant Properties of Wine and Wine Phenolics. *Journal of Agricultural and Food Chemistry* **2001**, *49*, 1957-1965.
105. Kuah, E.; Toh, S.; Yee, J.; Ma, Q.; Gao, Z. Enzyme Mimics: Advances and Applications. *Chemistry – A European Journal* **2016**, *22*, 8404-8430.
106. Kupcewicz, B.; Sobiesiak, K.; Malinowska, K.; Koprowska, K.; Czyz, M.; Keppler, B.; Budzisz, E. Copper(II) complexes with derivatives of pyrazole as potential antioxidant enzyme mimics. *Med Chem Res* **2013**, *22*, 2395-2402.
107. Samuni, A.; Krishna, C. M.; Riesz, P.; Finkelstein, E.; Russo, A. A novel metal-free low molecular weight superoxide dismutase mimic. *J Biol Chem* **1988**, *263*, 17921-17924.

7. Supplementary Material

7.1. Supplementary Material for Publication 1: Electrochemical Selenation/Cyclization of Quinones: A Rapid, Green and Efficient Access to Functionalized Trypanocidal and Antitumor Compounds

EurJOC
European Journal of Organic Chemistry

Supporting Information

Electrochemical Selenation/Cyclization of Quinones: A Rapid, Green and Efficient Access to Functionalized Trypanocidal and Antitumor Compounds

Ammar Kharma, Claus Jacob,* Ícaro A. O. Bozzi, Guilherme A. M. Jardim, Antonio L. Braga, Kelly Salomão, Claudia C. Gatto, Maria Francilene S. Silva, Claudia Pessoa, Maximilian Stangier, Lutz Ackermann,* Eufrânio N. da Silva Júnior*

Table of Contents

General electrochemical apparatus

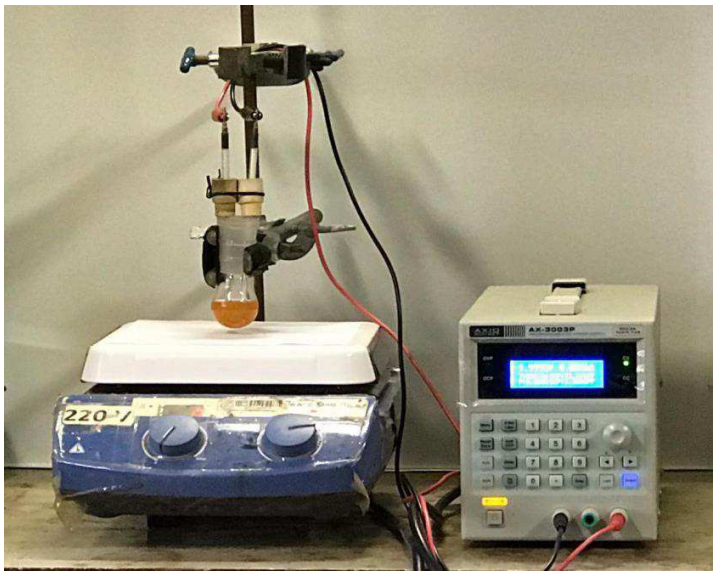

Figure S1. General apparatus for the synthesis of compounds **3**, **5** and **7**.

Cyclic Voltammetry

The cyclic voltammetry was carried out with a Metrohm Autolab PGSTAT204 workstation and following analysis was performed with Nova 2.1 software. A glassy-carbon electrode (3 mm-diameter, disc-electrode) was used as the working electrode, a Pt wire as auxiliary electrode and a SCE electrode was used as the reference. The measurements were carried out at a scan rate of 100 mVs^{-1}.

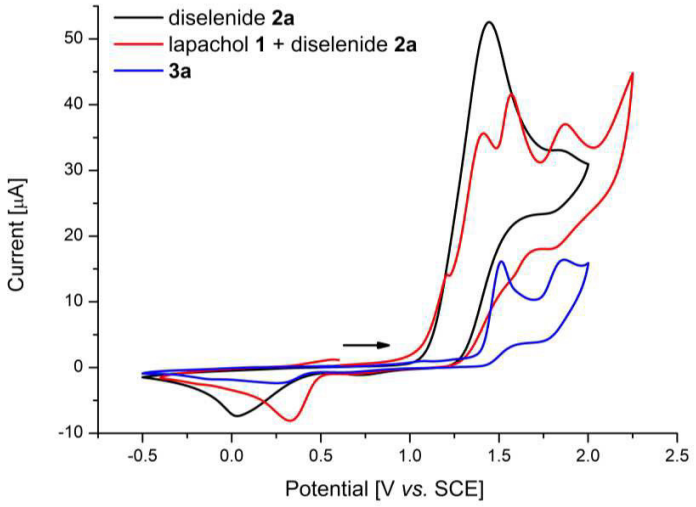

Figure S2. Cyclic voltammograms in MeCN at 100 mVs^{-1}. nBu_4NPF_6 (0.1 M in MeCN), concentration of lapachol **1** and selenide **2a** 5.0 mM. Diselenide **2a** (black); lapachol **1** + diselenide **2a** (red); **3a** (blue).

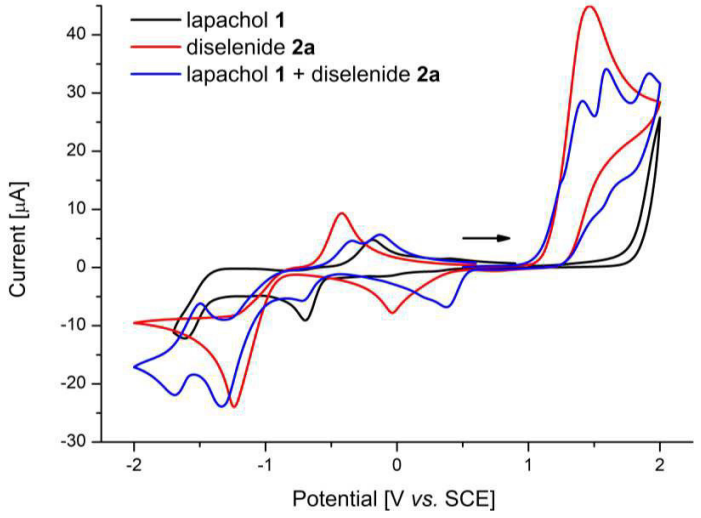

Figure S3. Cyclic voltammograms in MeCN at mVs^{-1}. nBu_4NPF_6 (0.1 M in MeCN), concentration of lapachol **1** and selenide **2a** 5.0 mM. Lapachol **1** (black); diselenide **2a** (red), lapachol **1** + diselenide **2a** (blue).

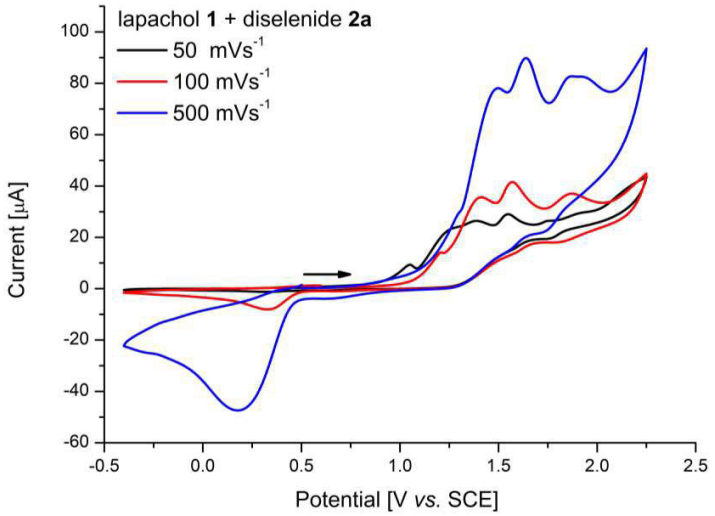

Figure S4. Cyclic voltammograms in MeCN. nBu$_4$NPF$_6$ (0.1 M in MeCN), concentration of lapachol **1** and selenide **2a** 5.0 mM. 50 mVs^{-1} (black); 100 mVs^{-1} (red); 500 mVs^{-1} (blue).

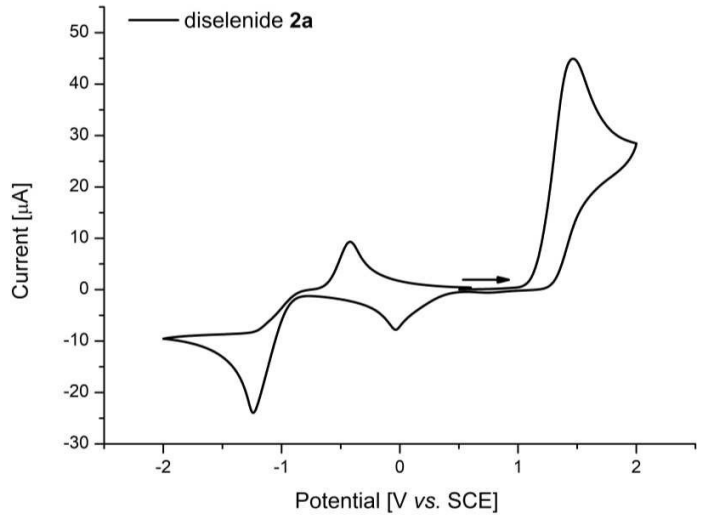

Figure S5. Cyclic voltammograms in MeCN at 100 mVs^{-1}. nBu$_4$NPF$_6$ (0.1 M in MeCN), concentration of diselenide **2a** 5.0 mM.

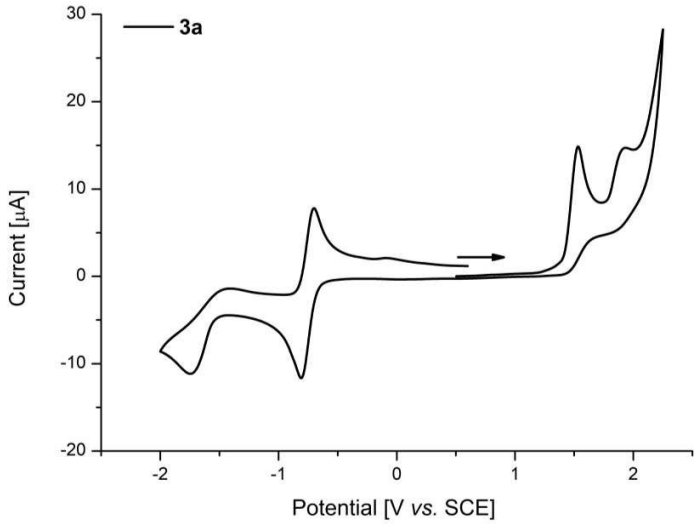

Figure S6. Cyclic voltammograms in MeCN at 100 mVs^{-1}. nBu_4NPF_6 (0.1 M in MeCN), concentration of **3a** 5.0 mM.

General analysis for the seleno-cyclization of compound 6

The correct regiochemistry for the seleno-cyclization reaction with compound **6** was determined by analysing the chemical shift of hydrogen 2 in compound **3a** and comparing the value with the chemical shift and the multiplicity of the hydrogen 3 of compound **7a** (Figure S7). Considering the two possibilities of intramolecular cyclization, 6-endo-tet cyclization is considered the main course of the reaction, due to the stabilization of the positive charge by the aromatic ring in the C-Se bond cleavage event (Scheme S1). This intramolecular path is characterized as an anti-Baldwin cyclization.[3] This type of cyclisation is also observed in many other products in literature.[4]

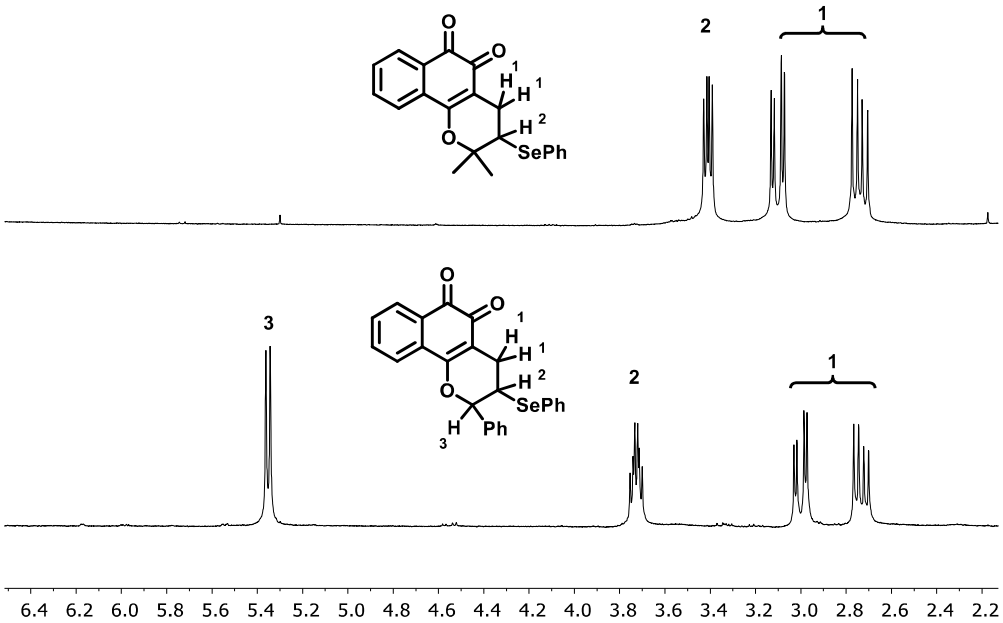

Figure S7. Stacked ^{1}H NMR spectrum (400 MHz, $CDCl_3$) of compounds **3a** and **7a**.

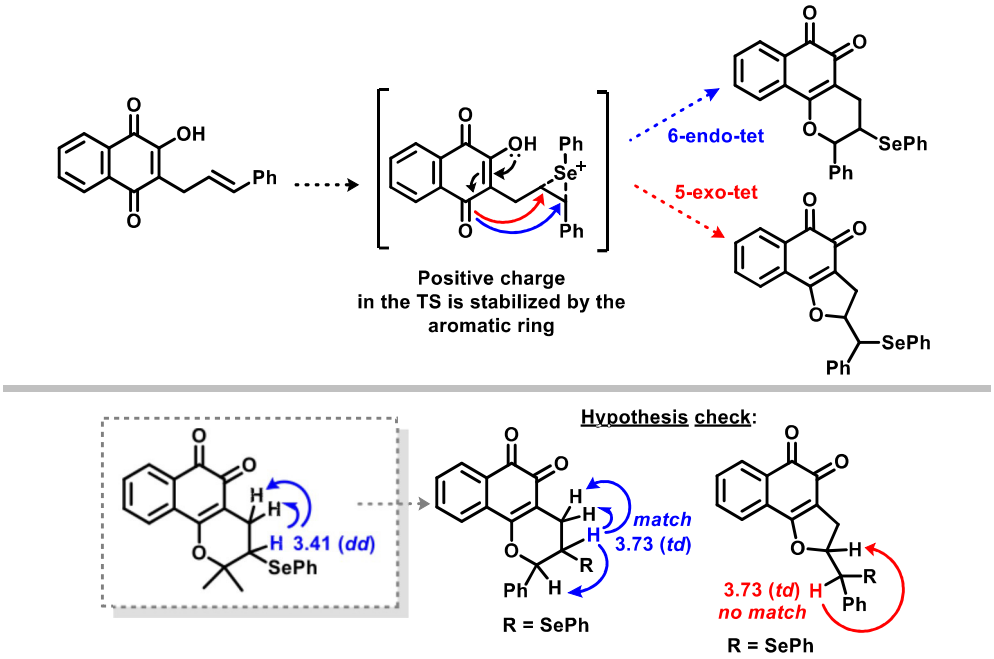

Scheme S1. Hypothesis for the seleno-cyclization of compound **6**.

Table S1. Selectivity index IC_{50} (non-tumor cells/tumor cells)

Compounds	IC_{50} (L929)/IC_{50} (tumor cells)				
	PC3	**SNB-19**	**HCT-116**	**MCF-7**	**B16F10**
3c	1.02	0.81	1.63	0.63	1.60
3f	0.40	0.34	0.57	0.31	0.62
3h	0.58	0.40	0.59	0.36	0.58
3g	0.87	0.61	0.79	0.40	0.79
5a	0.77	0.56	0.71	0.50	0.91
5b	0.71	0.85	1.10	0.56	1.10
5c	0.83	0.52	1.04	0.60	2.05
5d	0.85	0.74	0.90	0.56	0.85
5e	0.98	0.55	0.94	0.51	1.66
5f	0.86	1.10	1.69	0.67	1.61
5g	0.83	0.43	0.64	0.39	1.01
5h	1.06	0.77	1.00	0.57	1.11
5i	1.03	0.57	1.01	0.76	1.26

References

1. J. E. Baldwin, *J. Chem. Soc., Chem. Commun.*, **1976**, *18*, 734.

2. (a) B. J. Smit, Z. M. Bugarcic, *J. Heterocyclic Chem.*, **2010**, *47*, 1443. (b) S. S. Badsara, Y.-C. Liu, P.-A. Hsieh, J.-W. Zeng, S.-Y. Lu, Y.-W. Liu, C.-F. Lee, *Chem. Commun.*, **2014**, *50*, 11374. (c) H. J. Lim, T. V. RajanBabu, *Org. Lett.*, **2009**, *11*, 2924.

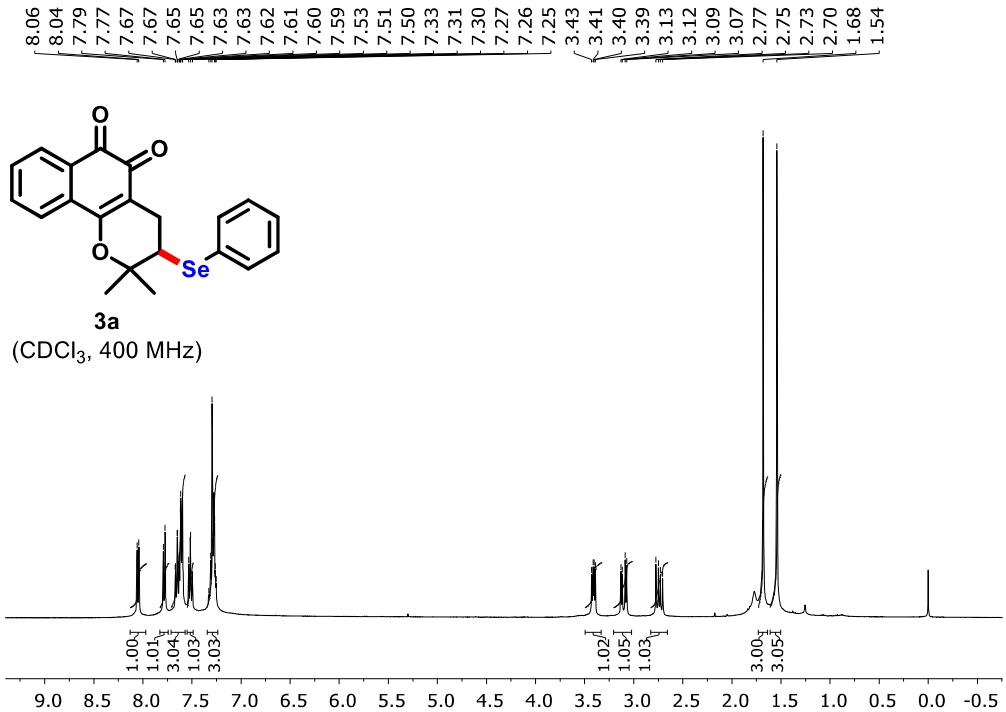
8.06 8.04 7.79 7.77 7.67 7.67 7.65 7.65 7.63 7.63 7.62 7.61 7.60 7.59 7.53 7.51 7.50 7.33 7.31 7.30 7.27 7.26 7.25 3.43 3.41 3.40 3.39 3.13 3.12 3.09 3.07 2.77 2.75 2.73 2.70 1.68 1.54
O
O
O
Se
3a
(CDCl3, 400 MHz)
1.00 1.01 3.04 1.03 3.03 1.02 1.05 1.03 3.00 3.05
9.0 8.5 8.0 7.5 7.0 6.5 6.0 5.5 5.0 4.5 4.0 3.5 3.0 2.5 2.0 1.5 1.0 0.5 0.0 -0.5

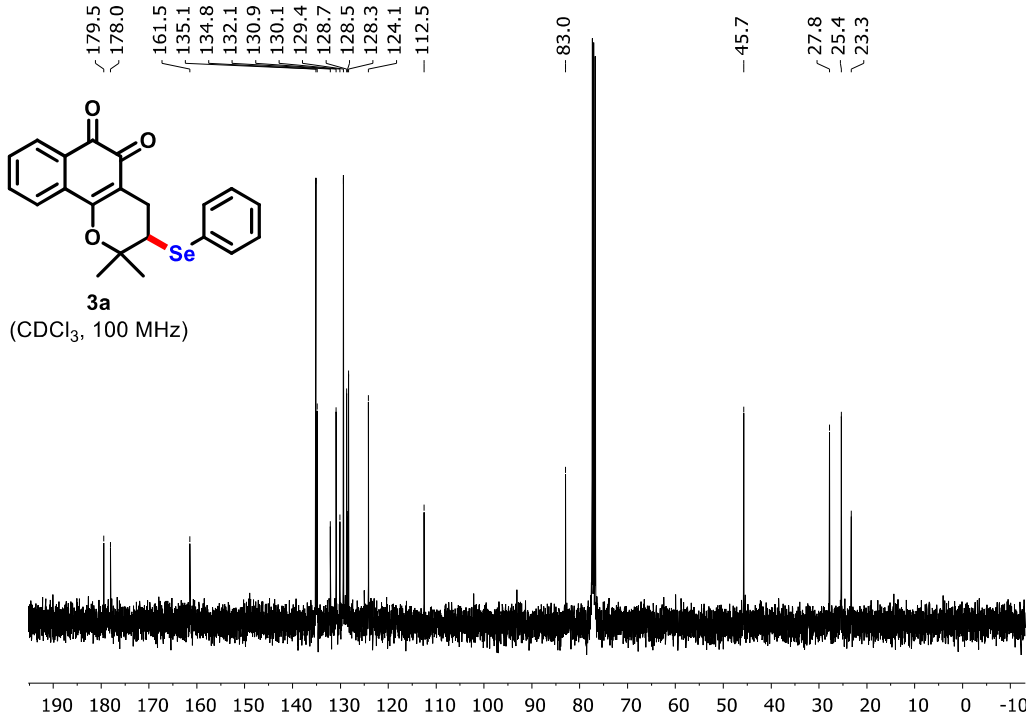
179.5 178.0 161.5 135.1 134.8 132.1 130.9 130.1 129.4 128.7 128.5 128.3 124.1 112.5 83.0 45.7 27.8 25.4 23.3
O
O
O
Se
3a
(CDCl3, 100 MHz)
190 180 170 160 150 140 130 120 110 100 90 80 70 60 50 40 30 20 10 0 -10

3a
($CDCl_3$, 76 MHz)

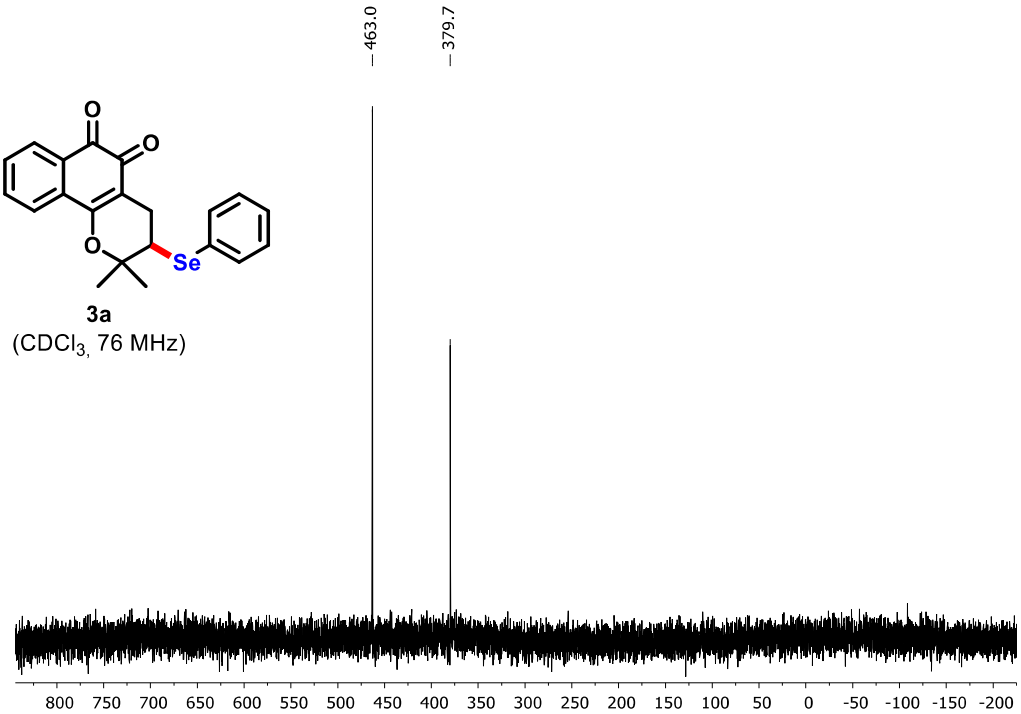

3b
($CDCl_3$, 400 MHz)

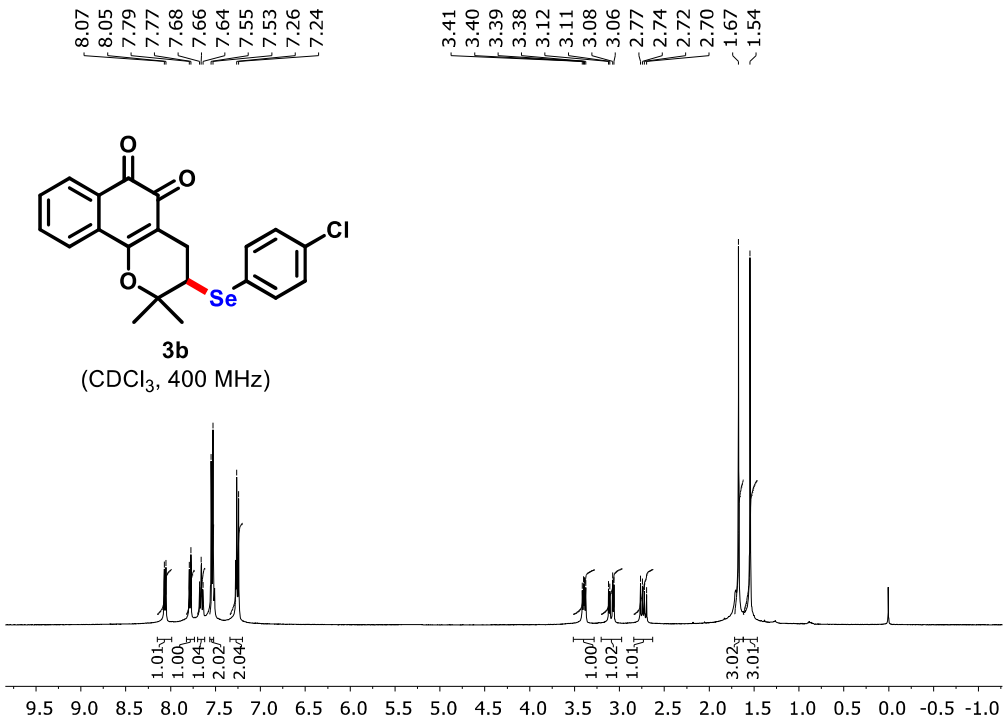

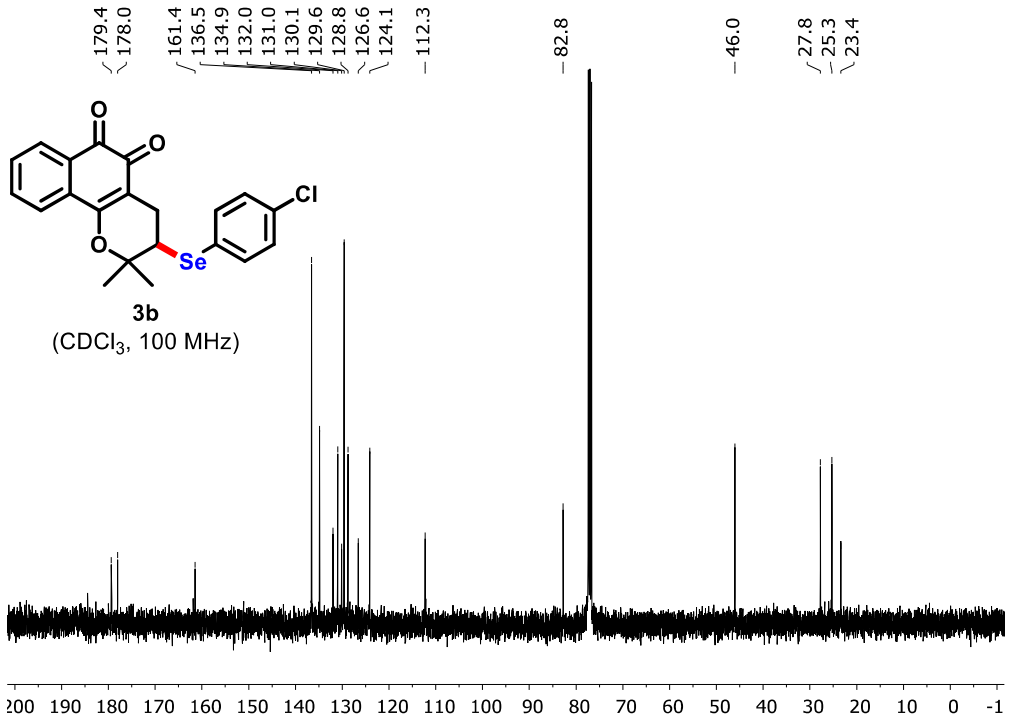
179.4
178.0
161.4
136.5
134.9
132.0
131.0
130.1
129.6
128.8
126.6
124.1
112.3
82.8
46.0
27.8
25.3
23.4
O
O
Cl
O
Se
3b
(CDCl3, 100 MHz)
200 190 180 170 160 150 140 130 120 110 100 90 80 70 60 50 40 30 20 10 0 -1

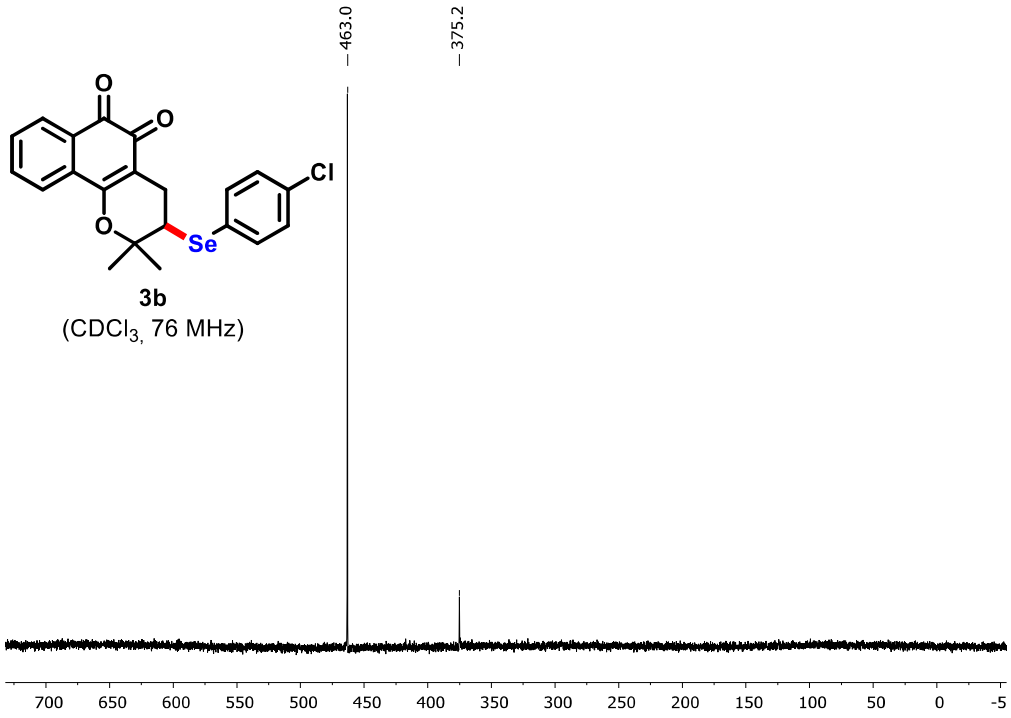
463.0
375.2
O
O
Cl
O
Se
3b
(CDCl3, 76 MHz)
700 650 600 550 500 450 400 350 300 250 200 150 100 50 0 -5

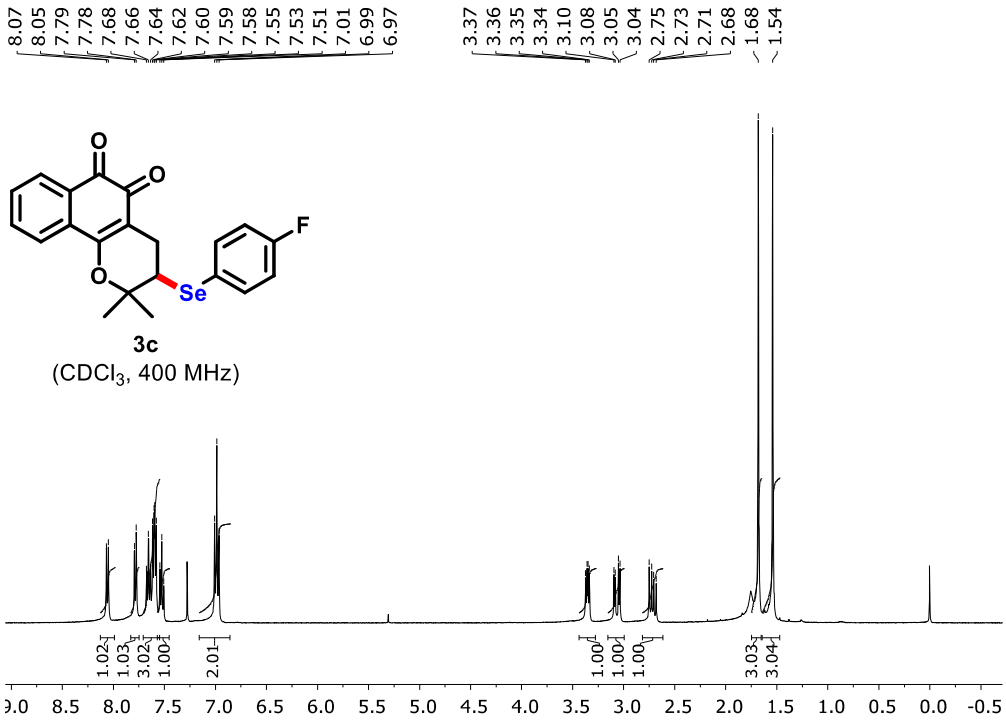
8.07
8.05
7.79
7.78
7.68
7.66
7.64
7.62
7.60
7.59
7.58
7.55
7.53
7.51
7.01
6.99
6.97
3.37
3.36
3.35
3.34
3.10
3.08
3.05
3.04
2.75
2.73
2.71
2.68
1.68
1.54
O
O
F
O
Se
3c
(CDCl3, 400 MHz)
1.02
1.03
3.02
1.00
2.01
1.00
1.00
1.00
3.03
3.04
9.0 8.5 8.0 7.5 7.0 6.5 6.0 5.5 5.0 4.5 4.0 3.5 3.0 2.5 2.0 1.5 1.0 0.5 0.0 -0.5

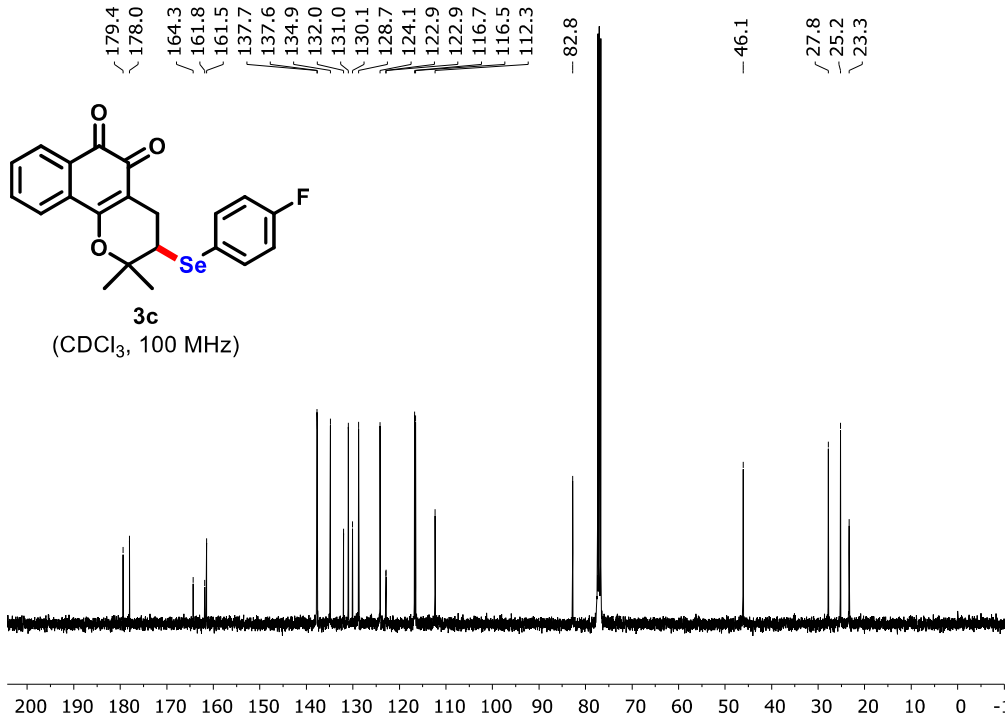
179.4
178.0
164.3
161.8
161.5
137.7
137.6
134.9
132.0
131.0
130.1
128.7
124.1
122.9
122.9
116.7
116.5
112.3
82.8
46.1
27.8
25.2
23.3
O
O
F
O
Se
3c
(CDCl3, 100 MHz)
200 190 180 170 160 150 140 130 120 110 100 90 80 70 60 50 40 30 20 10 0

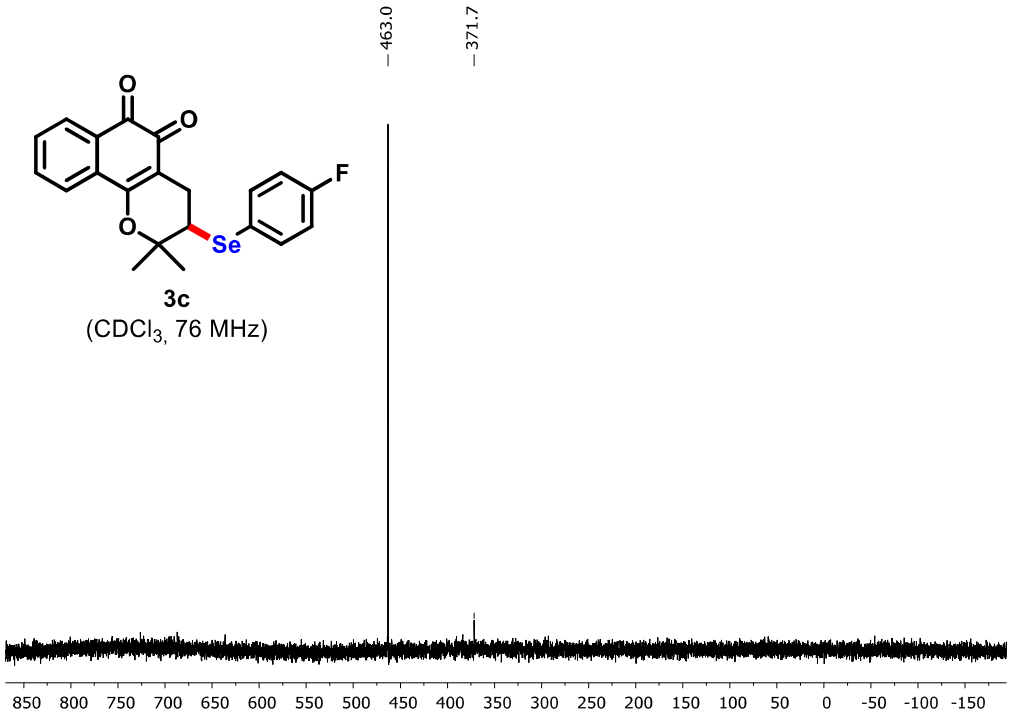
463.0
371.7
O
O
F
O
Se
3c
(CDCl3, 76 MHz)
850 800 750 700 650 600 550 500 450 400 350 300 250 200 150 100 50 0 -50 -100 -150

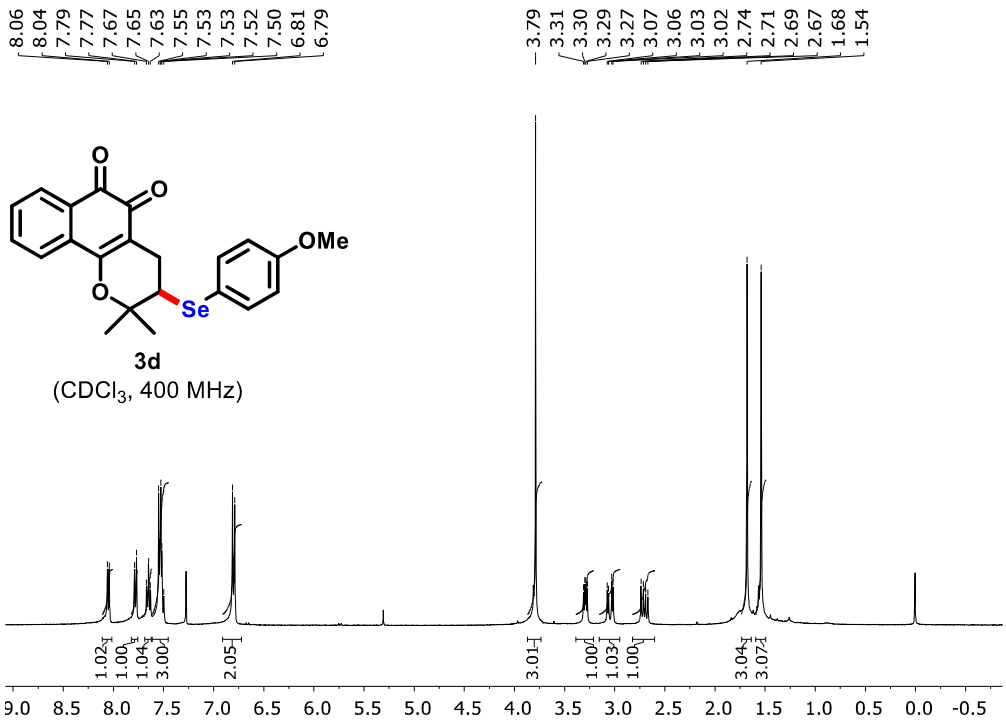
8.06
8.04
7.79
7.77
7.67
7.65
7.63
7.55
7.53
7.53
7.52
7.50
6.81
6.79
3.79
3.31
3.30
3.29
3.27
3.07
3.06
3.03
3.02
2.74
2.71
2.69
2.67
1.68
1.54
O
O
OMe
O
Se
3d
(CDCl3, 400 MHz)
1.02
1.00
1.04
3.00
2.05
3.01
1.00
1.03
1.00
3.04
3.07
9.0 8.5 8.0 7.5 7.0 6.5 6.0 5.5 5.0 4.5 4.0 3.5 3.0 2.5 2.0 1.5 1.0 0.5 0.0 -0.5

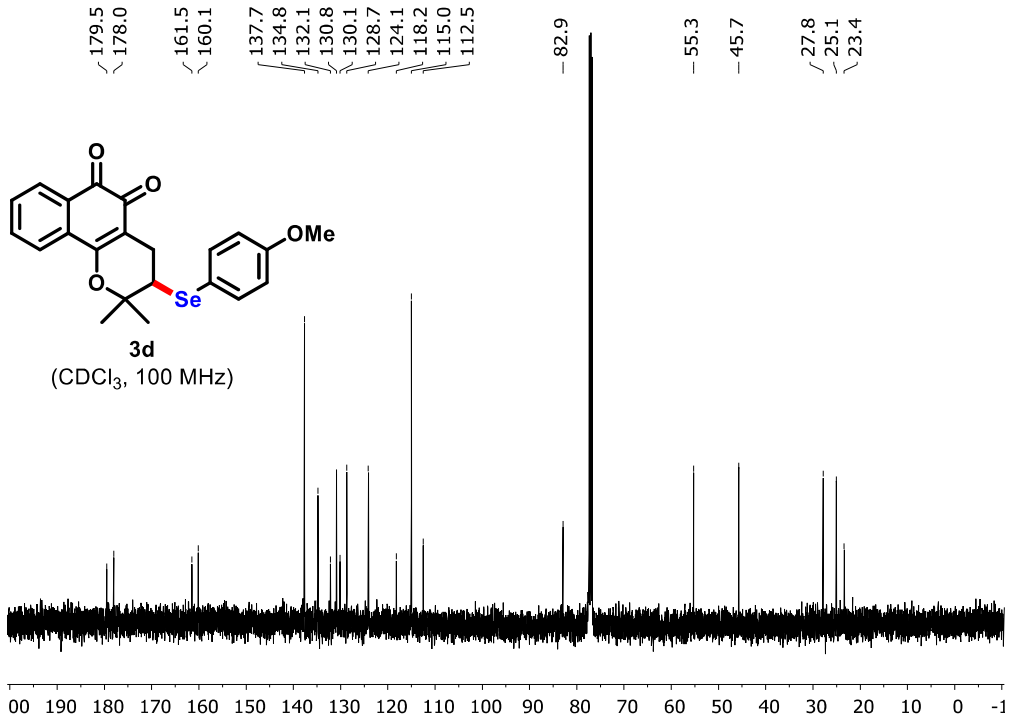
179.5
178.0
161.5
160.1
137.7
134.8
132.1
130.8
130.1
128.7
124.1
118.2
115.0
112.5
82.9
55.3
45.7
27.8
25.1
23.4
O
O
OMe
O
Se
3d
(CDCl3, 100 MHz)
00 190 180 170 160 150 140 130 120 110 100 90 80 70 60 50 40 30 20 10 0 -1

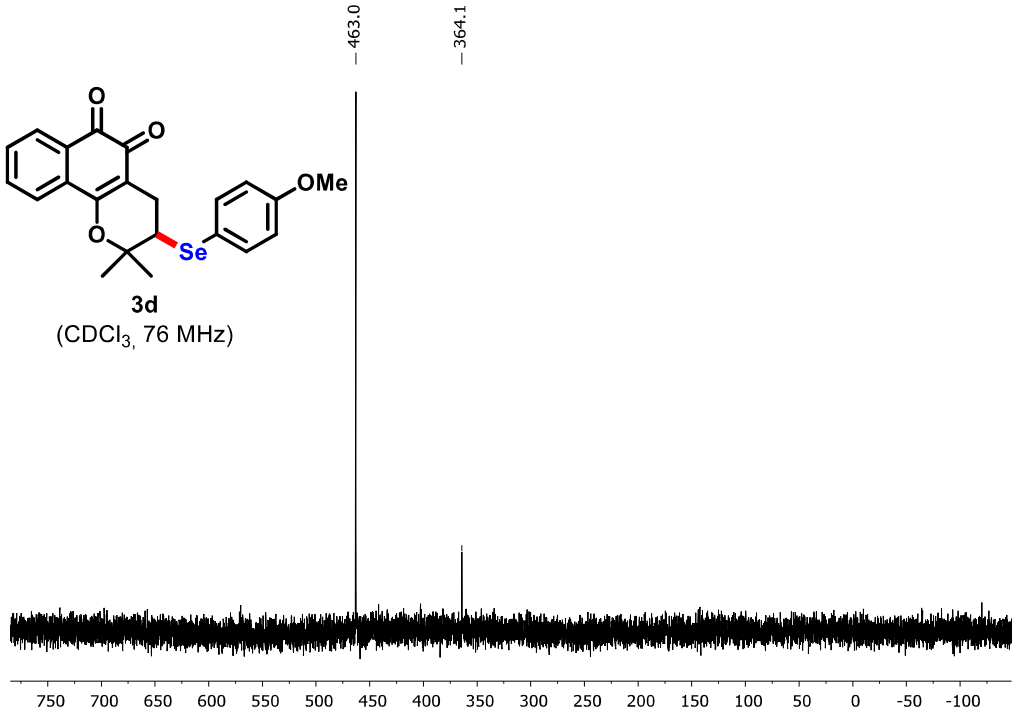
463.0
364.1
O
O
OMe
O
Se
3d
(CDCl3, 76 MHz)
750 700 650 600 550 500 450 400 350 300 250 200 150 100 50 0 -50 -100

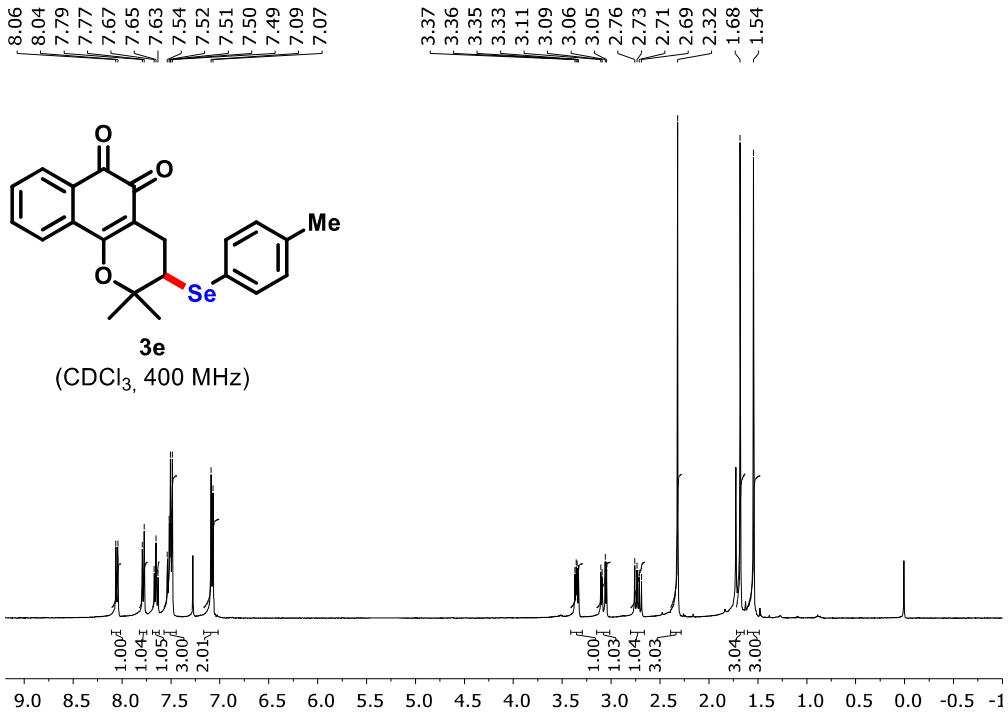
8.06
8.04
7.79
7.77
7.67
7.65
7.63
7.54
7.52
7.51
7.50
7.49
7.09
7.07
3.37
3.36
3.35
3.33
3.11
3.09
3.06
3.05
2.76
2.73
2.71
2.69
2.32
1.68
1.54
O
O
Me
O
Se
3e
(CDCl3, 400 MHz)
1.00
1.04
1.05
3.00
2.01
1.00
1.03
1.04
3.03
3.04
3.00
9.0 8.5 8.0 7.5 7.0 6.5 6.0 5.5 5.0 4.5 4.0 3.5 3.0 2.5 2.0 1.5 1.0 0.5 0.0 -0.5 -1

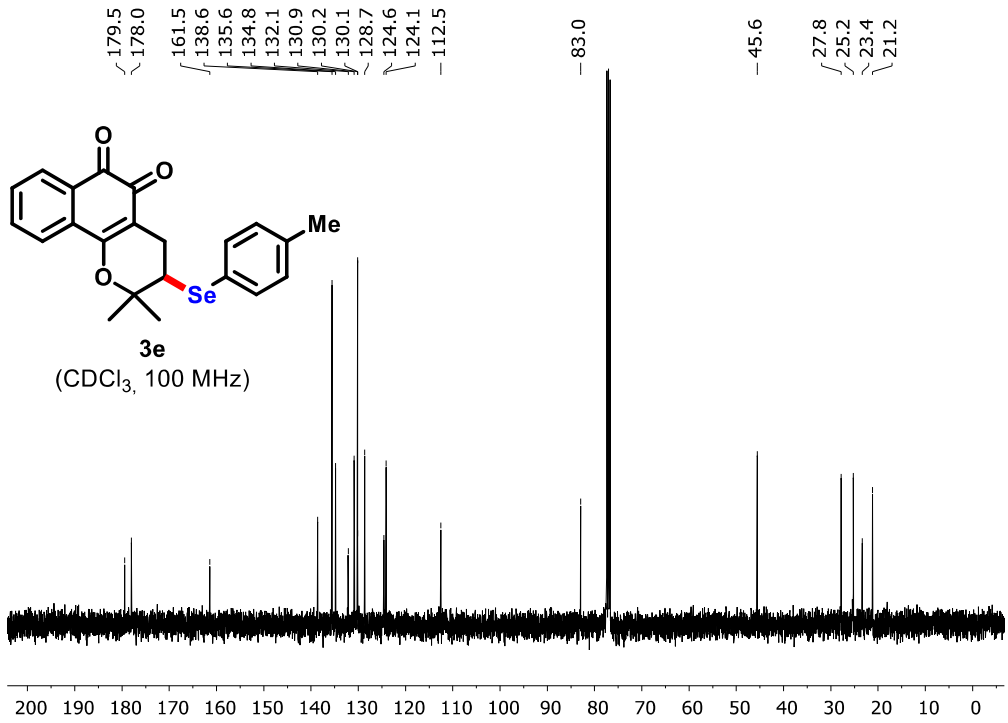
179.5
178.0
161.5
138.6
135.6
134.8
132.1
130.9
130.2
130.1
128.7
124.6
124.1
112.5
83.0
45.6
27.8
25.2
23.4
21.2
O
O
Me
O
Se
3e
(CDCl3, 100 MHz)
200 190 180 170 160 150 140 130 120 110 100 90 80 70 60 50 40 30 20 10 0

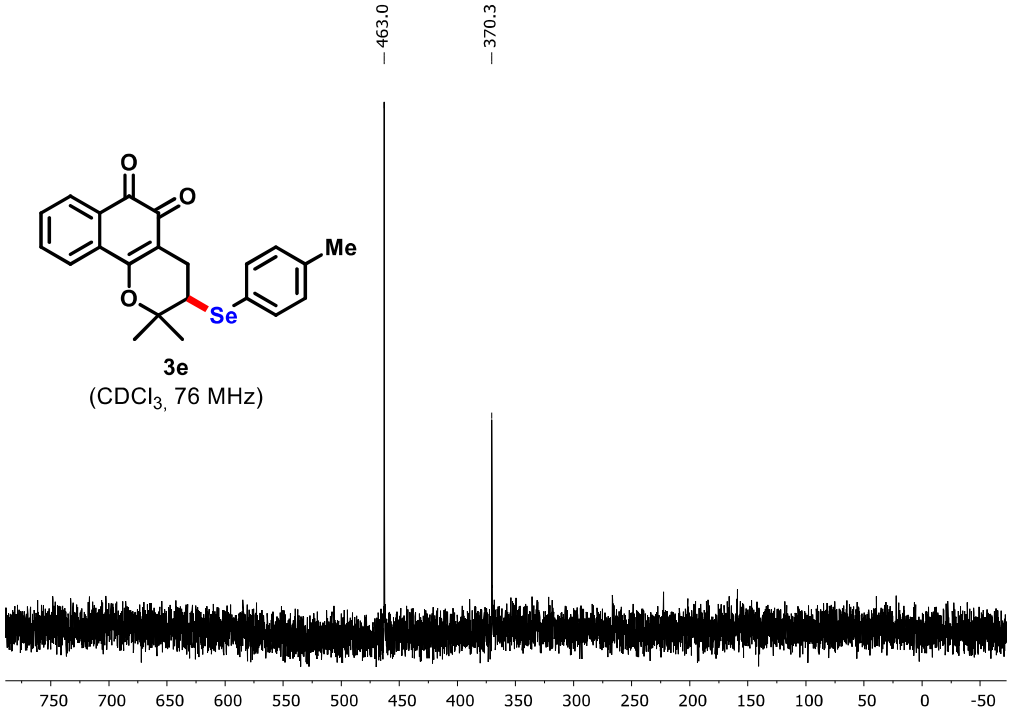

3e
($CDCl_3$, 76 MHz)

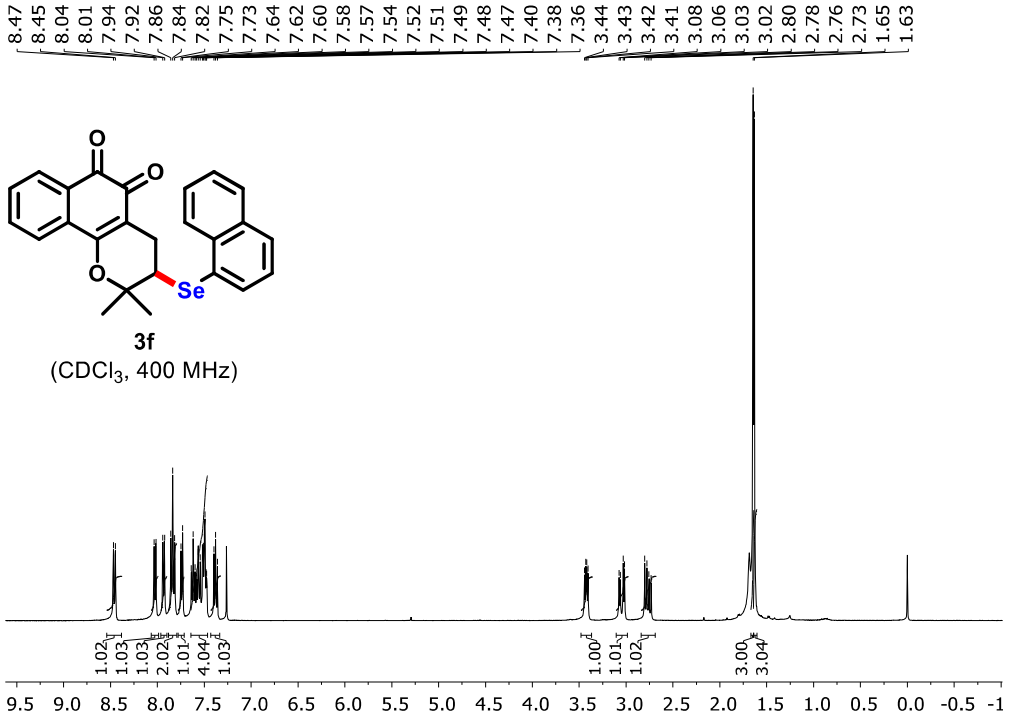

3f
($CDCl_3$, 400 MHz)

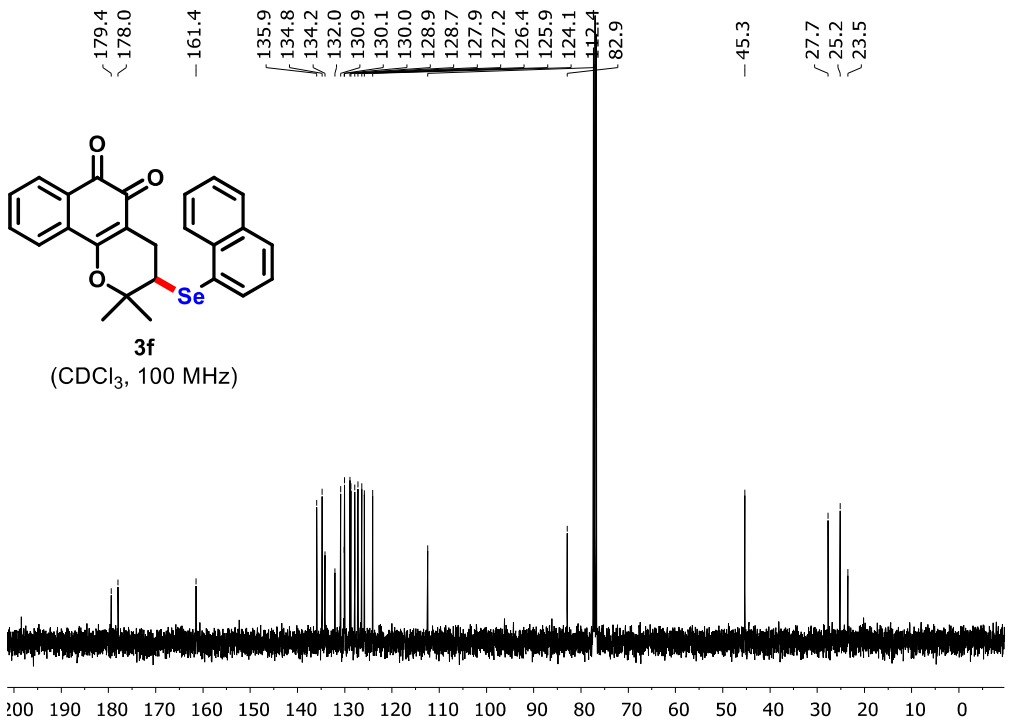
179.4
178.0
161.4
135.9
134.8
134.2
132.0
130.9
130.1
130.0
128.9
128.7
127.9
127.2
126.4
125.9
124.1
112.4
82.9
45.3
27.7
25.2
23.5
O
O
O
Se
3f
(CDCl3, 100 MHz)
200 190 180 170 160 150 140 130 120 110 100 90 80 70 60 50 40 30 20 10 0

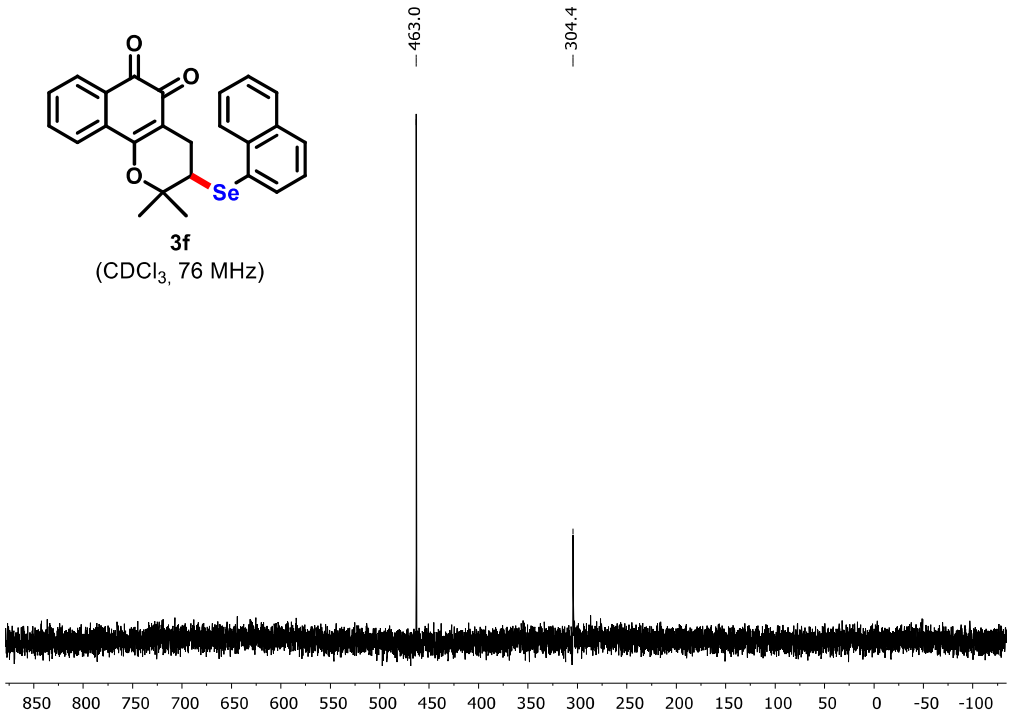
463.0
304.4
O
O
O
Se
3f
(CDCl3, 76 MHz)
850 800 750 700 650 600 550 500 450 400 350 300 250 200 150 100 50 0 -50 -100

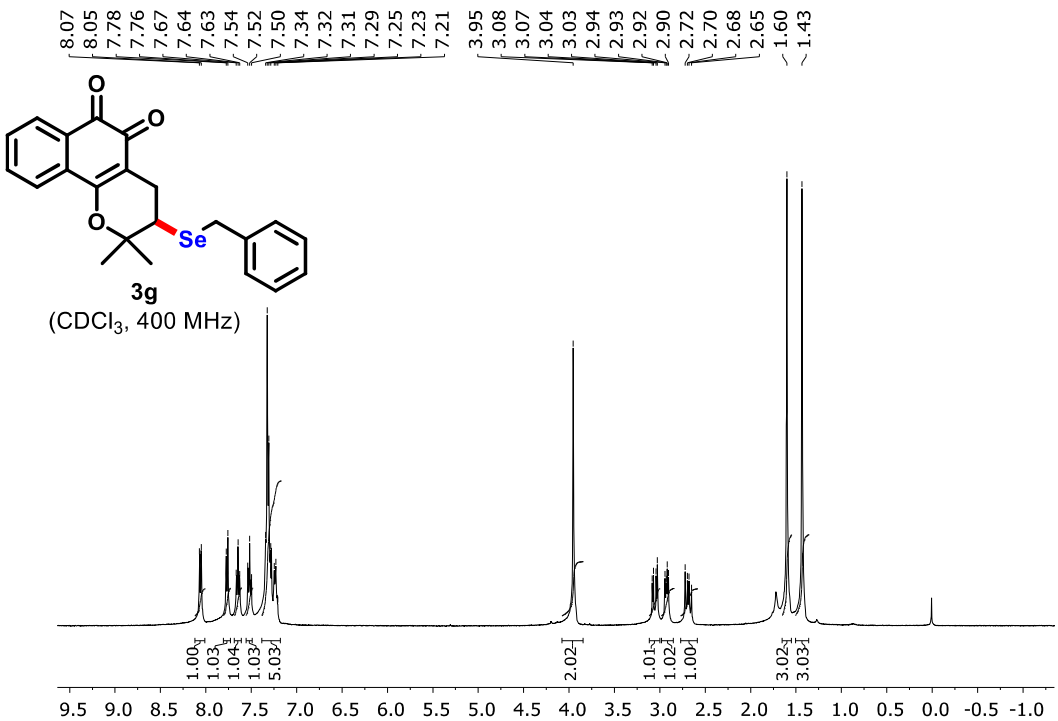
8.07
8.05
7.78
7.76
7.67
7.64
7.63
7.54
7.52
7.50
7.34
7.32
7.31
7.29
7.25
7.23
7.21
3.95
3.08
3.07
3.04
3.03
2.94
2.93
2.92
2.90
2.72
2.70
2.68
2.65
1.60
1.43
O
O
O
Se
3g
(CDCl3, 400 MHz)
1.00
1.03
1.04
1.03
5.03
2.02
1.01
1.02
1.00
3.02
3.03
9.5 9.0 8.5 8.0 7.5 7.0 6.5 6.0 5.5 5.0 4.5 4.0 3.5 3.0 2.5 2.0 1.5 1.0 0.5 0.0 -0.5 -1.0

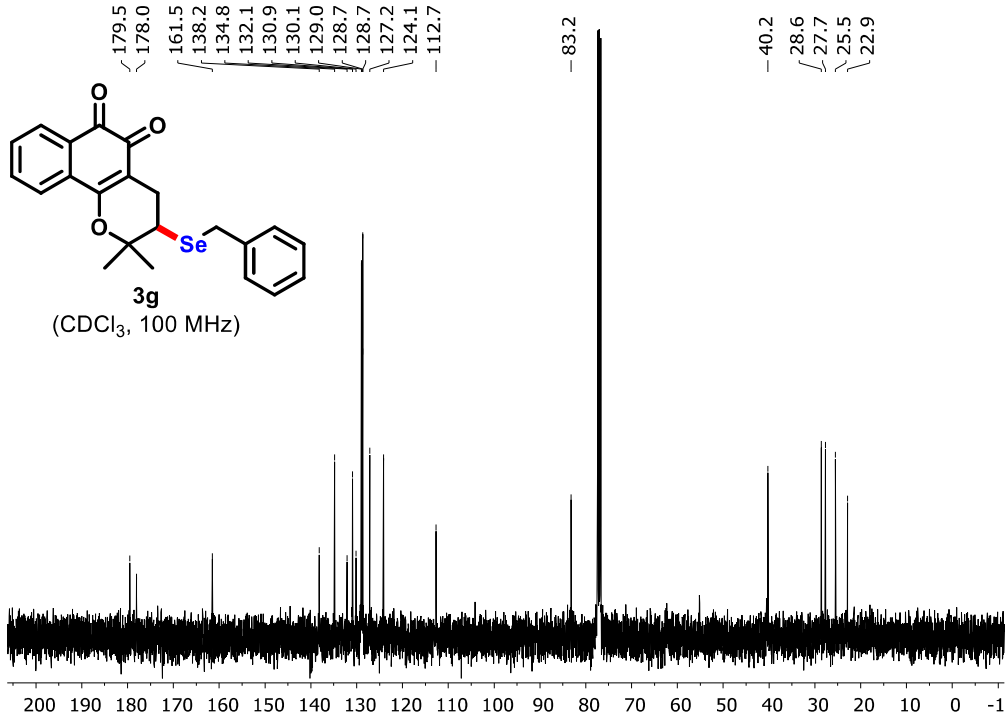
179.5
178.0
161.5
138.2
134.8
132.1
130.9
130.1
129.0
128.7
128.7
127.2
124.1
112.7
83.2
40.2
28.6
27.7
25.5
22.9
O
O
O
Se
3g
(CDCl3, 100 MHz)
200 190 180 170 160 150 140 130 120 110 100 90 80 70 60 50 40 30 20 10 0 -1

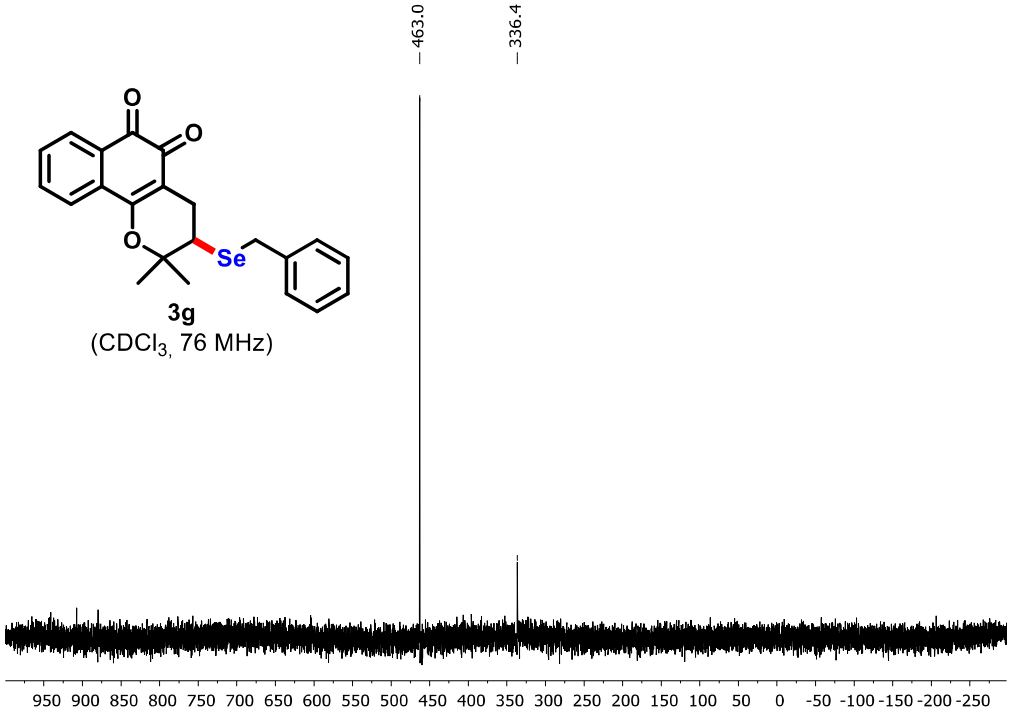

3g
($CDCl_3$, 76 MHz)

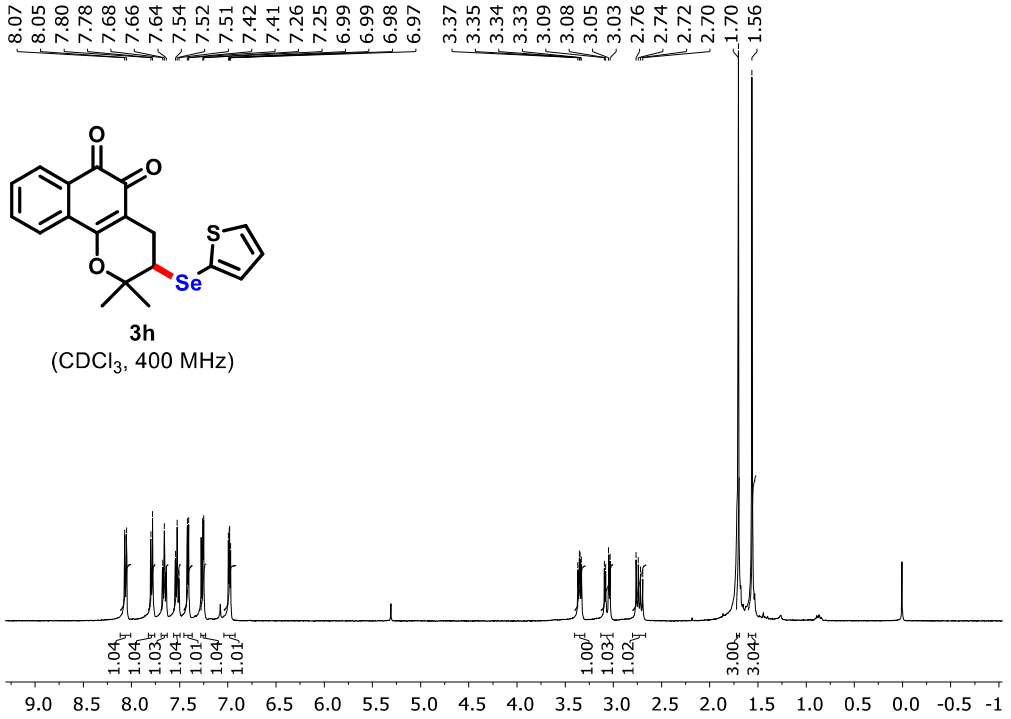

3h
($CDCl_3$, 400 MHz)

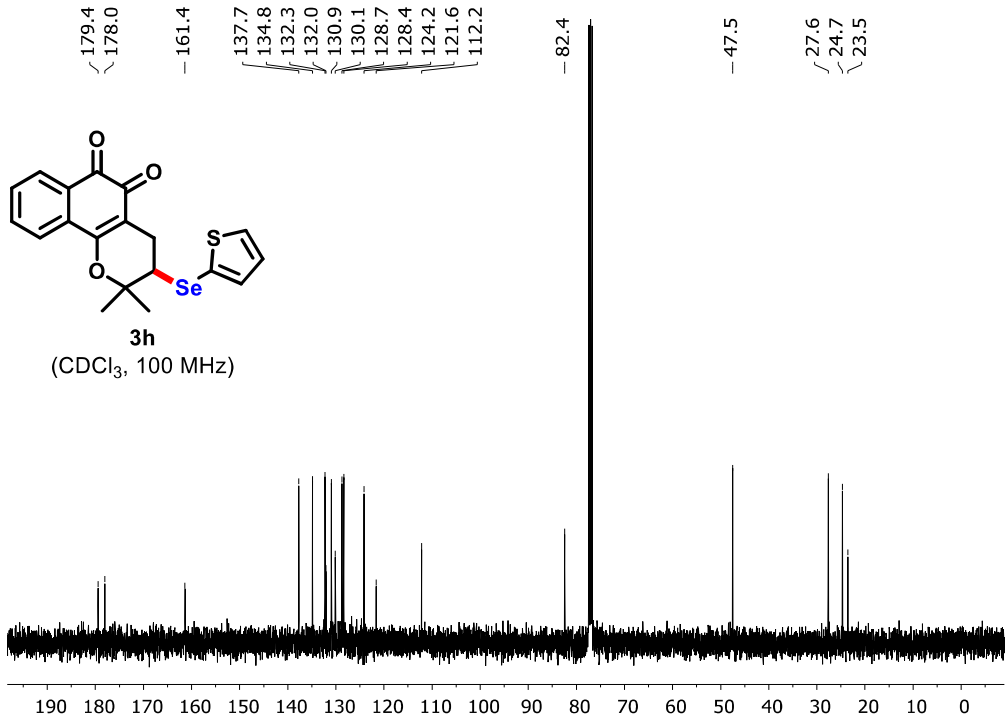
179.4
178.0
161.4
137.7
134.8
132.3
132.0
130.9
130.1
128.7
128.4
124.2
121.6
112.2
82.4
47.5
27.6
24.7
23.5
O
O
S
O
Se
3h
(CDCl3, 100 MHz)
190 180 170 160 150 140 130 120 110 100 90 80 70 60 50 40 30 20 10 0

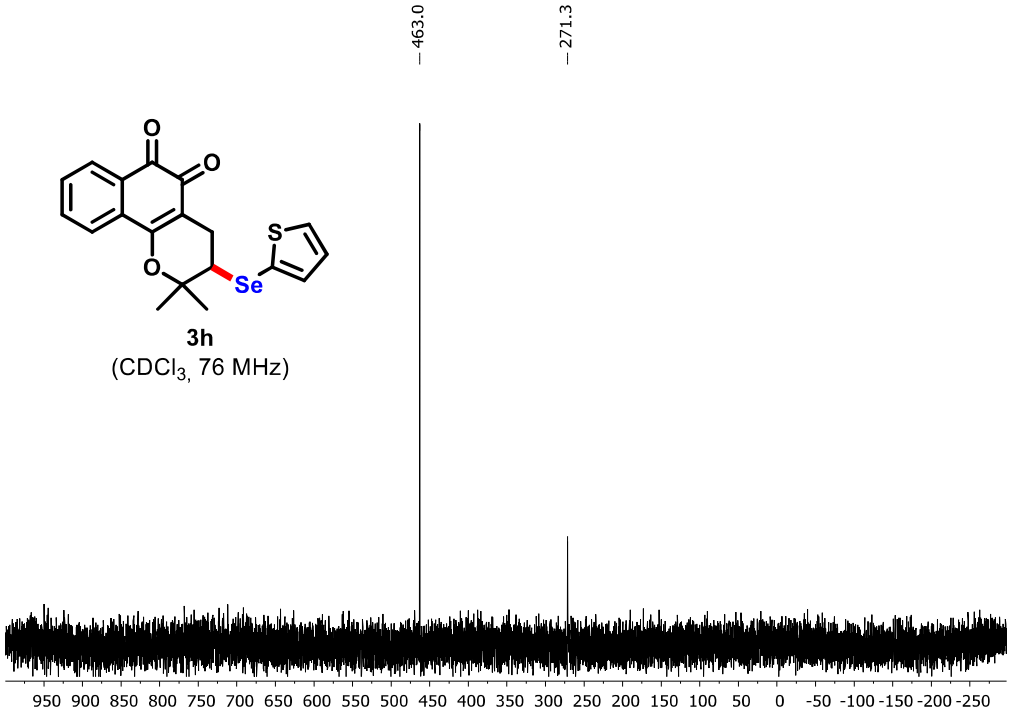
463.0
271.3
O
O
S
O
Se
3h
(CDCl3, 76 MHz)
950 900 850 800 750 700 650 600 550 500 450 400 350 300 250 200 150 100 50 0 -50 -100 -150 -200 -250

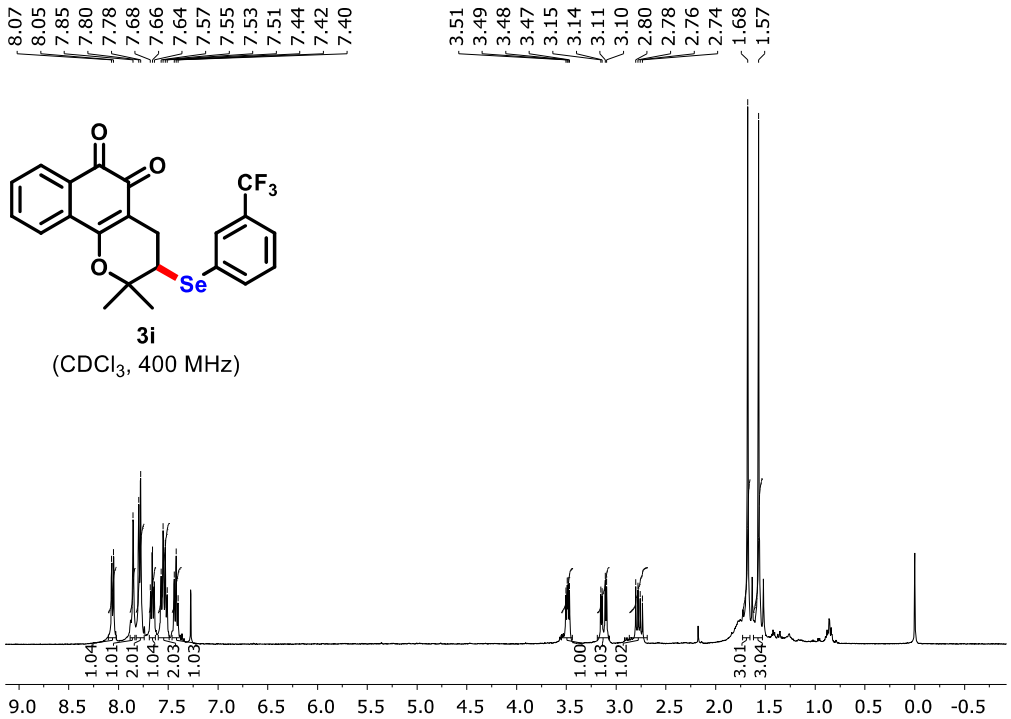
8.07
8.05
7.85
7.80
7.78
7.68
7.66
7.64
7.57
7.55
7.53
7.51
7.44
7.42
7.40
3.51
3.49
3.48
3.47
3.15
3.14
3.11
3.10
2.80
2.78
2.76
2.74
1.68
1.57
O
O
CF3
O
Se
3i
(CDCl3, 400 MHz)
1.04
1.01
2.01
1.04
2.03
1.03
1.00
1.03
1.02
3.01
3.04
9.0 8.5 8.0 7.5 7.0 6.5 6.0 5.5 5.0 4.5 4.0 3.5 3.0 2.5 2.0 1.5 1.0 0.5 0.0 -0.5

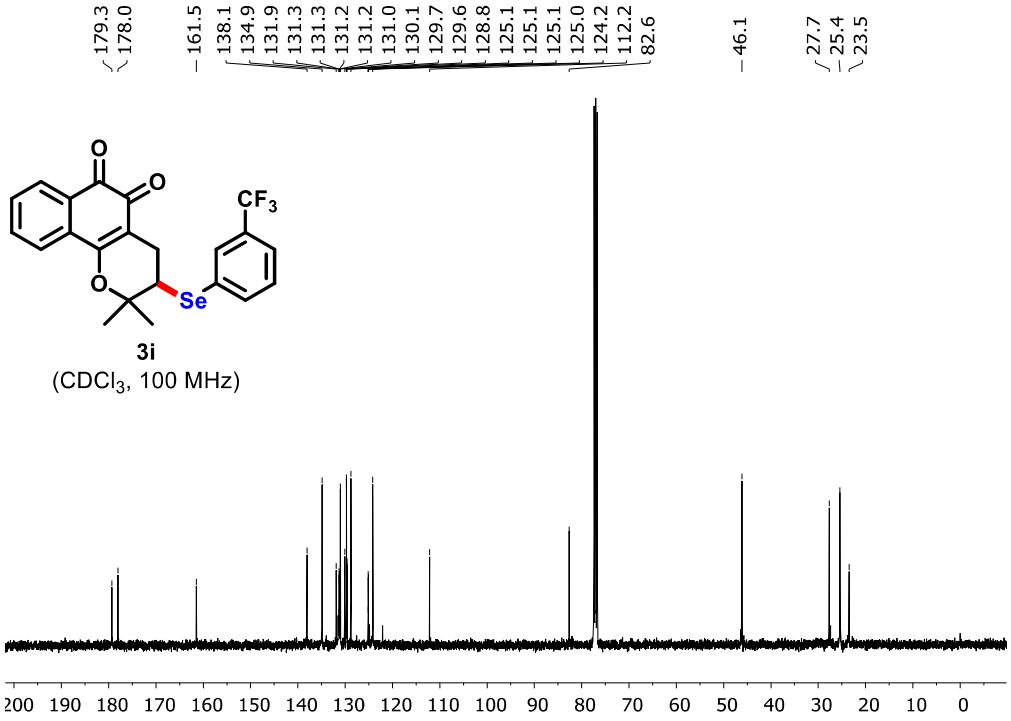
179.3
178.0
161.5
138.1
134.9
131.9
131.3
131.3
131.2
131.2
131.0
130.1
129.7
129.6
128.8
125.1
125.1
125.1
125.0
124.2
112.2
82.6
46.1
27.7
25.4
23.5
O
O
CF3
O
Se
3i
(CDCl3, 100 MHz)
200 190 180 170 160 150 140 130 120 110 100 90 80 70 60 50 40 30 20 10 0

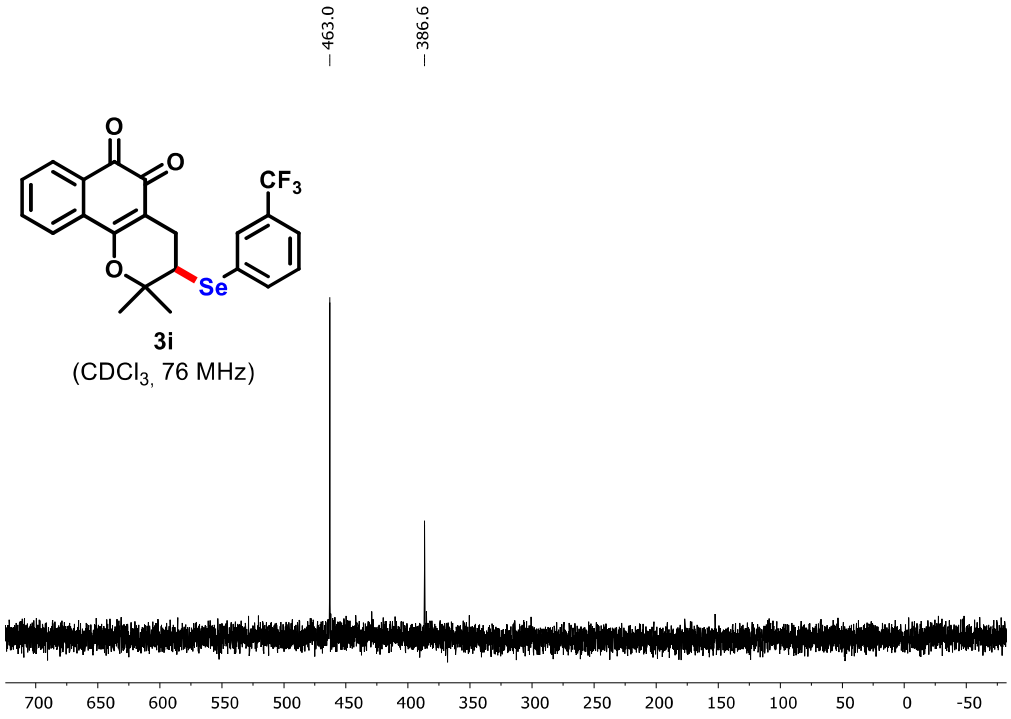
463.0
386.6
O
O
CF3
O
Se
3i
(CDCl3, 76 MHz)
700 650 600 550 500 450 400 350 300 250 200 150 100 50 0 -50

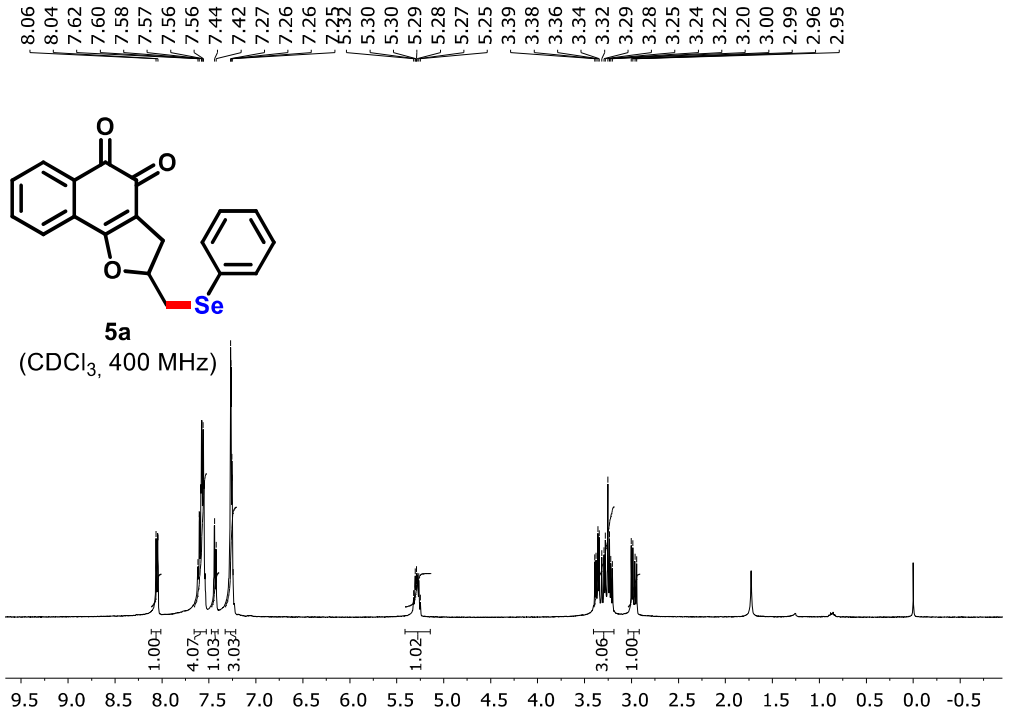
8.06 8.04 7.62 7.60 7.58 7.57 7.56 7.56 7.44 7.42 7.27 7.26 7.26 7.25 5.32 5.30 5.30 5.29 5.28 5.27 5.25 3.39 3.38 3.36 3.34 3.32 3.29 3.28 3.25 3.24 3.22 3.20 3.00 2.99 2.96 2.95
O
O
O
Se
5a
(CDCl3, 400 MHz)
1.00 4.07 1.03 3.03 1.02 3.06 1.00
9.5 9.0 8.5 8.0 7.5 7.0 6.5 6.0 5.5 5.0 4.5 4.0 3.5 3.0 2.5 2.0 1.5 1.0 0.5 0.0 -0.5

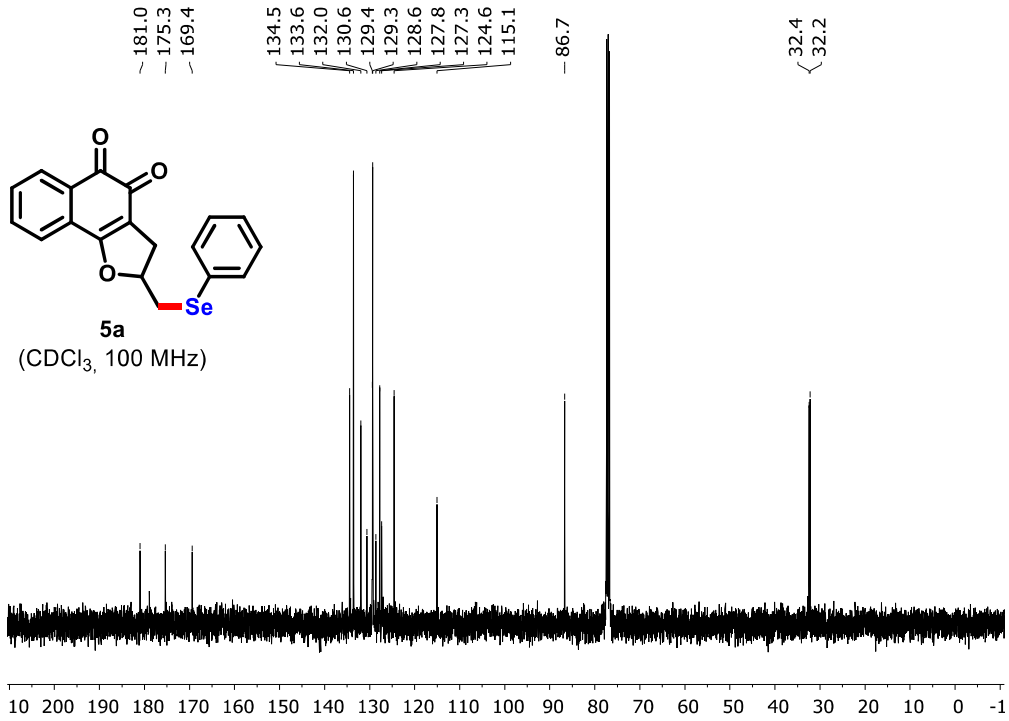
181.0
175.3
169.4
134.5
133.6
132.0
130.6
129.4
129.3
128.6
127.8
127.3
124.6
115.1
86.7
32.4
32.2
O
O
O
Se
5a
(CDCl3, 100 MHz)
10 200 190 180 170 160 150 140 130 120 110 100 90 80 70 60 50 40 30 20 10 0 -1

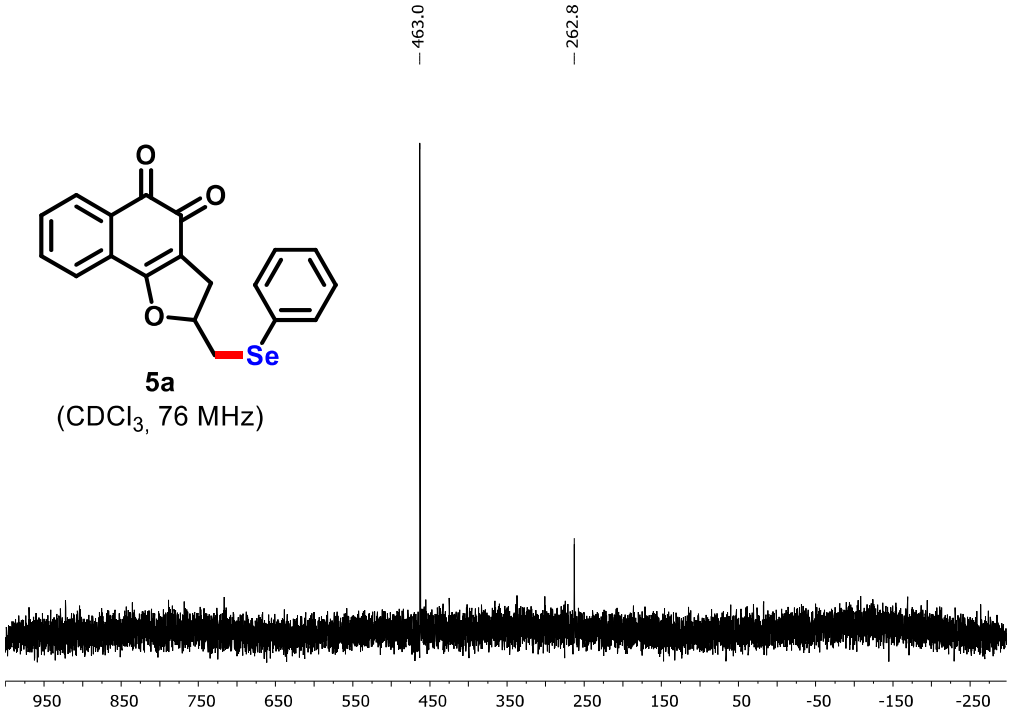
463.0
262.8
O
O
O
Se
5a
(CDCl3, 76 MHz)
950 850 750 650 550 450 350 250 150 50 -50 -150 -250

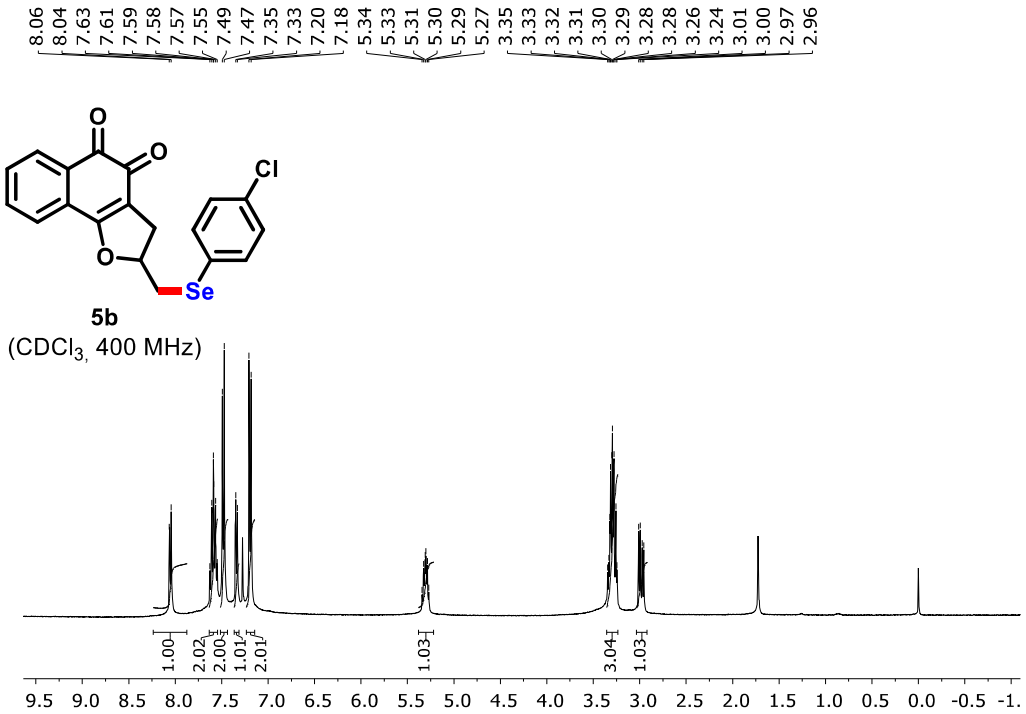
8.06
8.04
7.63
7.61
7.59
7.58
7.57
7.55
7.49
7.47
7.35
7.33
7.20
7.18
5.34
5.33
5.31
5.30
5.29
5.27
3.35
3.33
3.32
3.31
3.30
3.29
3.28
3.28
3.26
3.24
3.01
3.00
2.97
2.96
O
O
Cl
O
Se
5b
(CDCl3, 400 MHz)
1.00
2.02
2.00
1.01
2.01
1.03
3.04
1.03
9.5 9.0 8.5 8.0 7.5 7.0 6.5 6.0 5.5 5.0 4.5 4.0 3.5 3.0 2.5 2.0 1.5 1.0 0.5 0.0 -0.5 -1.

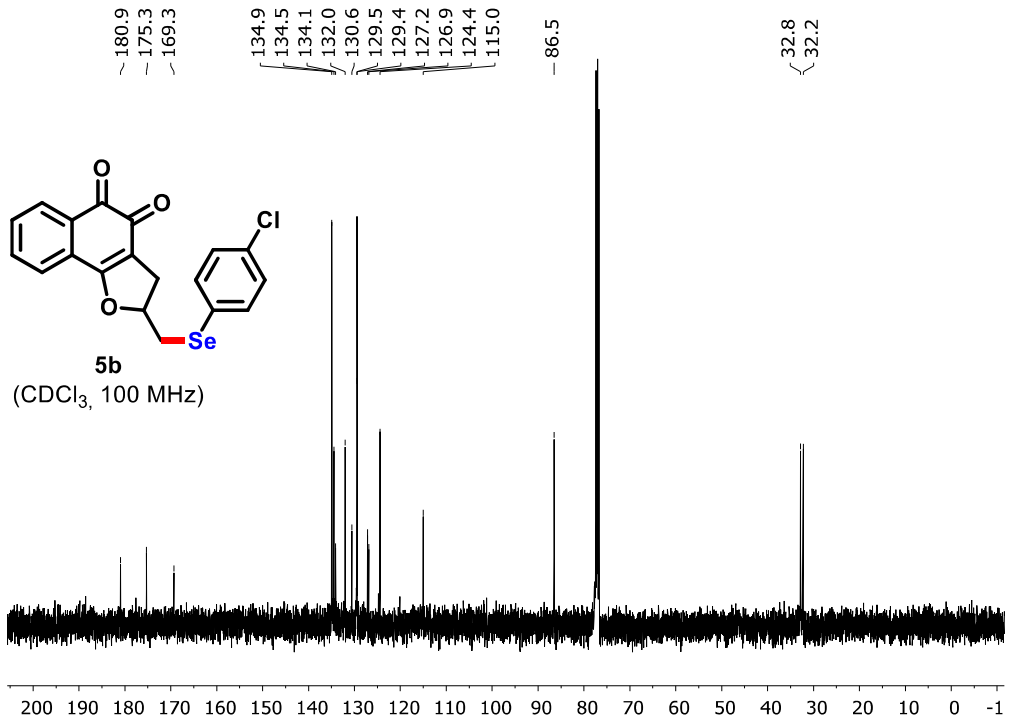
180.9
175.3
169.3
134.9
134.5
134.1
132.0
130.6
129.5
129.4
127.2
126.9
124.4
115.0
86.5
32.8
32.2
O
O
Cl
O
Se
5b
(CDCl3, 100 MHz)
200 190 180 170 160 150 140 130 120 110 100 90 80 70 60 50 40 30 20 10 0 -1

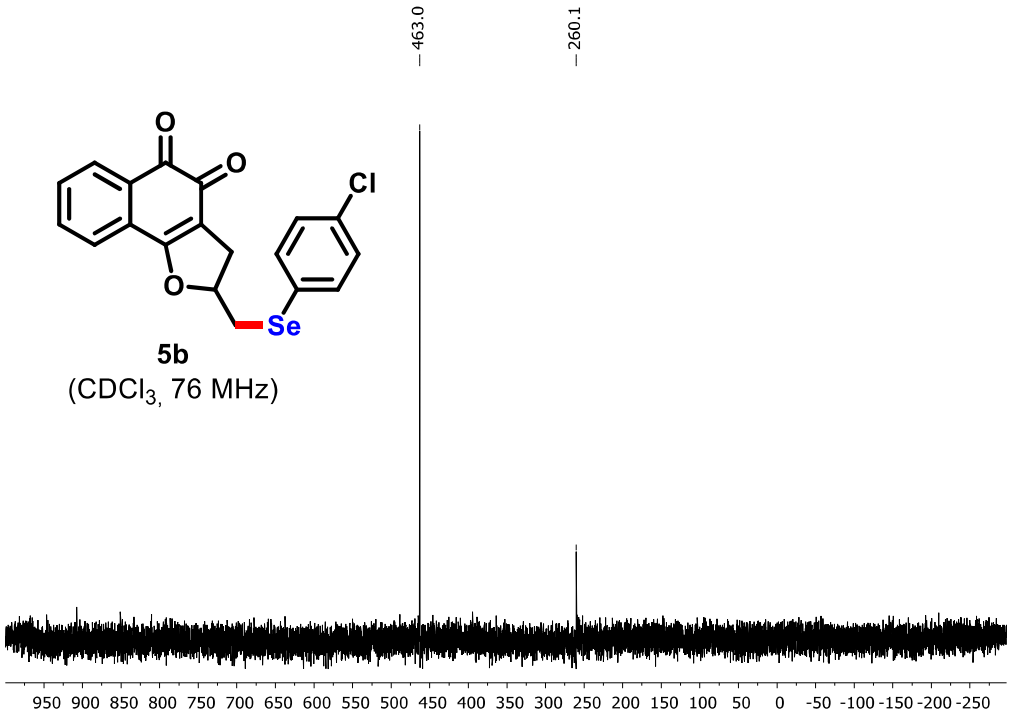
463.0
260.1
O
O
Cl
O
Se
5b
(CDCl3, 76 MHz)
950 900 850 800 750 700 650 600 550 500 450 400 350 300 250 200 150 100 50 0 -50 -100 -150 -200 -250

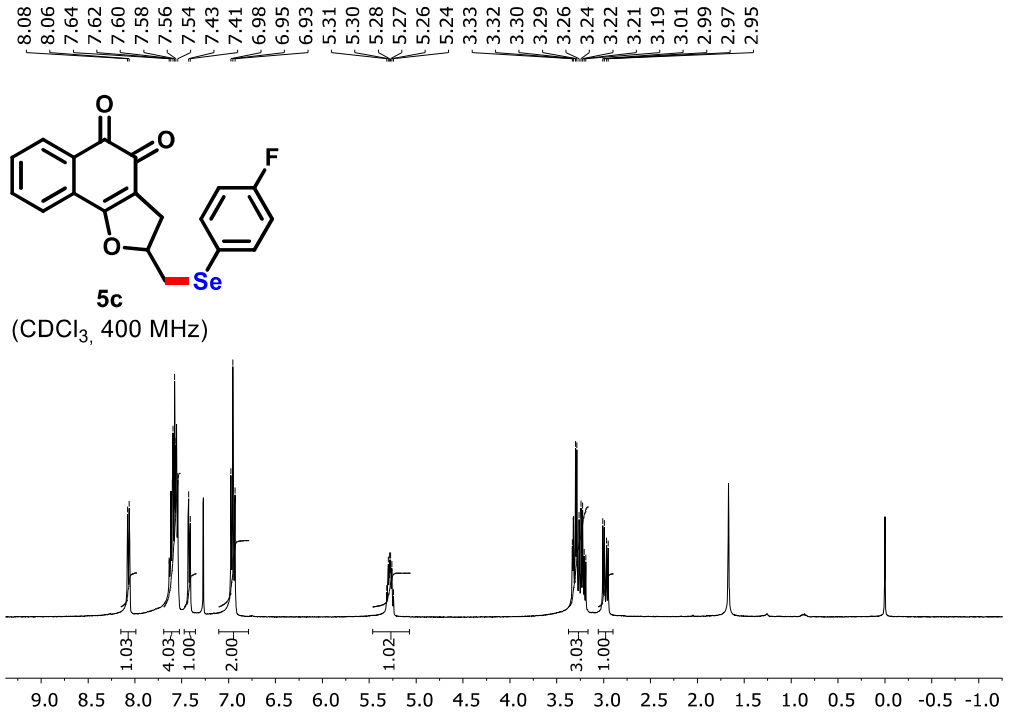
8.08 8.06 7.64 7.62 7.60 7.58 7.56 7.54 7.43 7.41 6.98 6.95 6.93 5.31 5.30 5.28 5.27 5.26 5.24 3.33 3.32 3.30 3.29 3.26 3.24 3.22 3.21 3.19 3.01 2.99 2.97 2.95
O
O
F
O
Se
5c
(CDCl3, 400 MHz)
1.03 4.03 1.00 2.00 1.02 3.03 1.00
9.0 8.5 8.0 7.5 7.0 6.5 6.0 5.5 5.0 4.5 4.0 3.5 3.0 2.5 2.0 1.5 1.0 0.5 0.0 -0.5 -1.0

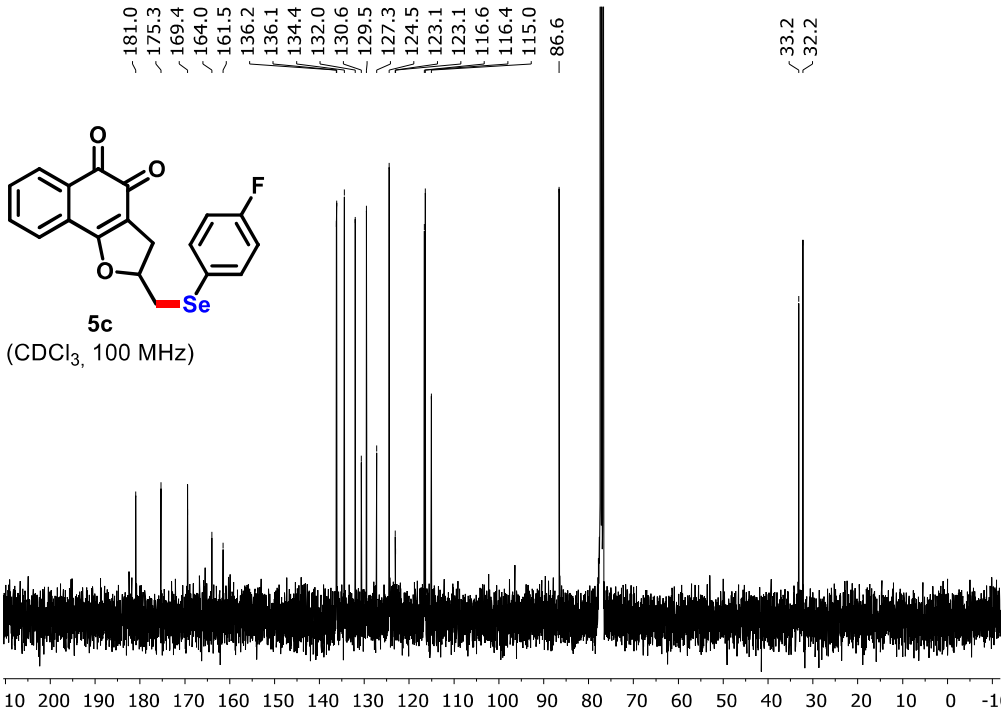
181.0
175.3
169.4
164.0
161.5
136.2
136.1
134.4
132.0
130.6
129.5
127.3
124.5
123.1
123.1
116.6
116.4
115.0
86.6
33.2
32.2
O
O
F
O
Se
5c
(CDCl3, 100 MHz)
10 200 190 180 170 160 150 140 130 120 110 100 90 80 70 60 50 40 30 20 10 0 -1

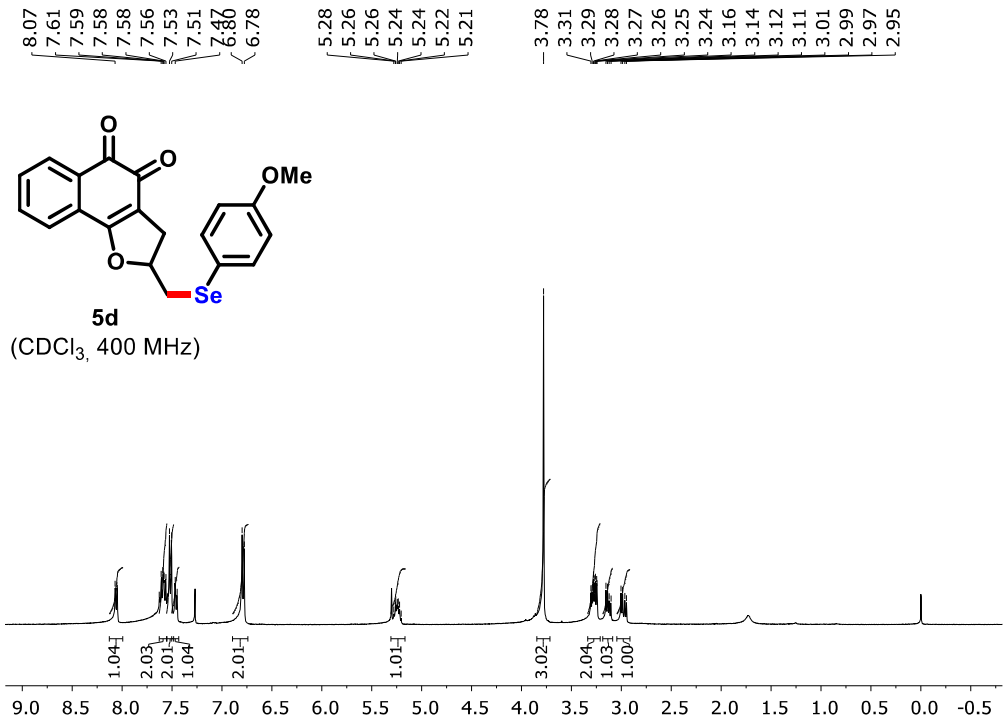
8.07
7.61
7.59
7.58
7.58
7.56
7.53
7.51
7.47
6.80
6.78
5.28
5.26
5.26
5.24
5.24
5.22
5.21
3.78
3.31
3.29
3.28
3.27
3.26
3.25
3.24
3.16
3.14
3.12
3.11
3.01
2.99
2.97
2.95
O
O
OMe
O
Se
5d
(CDCl3, 400 MHz)
1.04
2.03
2.01
1.04
2.01
1.01
3.02
2.04
1.03
1.00
9.0 8.5 8.0 7.5 7.0 6.5 6.0 5.5 5.0 4.5 4.0 3.5 3.0 2.5 2.0 1.5 1.0 0.5 0.0 -0.5

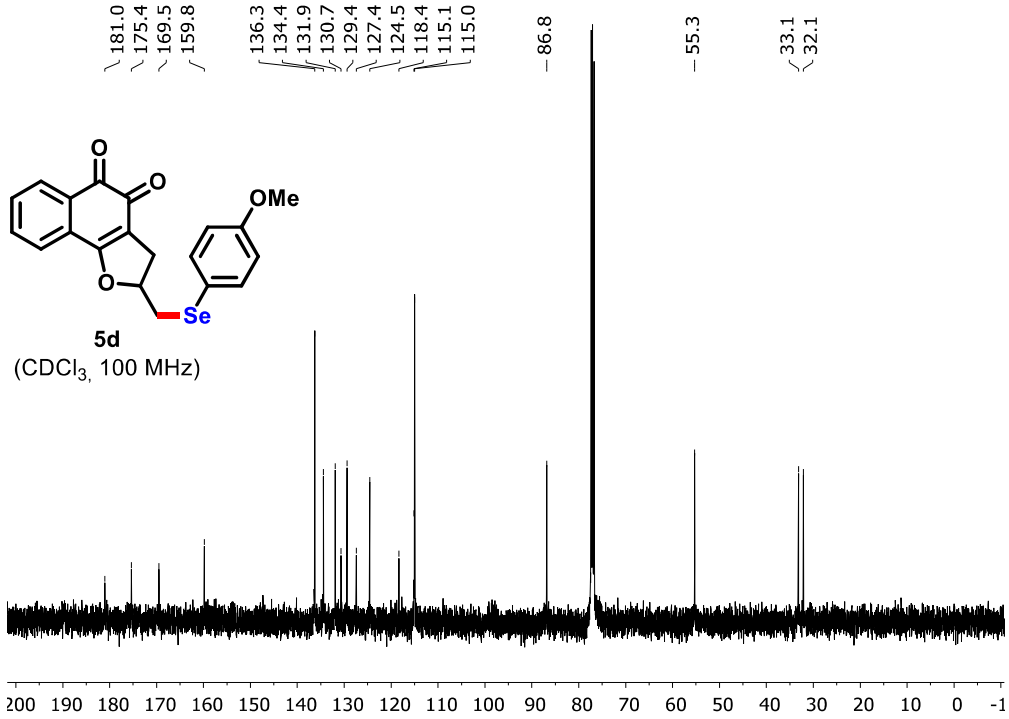
181.0
175.4
169.5
159.8
136.3
134.4
131.9
130.7
129.4
127.4
124.5
118.4
115.1
115.0
86.8
55.3
33.1
32.1
O
O
OMe
O
Se
5d
(CDCl3, 100 MHz)
200 190 180 170 160 150 140 130 120 110 100 90 80 70 60 50 40 30 20 10 0 -1

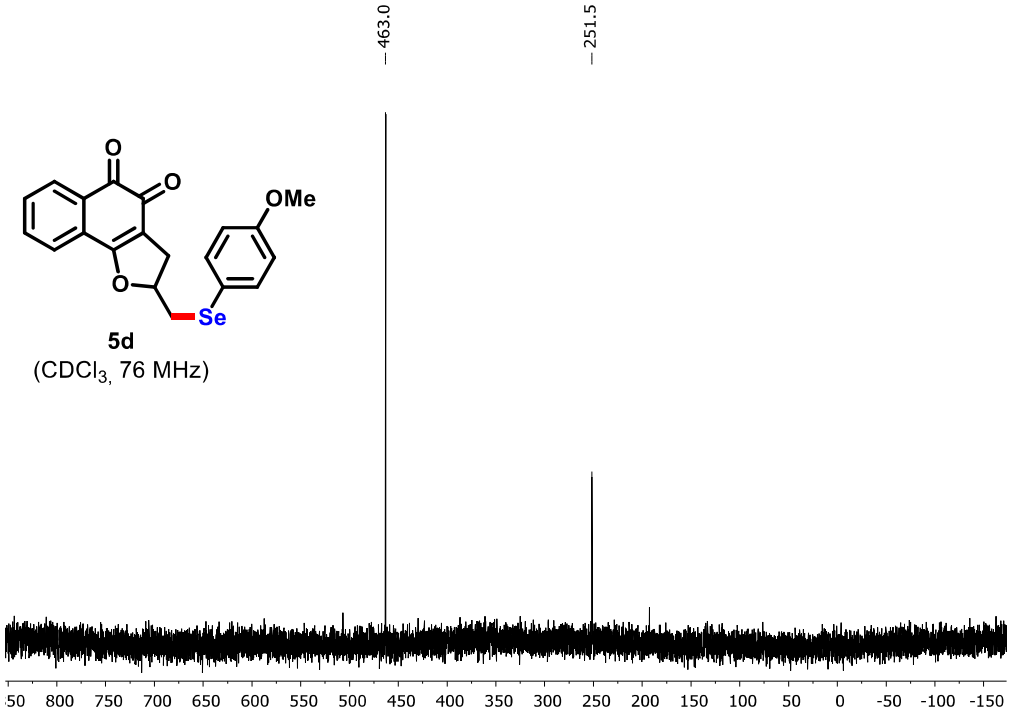
463.0
251.5
O
O
OMe
O
Se
5d
(CDCl3, 76 MHz)
50 800 750 700 650 600 550 500 450 400 350 300 250 200 150 100 50 0 -50 -100 -150

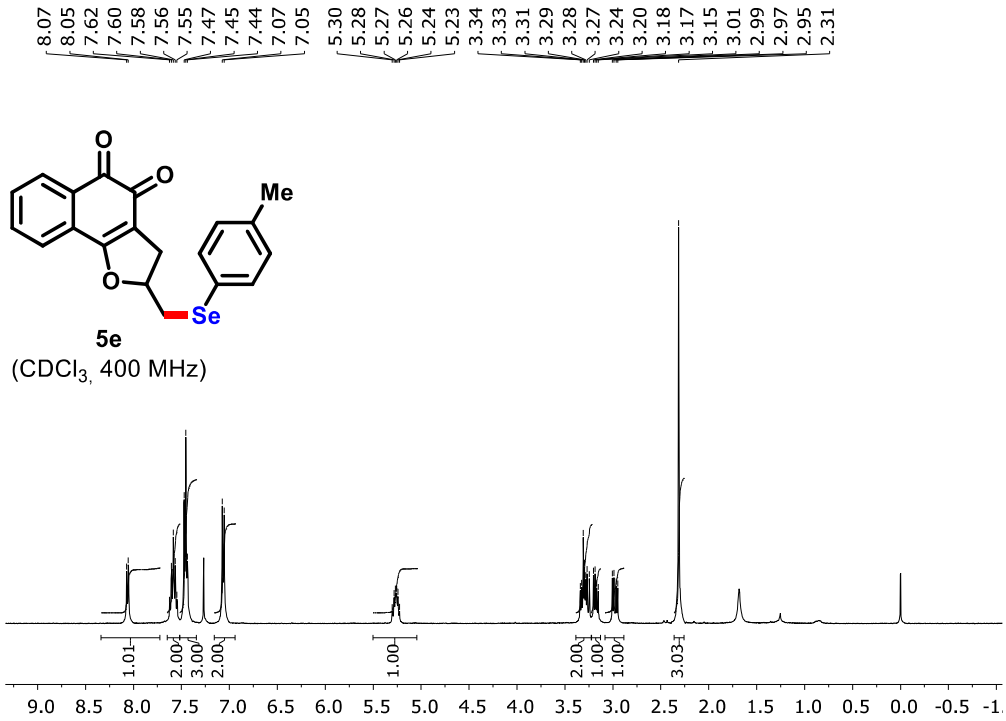
8.07
8.05
7.62
7.60
7.58
7.56
7.55
7.47
7.45
7.44
7.07
7.05
5.30
5.28
5.27
5.26
5.24
5.23
3.34
3.33
3.31
3.29
3.28
3.27
3.24
3.20
3.18
3.17
3.15
3.01
2.99
2.97
2.95
2.31
O
O
Me
O
Se
5e
(CDCl3, 400 MHz)
1.01
2.00
3.00
2.00
1.00
2.00
1.00
1.00
3.03
9.0 8.5 8.0 7.5 7.0 6.5 6.0 5.5 5.0 4.5 4.0 3.5 3.0 2.5 2.0 1.5 1.0 0.5 0.0 -0.5

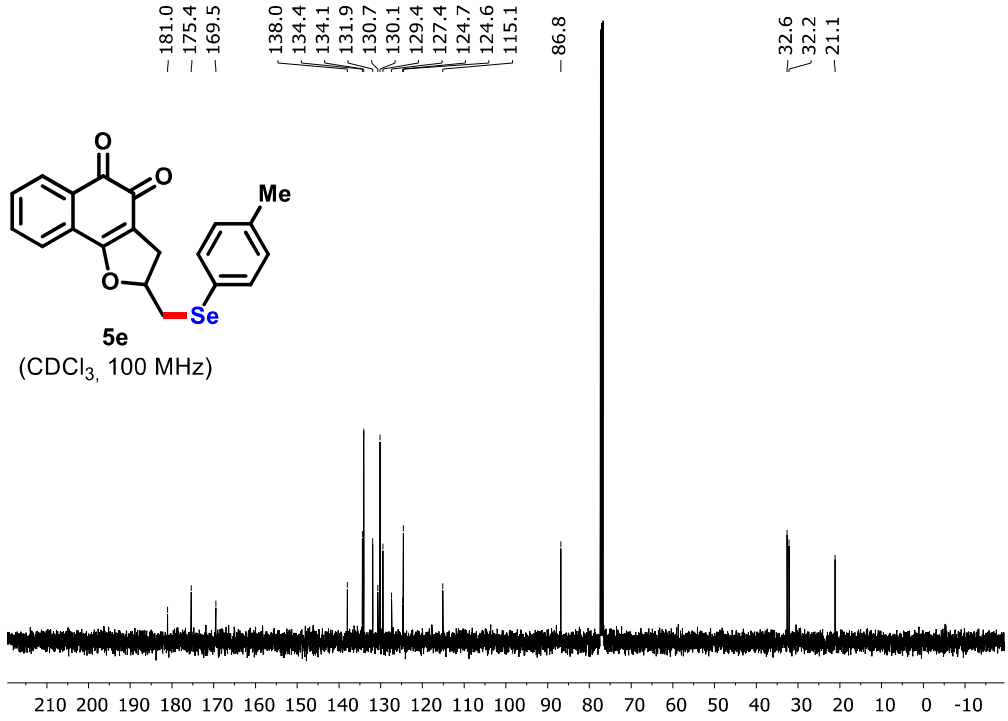
181.0
175.4
169.5
138.0
134.4
134.1
131.9
130.7
130.1
129.4
127.4
124.7
124.6
115.1
86.8
32.6
32.2
21.1
O
O
Me
O
Se
5e
(CDCl3, 100 MHz)
210 200 190 180 170 160 150 140 130 120 110 100 90 80 70 60 50 40 30 20 10 0 -10

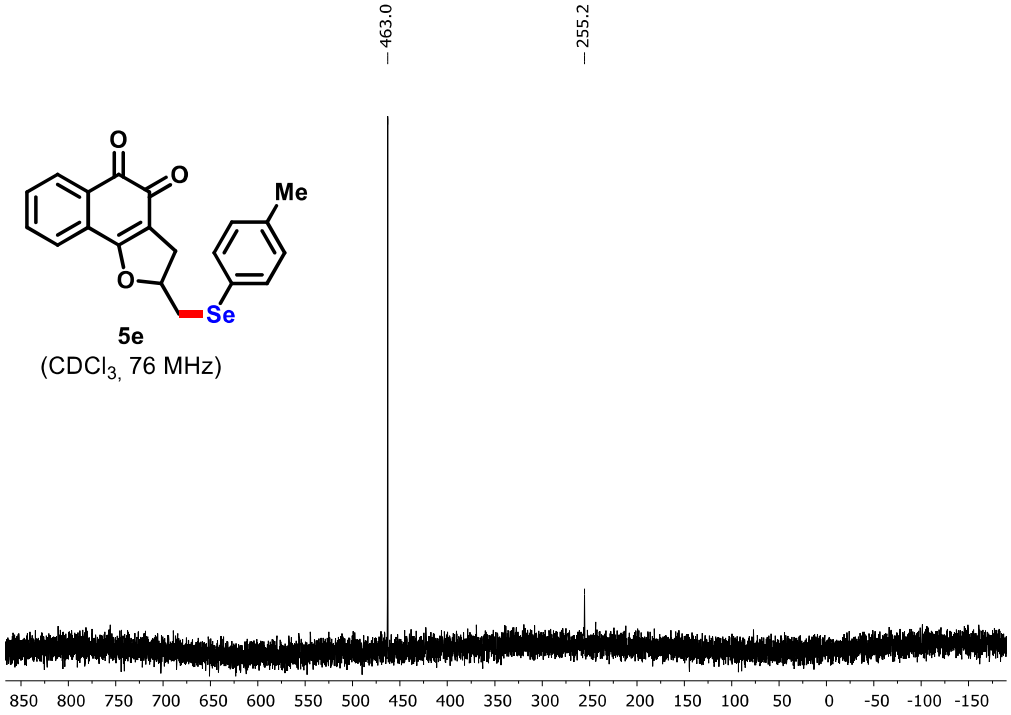

5e
($CDCl_3$, 76 MHz)

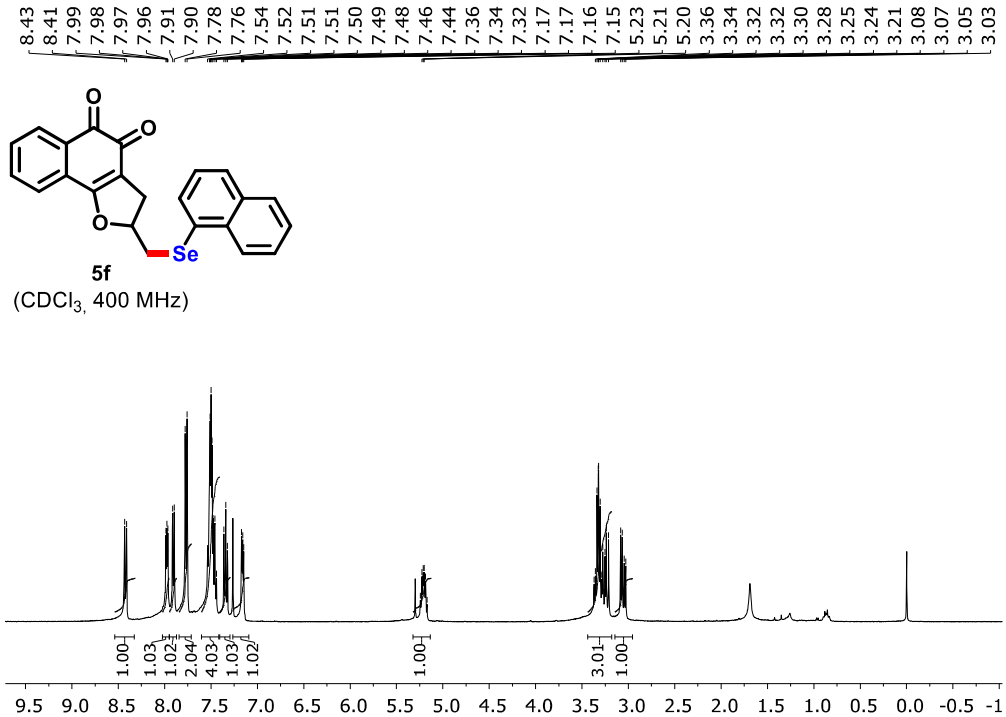

5f
($CDCl_3$, 400 MHz)

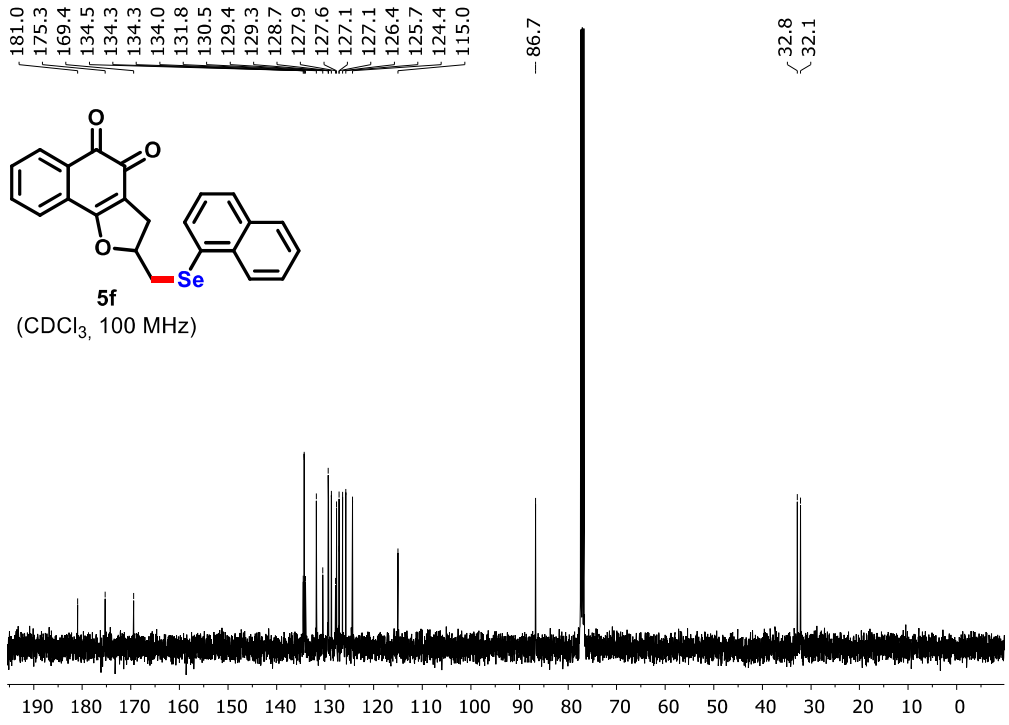
181.0
175.3
169.4
134.5
134.3
134.3
134.0
131.8
130.5
129.4
129.3
128.7
127.9
127.6
127.1
127.1
126.4
125.7
124.4
115.0
86.7
32.8
32.1
O
O
O
Se
5f
(CDCl3, 100 MHz)
190 180 170 160 150 140 130 120 110 100 90 80 70 60 50 40 30 20 10 0

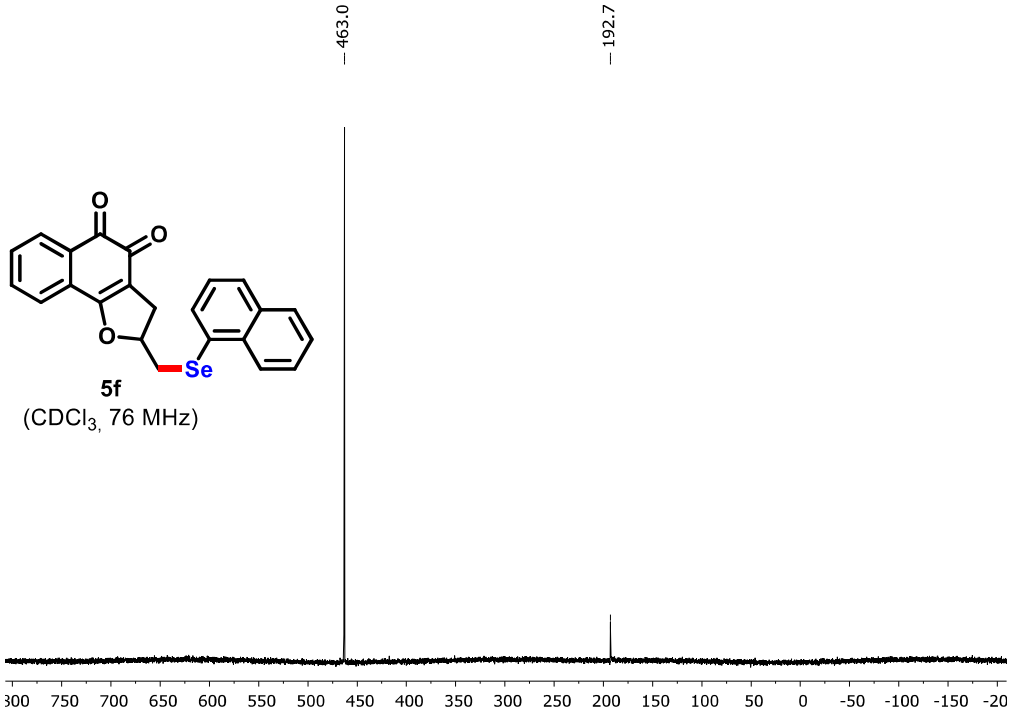
463.0
192.7
O
O
O
Se
5f
(CDCl3, 76 MHz)
750 700 650 600 550 500 450 400 350 300 250 200 150 100 50 0 -50 -100 -150

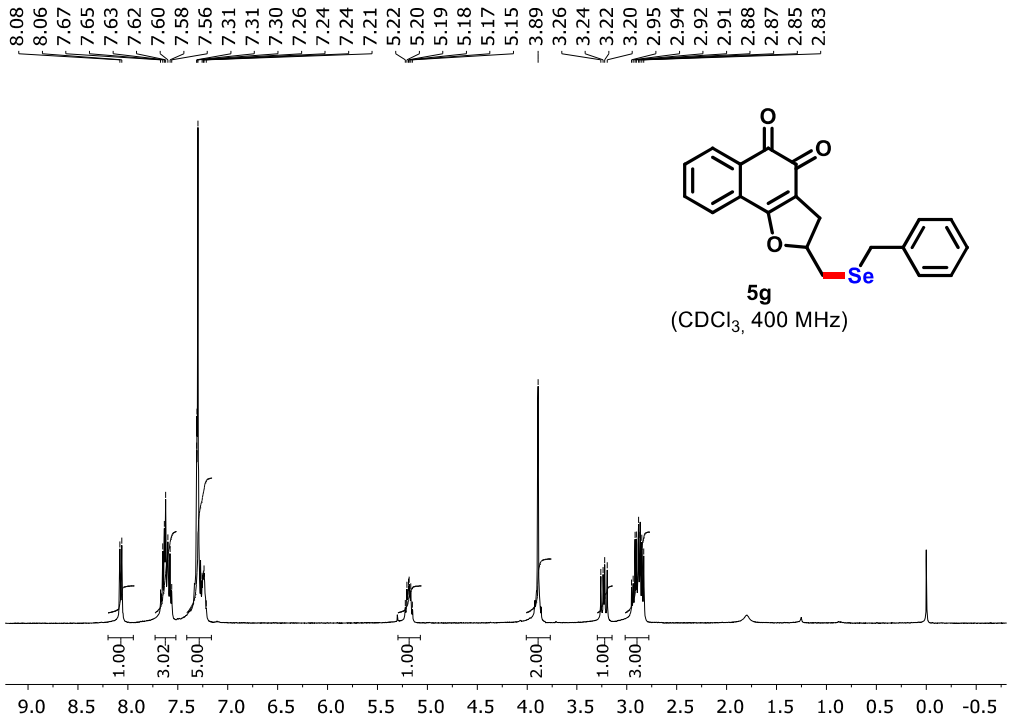
8.08
8.06
7.67
7.65
7.63
7.62
7.60
7.58
7.56
7.31
7.31
7.30
7.26
7.24
7.24
7.21
5.22
5.20
5.19
5.18
5.17
5.15
3.89
3.26
3.24
3.22
3.20
2.95
2.94
2.92
2.91
2.88
2.87
2.85
2.83
O
O
O
Se
5g
(CDCl3, 400 MHz)
1.00
3.02
5.00
1.00
2.00
1.00
3.00
9.0 8.5 8.0 7.5 7.0 6.5 6.0 5.5 5.0 4.5 4.0 3.5 3.0 2.5 2.0 1.5 1.0 0.5 0.0 -0.5

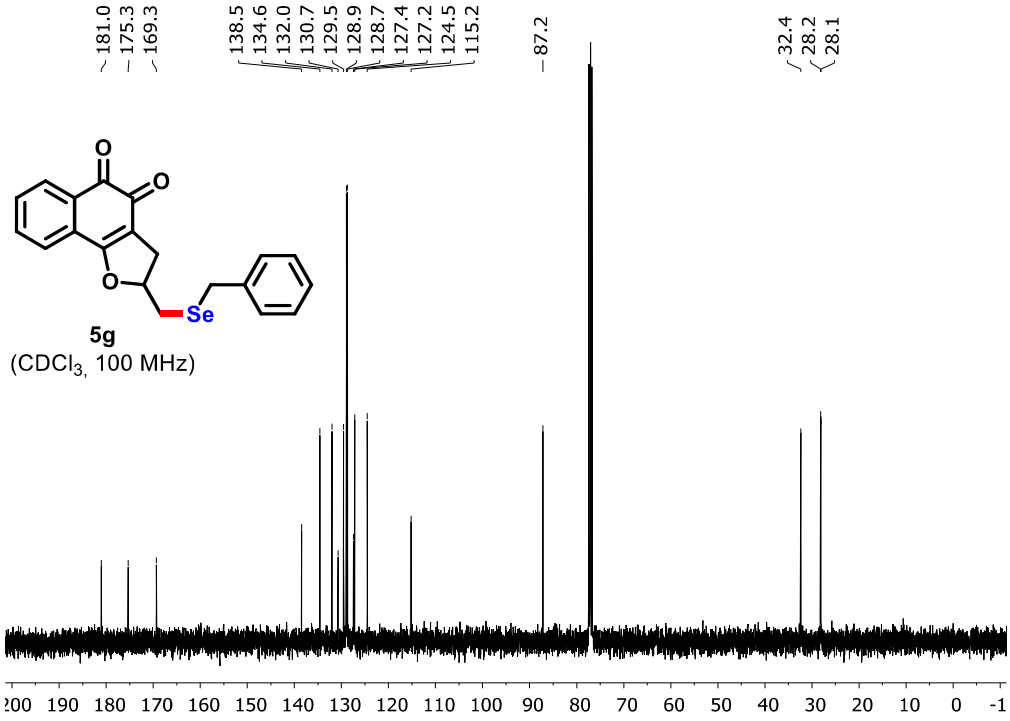
181.0
175.3
169.3
138.5
134.6
132.0
130.7
129.5
128.9
128.7
127.4
127.2
124.5
115.2
87.2
32.4
28.2
28.1
O
O
O
Se
5g
(CDCl3, 100 MHz)
200 190 180 170 160 150 140 130 120 110 100 90 80 70 60 50 40 30 20 10 0 -1

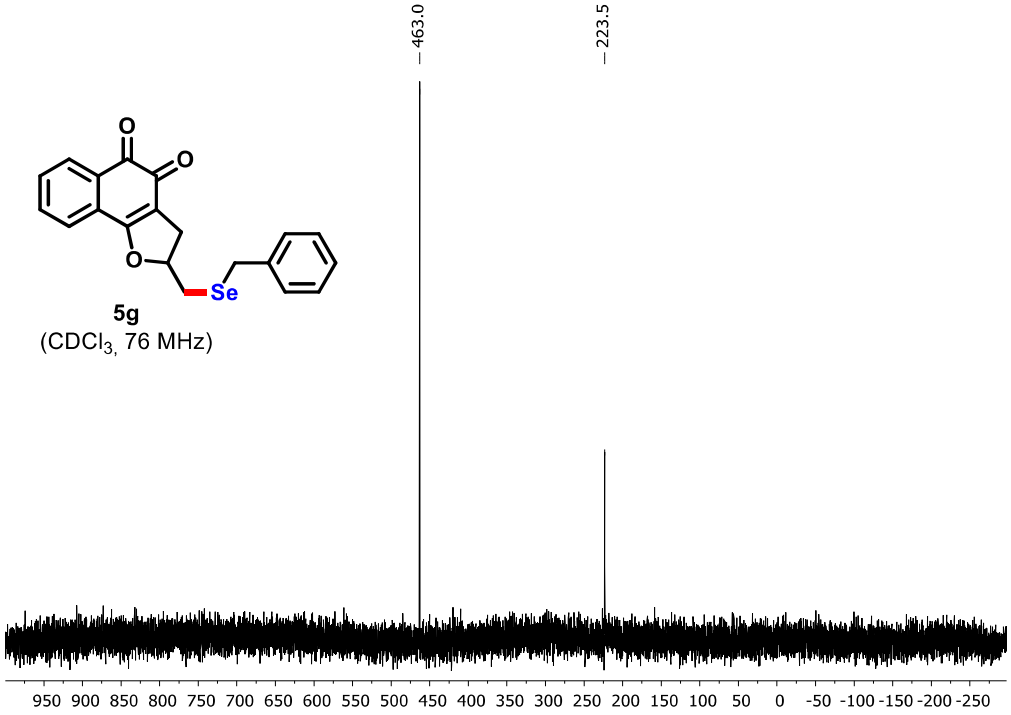

5g
($CDCl_3$, 76 MHz)

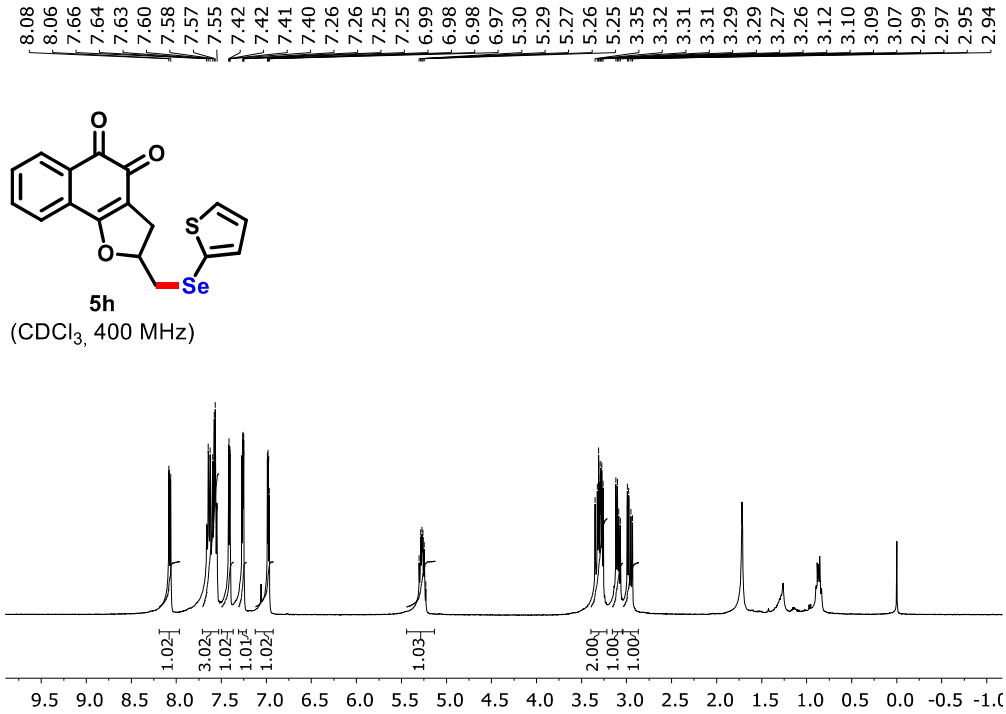

5h
($CDCl_3$, 400 MHz)

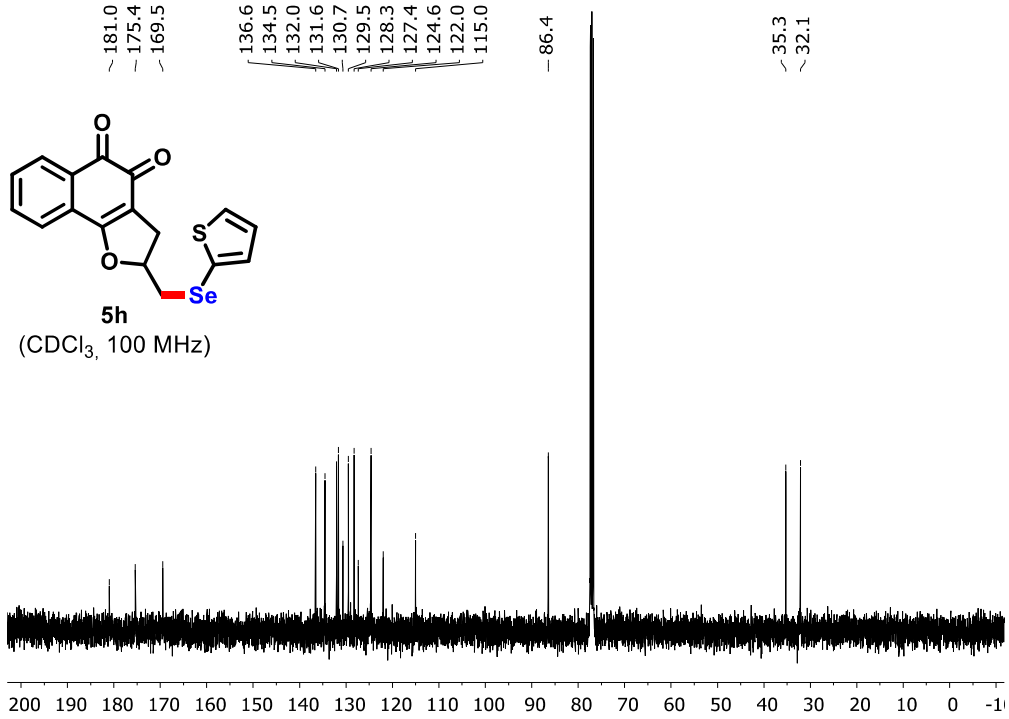
181.0
175.4
169.5
136.6
134.5
132.0
131.6
130.7
129.5
128.3
127.4
124.6
122.0
115.0
86.4
35.3
32.1
O
O
S
O
Se
5h
(CDCl3, 100 MHz)
200 190 180 170 160 150 140 130 120 110 100 90 80 70 60 50 40 30 20 10 0

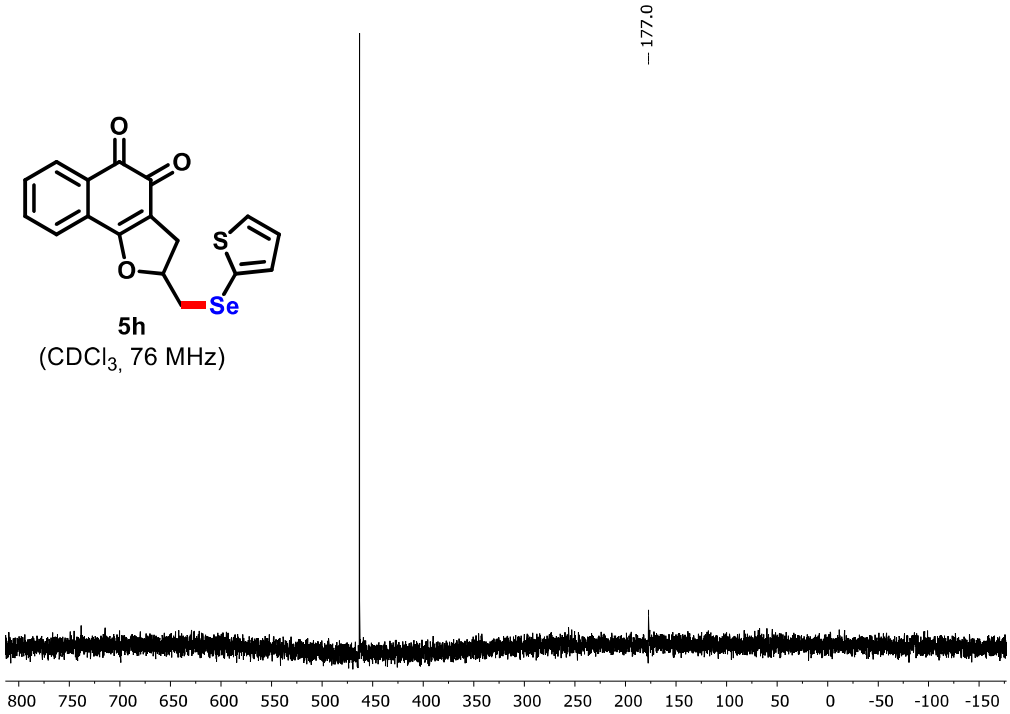
177.0
O
O
S
O
Se
5h
(CDCl3, 76 MHz)
800 750 700 650 600 550 500 450 400 350 300 250 200 150 100 50 0 -50 -100 -150

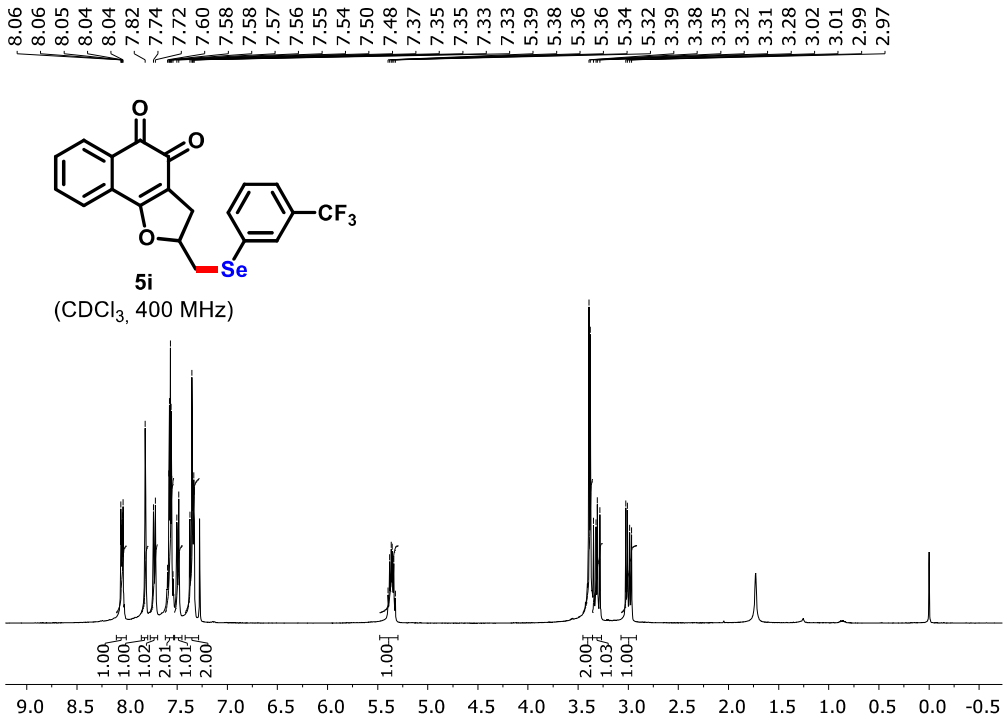
8.06
8.06
8.05
8.04
8.04
7.82
7.74
7.72
7.60
7.58
7.58
7.57
7.56
7.55
7.54
7.50
7.48
7.37
7.35
7.35
7.33
7.33
5.39
5.38
5.36
5.36
5.34
5.32
3.39
3.38
3.35
3.32
3.31
3.28
3.02
3.01
2.99
2.97
O
O
CF3
O
Se
5i
(CDCl3, 400 MHz)
1.00
1.00
1.02
2.01
1.01
2.00
1.00
2.00
1.03
1.00
9.0 8.5 8.0 7.5 7.0 6.5 6.0 5.5 5.0 4.5 4.0 3.5 3.0 2.5 2.0 1.5 1.0 0.5 0.0 -0.5

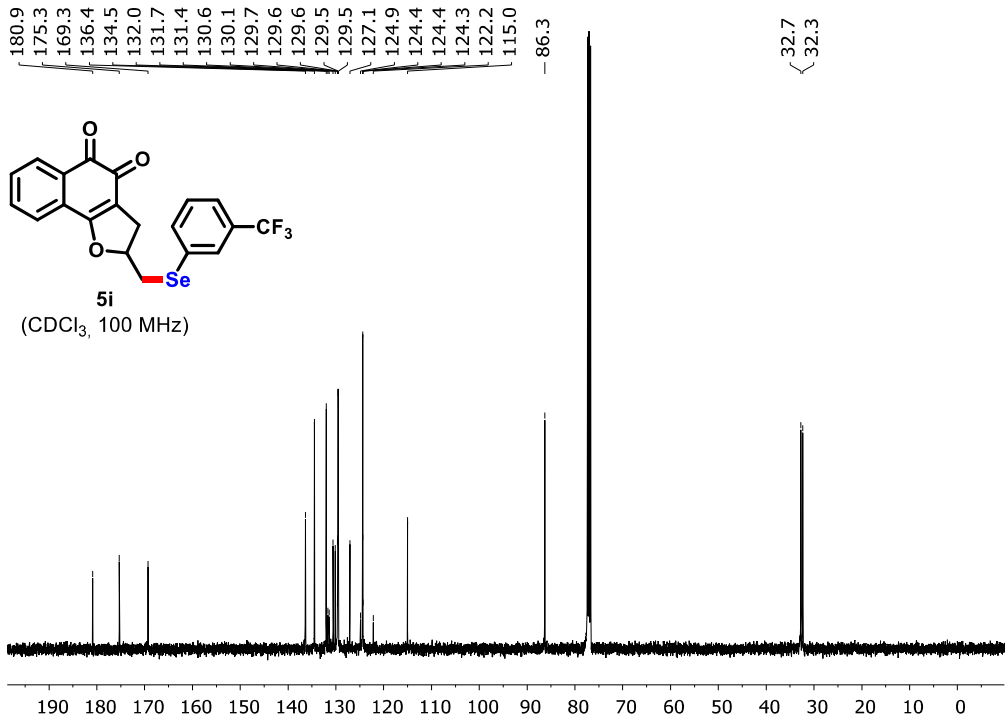
180.9
175.3
169.3
136.4
134.5
132.0
131.7
131.4
130.6
130.1
129.7
129.6
129.6
129.5
129.5
127.1
124.9
124.4
124.4
124.3
122.2
115.0
86.3
32.7
32.3
O
O
CF3
O
Se
5i
(CDCl3, 100 MHz)
190 180 170 160 150 140 130 120 110 100 90 80 70 60 50 40 30 20 10 0

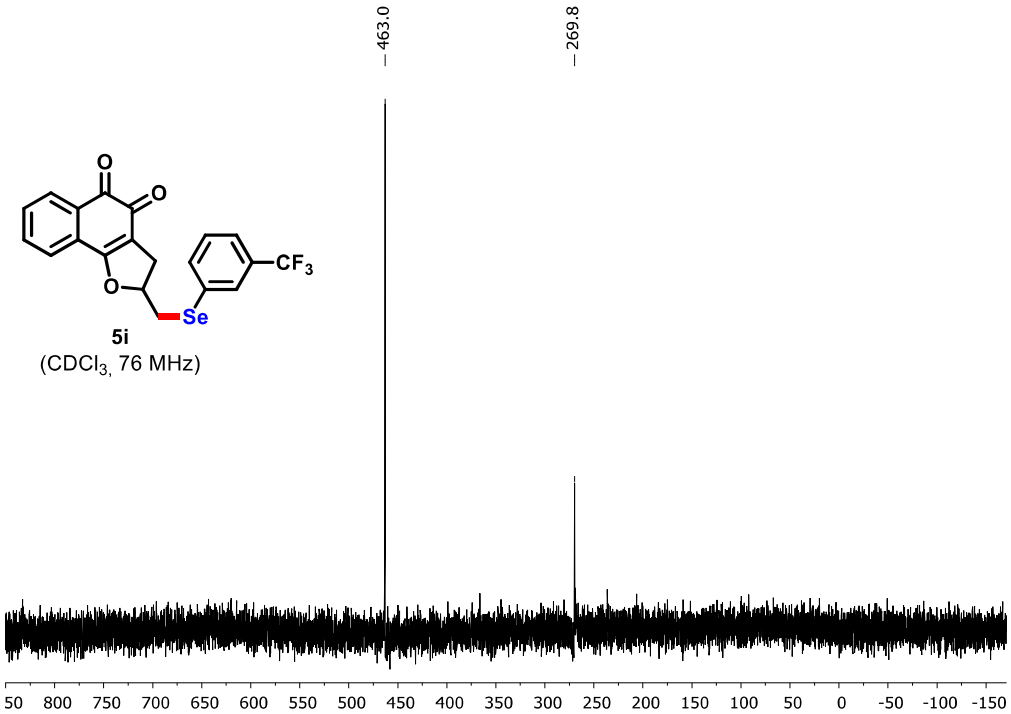
463.0
269.8
O
O
CF3
O
Se
5i
(CDCl3, 76 MHz)
50 800 750 700 650 600 550 500 450 400 350 300 250 200 150 100 50 0 -50 -100 -150

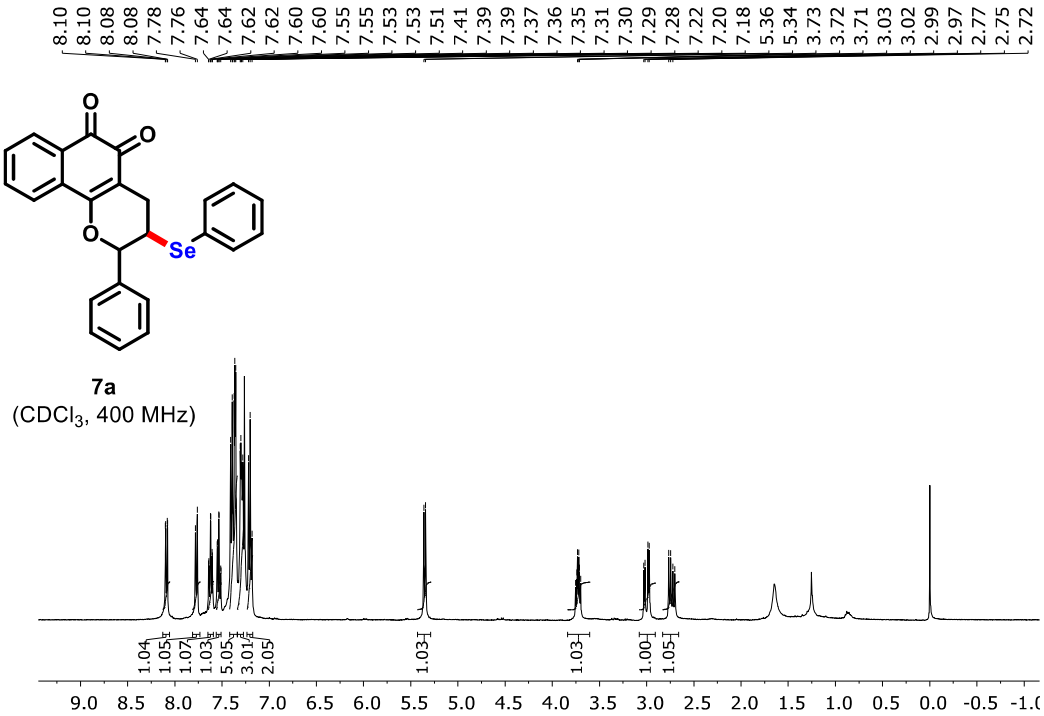
8.10 8.10 8.08 8.08 7.78 7.76 7.64 7.64 7.62 7.62 7.60 7.60 7.55 7.55 7.53 7.53 7.51 7.41 7.39 7.39 7.37 7.36 7.35 7.31 7.30 7.29 7.28 7.22 7.20 7.18 5.36 5.34 3.73 3.72 3.71 3.03 3.02 2.99 2.97 2.77 2.75 2.72
O
O
O
Se
7a
(CDCl3, 400 MHz)
1.04 1.05 1.07 1.03 5.05 3.01 2.05 1.03 1.03 1.00 1.05
9.0 8.5 8.0 7.5 7.0 6.5 6.0 5.5 5.0 4.5 4.0 3.5 3.0 2.5 2.0 1.5 1.0 0.5 0.0 -0.5

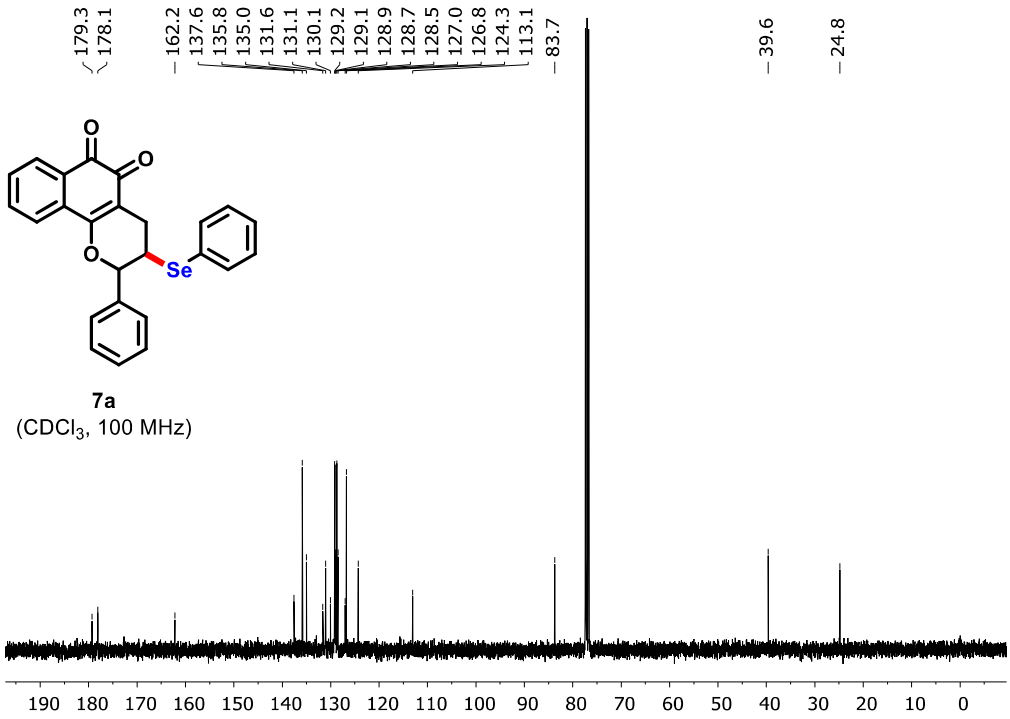

7a
($CDCl_3$, 100 MHz)

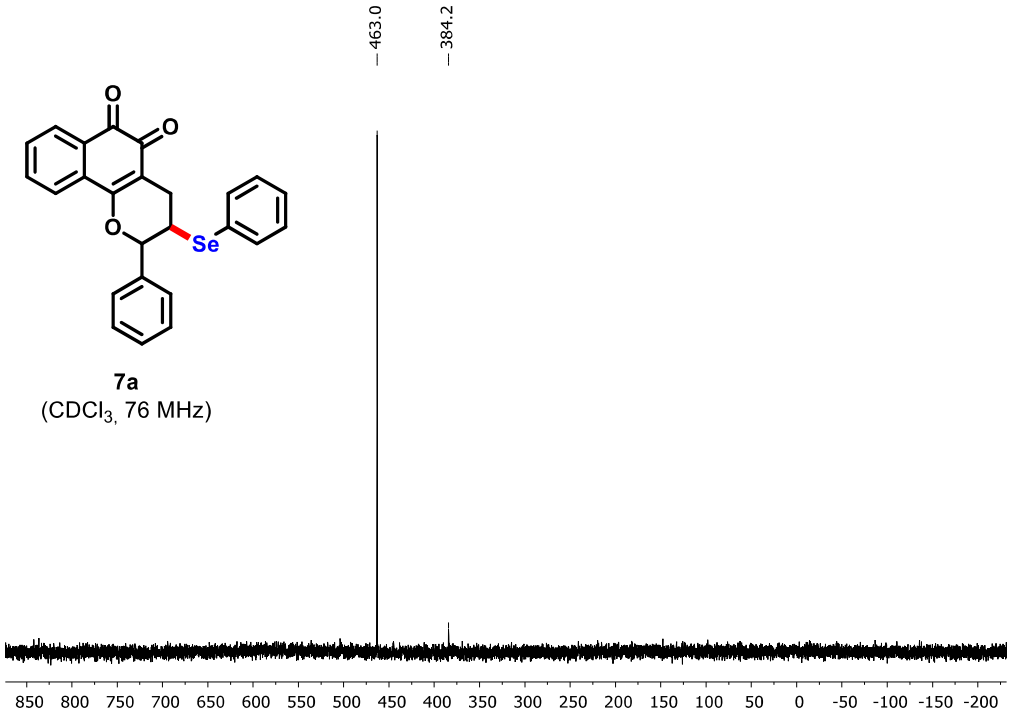

7a
($CDCl_3$, 76 MHz)

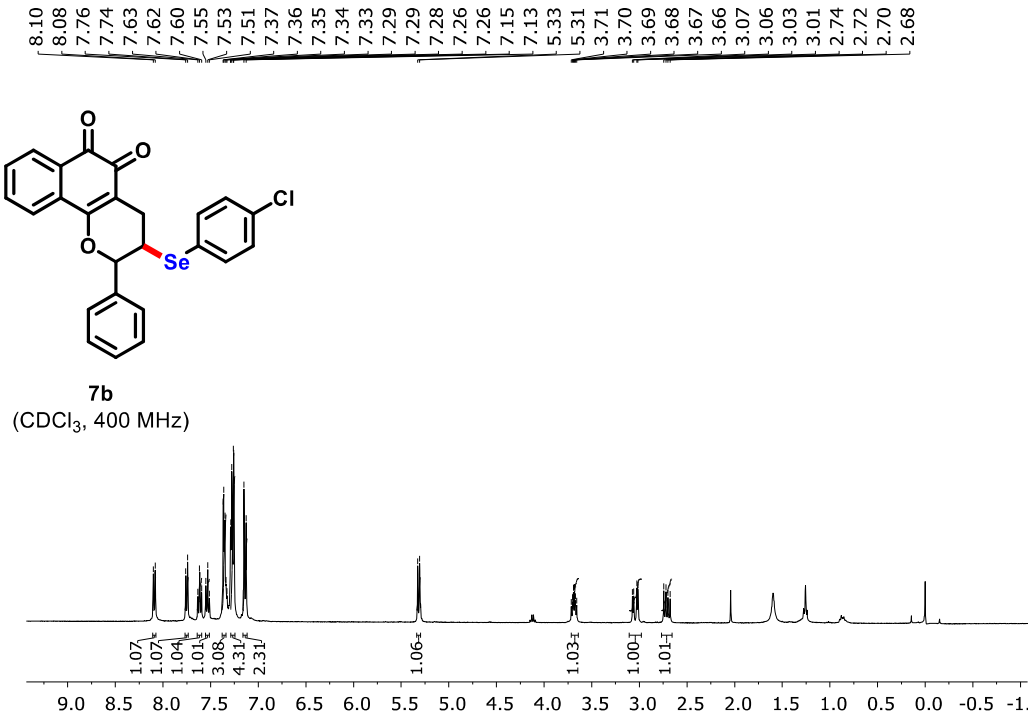
8.10
8.08
7.76
7.74
7.63
7.62
7.60
7.55
7.53
7.51
7.37
7.36
7.35
7.34
7.33
7.29
7.29
7.28
7.26
7.26
7.15
7.13
5.33
5.31
3.71
3.70
3.69
3.68
3.67
3.66
3.07
3.06
3.03
3.01
2.74
2.72
2.70
2.68
O
O
Cl
O
Se
7b
(CDCl3, 400 MHz)
1.07
1.07
1.04
1.01
3.08
4.31
2.31
1.06
1.03
1.00
1.01
9.0 8.5 8.0 7.5 7.0 6.5 6.0 5.5 5.0 4.5 4.0 3.5 3.0 2.5 2.0 1.5 1.0 0.5 0.0 -0.5 -1.

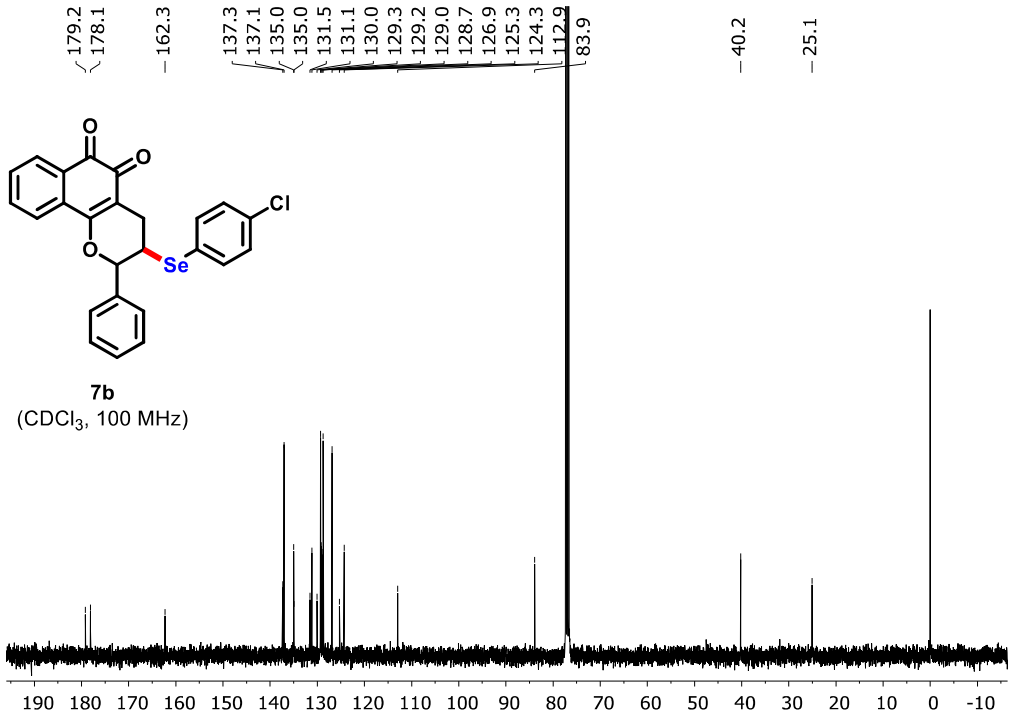
179.2
178.1
162.3
137.3
137.1
135.0
135.0
131.5
131.1
130.0
129.3
129.2
129.0
128.7
126.9
125.3
124.3
112.9
83.9
40.2
25.1
O
O
Cl
O
Se
7b
(CDCl3, 100 MHz)
190 180 170 160 150 140 130 120 110 100 90 80 70 60 50 40 30 20 10 0 -10

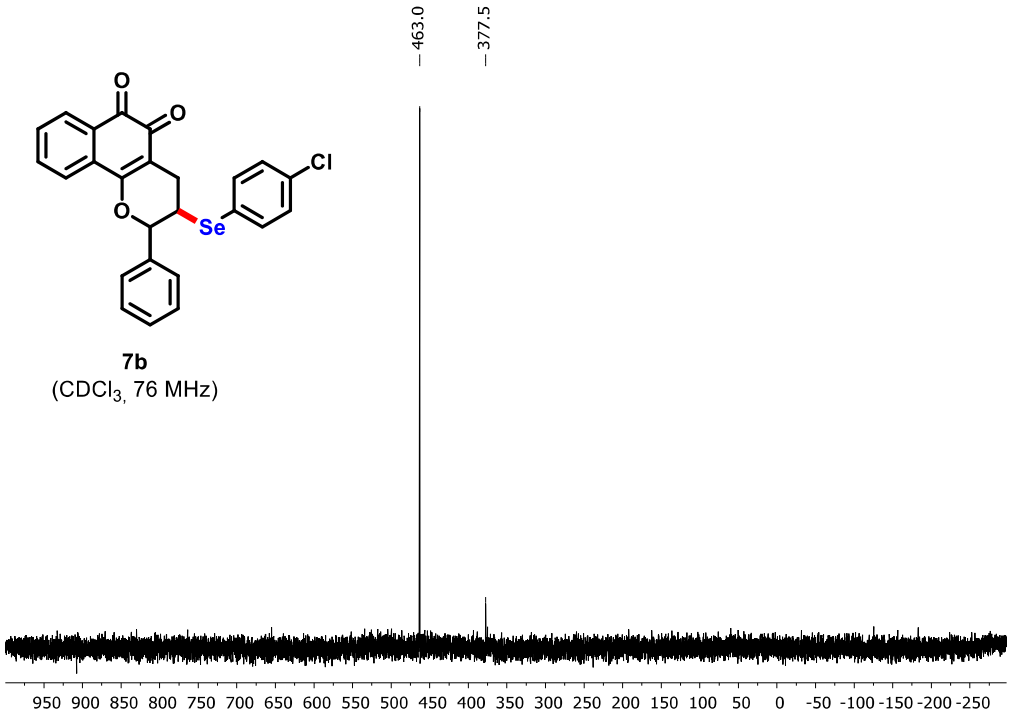

7b
($CDCl_3$, 76 MHz)

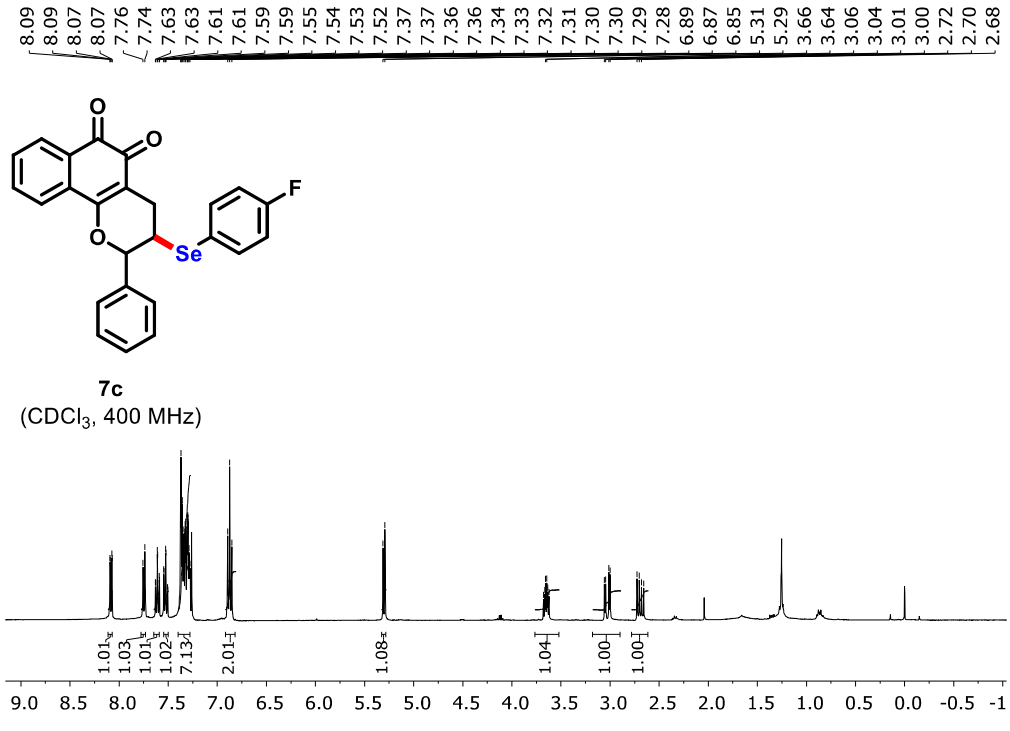

7c
($CDCl_3$, 400 MHz)

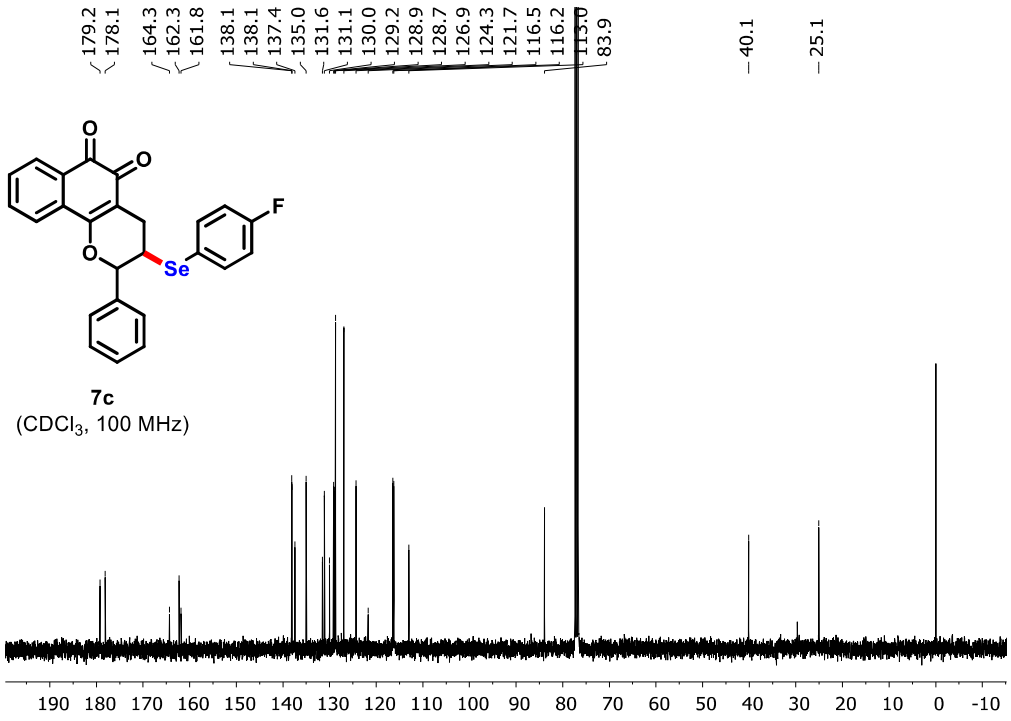
179.2
178.1
164.3
162.3
161.8
138.1
138.1
137.4
135.0
131.6
131.1
130.0
129.2
128.9
128.7
126.9
124.3
121.7
116.5
116.2
113.0
83.9
40.1
25.1
O
O
O
Se
F
7c
(CDCl3, 100 MHz)
190 180 170 160 150 140 130 120 110 100 90 80 70 60 50 40 30 20 10 0 -10

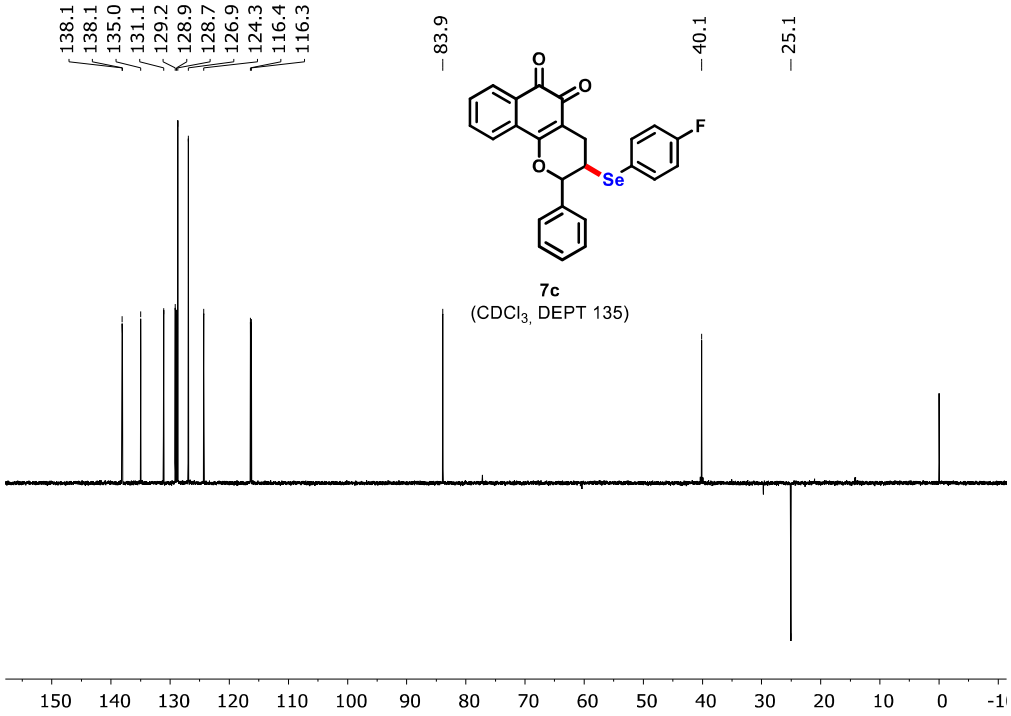
138.1
138.1
135.0
131.1
129.2
128.9
128.7
126.9
124.3
116.4
116.3
83.9
40.1
25.1
O
O
O
Se
F
7c
(CDCl3, DEPT 135)
150 140 130 120 110 100 90 80 70 60 50 40 30 20 10 0 -1

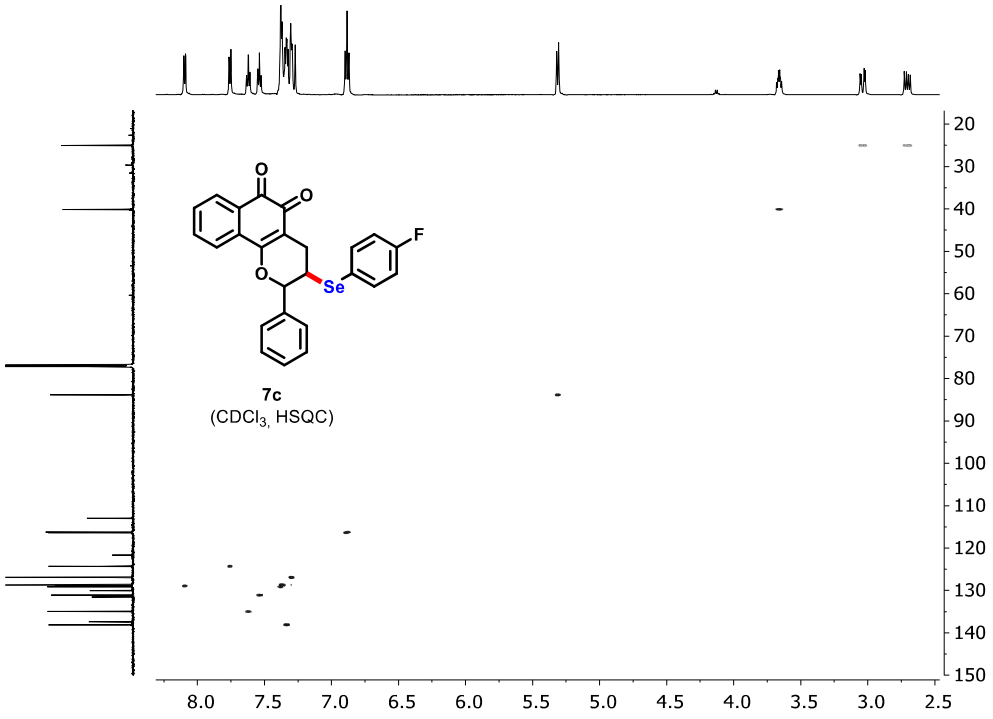
7c
(CDCl3, HSQC)

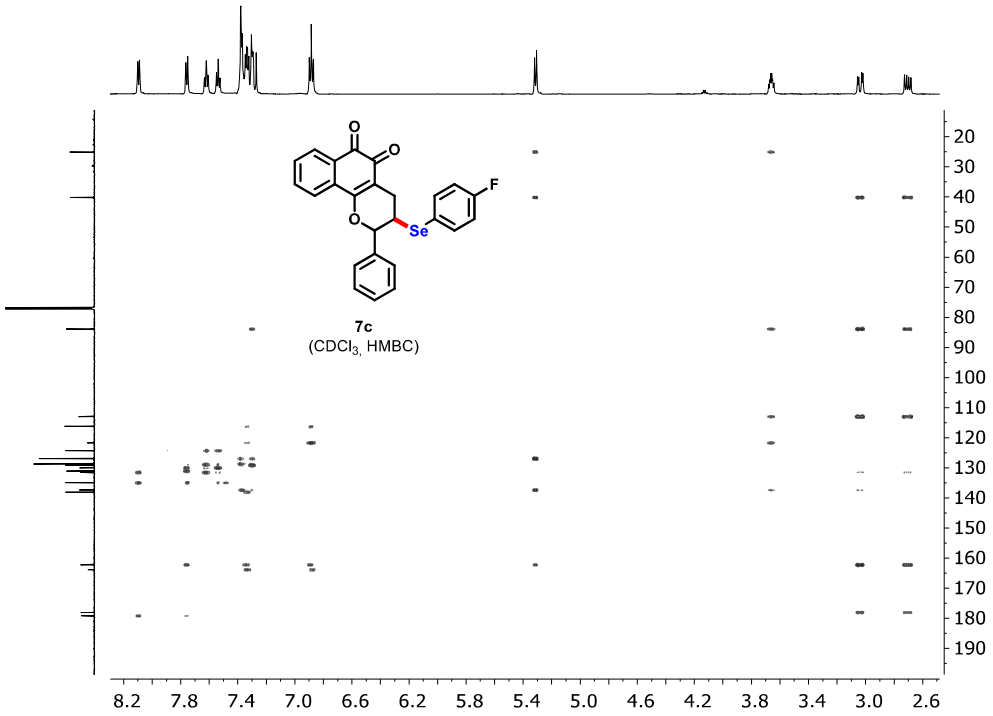
7c
(CDCl3, HMBC)

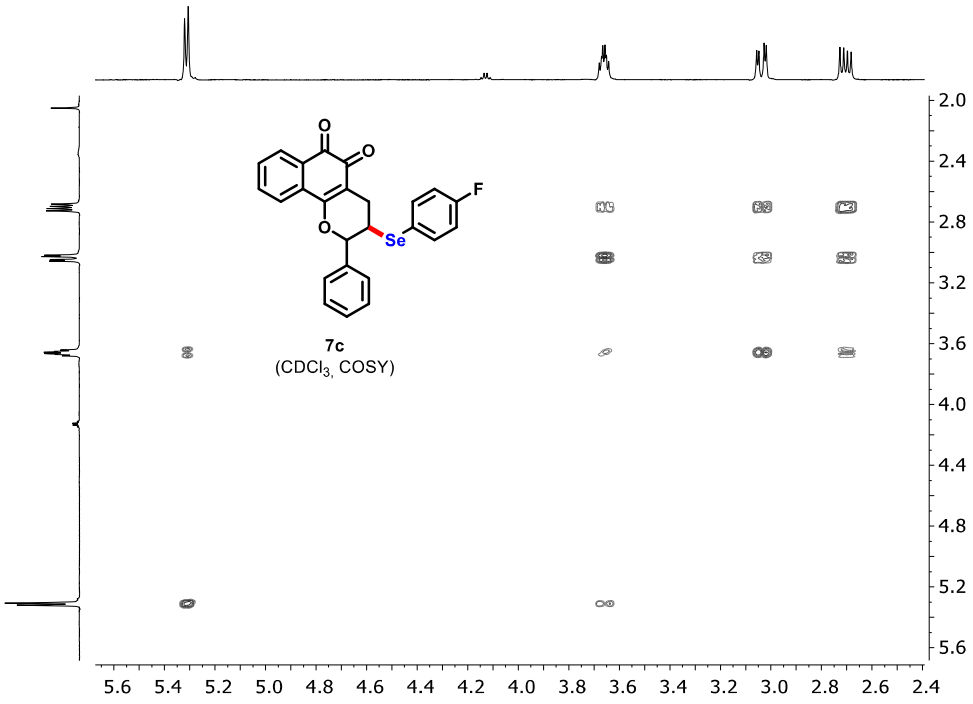
7c
(CDCl3, COSY)

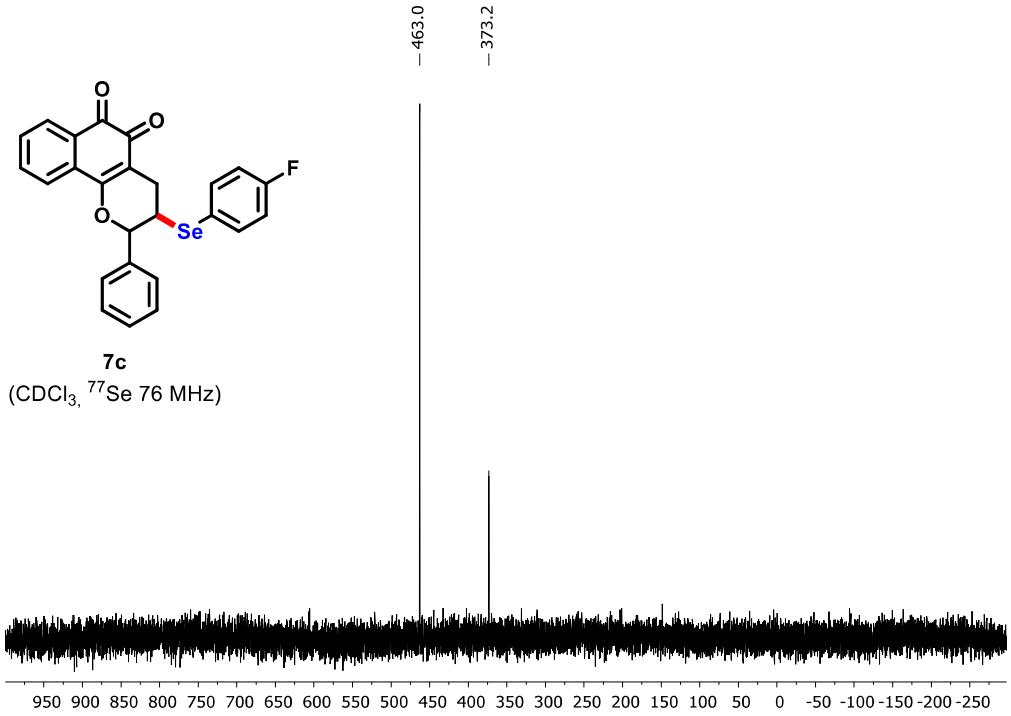
463.0
373.2
7c
(CDCl3, 77Se 76 MHz)

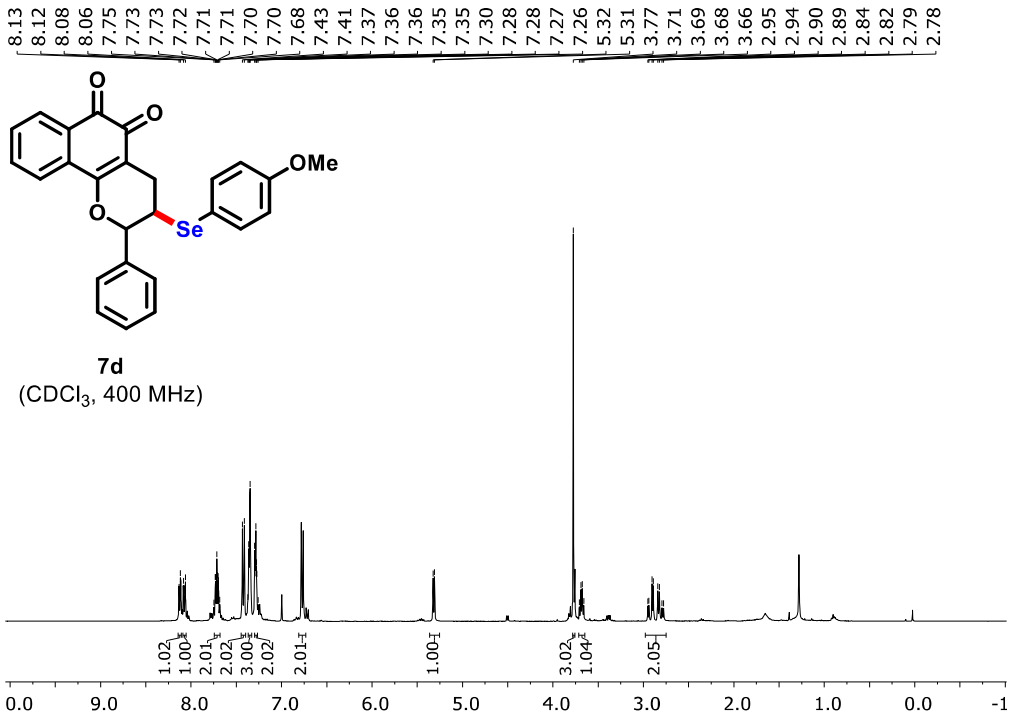

7d
($CDCl_3$, 400 MHz)

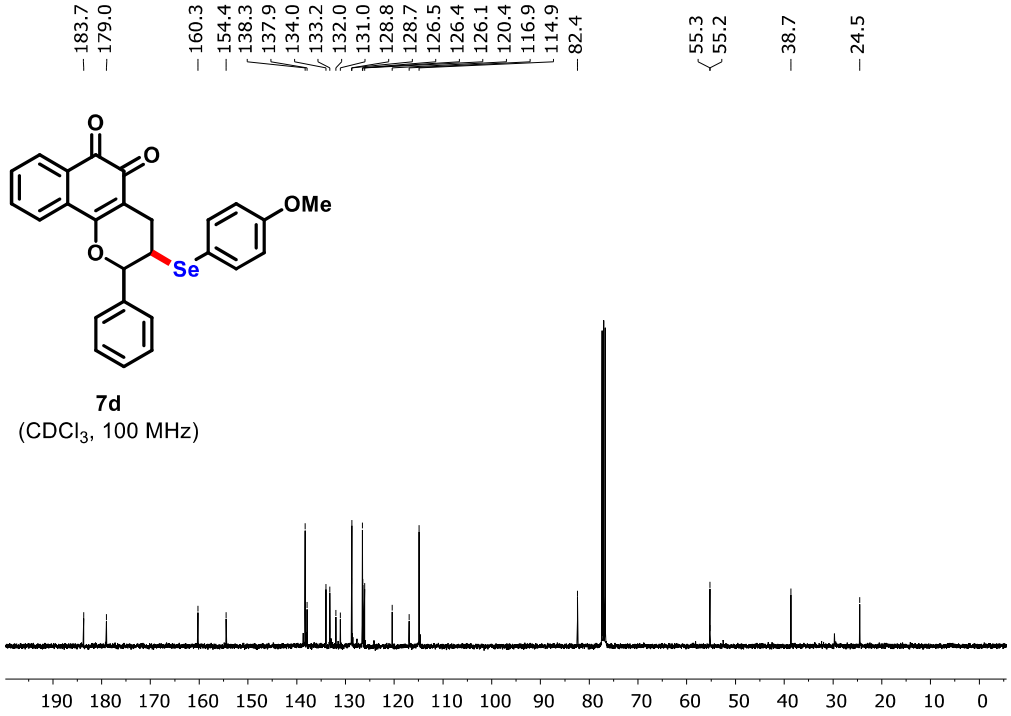

7d
($CDCl_3$, 100 MHz)

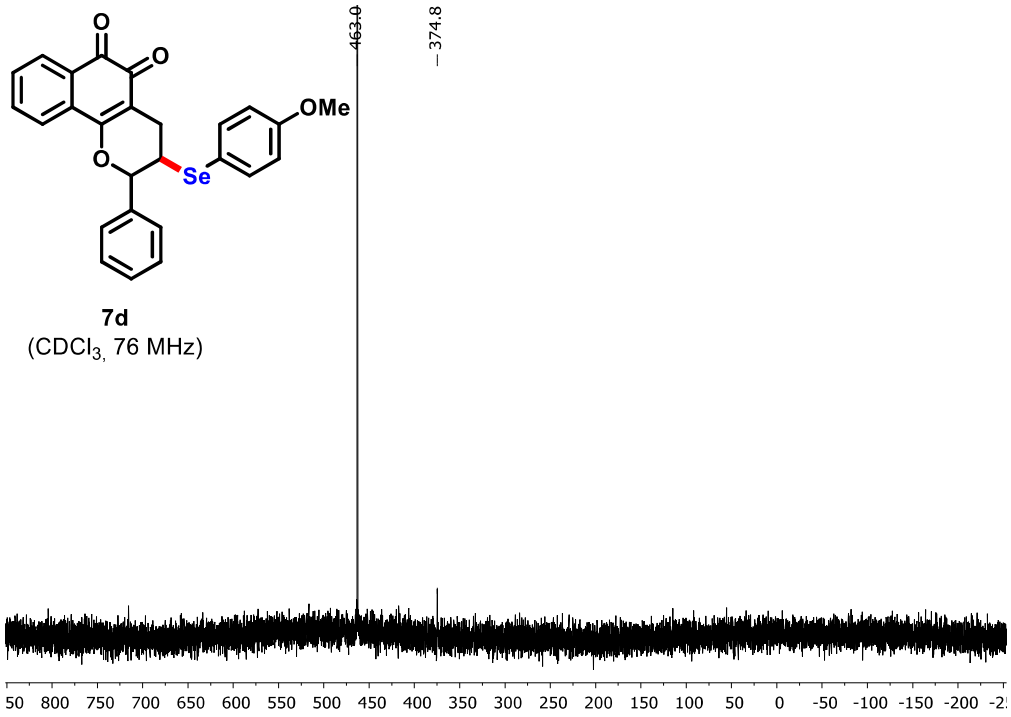

7d
($CDCl_3$, 76 MHz)

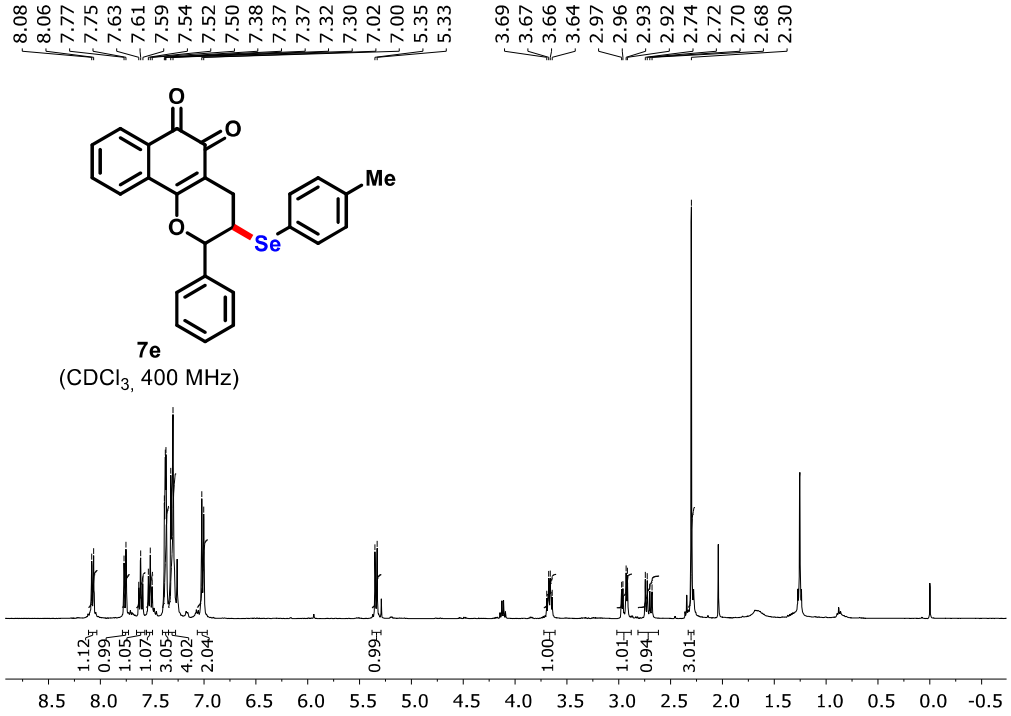

7e
($CDCl_3$, 400 MHz)

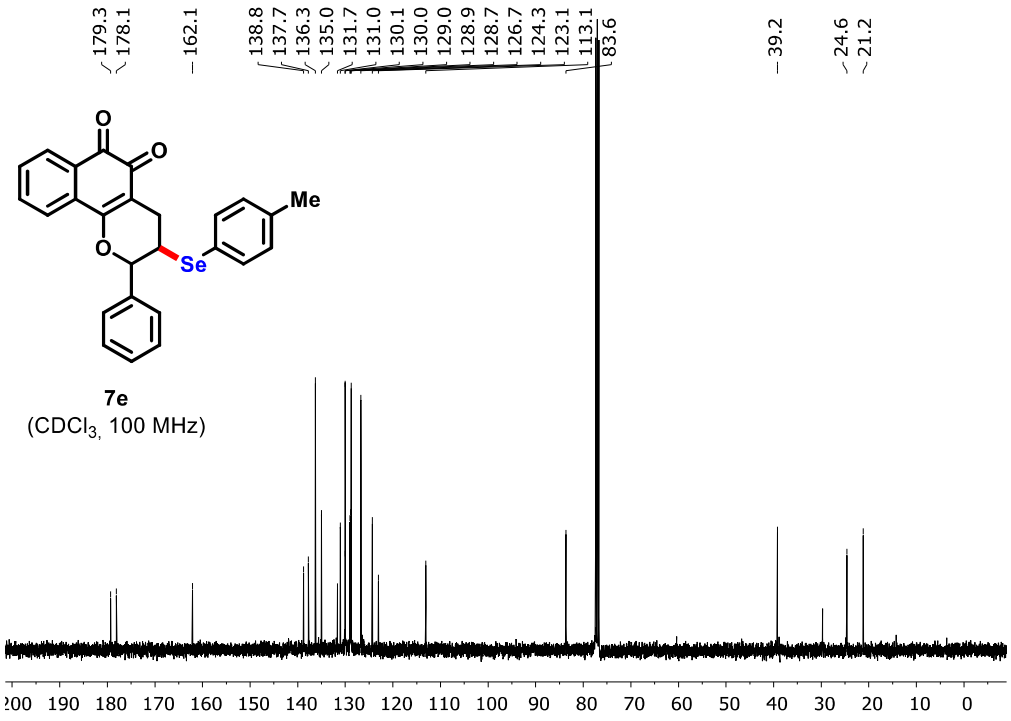
179.3
178.1
162.1
138.8
137.7
136.3
135.0
131.7
131.0
130.1
130.0
129.0
128.9
128.7
126.7
124.3
123.1
113.1
83.6
39.2
24.6
21.2
O
O
Me
O
Se
7e
(CDCl3, 100 MHz)
200 190 180 170 160 150 140 130 120 110 100 90 80 70 60 50 40 30 20 10 0

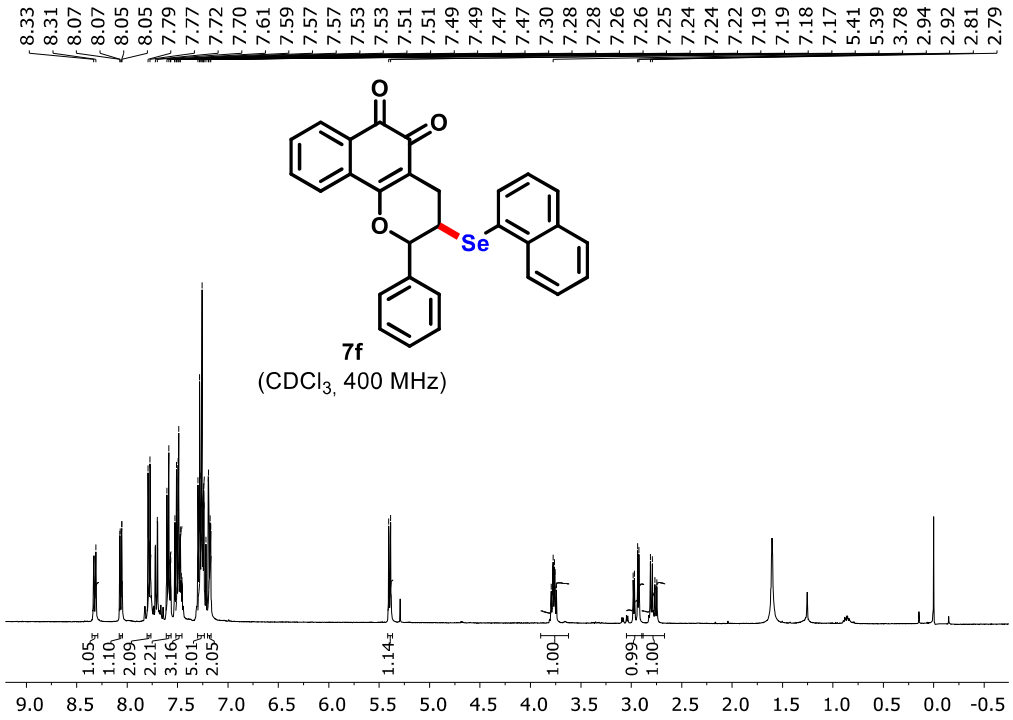
8.33
8.31
8.07
8.07
8.05
8.05
7.79
7.77
7.72
7.70
7.61
7.59
7.57
7.57
7.53
7.53
7.51
7.51
7.49
7.49
7.47
7.47
7.30
7.28
7.28
7.26
7.26
7.25
7.24
7.24
7.22
7.19
7.19
7.18
7.17
5.41
5.39
3.78
2.94
2.92
2.81
2.79
O
O
O
Se
7f
(CDCl3, 400 MHz)
1.05
1.10
2.09
2.21
3.16
5.01
2.05
1.14
1.00
0.99
1.00
9.0 8.5 8.0 7.5 7.0 6.5 6.0 5.5 5.0 4.5 4.0 3.5 3.0 2.5 2.0 1.5 1.0 0.5 0.0 -0.5

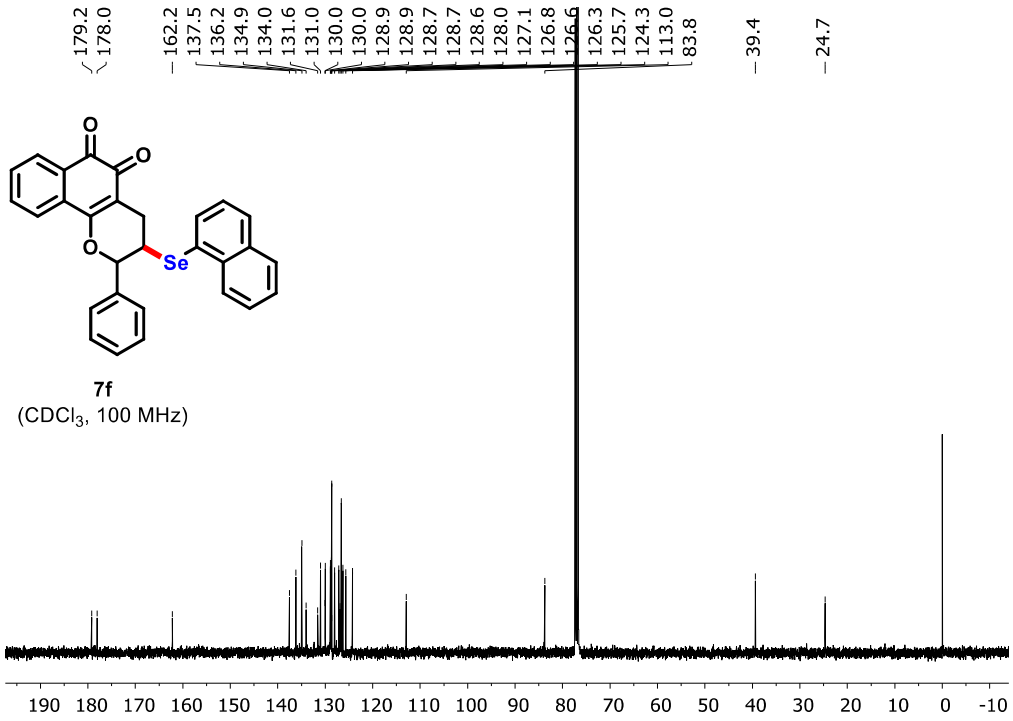
179.2
178.0
162.2
137.5
136.2
134.9
134.0
131.6
131.0
130.0
130.0
128.9
128.9
128.7
128.7
128.6
128.0
127.1
126.8
126.6
126.3
125.7
124.3
113.0
83.8
39.4
24.7
O
O
O
Se
7f
(CDCl3, 100 MHz)
190 180 170 160 150 140 130 120 110 100 90 80 70 60 50 40 30 20 10 0 -10

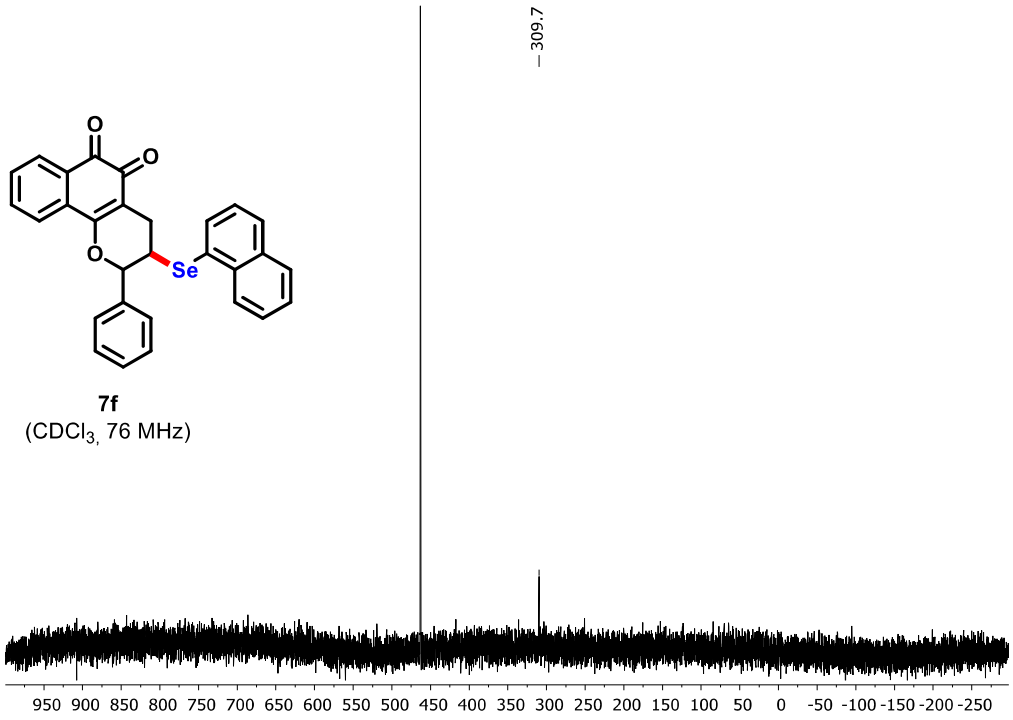
309.7
O
O
O
Se
7f
(CDCl3, 76 MHz)
950 900 850 800 750 700 650 600 550 500 450 400 350 300 250 200 150 100 50 0 -50 -100 -150 -200 -250

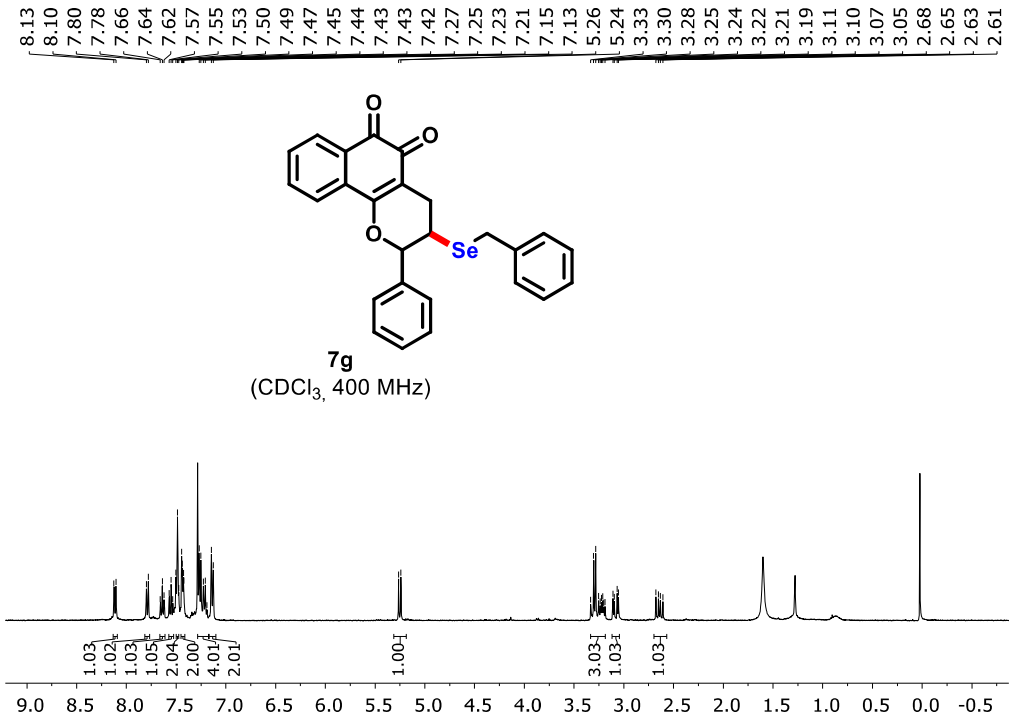
8.13
8.10
7.80
7.78
7.66
7.64
7.62
7.57
7.55
7.53
7.50
7.49
7.47
7.45
7.44
7.43
7.43
7.42
7.27
7.25
7.23
7.21
7.15
7.13
5.26
5.24
3.33
3.30
3.28
3.25
3.24
3.22
3.21
3.19
3.11
3.10
3.07
3.05
2.68
2.65
2.63
2.61
O
O
O
Se
7g
(CDCl3, 400 MHz)
1.03
1.02
1.03
1.05
2.04
2.00
4.01
2.01
1.00
3.03
1.03
1.03
9.0 8.5 8.0 7.5 7.0 6.5 6.0 5.5 5.0 4.5 4.0 3.5 3.0 2.5 2.0 1.5 1.0 0.5 0.0 -0.5

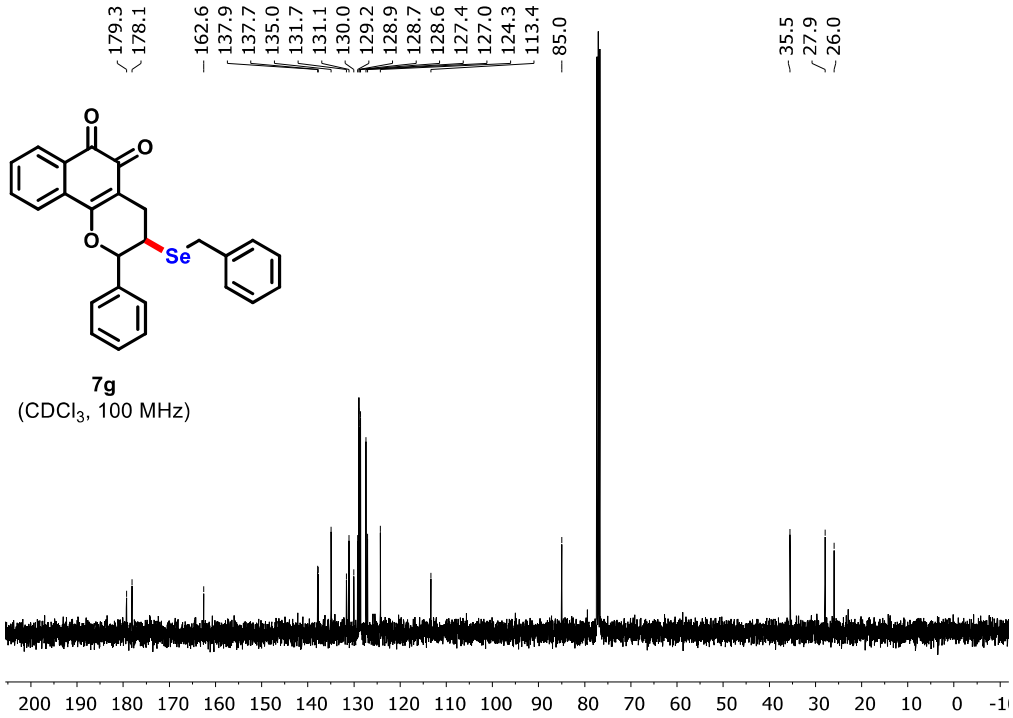
179.3
178.1
162.6
137.9
137.7
135.0
131.7
131.1
130.0
129.2
128.9
128.7
128.6
127.4
127.0
124.3
113.4
85.0
35.5
27.9
26.0
O
O
O
Se
7g
(CDCl3, 100 MHz)
200 190 180 170 160 150 140 130 120 110 100 90 80 70 60 50 40 30 20 10 0 -1

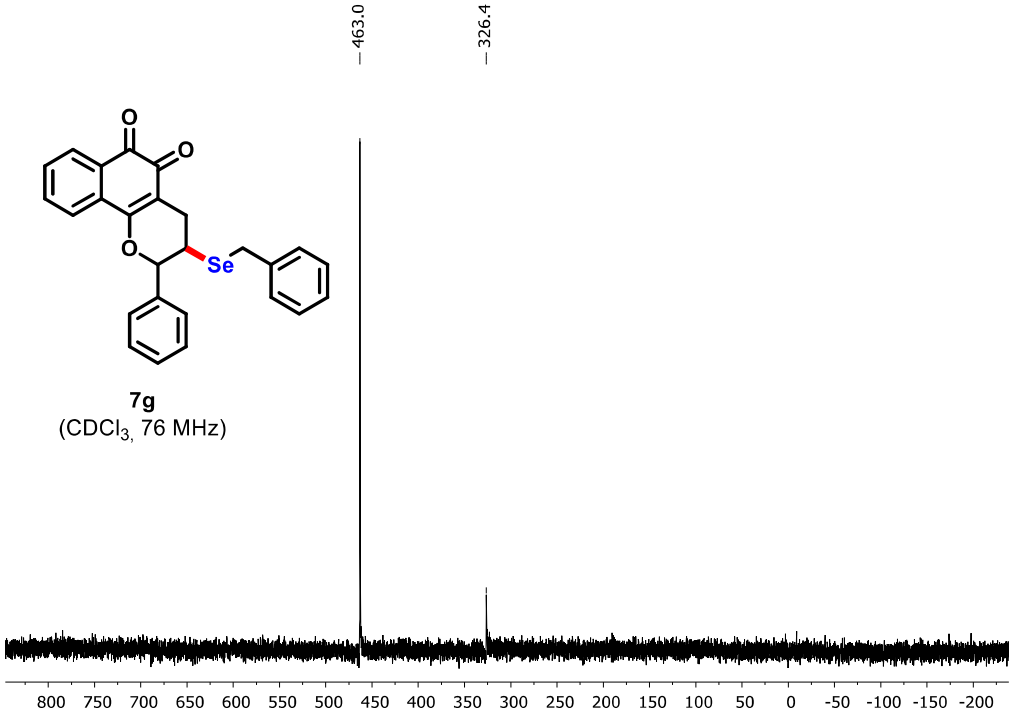

7g
($CDCl_3$, 76 MHz)

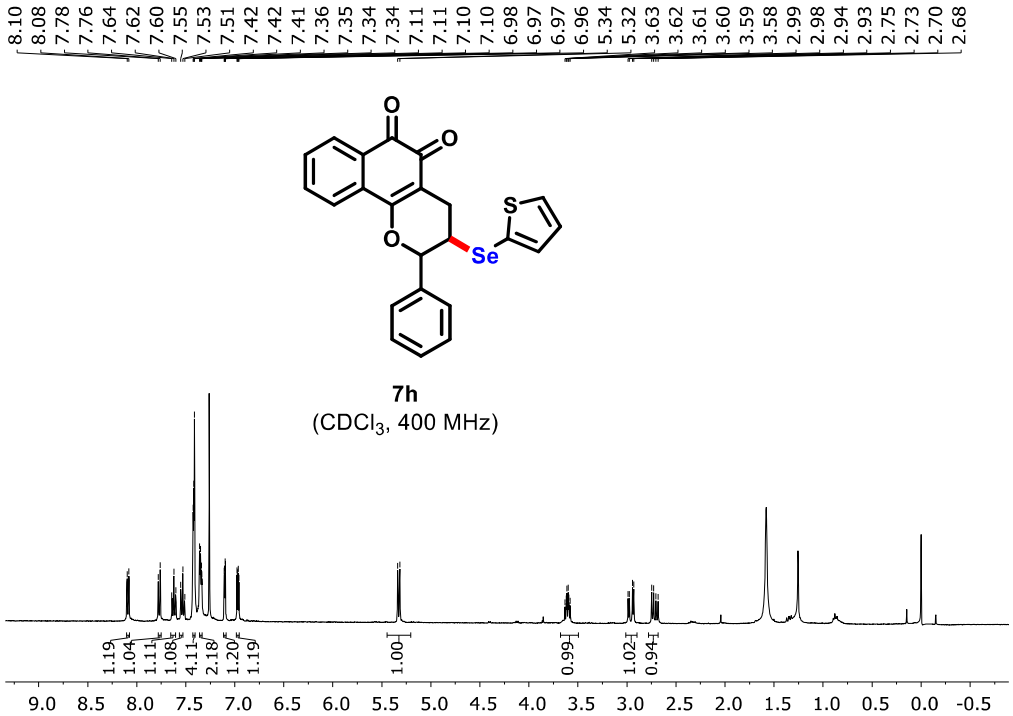

7h
($CDCl_3$, 400 MHz)

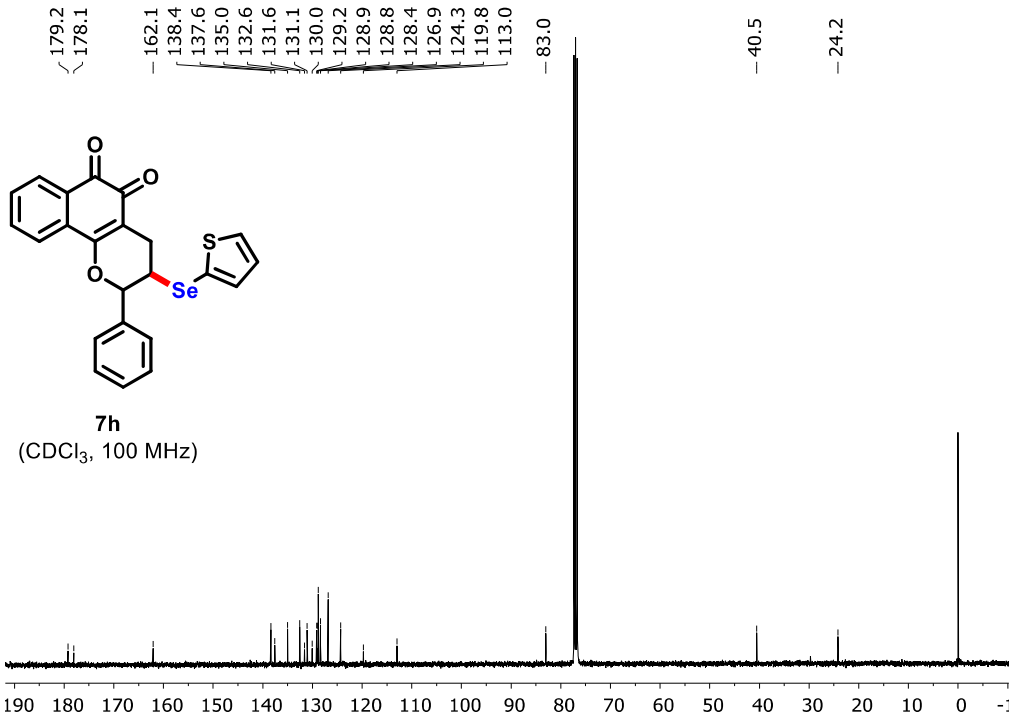

7h
($CDCl_3$, 100 MHz)

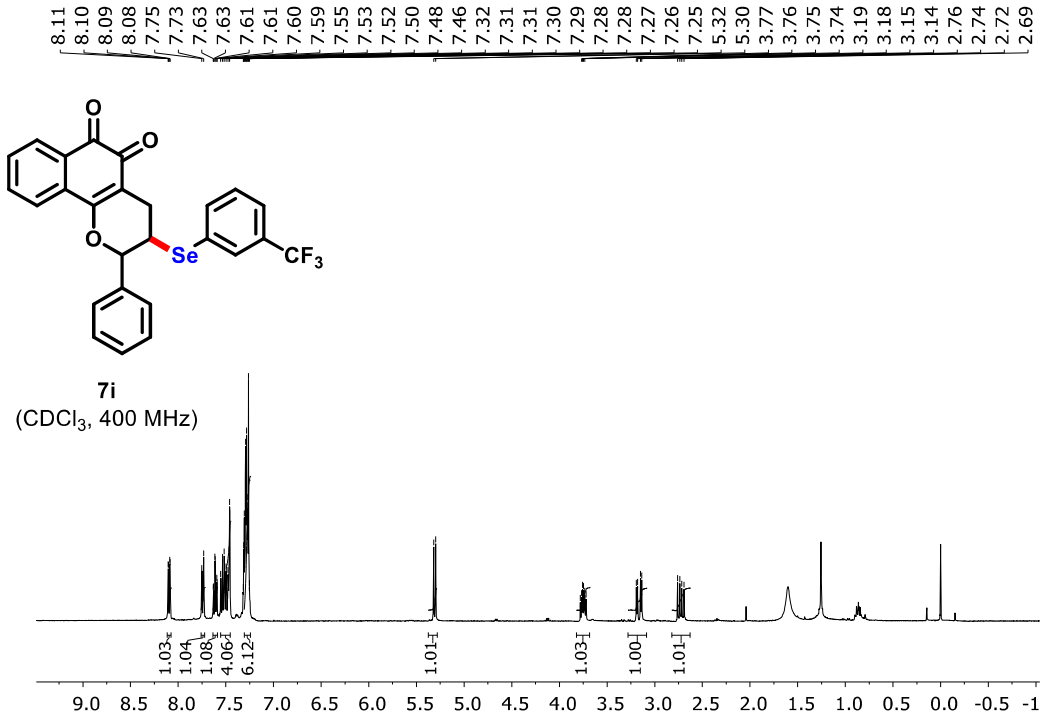

7i
($CDCl_3$, 400 MHz)

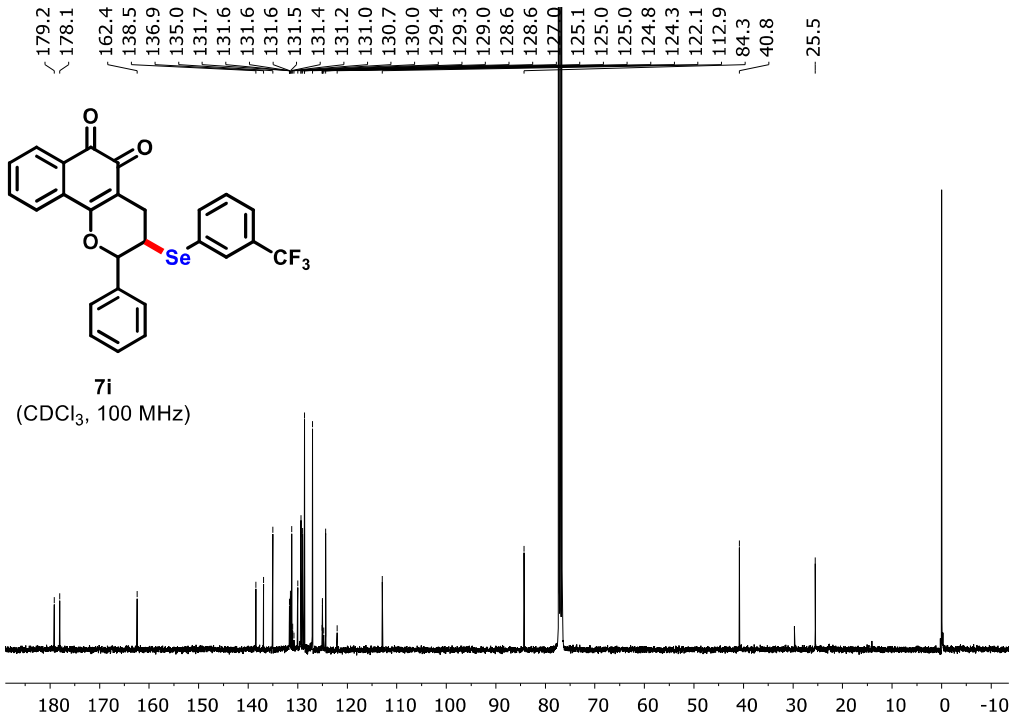
179.2
178.1
162.4
138.5
136.9
135.0
131.7
131.6
131.6
131.6
131.5
131.4
131.2
131.0
130.7
130.0
129.4
129.3
129.0
128.6
128.6
127.0
125.1
125.0
125.0
124.8
124.3
122.1
112.9
84.3
40.8
25.5
O
O
O
Se
CF3
7i
(CDCl3, 100 MHz)
180 170 160 150 140 130 120 110 100 90 80 70 60 50 40 30 20 10 0 -10

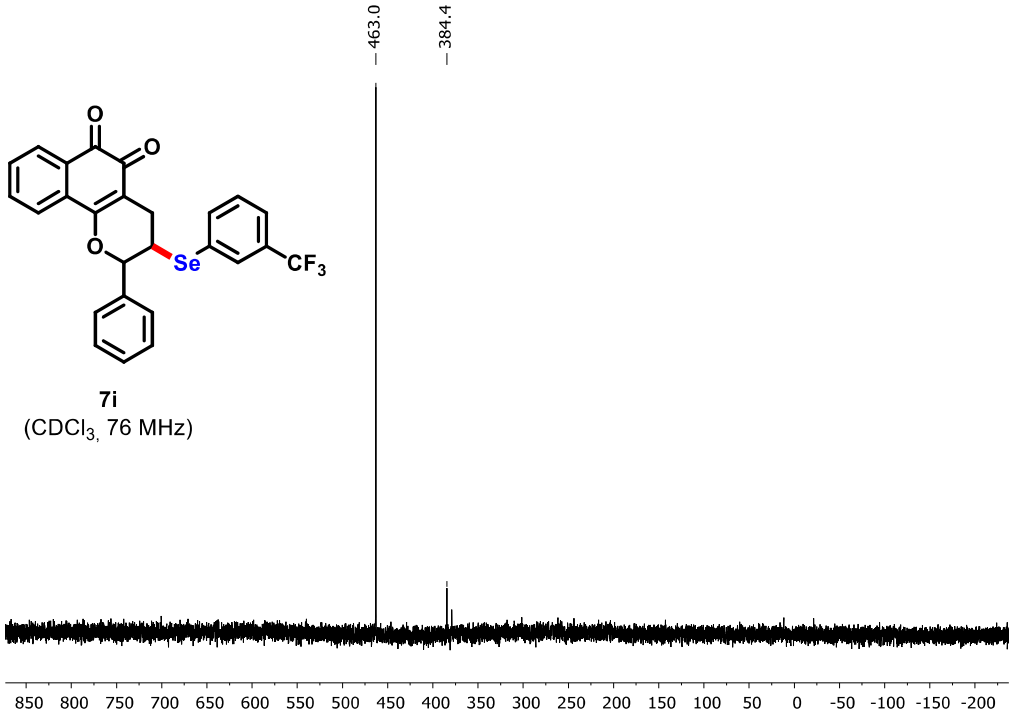
463.0
384.4
O
O
O
Se
CF3
7i
(CDCl3, 76 MHz)
850 800 750 700 650 600 550 500 450 400 350 300 250 200 150 100 50 0 -50 -100 -150 -200

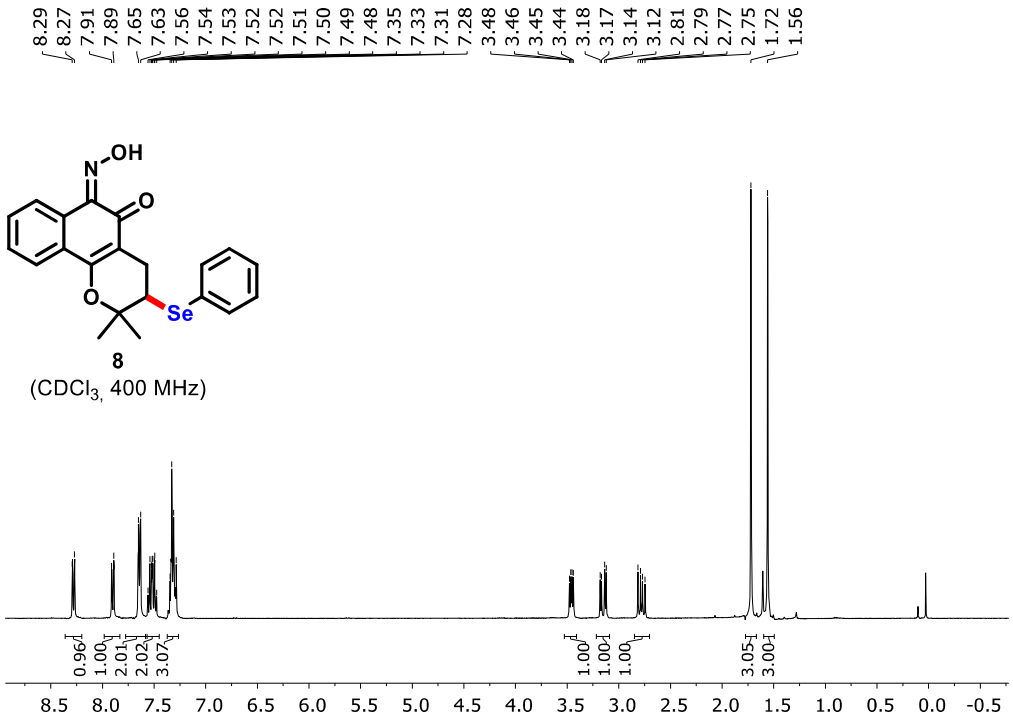
8.29
8.27
7.91
7.89
7.65
7.63
7.56
7.54
7.53
7.52
7.52
7.51
7.50
7.49
7.48
7.35
7.33
7.31
7.28
3.48
3.46
3.45
3.44
3.18
3.17
3.14
3.12
2.81
2.79
2.77
2.75
1.72
1.56
N-OH
O
O
Se
8
(CDCl3, 400 MHz)
0.96
1.00
2.01
2.02
3.07
1.00
1.00
1.00
3.05
3.00
8.5 8.0 7.5 7.0 6.5 6.0 5.5 5.0 4.5 4.0 3.5 3.0 2.5 2.0 1.5 1.0 0.5 0.0 -0.5

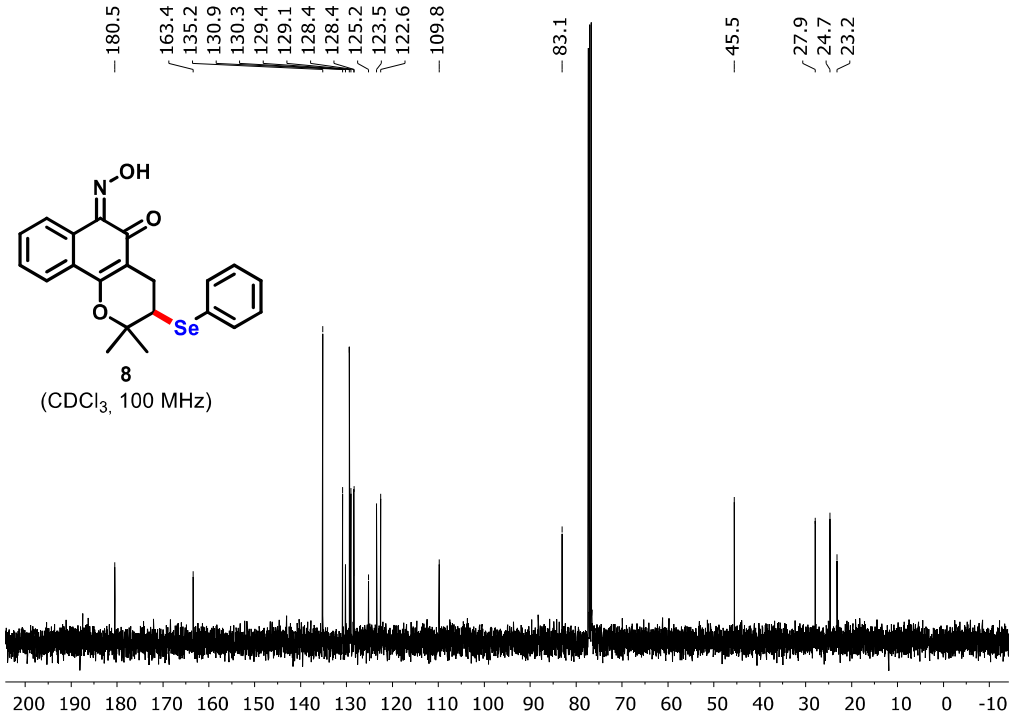
180.5
163.4
135.2
130.9
130.3
129.4
129.1
128.4
128.4
125.2
123.5
122.6
109.8
83.1
45.5
27.9
24.7
23.2
N-OH
O
O
Se
8
(CDCl3, 100 MHz)
200 190 180 170 160 150 140 130 120 110 100 90 80 70 60 50 40 30 20 10 0 -10

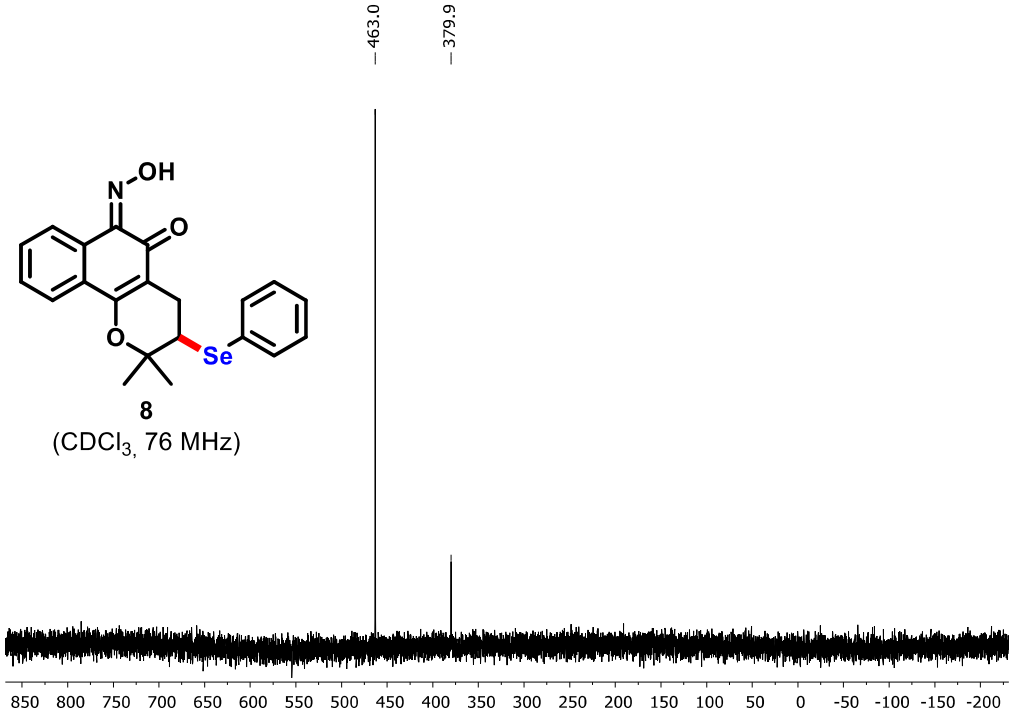
463.0
379.9
N
OH
O
O
Se
8
(CDCl3, 76 MHz)
850 800 750 700 650 600 550 500 450 400 350 300 250 200 150 100 50 0 -50 -100 -150 -200

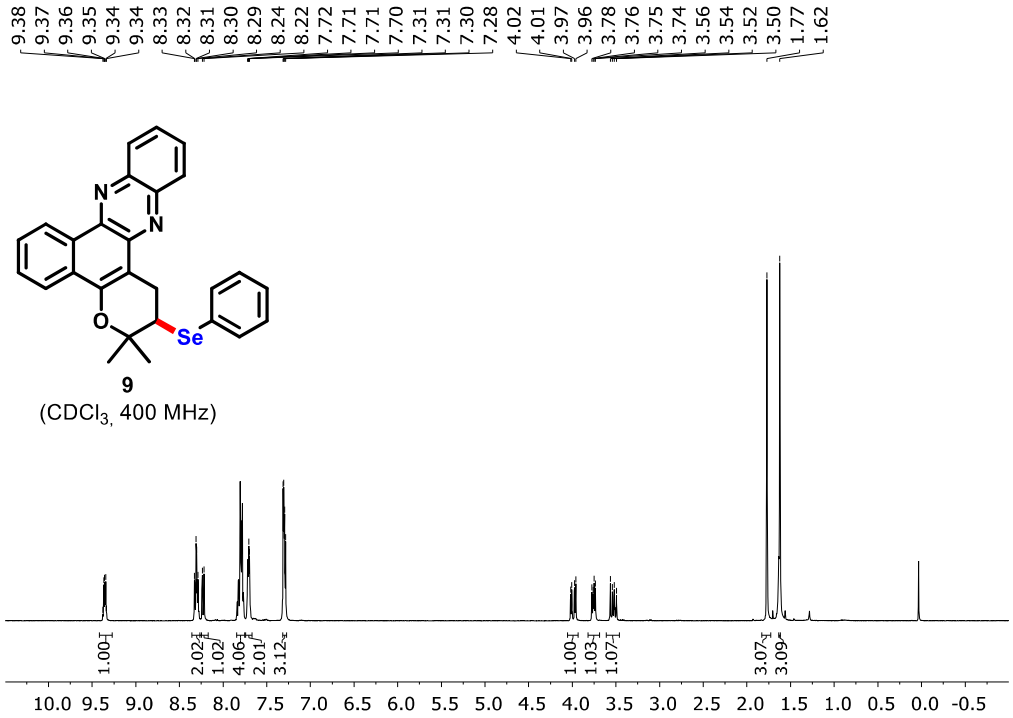
9.38 9.37 9.36 9.35 9.34 9.34 8.33 8.32 8.31 8.30 8.29 8.24 8.22 7.72 7.71 7.71 7.70 7.31 7.31 7.30 7.28 4.02 4.01 3.97 3.96 3.78 3.76 3.75 3.74 3.56 3.54 3.52 3.50 1.77 1.62
N
N
O
Se
9
(CDCl3, 400 MHz)
1.00 2.02 1.02 4.06 2.01 3.12 1.00 1.03 1.07 3.07 3.09
10.0 9.5 9.0 8.5 8.0 7.5 7.0 6.5 6.0 5.5 5.0 4.5 4.0 3.5 3.0 2.5 2.0 1.5 1.0 0.5 0.0 -0.5

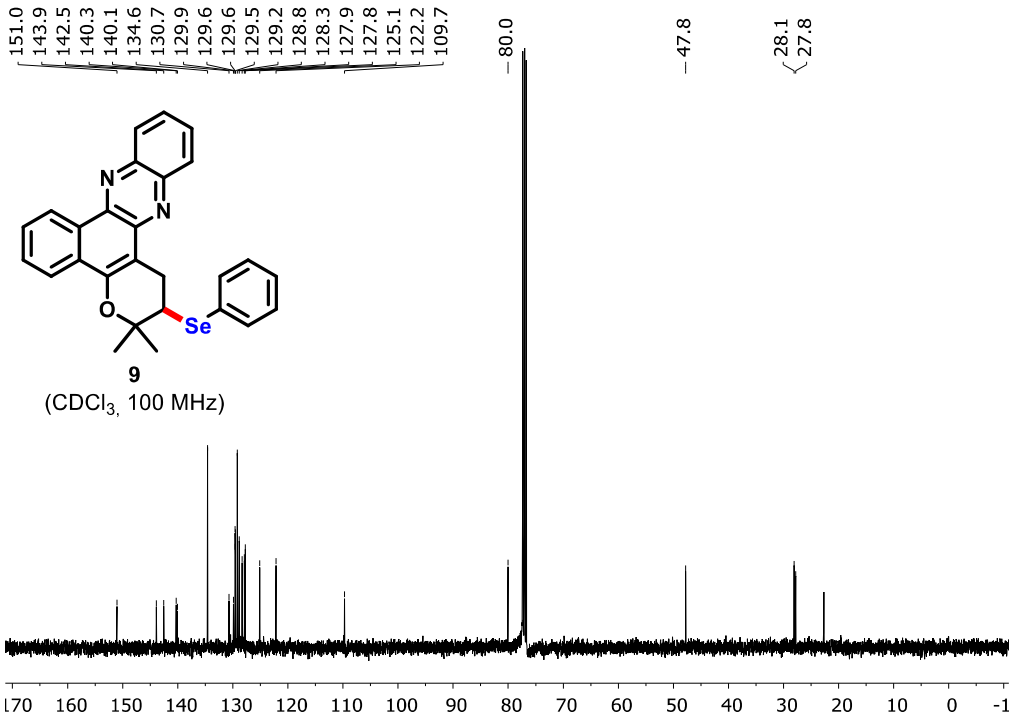
151.0
143.9
142.5
140.3
140.1
134.6
130.7
129.9
129.6
129.6
129.5
129.2
128.8
128.3
127.9
127.8
125.1
122.2
109.7
80.0
47.8
28.1
27.8
N
N
O
Se
9
(CDCl3, 100 MHz)
170 160 150 140 130 120 110 100 90 80 70 60 50 40 30 20 10 0 -1

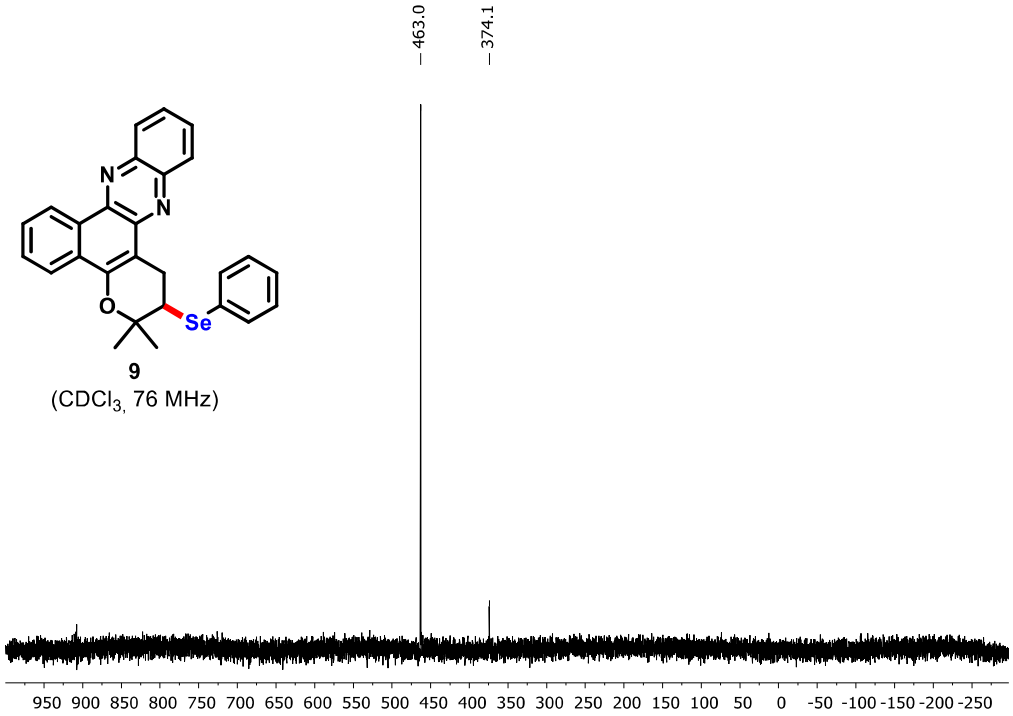
463.0
374.1
N
N
O
Se
9
(CDCl3, 76 MHz)
950 900 850 800 750 700 650 600 550 500 450 400 350 300 250 200 150 100 50 0 -50 -100 -150 -200 -250

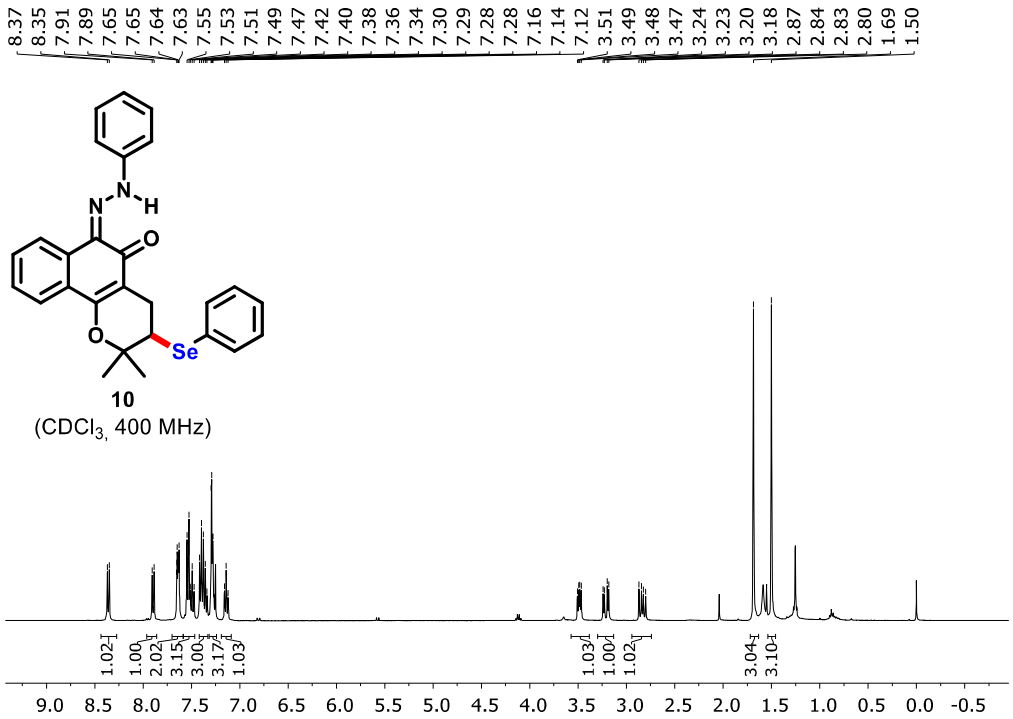
8.37
8.35
7.91
7.89
7.65
7.65
7.64
7.63
7.55
7.53
7.51
7.49
7.47
7.42
7.40
7.38
7.36
7.34
7.30
7.29
7.28
7.28
7.16
7.14
7.12
3.51
3.49
3.48
3.47
3.24
3.23
3.20
3.18
2.87
2.84
2.83
2.80
1.69
1.50
N
N
H
O
O
Se
10
(CDCl3, 400 MHz)
1.02
1.00
2.02
3.15
3.00
3.17
1.03
1.03
1.00
1.02
3.04
3.10
9.0 8.5 8.0 7.5 7.0 6.5 6.0 5.5 5.0 4.5 4.0 3.5 3.0 2.5 2.0 1.5 1.0 0.5 0.0 -0.5

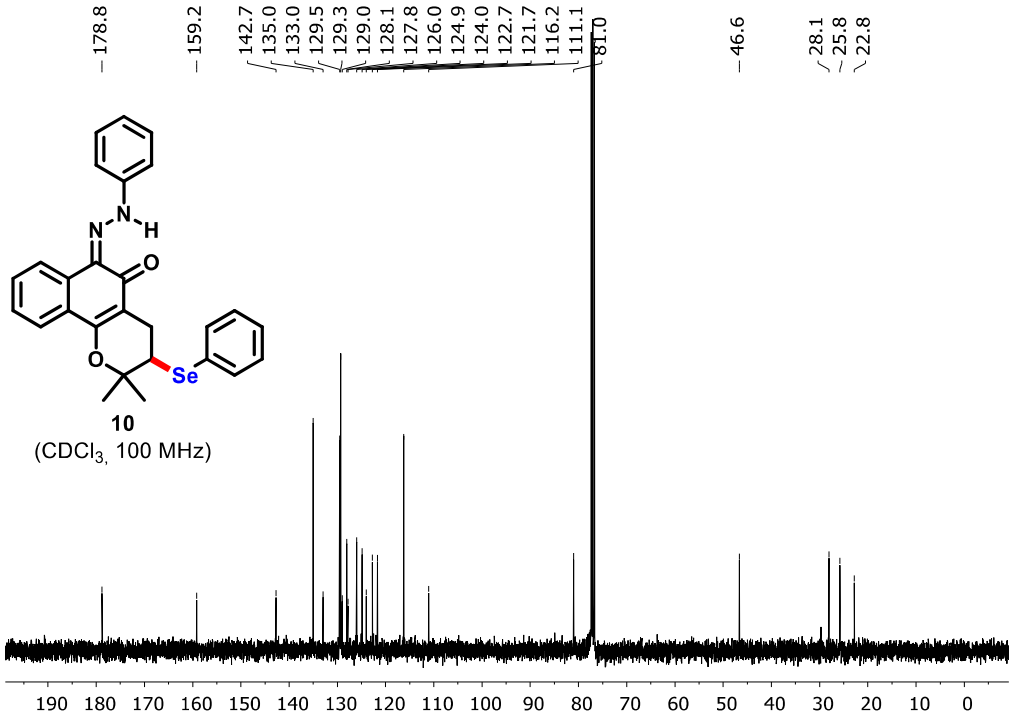
178.8
159.2
142.7
135.0
133.0
129.5
129.3
129.0
128.1
127.8
126.0
124.9
124.0
122.7
121.7
116.2
111.1
81.0
46.6
28.1
25.8
22.8
N
N
H
O
O
Se
10
(CDCl3, 100 MHz)
190 180 170 160 150 140 130 120 110 100 90 80 70 60 50 40 30 20 10 0

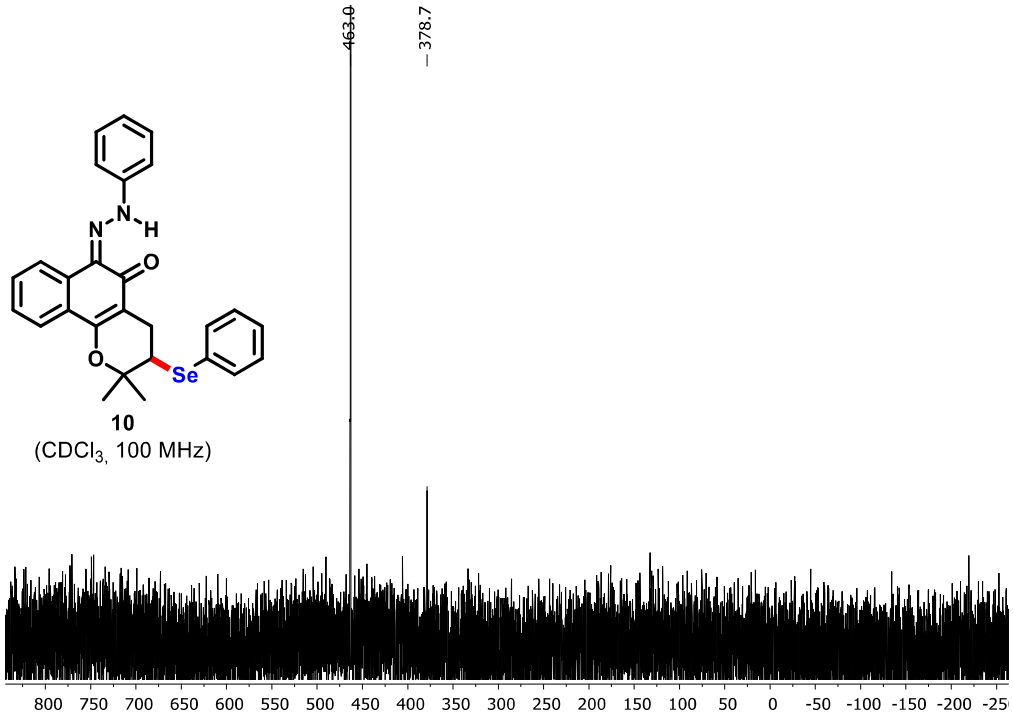
463.0
378.7
N
N
H
O
O
Se
10
(CDCl3, 100 MHz)
800 750 700 650 600 550 500 450 400 350 300 250 200 150 100 50 0 -50 -100 -150 -200 -25

7.2. Supplementary Material for Publication 2: Release of reactive selenium species from phthalic selenoanhydride in the presence of hydrogen sulfide and glutathione with implications for cancer research

Electronic Supplementary Information – New Journal of Chemistry

Release of Reactive Selenium Species from phthalic selenoanhydride in the presence of hydrogen sulfide and glutathione with implications for cancer research

Received 00th January 20xx,
Accepted 00th January 20xx

DOI: 10.1039/x0xx00000x

Ammar Kharma[a,b], Anton Misak[a], Marian Grman[a], Vlasta Brezova[c], Lucia Kurakova[d], Peter Baráth[e], Claus Jacob[b], Miroslav Chovanec[f], Karol Ondrias[a] and Enrique Domínguez-Álvarez*[g]

General procedure for the synthesis of chalcogen anhydrides

The phthalic selenoanhydride (R-Se) and the phthalic thioanhydride (R-S) have been synthetized following a modification of a procedure previously described[1,2]. Briefly, a suspension of grey selenium (7.0 mmol) for R-Se or elemental sulfur for R-S (7.0 mmol) in water-free tetrahydrofuran is reduced by a dropwise addition of lithium aluminium hydride (7 mL of a 1M solution in tetrahydrofuran). After the completion of the reaction (easily monitored thanks to the ceasing of the generation of molecular hydrogen), 1.41 g (6.9 mmol) of phthaloyl chloride solved in 20 mL of dichlorometane is added to the reaction. The mixture is left reacting 1 h at 50ºC with magnetic stirring). Then, the solution is filtered to eliminate the metallic salts generated during the process, and over the filtrate, 10 mL of concentrated sulfuric acid are added dropwise during 5 min. The solid is filtered and washed with chloroform (4×15 mL). The evaporation of the organic layer allowed the isolation of the impure desired product.

Synthesis of R-Se

Elemental grey selenium (1.10 g, 7.0 mmol), 1 M solution of lithium aluminium hydride (7 mL, 7.0 mmol), phthaloyl chloride (1.41 g, 6.9 mmol) and concentrated sulphuric acid (10 mL) were employed. 1-benzo[*c*]selenophene-1,3-dione (R-Se) was obtained as a brown solid that was recrystallized from hexane to isolate a light orange/yellow solid. Yield: 80% (1160 mg). ^{1}H NMR (400 MHz, $CDCl_3$) δ: 7.96 (dd, 2H, H_3+H_6, J_1 = 5.7 Hz, J_2 = 3.2 Hz,); 7.76 (dd, 2H, H_4+H_5). ^{13}C NMR (100 MHz, $CDCl_3$) δ: 123.8 (C_3+C_6); 135.1 (C_1+C_2), 141.9 (C_4+C_5), 194.2 (COSeCO). LC/MS±: purity: 100.0%, tR = 6.49 min.

Synthesis of R-S

Elemental sulfur (0.45 g, 7.0 mmol), 1 M solution of lithium aluminium hydride (7 mL, 7.0 mmol), phthaloyl chloride (1.41 g, 6.9 mmol) and concentrated sulphuric acid (10 mL) were employed. 1-benzo[*c*]thiophene-1,3-dione (R-S) was obtained as a yellow solid that was recrystallized from hexane to isolate a light yellow solid. Yield: 84% (951 mg). ^{1}H NMR (400 MHz, $CDCl_3$) δ: 7.97 (dd, 2H, H_3+H_6, J_1 = 5.7 Hz, J_2 = 3.0 Hz,); 7.81 (dd, 2H, H_4+H_5). ^{13}C NMR (100 MHz, $CDCl_3$) δ: 123.9 (C_3+C_6); 135.2 (C_1+C_2), 138.9 (C_4+C_5), 190.0 (COSCO). LC/MS±: purity: 100.0%, tR = 5.84 min.

NMR and LC-MS data

In next pages are provided as images the ^{1}H NMR, the ^{13}C NMR and LC-MS spectra of R-Se and R-S. The spectroscopic results are in accordance with previously published data. The molecular ion is no visible, but it is also in accordance with previous results, its abundance is low in this structures.

Notes and references

1 E. Domínguez-Álvarez, D. Plano, M. Font, A. Calvo, C. Prior, C. Jacob, J.A. Palop and C. Sanmartín, *Eur J Med Chem*, 2014, **73**, 153-166.
2 Domínguez-Álvarez E. PhD Dissertation. University of Navarra (Spain), 2012.

[a] *Institute of Clinical and Translational Research, Biomedical Research Center of the Slovak Academy of Sciences, Dúbravská cesta 9, 845 05 Bratislava, Slovak Republic.*
[b] *Division of Bioorganic Chemistry, School of Pharmacy, Saarland University, Campus B2 1, D-66123 Saarbruecken, Germany.*
[c] *Faculty of Chemical and Food Technology, Slovak University of Technology, Radlinskeho 9, 812 37 Bratislava, Slovak Republic.*
[d] *Department of Pharmacology and Toxicology, Faculty of Pharmacy, Comenius University, Ulica Odbojárov 10, 832 32 Bratislava, Slovak Republic.*
[e] *Institute of Chemistry, Slovak Academy of Sciences, Dúbravská cesta 9, 845 38 Bratislava, Slovakia.*
[f] *Cancer Research Institute, Biomedical Research Center of the Slovak Academy of Sciences, Dúbravská cesta 9, 845 05 Bratislava, Slovak Republic.*
[g] *Instituto de Química Orgánica General, Consejo Superior de Investigaciones Científicas (IQOG, CSIC), Juan de la Cierva 3, 28006 Madrid, Spain.*
Electronic Supplementary Information (ESI) available: [details of any supplementary information available should be included here]. See DOI: 10.1039/x0xx00000x

^{1}H NMR of R-Se and R-S

R-Se (1H NMR)

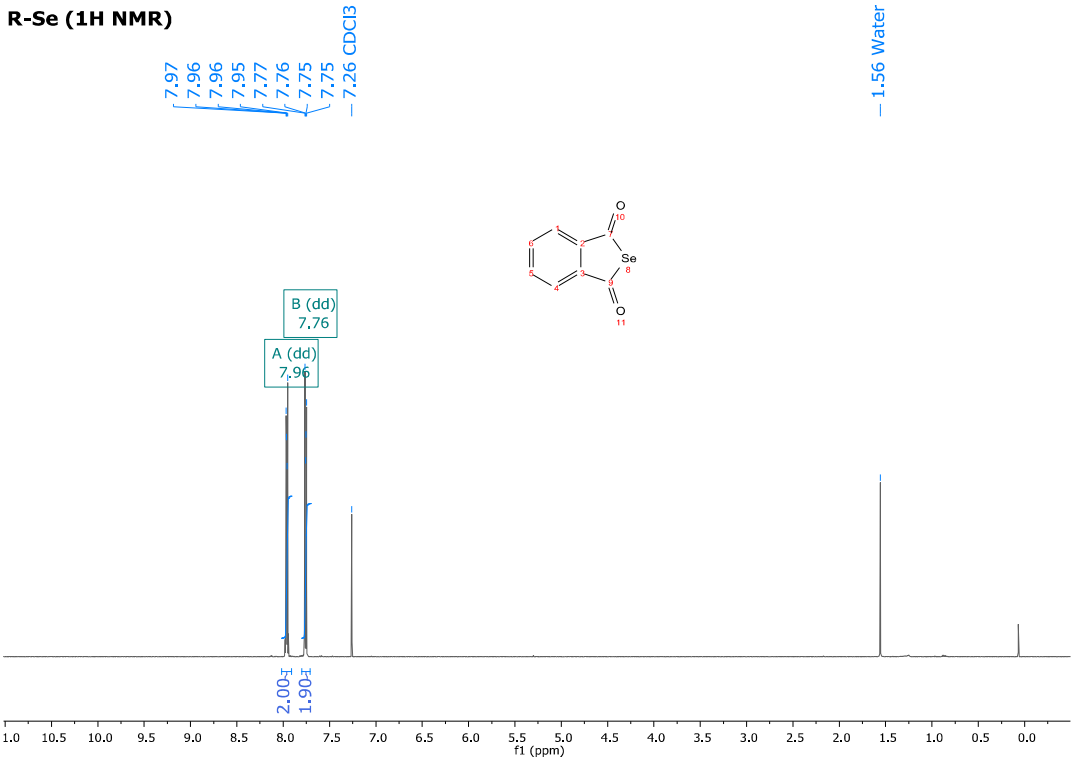

R-Se (1H NMR, Zoom)

R-S (1H NMR)

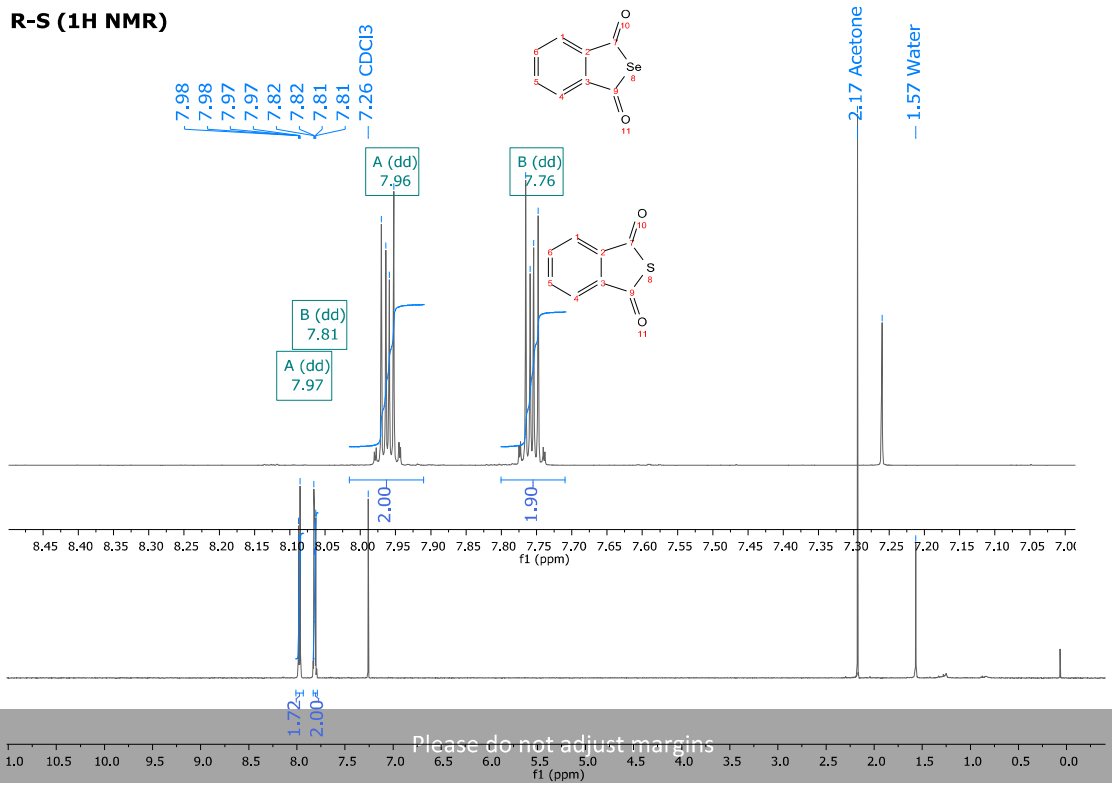

R-S (1H NMR, Zoom)

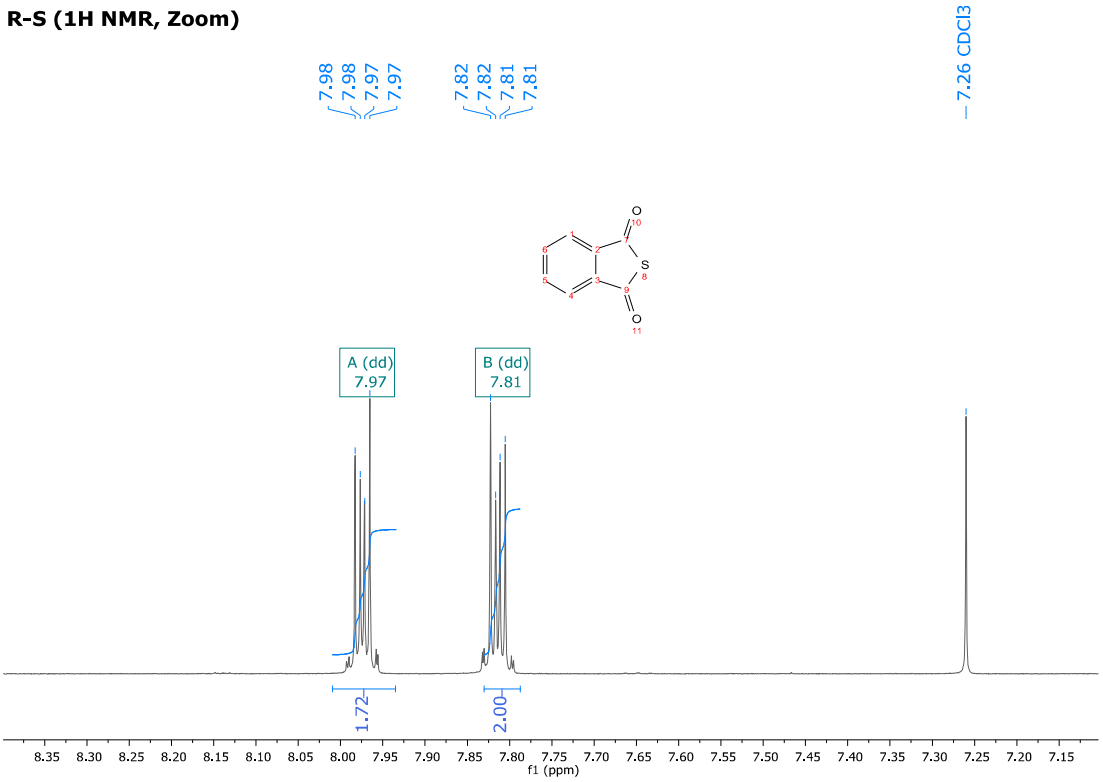

^{13}C NMR of R-Se and R-S

R-Se (13C NMR)

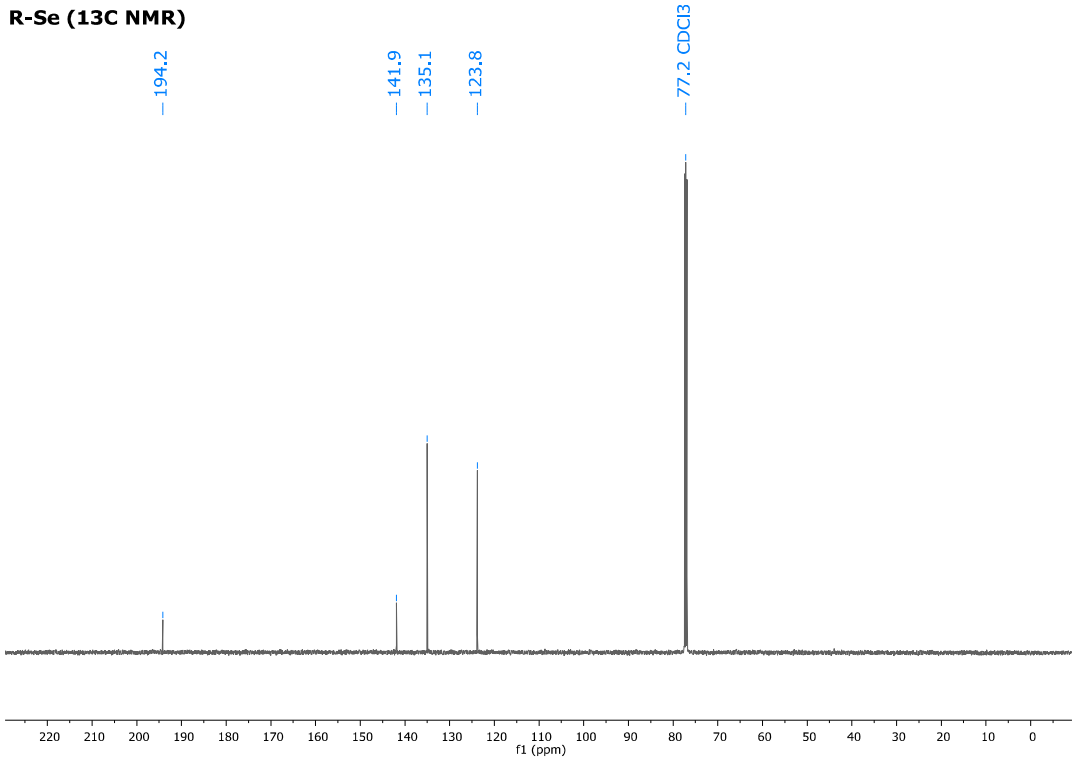

R-S (13C NMR)

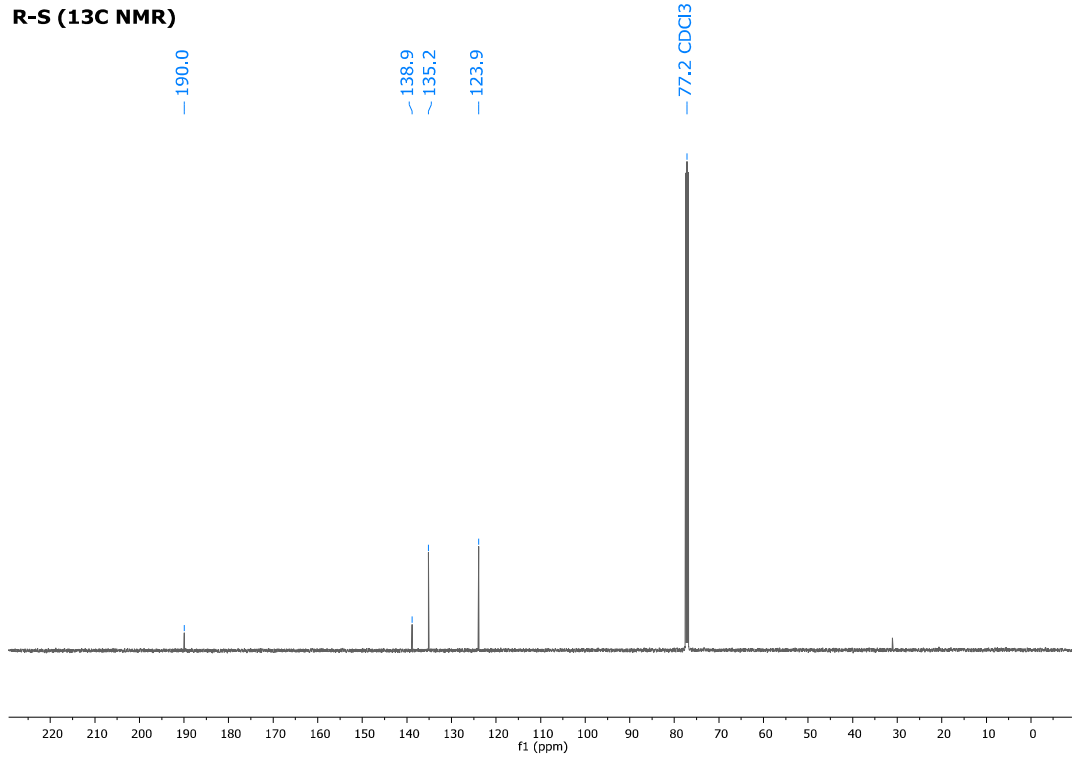

LC-MS of R-Se

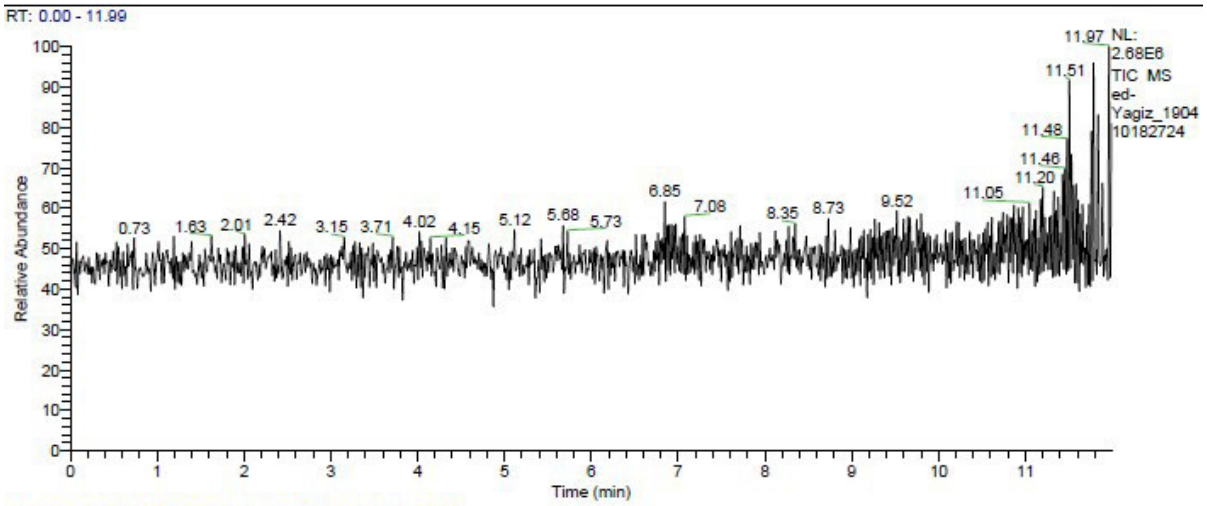

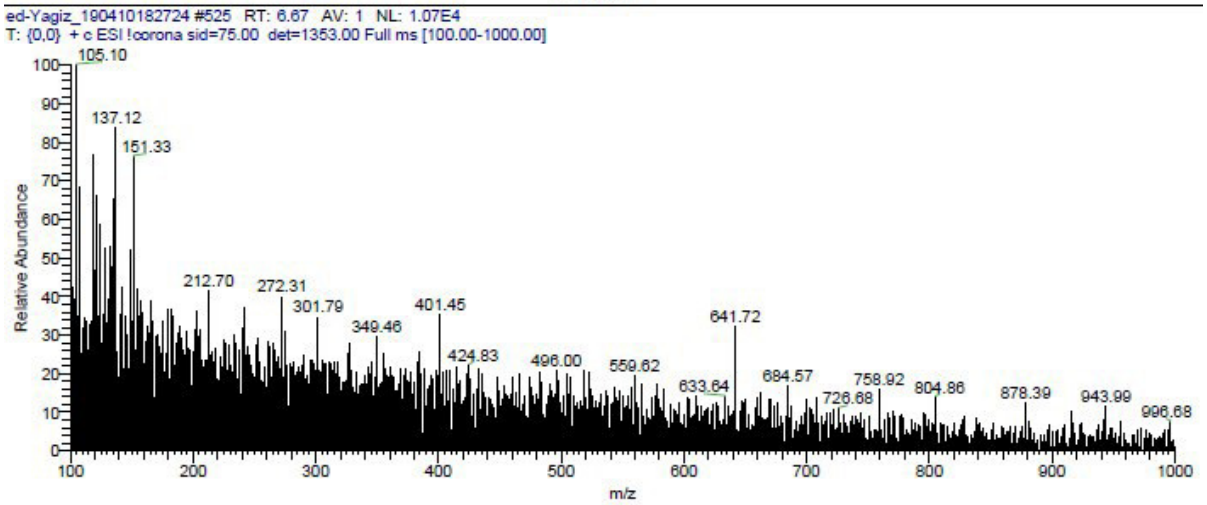

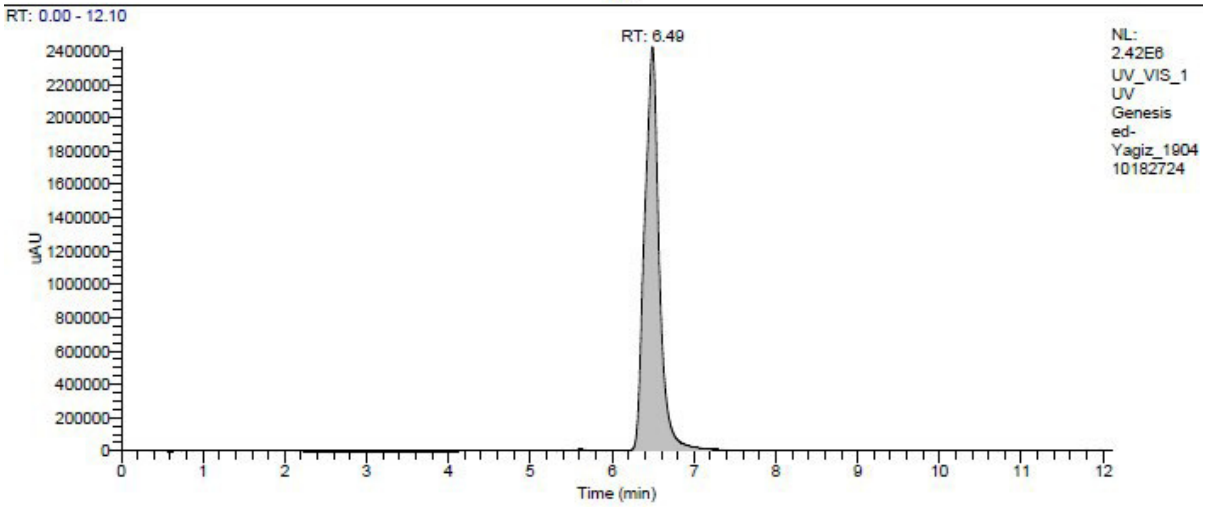

LC-MS of R-S

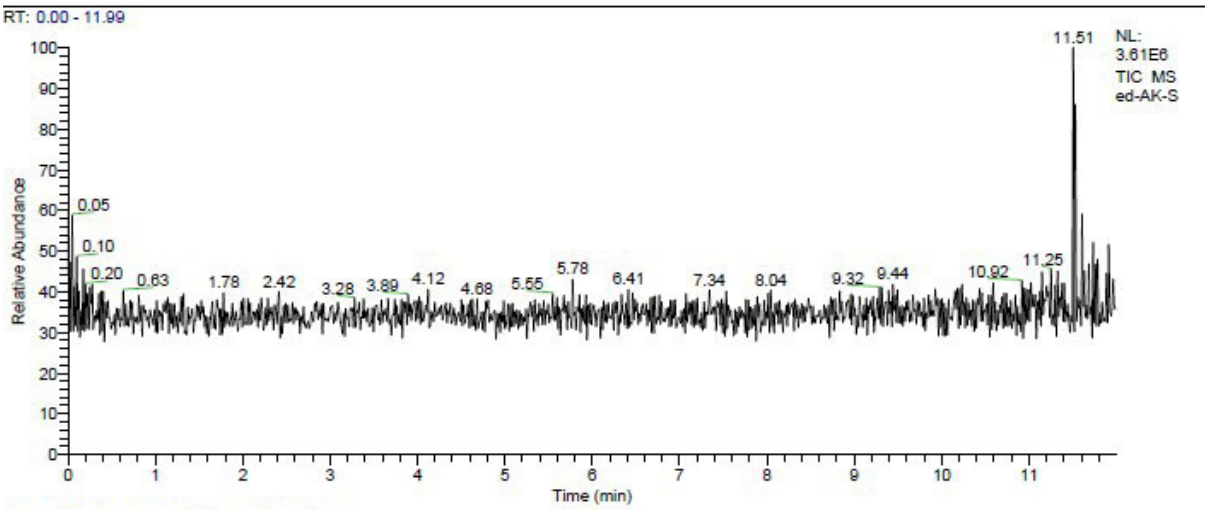

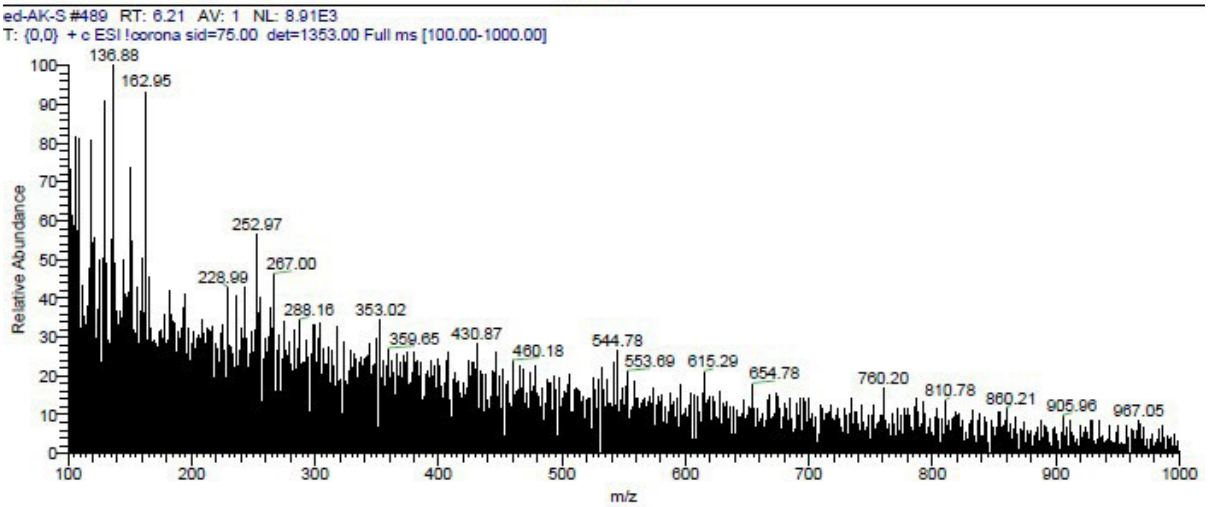

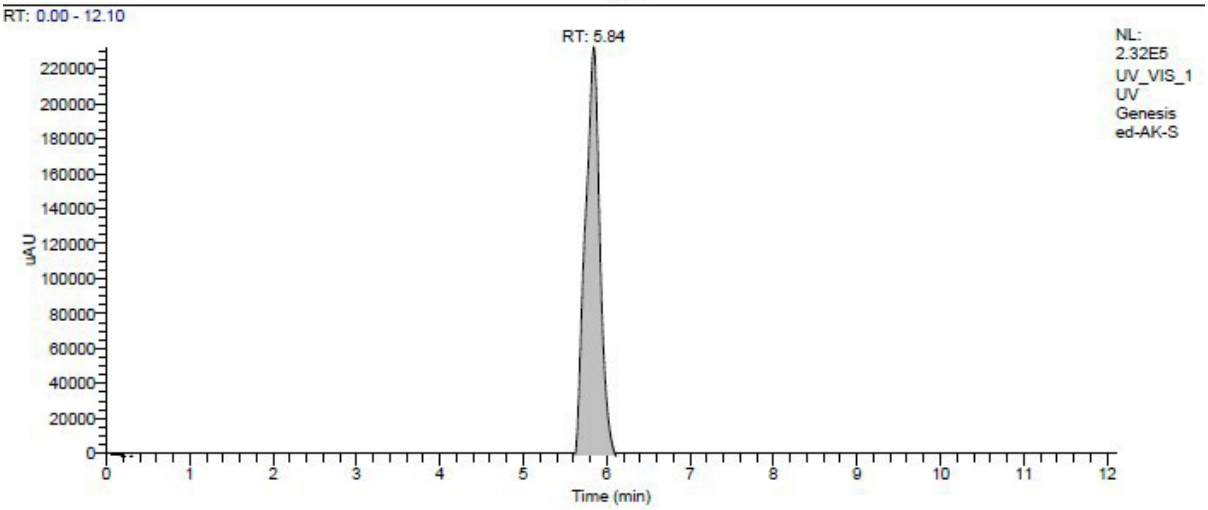

7.3. Supplementary Material for Publication 3: Synthesis of quinone imine and sulphur containing-compounds with antitumor and trypanocidal activities: redox and biological implications

Electronic Supplementary Information

Synthesis of quinone imine and sulphur-containing compounds with antitumor and trypanocidal activities: Redox and biological implications

Renata G. Almeida,[a1] Wagner O. Valença,[a,b1] Luisa G. Rosa,[a] Carlos A. de Simone,[c] Solange L. de Castro,[d] Juliana M. C. Barbosa,[d] Daniel P. Pinheiro,[e] Carlos R. K. Paier,[e] Guilherme G. C. de Carvalho,[e] Claudia Pessoa,[e] Marilia O. F. Goulart,[f] Ammar Kharma,[a,g] and Eufrânio N. da Silva Júnior[a]*

[a]Institute of Exact Sciences, Department of Chemistry, Federal University of Minas Gerais, Belo Horizonte, 31270-901, MG, Brazil; [b]Center for the Development of Chemical Technologies, State University of Mato Grosso do Sul, Naviraí, 79950-000, MS, Brasil; [c]Department of Physics and Informatics, Institute of Physics, University of São Paulo, São Carlos, 13560-160, SP, Brazil; [d]Oswaldo Cruz Institute, FIOCRUZ, Rio de Janeiro, 21045-900, RJ, Brazil; [e]Department of Physiology and Pharmacology, Federal University of Ceará, Fortaleza, CE, 60430-270, Brazil; [f]Institute of Chemistry and Biotechnology, Federal University of Alagoas, CEP 57072-970, Maceió, AL, Brazil; [g]Division of Bioorganic Chemistry, School of Pharmacy, University of Saarland D-66123 Saarbruecken, Germany.

E-mail: eufranio@ufmg.br

[1]*These authors contributed equally to this work*

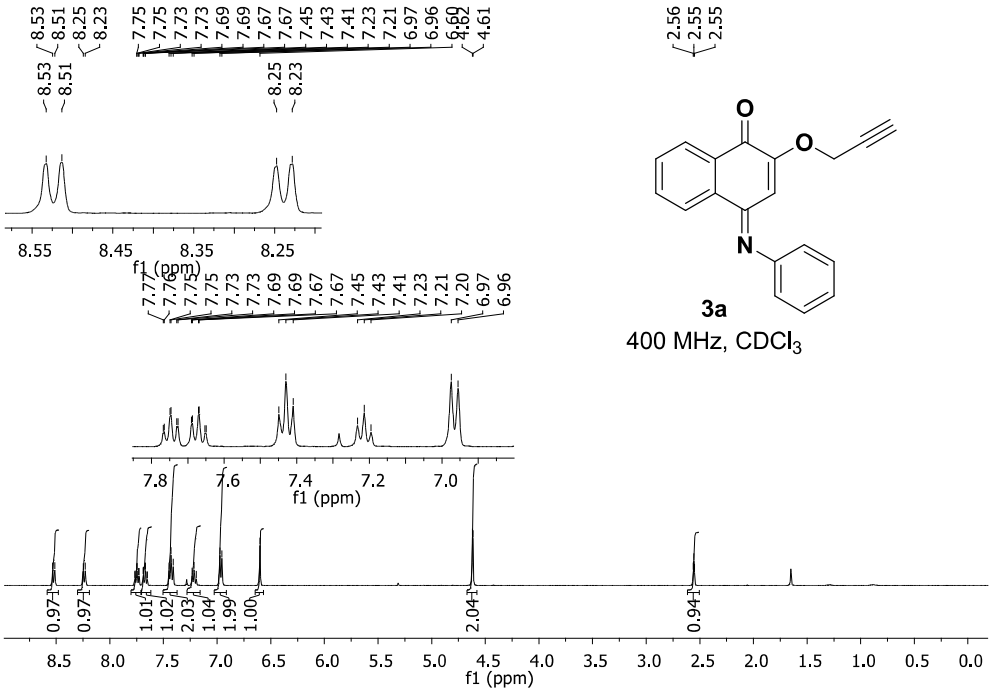

Figure S1. ^{1}H NMR spectrum (400 MHz, $CDCl_3$) of compound **3a**.

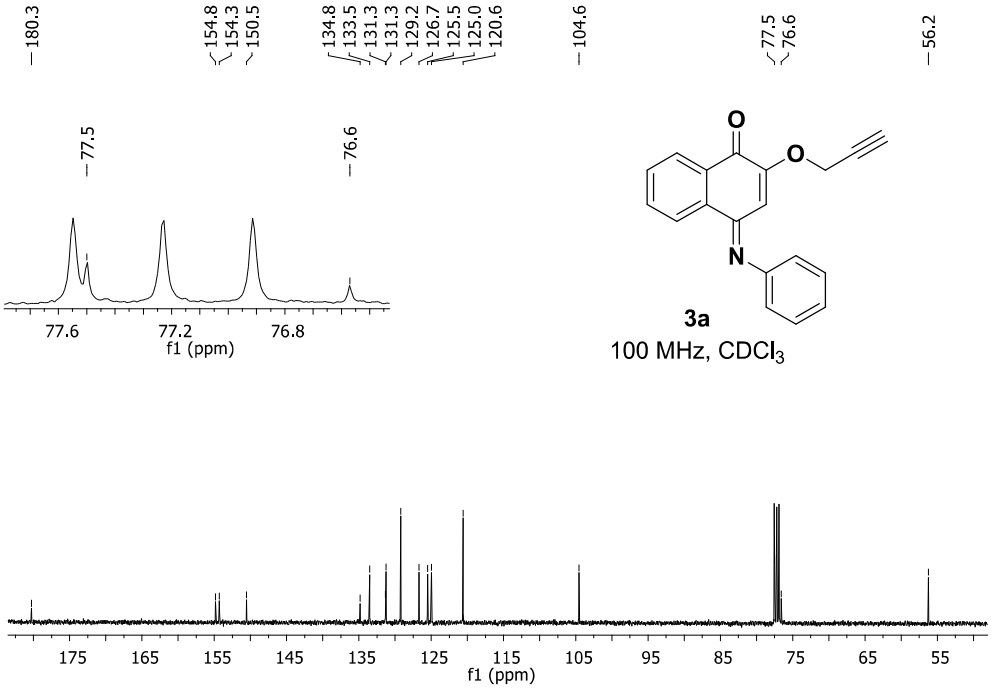

Figure S2. ^{13}C NMR spectrum (100 MHz, $CDCl_3$) of compound **3a**.

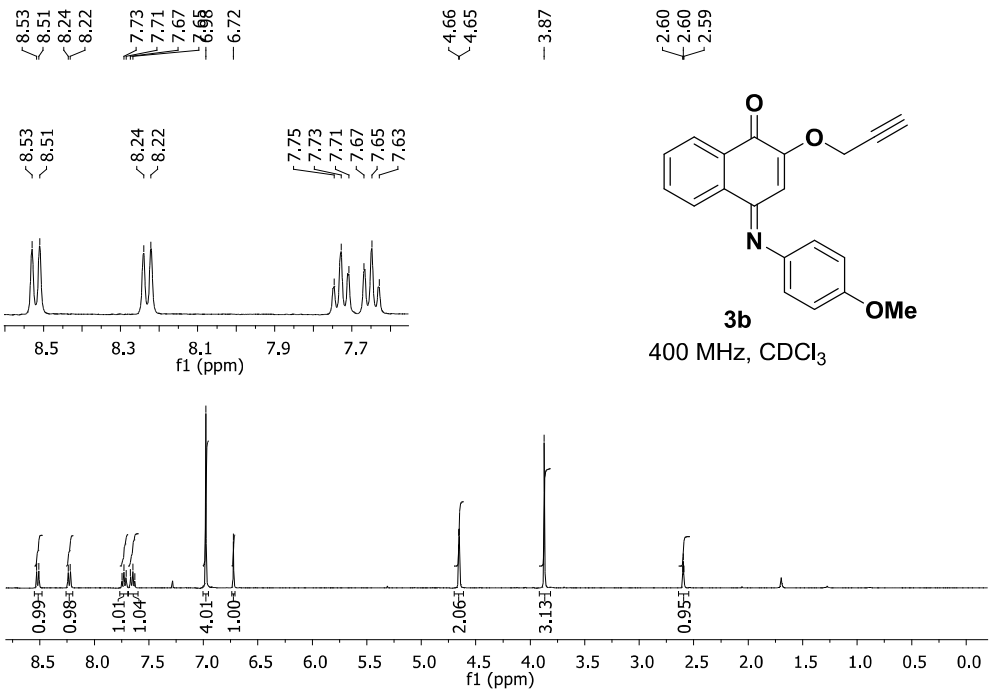

Figure S3. ^{1}H NMR spectrum (400 MHz, $CDCl_3$) of compound **3b**.

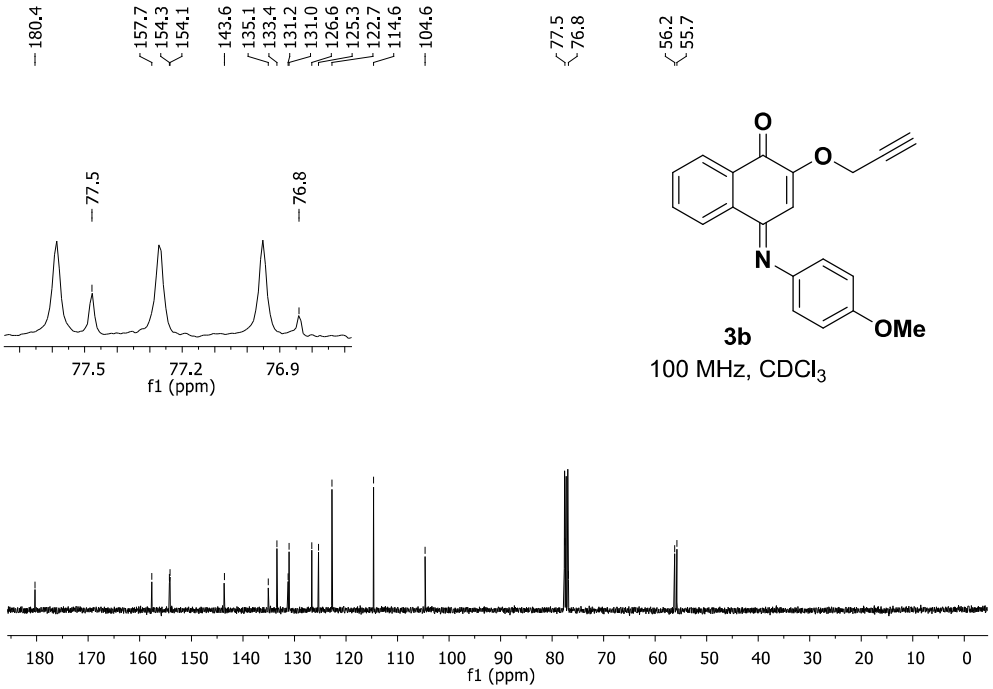

Figure S4. ^{13}C NMR spectrum (100 MHz, $CDCl_3$) of compound **3b**.

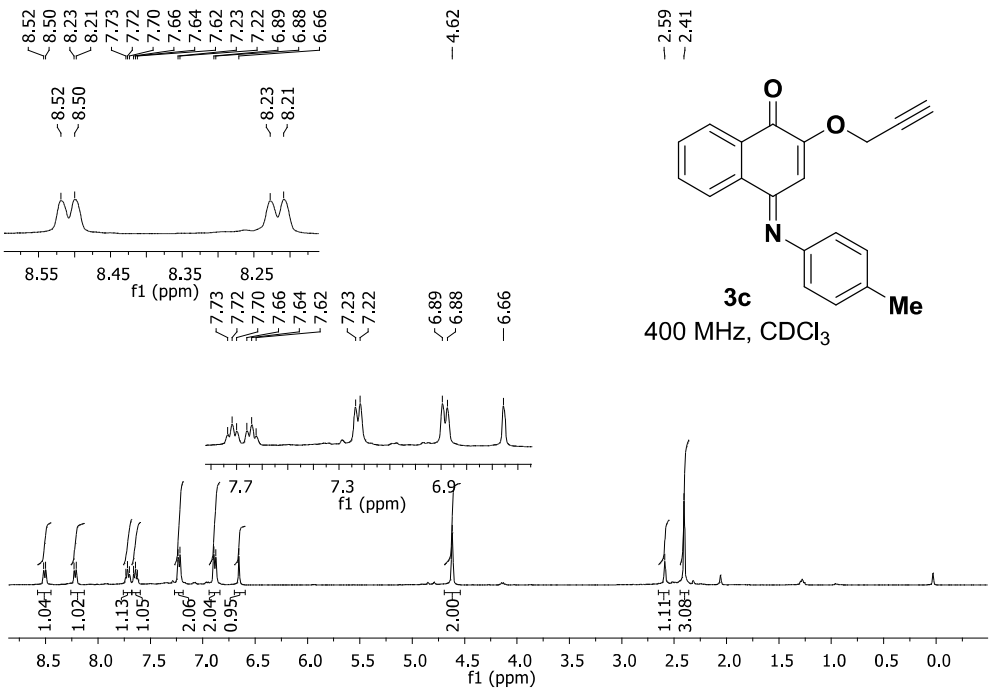

Figure S5. ^{1}H NMR spectrum (400 MHz, $CDCl_3$) of compound **3c**.

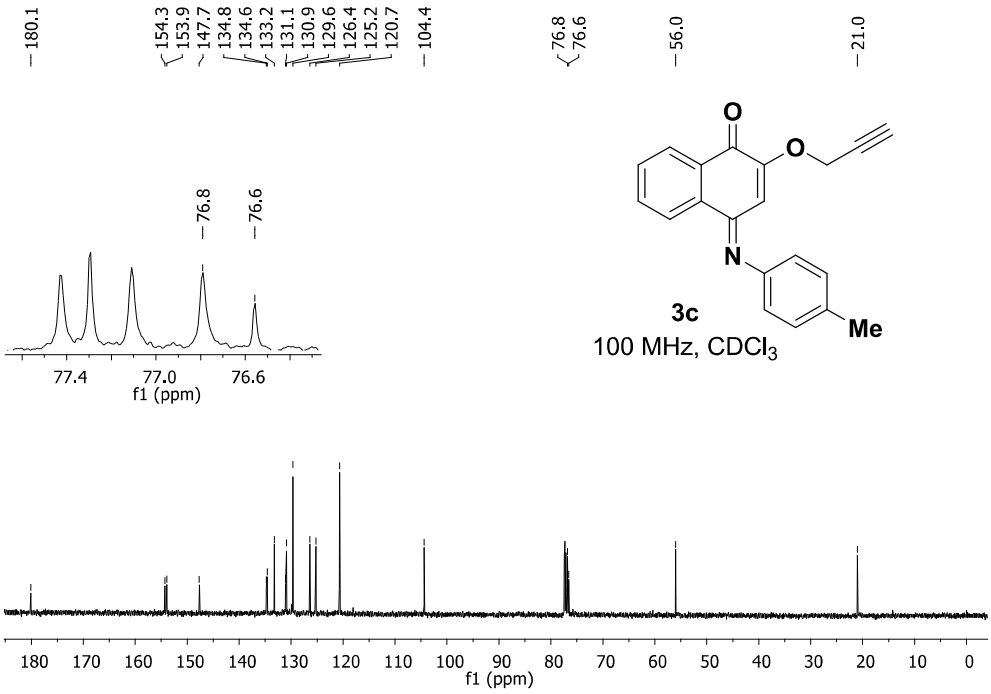

Figure S6. ^{13}C NMR spectrum (100 MHz, $CDCl_3$) of compound **3c**.

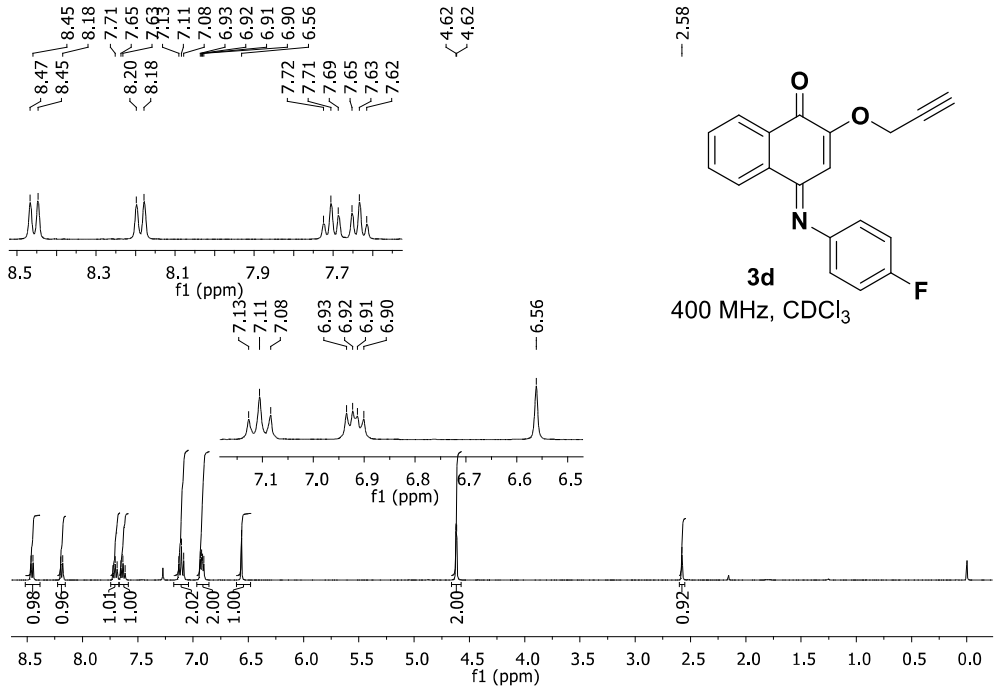

Figure S7. ^{1}H NMR spectrum (400 MHz, $CDCl_3$) of compound **3d**.

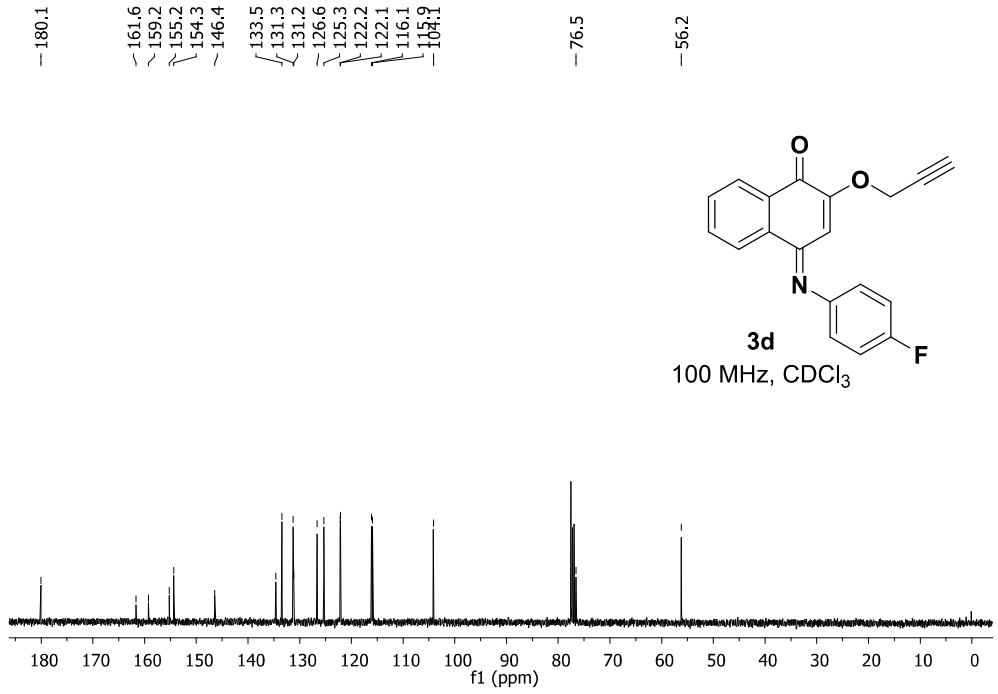

Figure S8. ^{13}C NMR spectrum (100 MHz, $CDCl_3$) of compound **3d**.

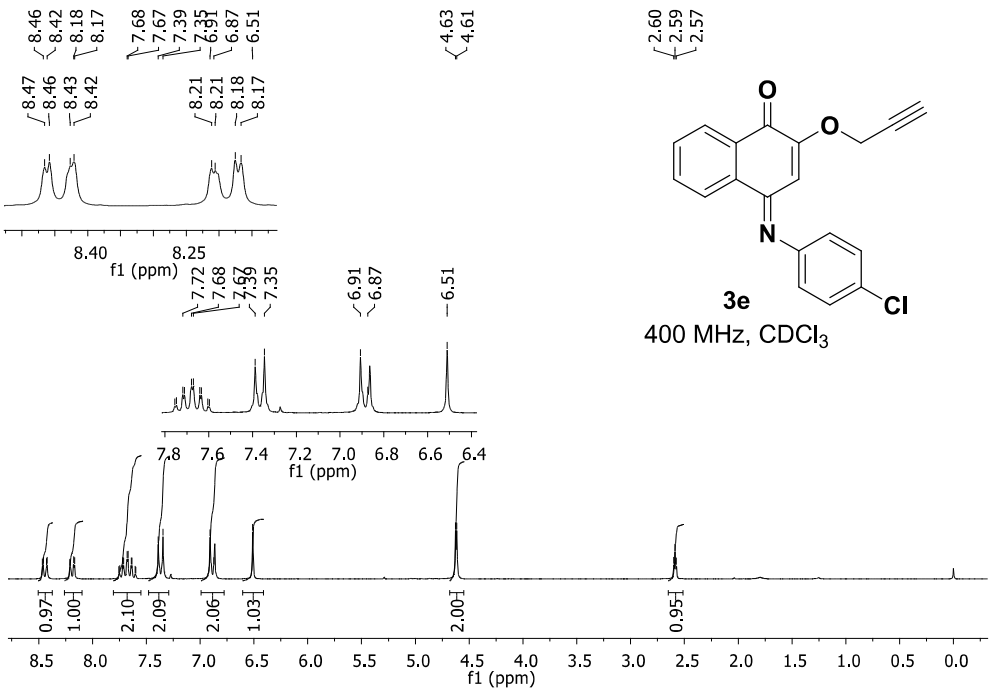

Figure S9. ^{1}H NMR spectrum (400 MHz, $CDCl_3$) of compound **3e**.

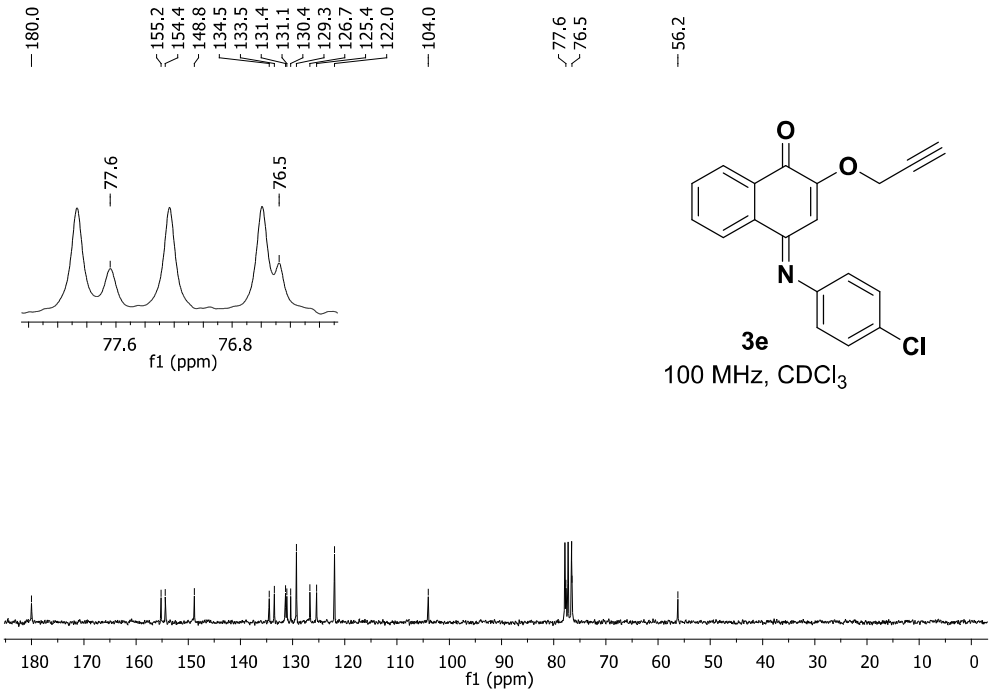

Figure S10. ^{13}C NMR spectrum (100 MHz, $CDCl_3$) of compound **3e**.

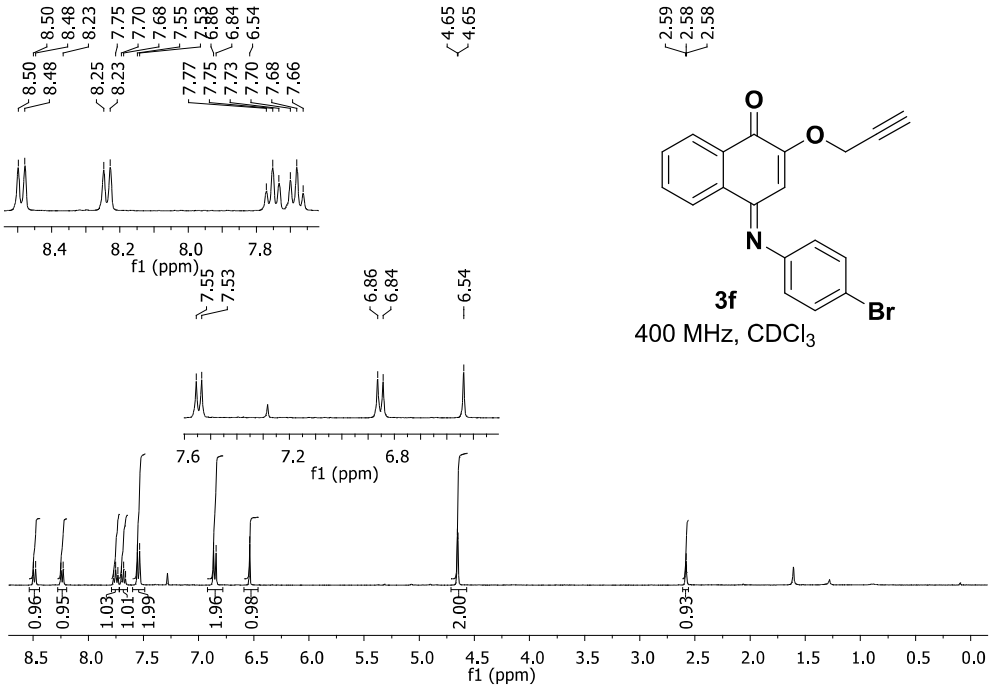

Figure S11. ^{1}H NMR spectrum (400 MHz, $CDCl_3$) of compound **3f**.

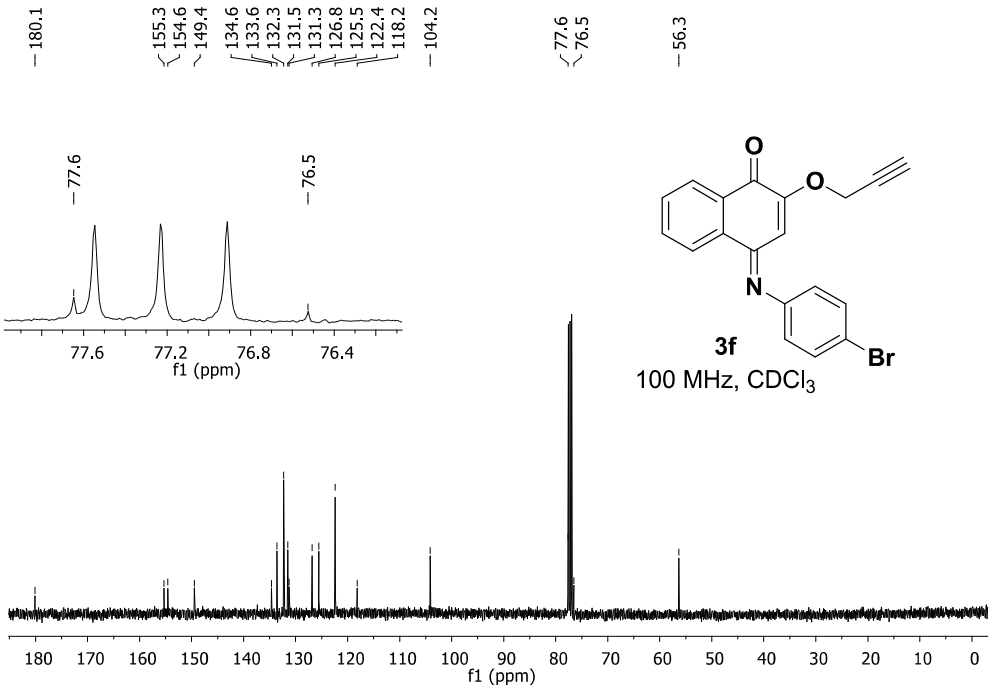

Figure S12. ^{13}C NMR spectrum (100 MHz, $CDCl_3$) of compound **3f**.

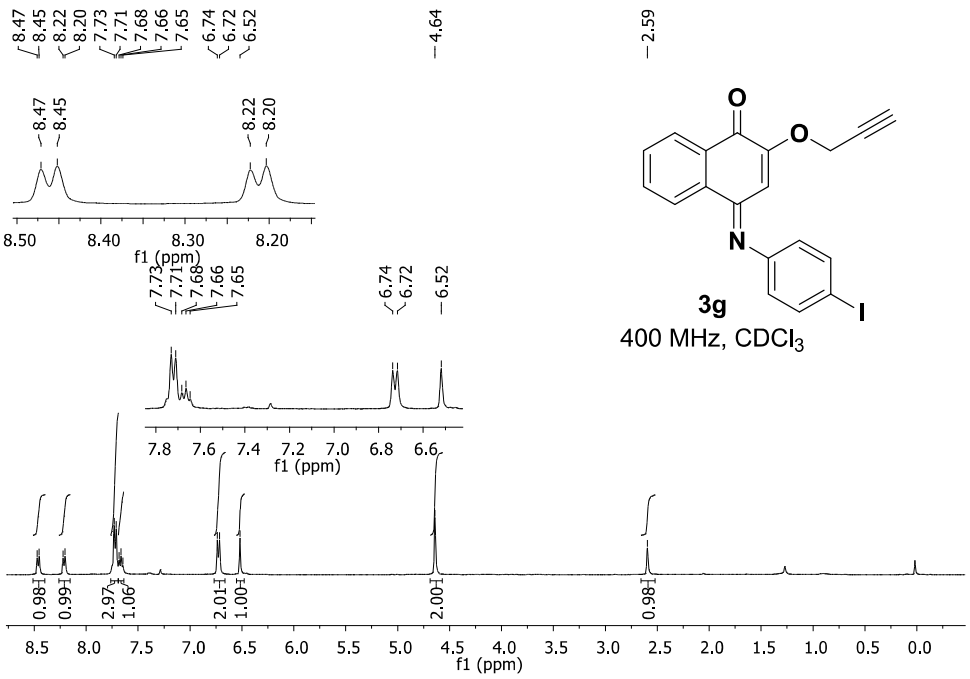

Figure S13. ^{1}H NMR spectrum (400 MHz, $CDCl_3$) of compound **3g**.

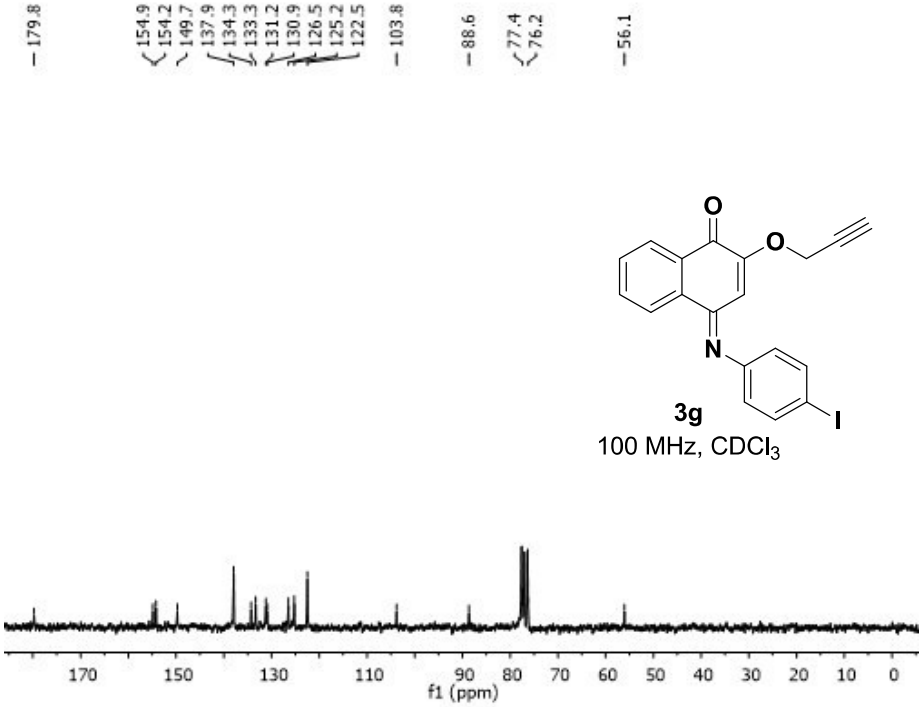

Figure S14. ^{13}C NMR spectrum (100 MHz, $CDCl_3$) of compound **3g**.

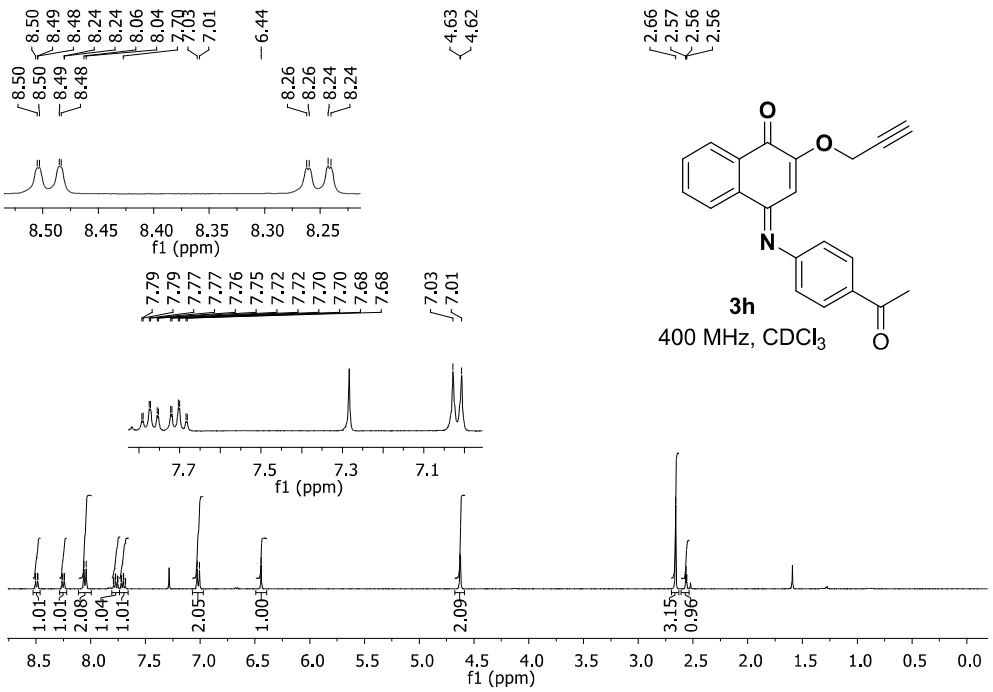

Figure S15. ^{1}H NMR spectrum (400 MHz, $CDCl_3$) of compound **3h**.

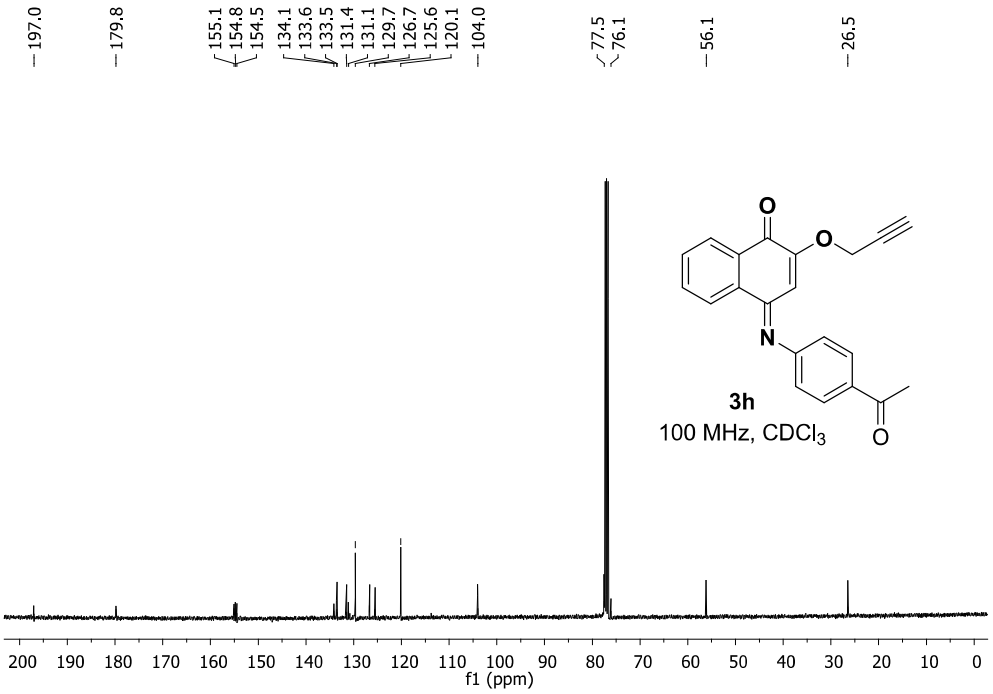

Figure S16. ^{13}C NMR spectrum (100 MHz, $CDCl_3$) of compound **3h**.

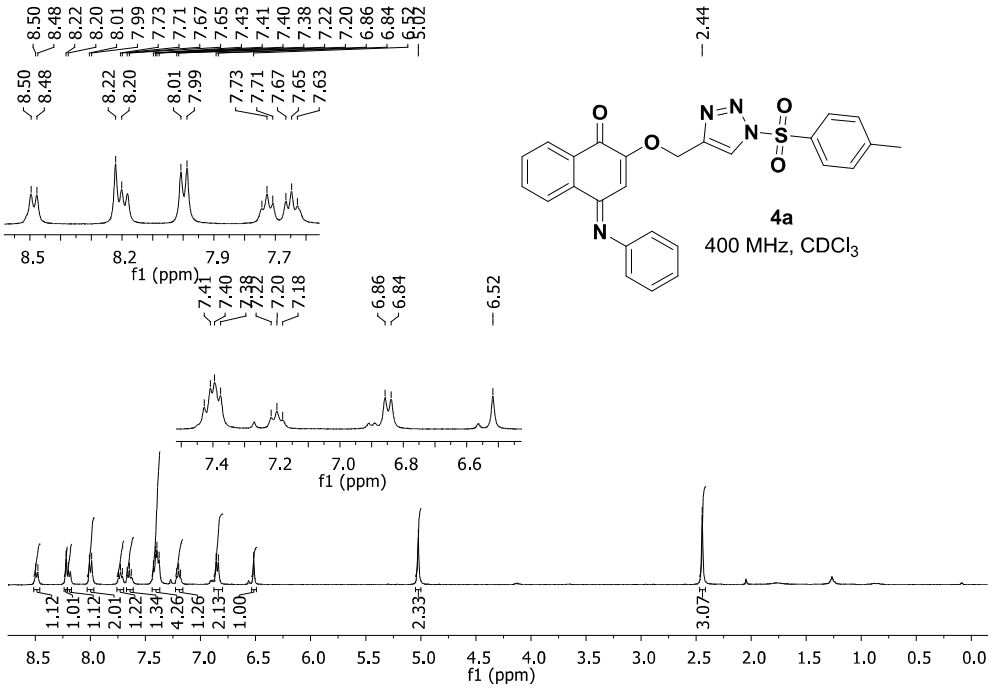

Figure S17. ^{1}H NMR spectrum (400 MHz, $CDCl_3$) of compound **4a**.

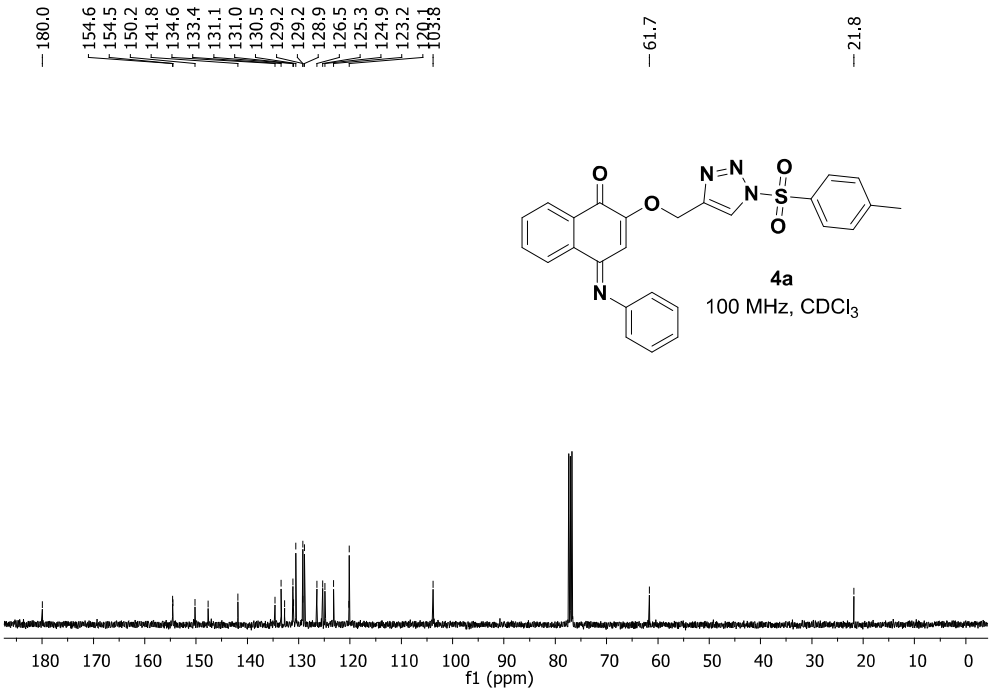

Figure S18. ^{13}C NMR spectrum (100 MHz, $CDCl_3$) of compound **4a**.

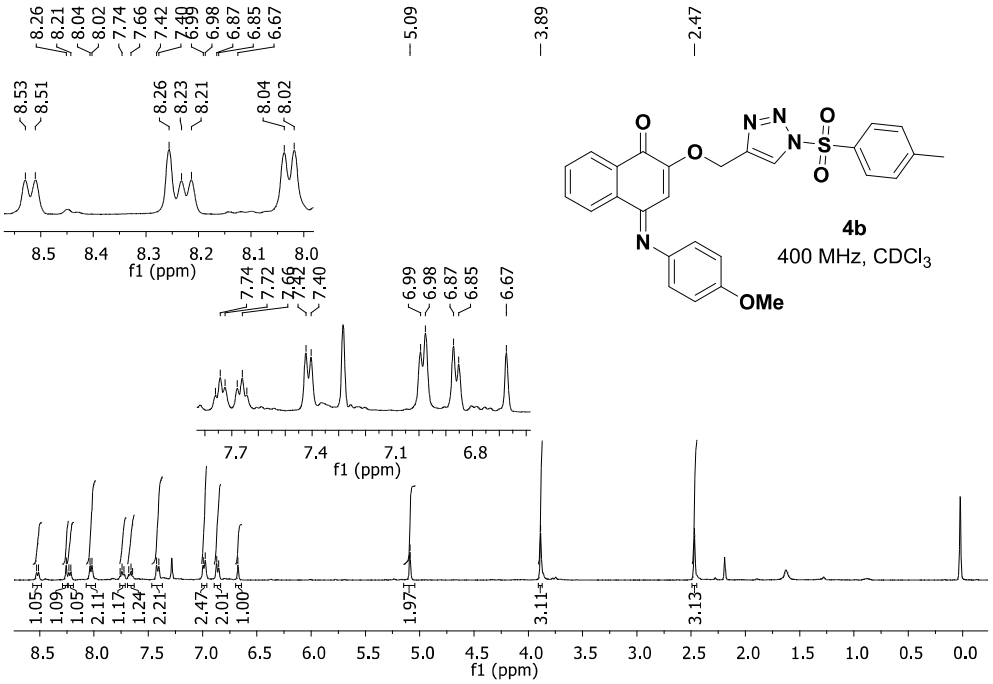

Figure S19. ^{1}H NMR spectrum (400 MHz, $CDCl_3$) of compound **4b**.

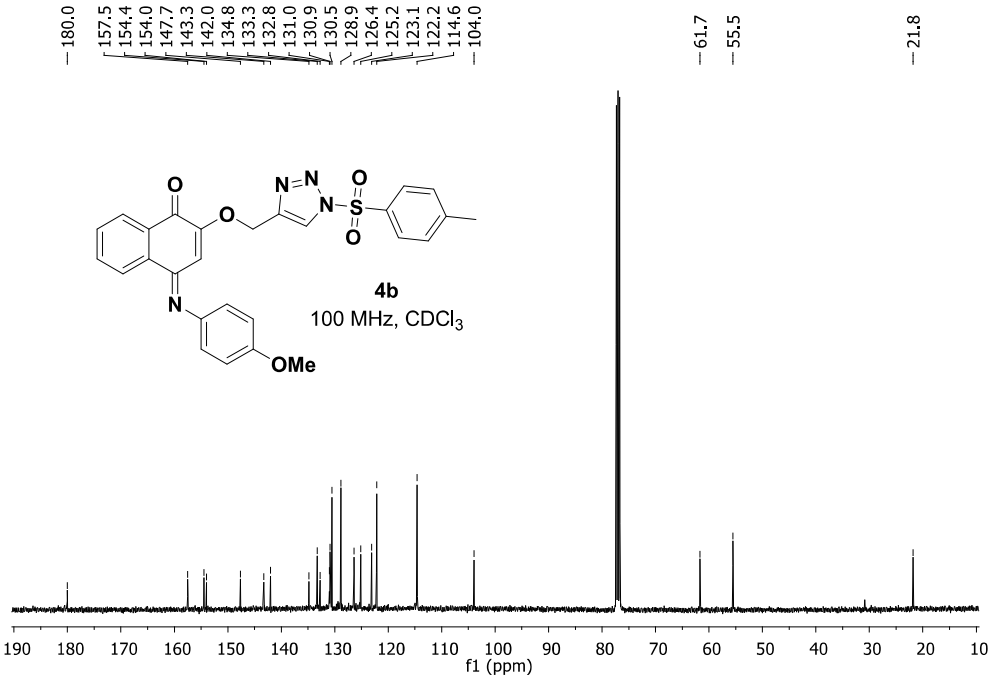

Figure S20. ^{13}C NMR spectrum (100 MHz, $CDCl_3$) of compound **4b**.

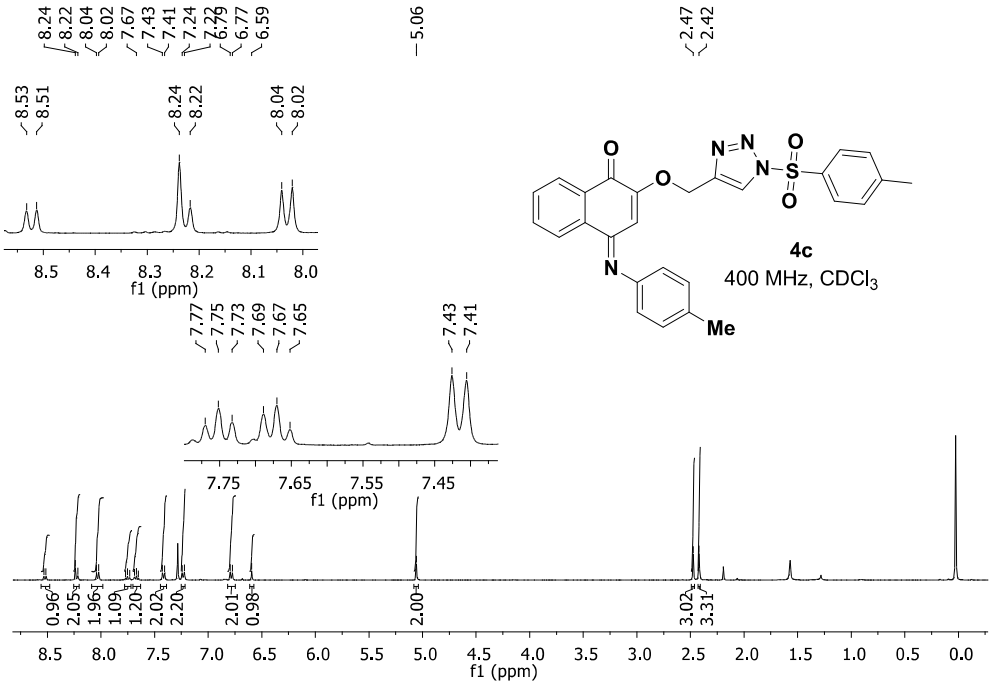

Figure S21. ^{1}H NMR spectrum (400 MHz, $CDCl_3$) of compound **4c**.

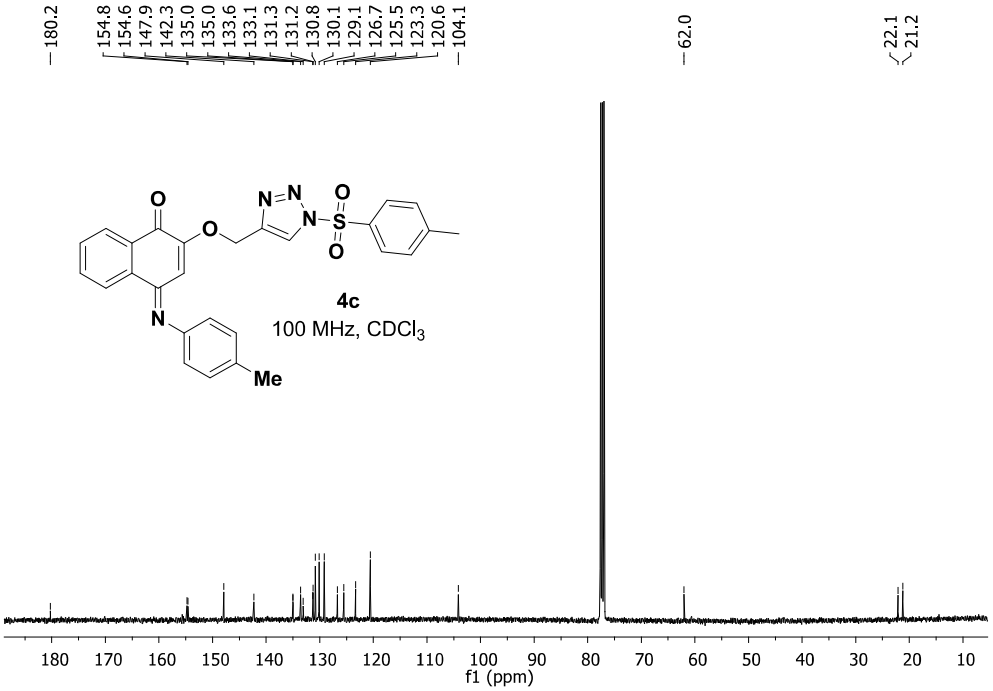

Figure S22. ^{13}C NMR spectrum (100 MHz, $CDCl_3$) of compound **4c**.

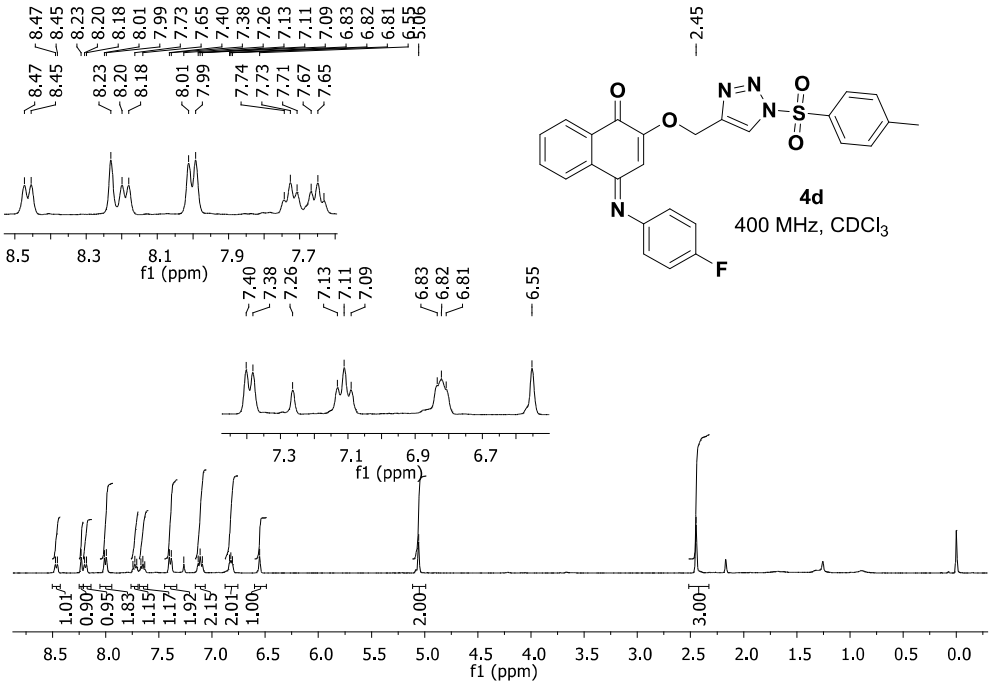

Figure S23. ^{1}H NMR spectrum (400 MHz, $CDCl_3$) of compound **4d**.

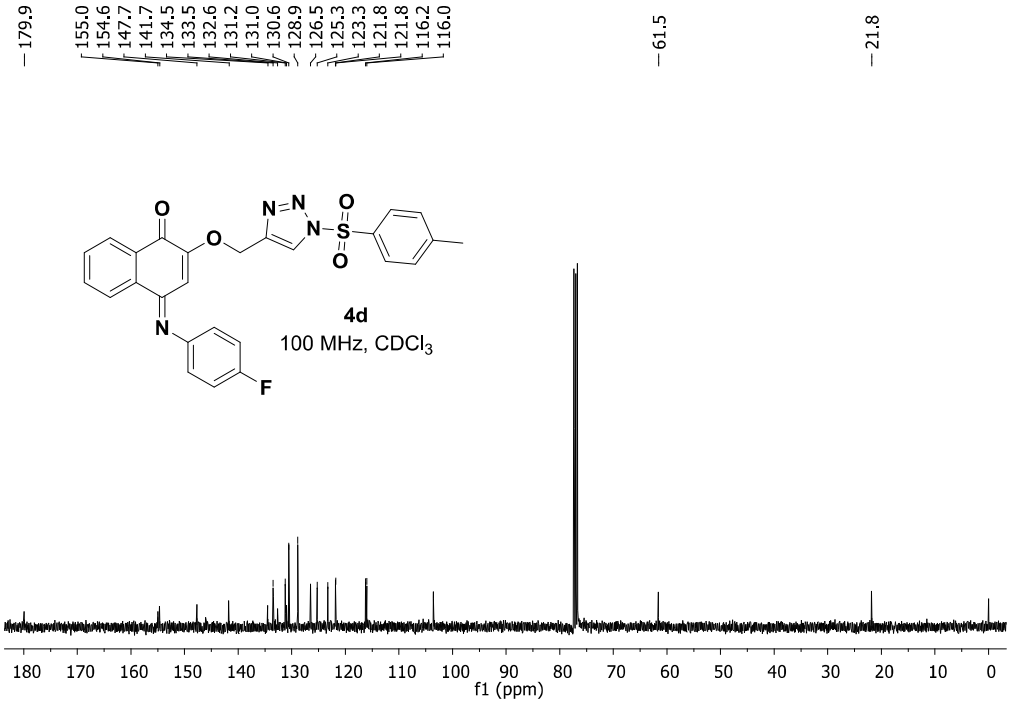

Figure S24. ^{13}C NMR spectrum (100 MHz, $CDCl_3$) of compound **4d**.

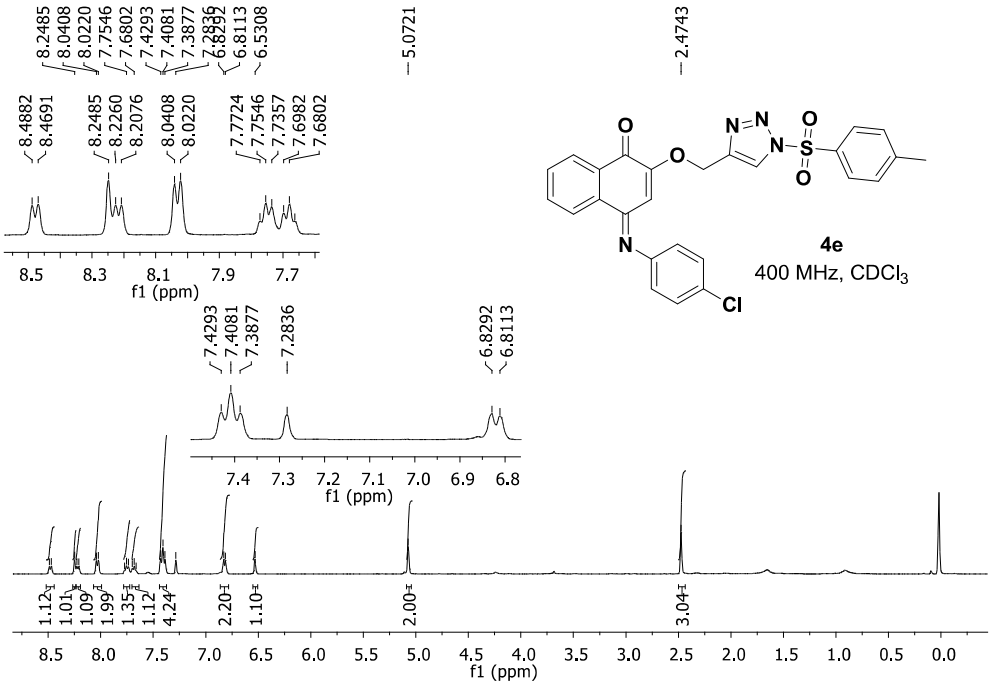

Figure S25. ^{1}H NMR spectrum (400 MHz, $CDCl_3$) of compound **4e**.

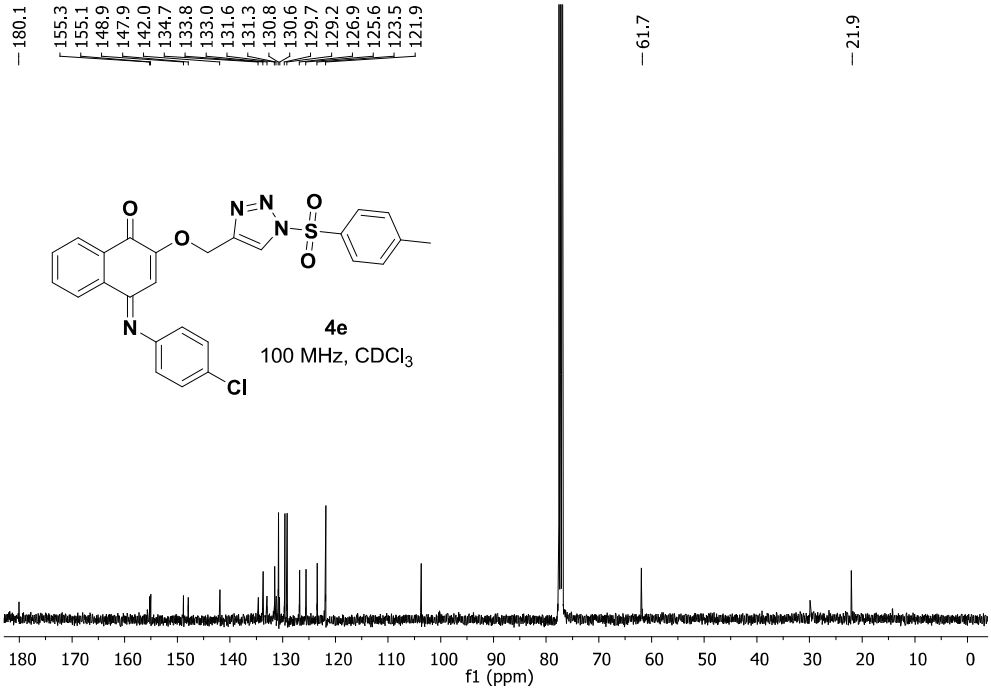

Figure S26. ^{13}C NMR spectrum (100 MHz, $CDCl_3$) of compound **4e**.

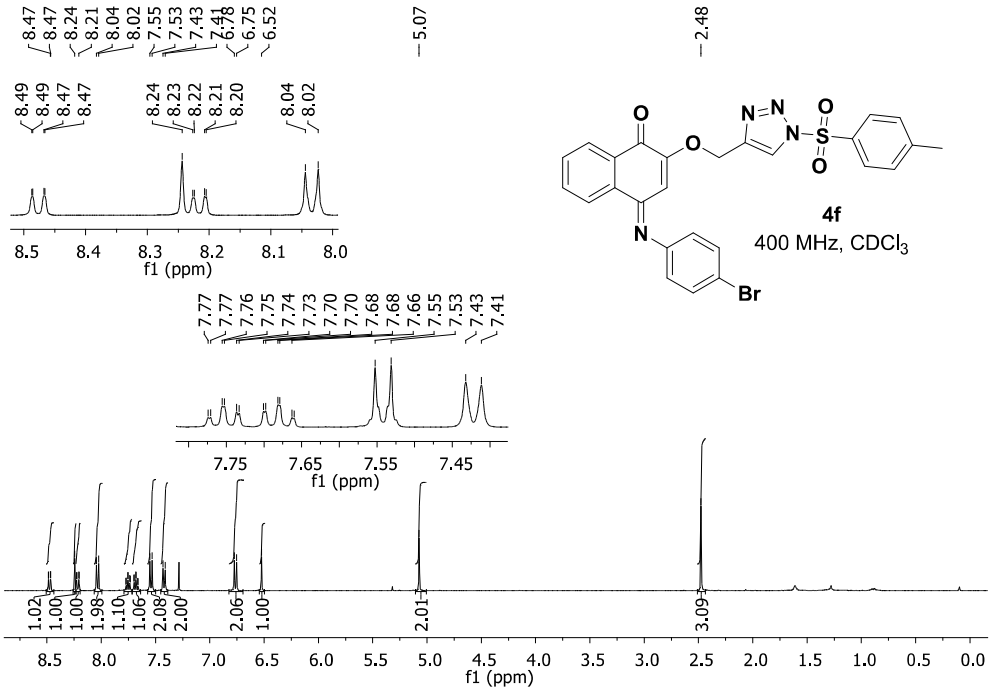

Figure S27. ^{1}H NMR spectrum (400 MHz, $CDCl_3$) of compound **4f**.

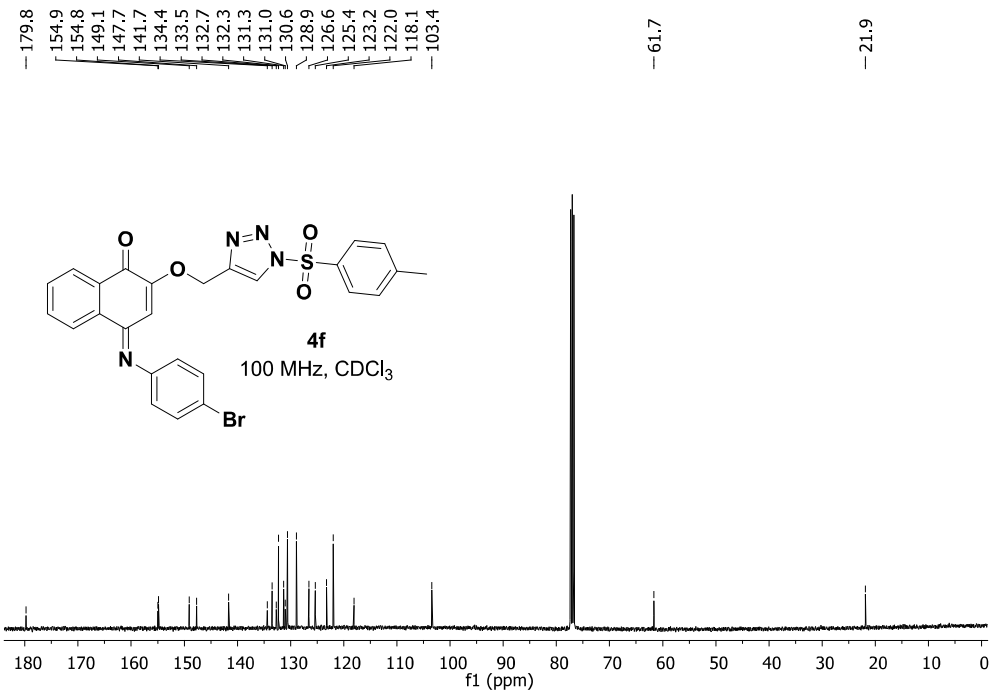

Figure S28. ^{13}C NMR spectrum (100 MHz, $CDCl_3$) of compound **4f**.

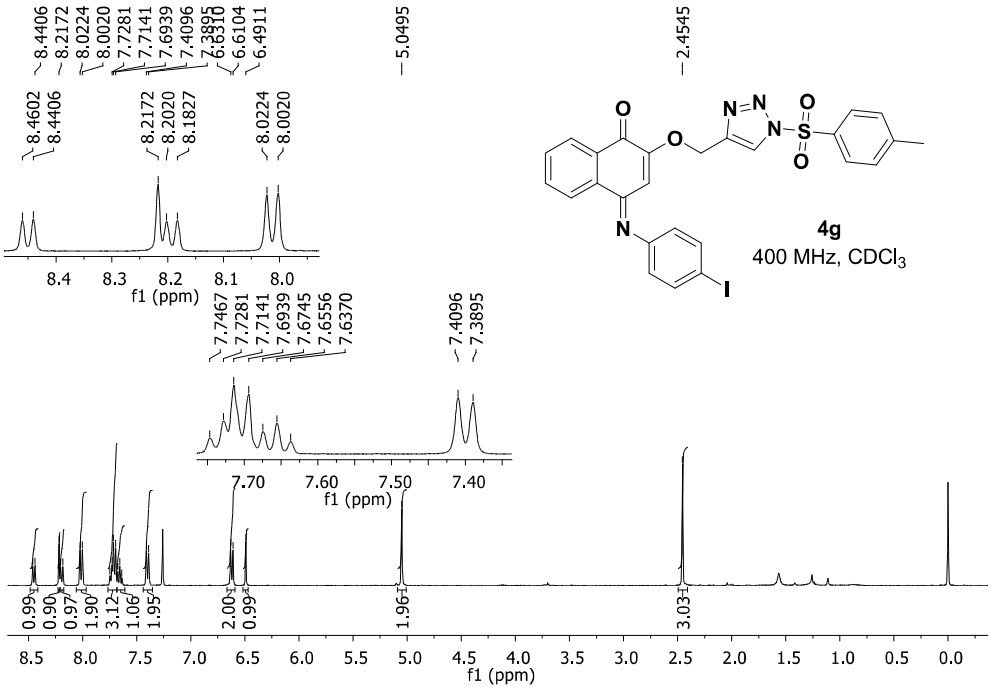

Figure S29. ^{1}H NMR spectrum (400 MHz, $CDCl_3$) of compound **4g**.

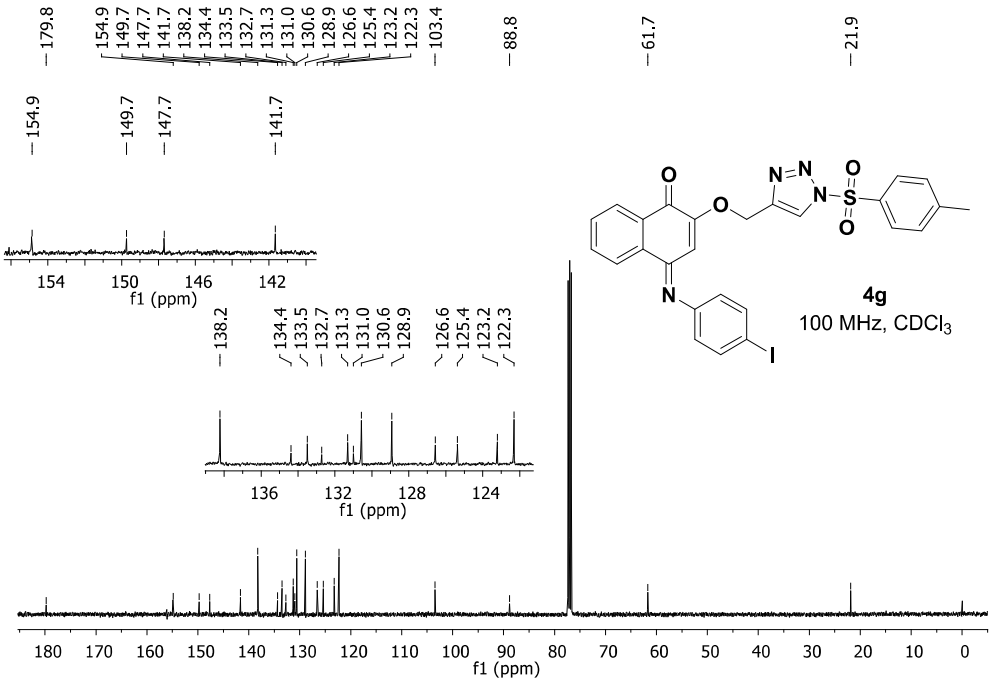

Figure S30. ^{13}C NMR spectrum (100 MHz, $CDCl_3$) of compound **4g**.

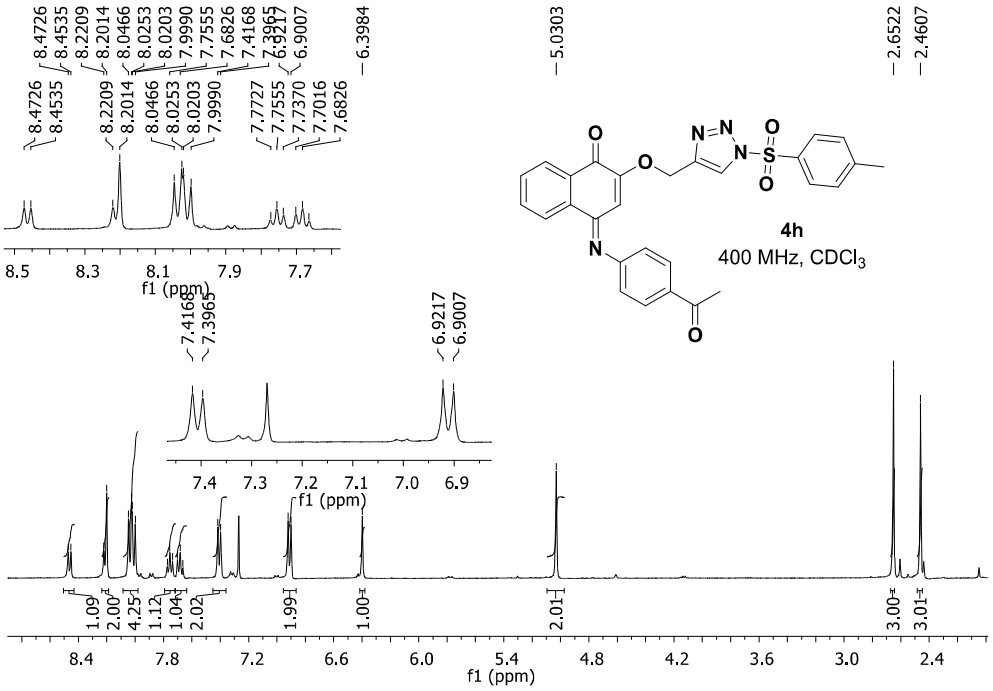

Figure S31. ^{1}H NMR spectrum (400 MHz, $CDCl_3$) of compound **4h**.

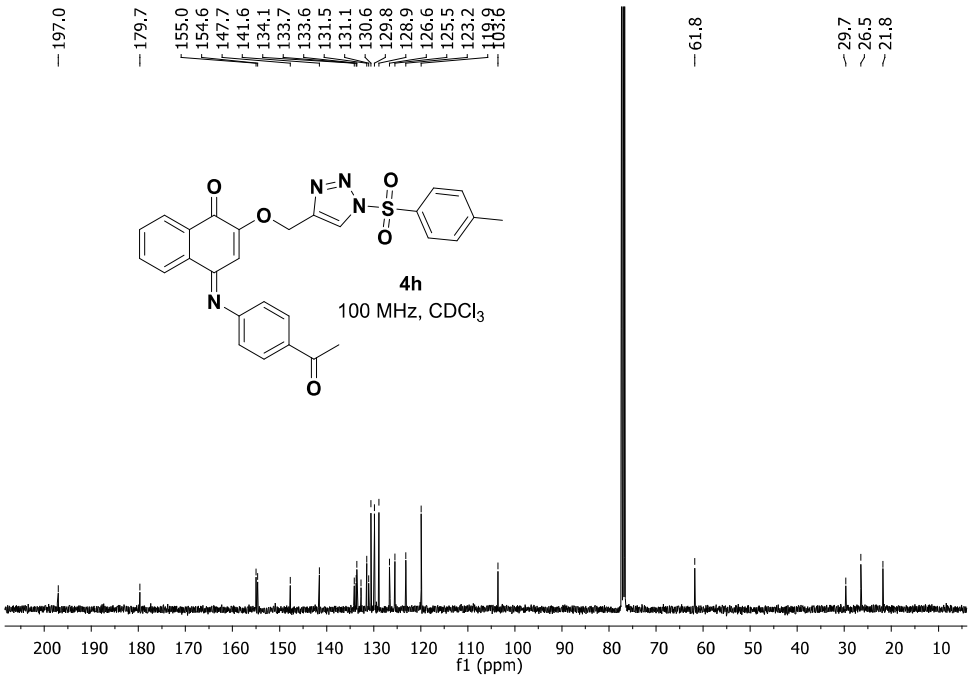

Figure S32. ^{13}C NMR spectrum (100 MHz, $CDCl_3$) of compound **4h**.

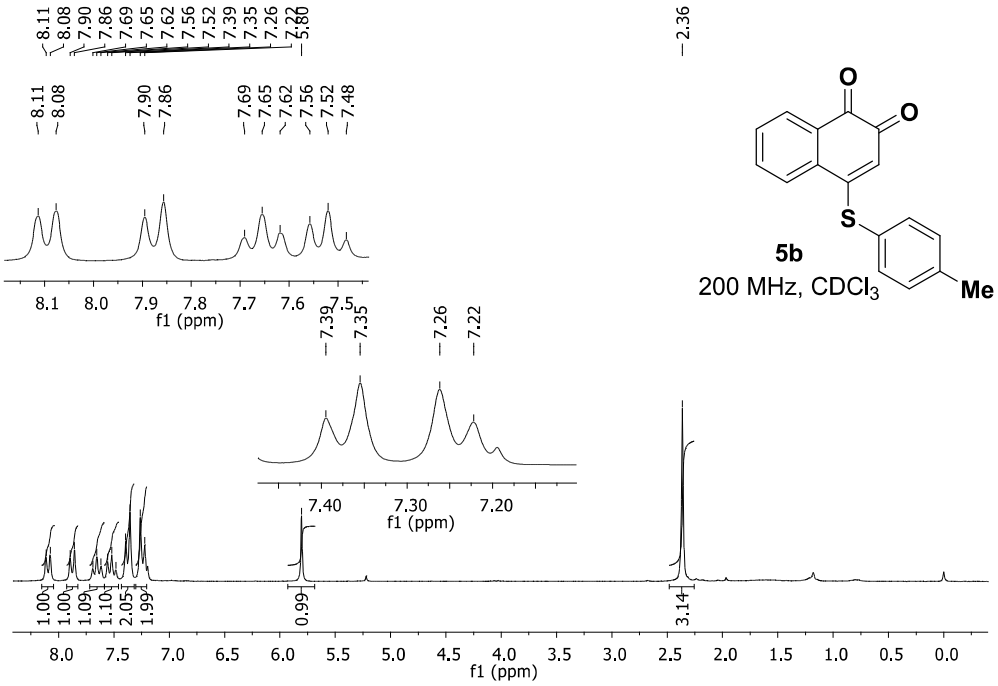

Figure S33. ^{1}H NMR spectrum (200 MHz, $CDCl_3$) of compound **5b**.

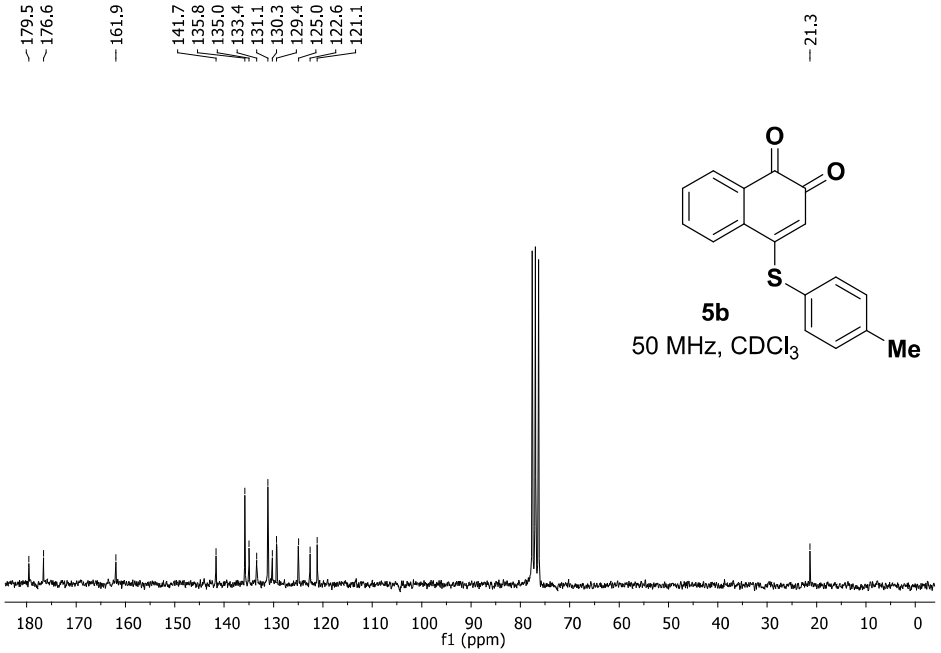

Figure S34. ^{13}C NMR spectrum (50 MHz, $CDCl_3$) of compound **5b**.

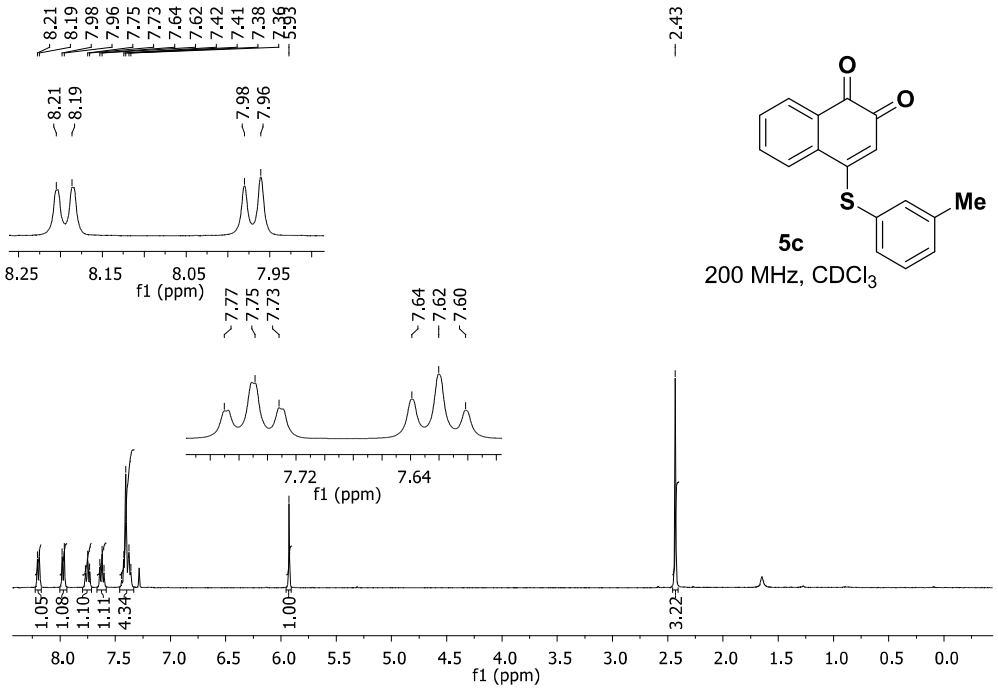

Figure S35. ^{1}H NMR spectrum (200 MHz, $CDCl_3$) of compound **5c**.

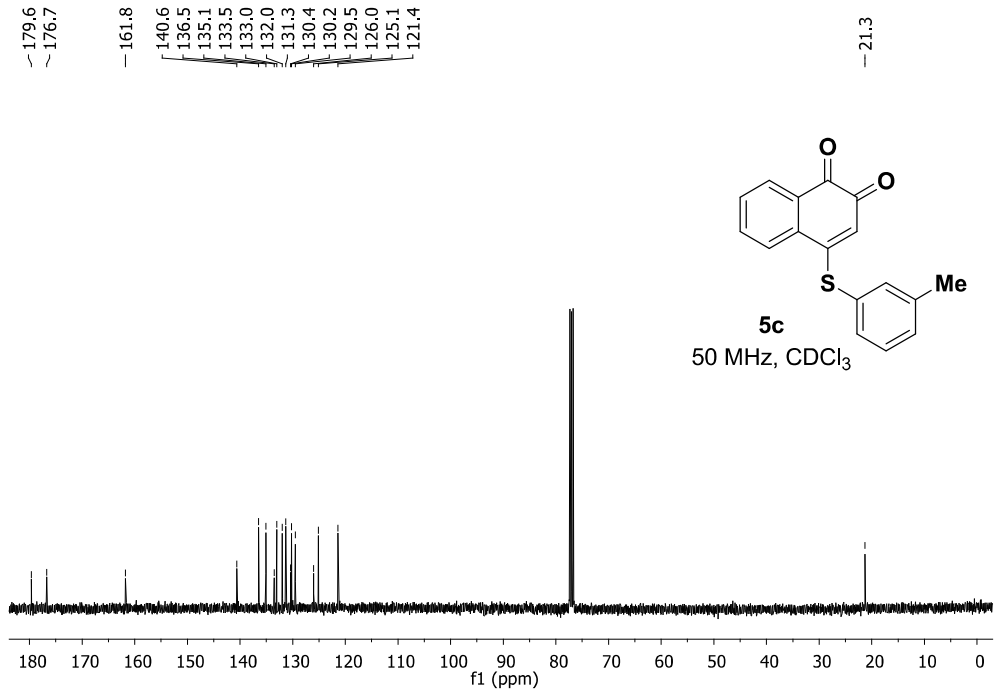

Figure S36. ^{13}C NMR spectrum (50 MHz, $CDCl_3$) of compound **5c**.

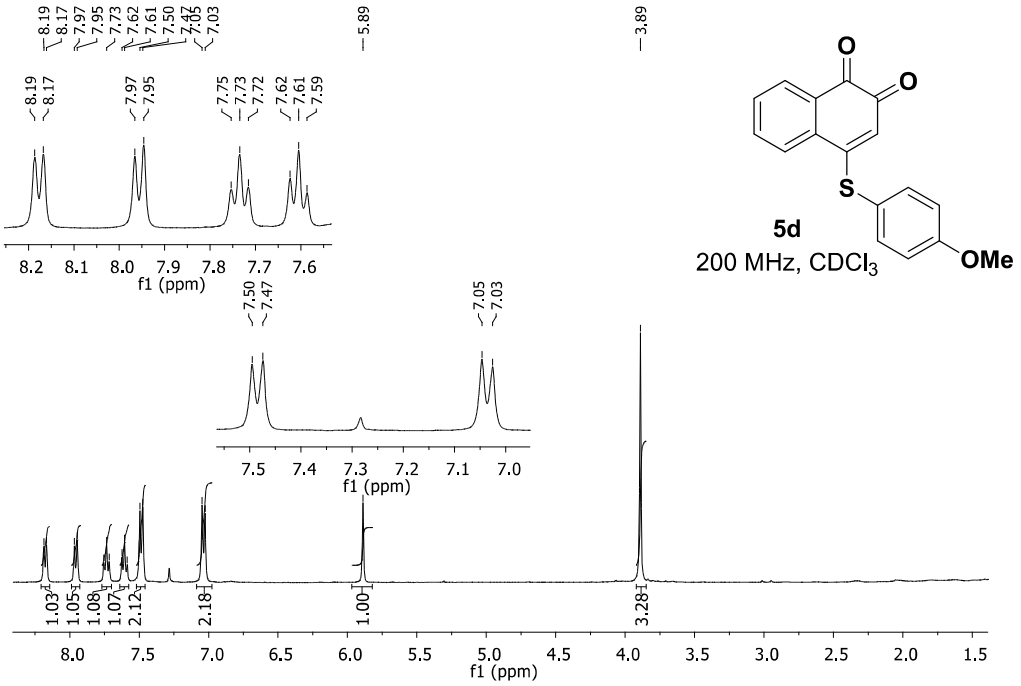

Figure S37. ^{1}H NMR spectrum (400 MHz, $CDCl_3$) of compound **5d**.

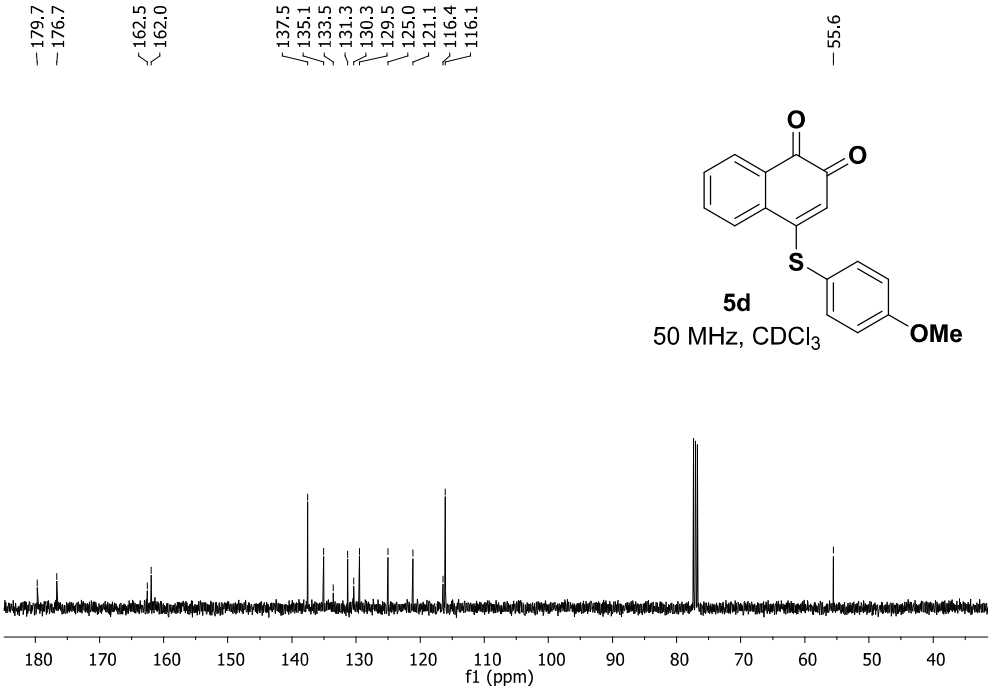

Figure S38. ^{13}C NMR spectrum (50 MHz, $CDCl_3$) of compound **5d**.

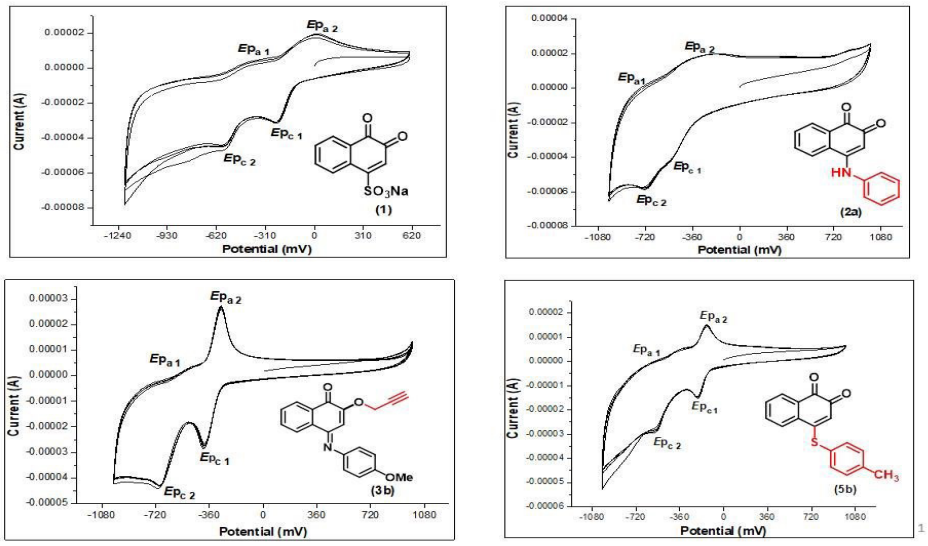

Figure S39. Representative cyclic voltammograms of selected compounds belonging to class 1 (insert a), class 2, class 3 (compound 3a, insert b) and class 5 (compound 5b, insert c). Phosphate buffer 0.1 M (pH 7.4) + 30% methanol; glassy carbon electrode, *E* vs. Ag/AgCl reference electrode (SSE), 200 mV s^{-1}. Potential range: +1.0 V to -1.0 V. Anodic direction. E initial: 0 V.

8. List of Publications:

1- Renata G. Almeida, Wagner O. Valença, Luísa G. Rosa, Carlos A. de Simone, Solange L. de Castro, Juliana M. C. Barbosa, Daniel P. Pinheiro, Carlos R. K. Paier, Guilherme G. C. de Carvalho, Claudia Pessoa, Marilia O. F. Goulart, **Ammar Kharma** and Eufrânio N. da Silva Júnior. Synthesis of quinone imine and sulphur containing-compounds with antitumor and trypanocidal activities: redox and biological implications, *RSC Medicinal Chemistry*, 11, 1145-1160, (2020) (Front Cover)

2- **A. Kharma**, C. Jacob, Í.A.O. Bozzi, G.A.M. Jardim, A.L. Braga, K. Salomão, C.C. Gatto, M.F.S. Silva, C. Pessoa, M. Stangier, L. Ackermann, E.N. da Silva Júnior. Electrochemical Selenation/Cyclization of Quinones: A Rapid, Green and Efficient Access to Functionalized Trypanocidal and Antitumor Compounds. *European. Journal of Organic Chemistry*. 4474-4486. (2020) (Front Cover)

3- Marian Grman, Anton Misak, Lucia Kurakova, Vlasta Brezova, Sona Cacanyiova, Andrea Berenyiova, Peter Balis, Lenka Tomasova, **Ammar Kharma**, Enrique Domínguez-Álvarez, Miroslav Chovanec, and Karol Ondrias. Products of Sulfide/Selenite Interaction Possess Antioxidant Properties, Scavenge Superoxide-Derived Radicals, React with DNA, and Modulate Blood Pressure and Tension of Isolated Thoracic Aorta. *Oxidative Medicine and Cellular Longevity* (2019).

4- **A. Kharma**, M. Grman, A. Misak, E. Domínguez-Álvarez, M.J. Nasim, K. Ondrias, M. Chovanec, C. Jacob. Inorganic Polysulfides and Related Reactive Sulfur–Selenium Species from the Perspective of Chemistry. *Molecules*, 24, 1359 (2019).

5- **A. Kharma**, A. Misak, M. Grman, V. Brezova, L. Kurakova, P. Baráth, C. Jacob, M. Chovanec, K. Ondrias, E. Domínguez-Álvarez. Release of reactive selenium species from phthalic selenoanhydride in the presence of hydrogen sulfide and glutathione

with implications for cancer research. *New Journal of Chemistry*, 43, 11771-11783 (2019).

6- R. Alhasan, **A. Kharma**, P. Leroy, C. Jacob, C. Gaucher. Selenium donors at the junction of inflammatory diseases. *Current Pharmaceutical Design*, 25(15):1707-1716 (2019).

7- R. Alhasan, **A. Kharma**, M. J. Nasim, A. Y. Abdin, J. Bonetti, P. Giummelli, C. E.C.C. Ejike, P. Leroy, C. Gaucher, C. Jacob, Flush with a flash: Natural three-component antimicrobial combinations based on S-nitrosothiols, controlled superoxide formation and "domino" reactions leading to peroxynitrite. *Medicinal. Chemistry. Communications*, 9(12), 1994-1999 (2018).

8- M. J. Nasim, P. Denezhkin, M. Sarfraz, R. Leontiev, Y. Ney, **A. Kharma**, S. Griffin, M. I. Masood, C. Jacob, The Small Matter of a Red Ox, a Particularly Sensitive Pink Cat, and the Quest for the Yellow Stone of Wisdom. *Current. Pharmacology. Reports*, 4:380-396 (2018).

9- Y. Ney, M. J. Nasim**, A. Kharma**, L. A. Youssef, C. Jacob, Small Molecule Catalysts with Therapeutic Potential. *Molecules*;23(4), 765 (2018).

10- L. Faulstich, S. Griffin, M.J. Nasim, M.I. Masood, W. Ali, S. Alhamound, Y. Omran, H. Kim, **A. Kharma**, K.H. Schaefer, R. Lilischkis, M. Montenarh, C. Keck, C. Jacob, Nature's Hat-trick: Can we use sulfur springs as ecological source for materials with agricultural and medical applications?, *International . Biodeterioration and Biodegradation*, 119, 678-686, (2017).